MANCHESTER 1824

The University of Manchester

Allyl and Pentadienyl Carbanion Complexes of Alkali Metals: Metal- and Functionality-directed Structure and Bonding

A thesis submitted to the University of Manchester for the degree of Doctor of Philosophy in the Faculty of Engineering and Physical Sciences.

2011

Sophia A. Solomon

Supervisor: Dr Richard Layfield

School of Chemistry

Table of Contents

Word Count – 43,156

Abstract

Five *ansa-tris*(allyl) complexes [(PhSi{$C_3H_3(SiMe_3)$}$_3$)(Li·tmeda)$_3$] (**2.1**), [(MeSi{$C_3H_3(SiMe_3)$}$_3$)(Li·pmdeta)$_3$] (**2.2**), [(MeSi{$C_3H_3(SiMe_3)$}$_3$)-(Na.tmeda)$_3$] (**2.3**), [(PhSi{$C_3H_3(SiMe_3)$}$_3$)(Na·tmeda)$_2$Na]$_2$ [**2.4**]$_2$ and [(MeSi-{$C_3H_3(SiMe_3)$}$_3$)(K·OEt$_2$)$_2$(KLi{O^{t}Bu})]$_2$ [**2.5**]$_2$ have been synthesised, and studied by X-ray crystallography and NMR spectroscopy. A collaboration was undertaken to study some of the complexes by DFT. Crystallographic studies have shown that the overall structure of the complex is dependent on a combination of several factors: the metal cation; the substituent on the central silicon atom for the *ansa-tris*(allyl) ligands; and the co-ligand, tmeda or pmdeta. (tmeda = *N,N,N',N'*-tetramethylethylenediamine and pmdeta = *N,N,N',N',N''*-pentamethyldiethylene-triamine). Solution studies of the *ansa-tris*(allyl) complexes showed that the solid-state structures are maintained in solution.

The first examples of donor-functionalised allyl pro-ligands have been synthesised and coordinated to a variety of s-block metals; [Li{$(SiMe_3)_2C_3H_2$(1-$CH_2C_4H_7O$)}]$_2$ [**4.1**]$_2$, [Li{$(SiMe_3)_2C_3H_2$(1-$CH_2CH_2OCH_3$)}]$_2$ [**4.2**]$_2$, [(thf)K{$(SiMe_3)_2C_3H_2$(1-$CH_2C_4H_7O$)}]$_2$ [**4.5**]$_\infty$ and [Mg{$(SiMe_3)_2C_3H_2$(1-$CH_2C_4H_7O$)}$_2$] (**4.6**). As with the *ansa-tris*(allyl) complexes, both X-ray crystallographic and NMR spectroscopy studies have been undertaken, and the structures of the donor-functionalised allyl complexes were found to be dependent on the metal cation, with each cation coordinated in a different manner by the allyl ligand. For the potassium allyl complex **4.5** there is complete delocalisation of the allyl negative charge, and it is η^3-coordinated in a polymeric structure. However for lithium complexes, **[4.1]$_2$** and **[4.2]$_2$**, the donor-functionalised allyl ligand is η^2-coordinated, and the negative charge is only partially delocalised. The magnesium complex **4.6** has the allyl ligand coordinated *via* a σ-bond to the metal and the allyl has localised single and double bonds.

Finally, the synthesis of the first two donor-functionalised pentadienyl ligands and their lithium complexes are reported. Complexes [(tmeda)Li{1,5-$(SiMe_3)_2C_5H_4(CH_2C_4H_7O)$}] (**6.1**) and [(tmeda)Li{1,5-$(SiMe_3)_2C_5H_4(CH_2CH_2OCH_3)$}] (**6.2**) are the first structurally characterised lithium pentadienyl complexes, and are the first donor-functionalised pentadienyl complex of any metal. As well as structural characterisation, complexes **6.1** and **6.2** have been investigated by NMR spectroscopy and collaborative DFT studies. X-ray crystallography revealed that both complexes have the W-conformation of the pentadienyl ligand η^2-coordinated to the lithium cation, as well as the ether oxygen atom and the tmeda nitrogen atoms. DFT studies showed that the most stable gas-phase structure of the 1,5-*bis*(trimethylsilyl)-pentadienyl anion is the W-conformation, but its lithium complex is most stable in the U-conformation. The $[Li\{1,5\text{-}(SiMe_3)_2C_5H_4(CH_2CH_2OCH_3)\}]^-$ anion has the W-conformation and the U-conformation is isoenergetic, but the addition of tmeda gives the W-conformation as the most stable in both the gas-phase and in toluene. Finally NMR spectroscopy studies showed that in solution complexes **6.1** and **6.2** are either in the symmetrical U-conformation or in fluxional process with a very low activation energy.

Declaration

No portion of the work referred to in the thesis has been submitted in support of an application for another degree or qualification of this or any other university or other institute of learning

Copyright

i. The author of this thesis (including any appendices and/or schedules to this thesis) owns certain copyright or related rights in it (the "Copyright") and s/he has given The University of Manchester certain rights to use such Copyright, including for administrative purposes.

ii. Copies of this thesis, either in full or in extracts and whether in hard or electronic copy, may be made **only** in accordance with the Copyright, Designs and Patents Act 1988 (as amended) and regulations issued under it or, where appropriate, in accordance with licensing agreements which the University has from time to time. This page must form part of any such copies made.

iii. The ownership of certain Copyright, patents, designs, trade marks and other intellectual property (the "Intellectual Property") and any reproductions of copyright works in the thesis, for example graphs and tables ("Reproductions"), which may be described in this thesis, may not be owned by the author and may be owned by third parties. Such Intellectual Property and Reproductions cannot and must not be made available for use without the prior written permission of the owner(s) of the relevant Intellectual Property and/or Reproductions.

iv. Further information on the conditions under which disclosure, publication and commercialisation of this thesis, the Copyright and any Intellectual Property and/or Reproductions described in it may take place is available in the University IP Policy (http://www.campus.manchester.ac.uk/medialibrary/policies/intellectual-property.pdf), in any relevant Thesis restriction declarations deposited in the University Library, The University Library's regulations (http://www.manchester.ac.uk/library/aboutus/regulations) and in The University's policy on presentation of Theses

Acknowledgements

Firstly I would like to thank Dr. Richard Layfield for all the support, guidance and advice he has given me throughout the last three years, without his support I would not have been able to complete this work. I would like to thank The University of Manchester's NMR spectroscopy service, microanalysis service and mass spectrometry service and Stephen Boyer (London Metropolitan University) for running my air-senstive elemental analysis samples. Thank you to Dr Chris Muryn, Dr. Madeleine Helliwell and Dr Robin Pritchard for their help with crystallography. Also, I'd like to thank Dr. Jordi Poater and Prof. Miquel Solà (Universitat de Girona, Spain) and Prof. Dr. F. Matthias Bickelhaupt (Department of Theoretical Chemistry and Amsterdam Centre for Multiscale Modeling, Amsterdam) for their work on DFT calculations. I would also like to thank lecturers and friends from my undergraduate, without their support and encouragement I would not have had the chance to do a PhD. I'd especially like to thank Dr. Philip Dyer and Dr. Andrew Beeby, and my friends Lucas Applegarth, Sebastian Spain, Pippa Monks and Ricky Ward. I would like to thank those in office 3.09, and others that joined us for tea breaks, for their help making the department a great place to work. I would like to thank to my parents, Peter and Jenny Solomon, they have always supported me, especially through my PhD, and I'd like to thank my brother, George Solomon, for being there to cheer me up, in a way only a sibling could. And to all of my extended family, especially my grandma, my aunts Anna Saif and Helen Solomon, and my uncle Chris Solomon for their support and understanding throughout the writing up process. Thank you to all my friends, for supporting me in so many ways, especially Freya Smith-Jack and Virginie Walker, my oldest and dearest friends. And finally I would like to thank Daniel Woodruff, who from all the people in my life has had to cope with more of my bad moods than any other. He has had to help me through each stage of my PhD and this thesis and for that I am very grateful.

Abbreviations

Cp − cyclopentadiene

Cp^- – Cyclopentadienyl

Cp* - Pentamethylcyclopentadienyl

COSMO - COnductor-like Screening Model

depe – 1,2-*bis*(diethylphosphino)ethane

DFT – Density Functional Theory

FTIR Spectroscopy – Fourier Transform Infra Red Spectroscopy

HSQC – Heteronuclear Single-Quantum Correlation

NMR − Nuclear Magnetic Resonance

pmdeta − *N,N,N',N',N''*-pentamethyldiethylenetriamine

Pn – Pentadienyl

SSEPOC − Site Specific Electrostatic Perturbation of Conjugation

thf − tetrahydrofuran

tmeda − *N,N,N',N'*-tetramethylethylenediamine

UV-Vis Spectroscopy – Ultraviolet-Visible Spectroscopy

VT –Variable Temperature

List of Isolated Ligands and Complexes

Chapter 2:

$PhSi\{C_3H_4(SiMe_3)\}_3$ (**L**^{2}H_3)

$[PhSi\{(C_3H_3SiMe_3)Li(tmeda)\}_3]$ (**2.1**)

$[MeSi\{(C_3H_3SiMe_3)Li(pmdeta)\}_3]$ (**2.2**)

$[MeSi\{(C_3H_3SiMe_3)Na(tmeda)\}_3]$(**2.3**)

$[PhSi\{(C_3H_3SiMe_3)Na\}_3]_2$ [**2.4**]$_2$

$[MeSi\{(C_3H_3SiMe_3)_3\}\{K(OEt_2)_2\}_2KLi(\mu_4\text{-}O^tBu)]_2$ [**2.5**]$_2$

Chapter 4:

$(1,3\text{-}SiMe_3)_2C_3H_2(1\text{-}CH_2C_4H_7O)$ (**L**^{8}H)

$(1,3\text{-}SiMe_3)_2C_3H_2(1\text{-}CH_2CH_2OCH_3)$ (**L**^{9}H)

$[Li\{(SiMe_3)_2C_3H_3(CH_2C_4H_7O)\}]_2$ [**4.1**]$_2$

$[Li\{(SiMe_3)_2C_3H_3(CH_2CH_2OCH_3)\}]_2$ [**4.2**]$_2$

$[(thf)K\{(SiMe_3)_2C_3H_2(CH_2C_4H_7O)\}]_\infty$ [**4.5**]$_\infty$

$[Mg\{(SiMe_3)_2C_3H_2(CH_2C_4H_7O)\}_2]$ (**4.6**)

Chapter 6:

$(1,5\text{-}SiMe_3)_2C_5H_5(3\text{-}CH_2C_4H_7O)$ (**L**^{8}H)

$(1,5\text{-}SiMe_3)_2C_5H_5(3\text{-}CH_2CH_2OCH_3)$ (**L**^{9}H)

$Me_2Si(C_6H_4\text{-}m\text{-}OCH_3)C_5H_6(SiMe_3)$ (**L**^{10}H)

$(1\text{-}Me_3Si)C_5H_6(5\text{-}CH_2CH_2OCH_3)$ (**L**^{12}H)

$[(tmeda)Li\{(SiMe_3)_2C_5H_4(CH_2C_4H_7O)]]$ (**6.1**)

$[(tmeda)Li\{(SiMe_3)_2C_5H_4(CH_2CH_2OCH_3)]$ **(6.2**)

Chapter 1

Introduction to Metal Allyl Complexes

1.1 An Introduction to Metal Allyl Chemistry

Over the last fifty years the area of allyl chemistry has been extensively developed, with the allyl anion and its derivatives being used widely as ligands in organometallic chemistry[1,2] and in organic synthesis.[3,4] G. Wilke and his group sparked interest in the chemistry of homoleptic metal allyl complexes with their ground-breaking work on complexes of the general formula $[(C_3H_5)_nM]$, and their investigations into the roles that metal allyl complexes play in homogeneous catalysis. Examples of metal allyl complexes are $[Ni(C_3H_5)_2]$ (**1.1**), synthesised according to Scheme 1, and $[Pd(C_3H_5)_2]$ (**1.2**) which were found to be active catalysts for the oligomerisation of dienes.[2]

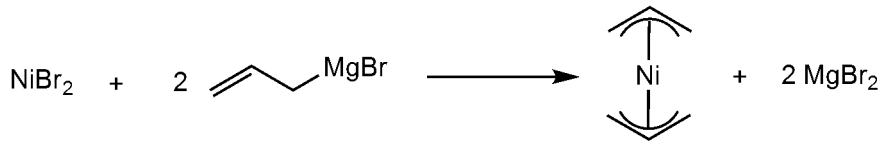

Scheme 1

In his original work, Wilke and his team synthesised a variety of different transition metal allyl complexes, and throughout their work they identified several trends in the chemical properties of the complexes. First, they noted the homoleptic transition metal allyl complexes were extremely sensitive to air and moisture; secondly that the diamagnetic metal allyls tended to be easier to synthesise and handle than the paramagnetic allyl complexes; and, finally, it was noted that the stability of the metal allyl complex in a particular triad increases in the order 3d < 4d < 5d. It was also noted that metal allyl complexes of the type $[(C_3H_5)_nM]$ were difficult to handle and characterise owing to their thermal instability, and the fact the complexes have access to decomposition pathways with low activation energies. However, in recent years, the problem of low thermal stability has been addressed through use of sterically bulky silyl (usually trimethylsilyl) substituents on to the allyl ligand. This has lead to the ability to

stabilise a much wider variety of metal allyl complexes, including those too unstable to isolate using just the parent allyl $[C_3H_5]^-$ as the ligand.[5,6]

1.1.1 Silyl-substituted Allyl Ligands

For an allyl ligand, there are three common coordination modes: the η^1, or σ-bonded mode (**A**), the enyl, or combined σ/π-bonded (**B**), or the η^3, π-bonded mode (**C**). If the allyl ligand has substituents on one or both of the terminal carbon atoms it is possible for an *exo* (*syn*) or *endo* (*anti*) isomers (**D**) to exist (Figure 1).

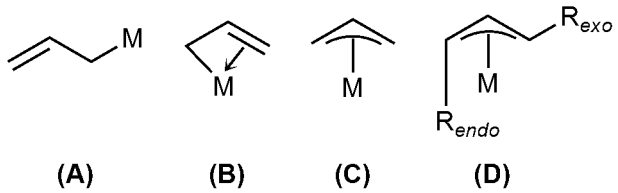

Figure 1: Different allyl bonding modes

Using steric bulk to give a complex kinetic stability is a well known strategy. However, it is only more recently that properties of silyl substituents have been utilised in metal allyl coordination chemistry. Not only do they provide steric protection for the metal, they also improve solubility and are easy to synthesise in high yields, usually from inexpensive and readily available starting materials.[4] Synthesis of silyl-allyl pro-ligands, usually involves a nucleophilic substitution reaction between silyl halides and main group metal allyls (Scheme 2).

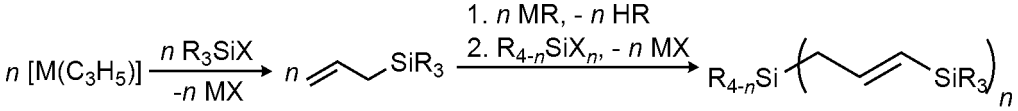

Scheme 2

There now exists a wide range of silyl-substituted pro-ligands: mono(silyl-allyl) (**E**), *ansa-bis*(silyl-allyl) (**F**) and the *ansa-tris*(silyl-allyl) (**G**), and, more recently, donor

functionalised-allyl pro-ligands (see Chapter 3 and Chapter 4). The large variety of available alkyl- and aryl-silyl halides means the steric bulk of the pro-ligand can be tailored to requirements.

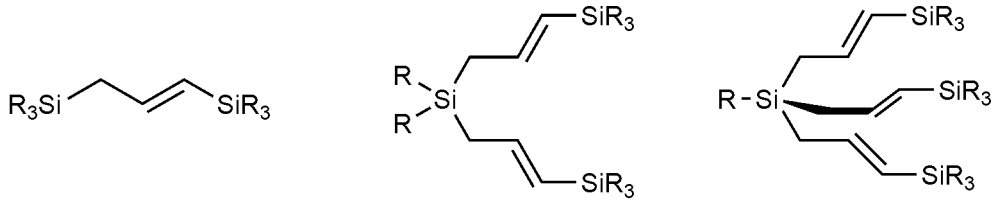

(**E**) (**F**) (**G**)

Figure 2: Types of silyl-allyl pro-ligand

1.1.2 s-Block Metal Allyl Complexes

A general synthetic route to lithium complexes of allyl ligands is usually *via* direct metallation of a carbon α- to the silicon by lithium alkyl. The lithium complexes of the silyl-allyl ligands can then be transmetallated with sodium or potassium *tert*-butoxide, in hexane, to give insoluble sodium or potassium allyls, which can be stored indefinitely under an inert atmosphere. Elemental caesium reacts directly with the acidic C−H bond of the silyl-allyl pro-ligand. Alkali metal silyl-allyl complexes have interesting and varied chemistry; the s-block metal centre in the complexes can vary the extent of delocalisation of the negative charge within the allyl. The heavier and larger metals such as sodium, potassium and caesium are often η^3 coordinated by allyl ligands exhibiting a fully delocalised charge. In lithium allyl complexes, a range of types of allyl coordination modes can be seen. Localised σ-bonds to lithium, with localised single and double bonds within the allyl is possible (**H**). In contrast, η^3 coordinated allyl ligands, in which the C−C bond lengths are roughly equal, suggests complete delocalisation of the negative charge (**I**). The structure with bonding between these two extremes has partial delocalisation of the negative charge (**J**). Partial delocalisation has been investigated thoroughly by Fraenkel *et al.*[7,8] and they have shown that complexes of donor-

functionalised allyl ligands tend to exhibit partial delocalisation, and have called the effect Site Specific Electrostatic Perturbation of Conjugation (SSEPOC).[9]

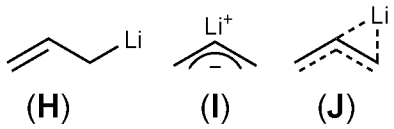

(**H**) (**I**) (**J**)

Figure 3: Possible coordination of the allyl ligand to the lithium cation.

As well as being interesting in their own right, alkali metal complexes also allow access to p-, d-, and f-block allyl complexes *via* metathesis, which will be discussed in the following sections.

1.1.2a Alkali Metal Allyl Complexes

The simplest metal allyl complex, allyllithium, [Li(C_3H_5)] (**1.3**), has been the subject of extensive investigations by calculations[10,11] and NMR spectroscopic experiments.[12] Crystallographic studies have also been reported on allyllithium complexes of tmeda (tmeda = *N,N,N',N'*-tetramethylethylenediamine) and pmdeta (pmdeta = *N,N,N',N',N''*-pentamethyldiethylenetriamine), [(tmeda)Li(C_3H_5)] (**1.4**)[13,14] and [(pmdeta)Li(C_3H_5)] (**1.5**)[15] respectively. The interest in the structure of allyllithium arose from the large discrepancy between the calculated and experimental data for the rotation of the terminal methylene about the C−C bond of the solution of **1.3** in thf (thf = tetrahydrofuran). The calculated *ab initio* rotational barrier suggested that the species should be a monomer, however it was found that **1.3** in thf existed as an unsymmetrical and rapidly equilibrating dimer [**1.3**$(thf)_2]_2$ (Scheme 3), in which the lithium cation is coordinated to one allyl and μ-bridges to another (Scheme 3).[12] This contrasts to the structures of the heavier alkali metal allyls, allylsodium, [Na(C_3H_5)] (**1.6**) and allylpotassium, [K(C_3H_5)] (**1.7**), which are thought to be monomers in thf solution.[12]

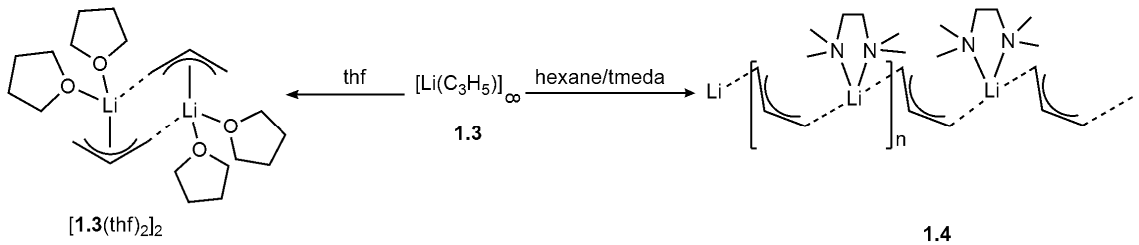

Scheme 3

Complex **1.3** is insoluble in hydrocarbons, suggesting that its solid-state structure is polymeric. However, if tmeda is added to a suspension of allyllithium in hexane it produces a polymer, which crystallises as complex **1.4** (Scheme 3). Within the structure of **1.4** a lithium-tmeda cation, $[Li(tmeda)]^+$, bridges $[C_3H_5]^-$ in a μ:η^1:η^1 fashion. If the denticity of the co-ligand is increased, i.e. tmeda is replaced with pmdeta, the aggregation state of the resulting complex is lower, and the structure of $[(pmdeta)Li(C_3H_5)]$ (**1.5**) is monomeric.[15]

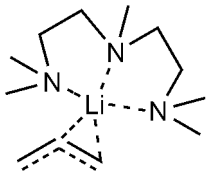

Figure 4: Structure of $[(pmdeta)Li(C_3H_5)]$ (**1.5**)

The allyl C−C bond lengths of complex **1.5** are 1.361(4) Å and 1.379(4) Å are similar enough for the negative charge to be regarded as fully delocalised across the allyl ligand. Despite the similarity in C−C bond lengths, the allyl ligand appears to be coordinated to the lithium in a η^2 fashion, with the Li−C bond lengths being 2.255(5) and 2.362(5) Å, and the third Li−C distance is 2.720(4) Å. Coordination of the allyl ligand in this fashion is unusual, however this is thought to be due to the steric bulk of the pmdeta co-ligand.

The first studies on silyl-substituted allyl complexes, in their own right, were reported by Fraenkel *et al.* in 1990 and were studied in solution *via* NMR spectroscopy. The complexes studied were either silyl-allyllithium complexes,[16] or the solvated silyl-

allyllithium(tmeda) complexes.[17,18] However the first solid-state structure of a silyl-allyllithium complex, [(tmeda)Li{$C_3H_3(SiMe_3)_2$}] (**1.8**) was not reported until 1992.[19] Complex **1.8** was synthesised by deprotonating *E*-1,3-*bis*(trimethylsilyl)propene with *sec*-butyllithium in hexane/tmeda (Scheme 4).

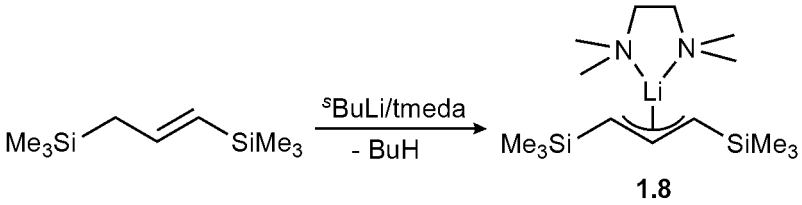

1.8

Scheme 4

The NMR spectroscopic studies of **1.8** showed that the silyl substituents were both in an *exo* conformation over a large temperature range. This is unusual when compared with alkyl- and aryl-substituted allyllithiums, which exist as mixtures of the *exo* and *endo* isomers and have a slight preference for the *endo* position.[14] The ^{13}C NMR spectrum of **1.8** shows slight differences in the terminal allyl carbon shifts, which is due to the asymmetry of the tmeda coordinating to the lithium cation. In agreement with the NMR spectroscopy, X-ray crystallographic studies on **1.8**, showed that the silyl substituents were in the *exo* position. However, in comparison to **1.4**, X-ray crystallography showed that complex **1.8** is a monomer in the solid-state. The difference in the terminal Li−C bond lengths (2.229(9) and 2.269(10) Å) is so small that the allyl can be considered to be coordinated in an η^3 manner to the lithium cation.

Complex [Li{$C_3H_3(SiPhMe_2)_2$}]$_\infty$ (**1.9**) was the first example of a Lewis-base-free silyl-allyllithium.[20] The allyl ligand is coordinated to the lithium in an η^3 fashion, which can be seen from the terminal Li−C bond lengths (2.314(6) Å and 2.318(6) Å) which are essentially the same. Consequently, monomers of **1.9** assemble in a μ:η^3:η^3 coordination polymer, which means that the lithium is formally 4-coordinate. There are two independent Li-allyl-Li chains, parallel to the *c*-axis, in the unit cell; one polymer chain

propagates along a crystallographic 4_1 screw axis and the other along the symmetry related 4_3 screw axis.

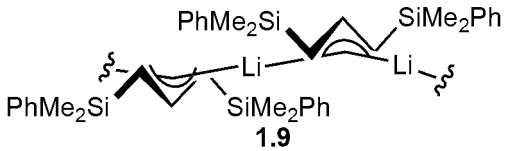

1.9

Figure 5: Lewis base free silyl-allyllithium $[Li\{C_3H_3(SiPhMe_2)_2\}]_\infty$

The structure of **1.9** is reminiscent of those of the heavier alkali metal silyl-allyls; for example $[(thf)_nM\{C_3H_3(SiMe_3)_2\}]_\infty$ where M = K, n = 1.5 (**1.10**) and M = Cs, n = 1 (**1.11**).[21] Potassium and caesium often form coordination polymers with π-bonded organo-ligands, such as allyls and cyclopentadienide (Cp) derivatives.[22]

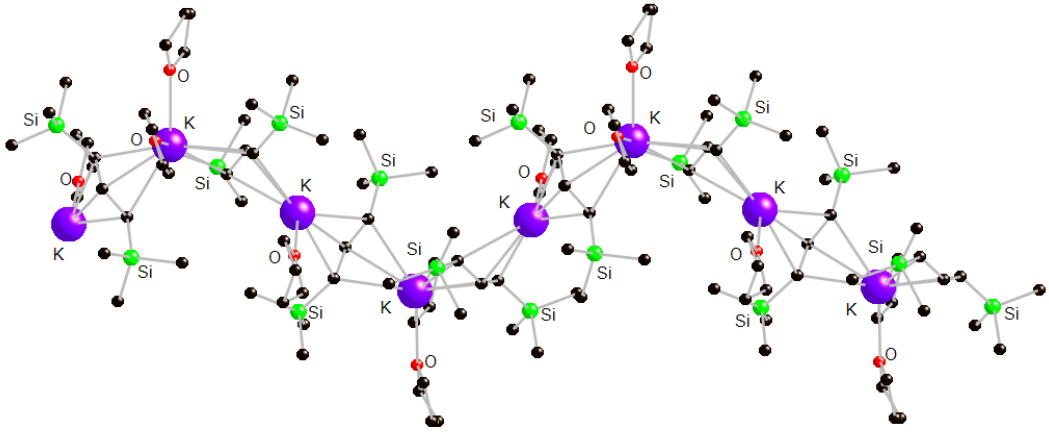

Figure 6: Polymeric zig-zag structure of $[(thf)_3K_2\{C_3H_3(SiMe_3)_2\}_2]_\infty$ (**1.10**). Hydrogen atoms have been omitted for clarity, carbon = black, silicon = green, oxygen = red, potassium = bright purple. Reproduced from ref. 21

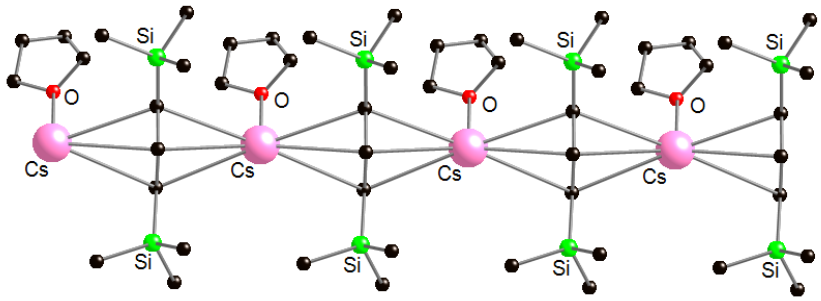

Figure 7: Polymeric linear structure of $[(thf)Cs\{C_3H_3(SiMe_3)_2\}]_\infty$ (**1.11**). Hydrogen atoms have been omitted for clarity, carbon = black, silicon = green, oxygen = red, caesium = light pink. Reproduced from ref. 21

In complexes **1.10** and **1.11** (Figure 6 and Figure 7 above), as with all the previous examples discussed so far, the silyl substituents are in the *exo* positions and in both structures the allyl ligands adopt the $\mu{:}\eta^3$ mode. Complex **1.10** consists of alternating linear and bent potassium coordination environments, with alternate potassium cations coordinated to one or two thf solvent molecules, respectively. The K−C bond lengths within **1.10** range from 2.93 to 3.12 Å (as quoted),[21] confirming η^3 coordinated allyl ligands. Similarly, complex **1.11** has Cs−C bond lengths within the range 3.331(6)-3.509(7) Å, indicating η^3 coordination of the silyl-allyl. However, unlike the potassium example, the caesium complex has a linear polymeric structure and has one thf molecule coordinated to each Cs^+ cation. Complex **1.11** is the only example of a caesium allyl complex, however there are other examples of potassium allyl complexes, such as $[(dme)K\{C_3H_3(SiMe_3)_2\}]_\infty$ (**1.12**).[23]

In recent years, solvent-free and base-free lithium and potassium monosilyl-allyl complexes were synthesised; $[Li\{C_3H_2(SiMe_3)_3\}]_2$ (**1.13**) and $[K\{C_3H_3(SiMe_3)_2\}]_\infty$ (**1.14**).[24] The allyl ligand in complex **1.13** was synthesised by Fraenkel and Winchester, and the solution-state structure of $[(tmeda)Li\{C_3H_2(SiMe_3)_3\}]_2$ (**1.15**) was investigated.[16] Complex **1.13** (Figure 8) is a dimer in the solid-state in which the Li cation is bridging the two allyl ligands. The bonding mode of the allyl ligands coordinated to the lithium cation are $\mu{:}\eta^2{:}\eta^1$; with a Li−C σ-bond distance of 2.232(7) Å and η^2 Li−C interactions at 2.230(7) and 2.241(6) Å and the difference between the allyl C−C bond lengths of 0.085 Å suggest partial delocalisation of the negative charge. DFT studies on $[Li(C_3H_5)]$ (**1.3**) showed that a monomeric structure is favoured, with η^3-symmetical coordination of allyl, rather than a σ-bonded allyl. The substitution of the three H atoms for SiH_3 makes little difference to the structure except a slight asymmetry of the Li cation over the allyl carbons. However, calculations on $[Li(C_3H_5)]_2$ $[\mathbf{1.3}]_2$ showed a head-to-tail dimer to be the lowest energy structure, with two σ-bonded Li−C

bridging units, in which the allyl ligand also interacts with the second Li cation; substitution of the three H atoms for SiH_3, does not change the structure but shifts the structural features to that of $[Li\{C_3H_2(SiMe_3)_3\}]_2$. Addition of solvent was also investigated using H_2O and thf, and in both cases the dimeric structure was not changed.[24]

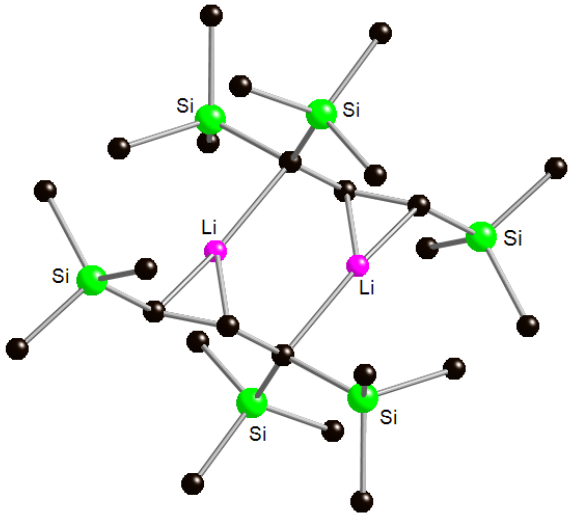

Figure 8: Molecular structure of $[Li\{C_3H_2(SiMe_3)_3\}]_2$ (**1.13**). Hydrogen atoms have been omitted for clarity, carbon = black, silicon = green, lithium = pink. Reproduced from ref. 24

The solid-state structure of $[K\{C_3H_3(SiMe_3)_2\}]_\infty$ (**1.14**) (Figure 9), as with other examples of potassium allyls, is a coordination polymer of potassium cations bridged by allyl ligands. However, **1.14** has helical chains running parallel to the *a*-axis, with three unique potassium ions in each chain. The K−C bond lengths range from 2.87 to 3.15 Å (as stated)[24] and are similar to other K−C bond distances in the solvated analogue $[(thf)_3K_2\{C_3H_3(SiMe_3)_2\}_2]_\infty$ (**1.10**)[21] which have a range of 2.93 to 3.12 Å (as quoted).

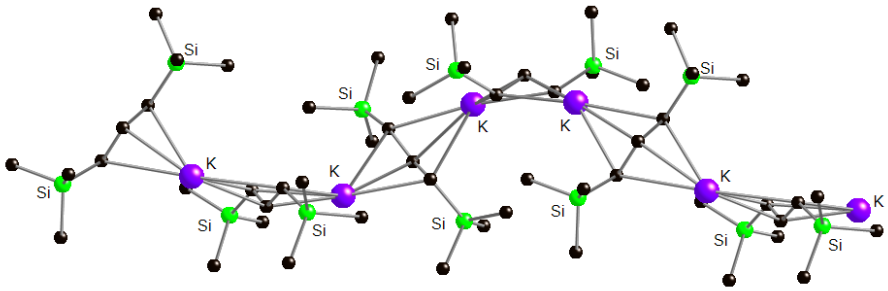

Figure 9: Molecular structure of $[K\{C_3H_3(SiMe_3)_2\}]_\infty$ (**1.14**) Hydrogen atoms have been omitted for clarity, carbon = black, silicon = green, potassium = bright purple. Reproduced from ref. 24

Sodium allyl complexes are uncommon. The first structurally characterised complex was the tetraphenyl(allyl)sodium diethyl ether complex, $[(OEt_2)Na(Ph_4C_3H)]$ (**1.16**), in which the sodium cation is coordinated between two of the phenyl rings, and not involved in bonding with the allyl unit (Figure 10).[25]

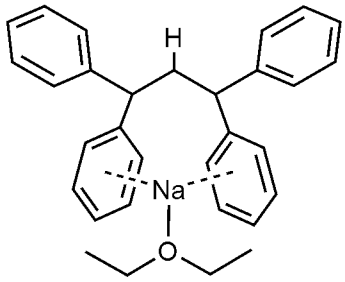

Figure 10: Structure of tetraphenyl(allyl)sodium diethyl ether (**1.16**). Allyl C−C bond distances 1.38 and 1.42 Å, Na−C_{Ph} bond distances range from 2.72-3.10 Å, error on bond distances ± 0.008 Å). Reproduced from ref. 25

The first structurally characterised allyl complex in which there is a sodium-allyl interaction was $[(pmdeta)Na(1\text{-}PhC_3H_4)]$ (**1.17**).[26] Complex **1.17** has a monomeric structure, in which the sodium is coordinated by the allyl ligand and is also coordinated by the three nitrogen atoms of the pmdeta. The Na−C bond distances are 2.791(9), 2.577(7) and 2.676(3) Å suggesting that the sodium cation is η^3-coordinated by the allyl. However, the C−C bond distances are 1.309(14) and 1.469(9) Å, which suggest localised bonds.

Very recently, another structurally characterised sodium allyl was reported, complex $[Na\{1,3\text{-}(SiMe_3)_2C_3H_3\}(thf)]_4$ (**1.18**) (Figure 11).[27] Complex **1.18** lies on a crystallographic two-fold axis, therefore there are only two unique metal sites. The tetramer is formed through $\mu{:}\eta^3{:}\eta^3$ allyl bridging between sodium cations, which are also coordinated by a thf ligand. The Na−C bond distances range from 2.590(3)-2.896(3) Å, and the C−C bond distances range from 1.381(3)-1.415(3), suggesting delocalisation of the negative charge across the allyl ligand.

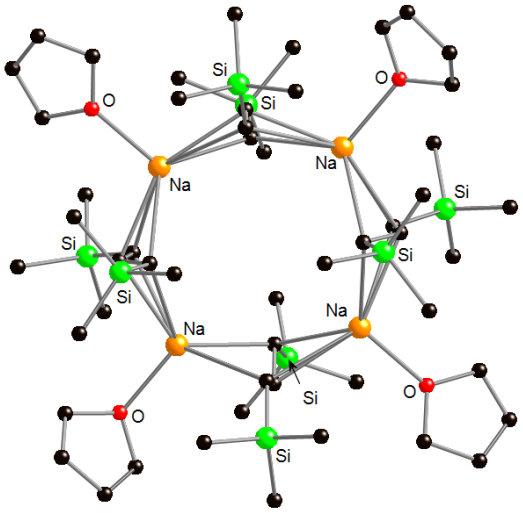

Figure 11: Molecular structure of $[Na\{1,3\text{-}(SiMe_3)_2C_3H_3\}(thf)]_4$ (**1.18**). Hydrogen atoms have been omitted for clarity, carbon = black, silicon = green, sodium = orange, oxygen = red. Reproduced from ref. 27

Ansa-bis(allyl) ligands, ligands of the formula $[R_2Si\{3\text{-}(C_3H_3\text{-}1\text{-}SiR'_3)_2\}_2]$ with R = Me or Ph and R´ = Me, Ph or R´$_3$ = ^{t}BuMe$_2$ are known, and both lithium and potassium complexes of these ligands have been characterised.[28] The complex $[Me_2Si\{Li(tmeda)\}_2\{3\text{-}(C_3H_3\text{-}1\text{-}SiMe_3)\}_2]$ (**1.19**) (Figure 12) has a crystallographically imposed 2-fold rotation axis, with the Li−C distances being 2.202(11) (terminal), 2.131(10) (central) and 2.210(10) Å (inner). This is indicative of the lithium cation being coordinated by the allyl ligand in a η^3 fashion. As well as the allyl ligand, the lithium is coordinated by the two tmeda nitrogen atoms, which gives the lithium an overall pseudo-tetrahedral coordination geometry. The three silyl groups on the allyl are in the *exo* conformation and can be considered as two pairs, with the central $SiMe_2$ group; give a [*exo,exo*]$_2$ overall stereochemistry, which is preserved in the solution-state according to ^{1}H and ^{13}C NMR spectroscopy. Complex **1.19** is essentially isostructural with complex **1.8.**

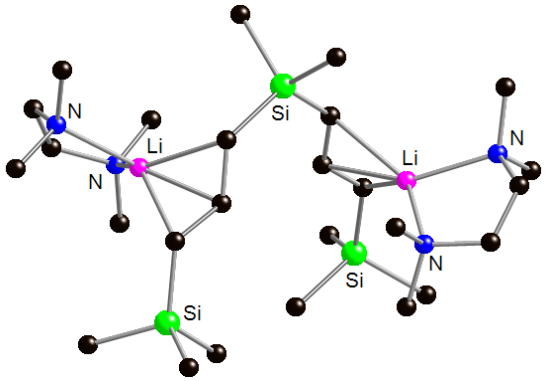

Figure 12: Molecular structure of $[Me_2Si\{Li(tmeda)\}_2\{3\text{-}(C_3H_3\text{-}1\text{-}SiMe_3)_2\}_2]$ (**1.19**) Hydrogen atoms have been omitted for clarity, carbon = black, silicon = green, nitrogen = blue, lithium = pink. Reproduced from ref. 28

The *ansa-bis*(allyl) ligand retained *exo,exo* stereochemistry and coordination for an allyl with a lithium cation; this is also true of the *ansa-bis*(allyl) potassium complex $[K_2\{(\eta^3\text{-}C_6H_4SiMe_3\text{-}6)_2SiMe_2\}(thf)_3]_\infty$ (**1.20**),[29] in which the known $\mu{:}\eta^3$ coordination of the allyl is maintained (Figure 13). As with complex **1.10** the coordination environment around each potassium cation alternates with two coordinated thf molecules and one thf molecule, as well as the η^3 coordinated bridging allyl ligands. The allyl C−C bond lengths range from 1.374(8) to 1.386(9) Å, suggesting full delocalisation of the negative charge across the three allyl carbon atoms.

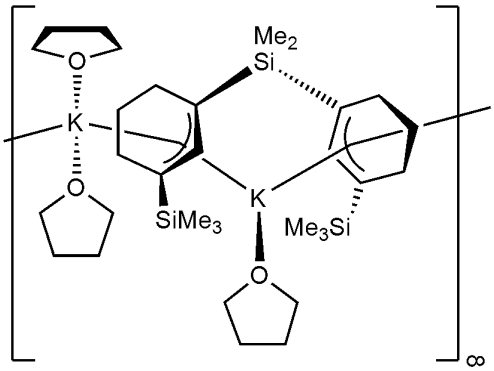

1.20

Figure 13: Structure of $[K_2\{(\eta^3\text{-}C_6H_4SiMe_3\text{-}6)_2SiMe_2\}(thf)_3]_\infty$

A new type of ligand, the *ansa-tris*(allyl) ligand was recently synthesised, and successfully coordinated to lithium. The complex $[MeSi\{(C_3H_3SiMe_3)Li(tmeda)\}_3]$

(**1.21**)[30] is intriguing because unlike previous examples of lithium complexes it has a [*exo*,*exo*]$_2$[*endo*,*exo*] conformation.

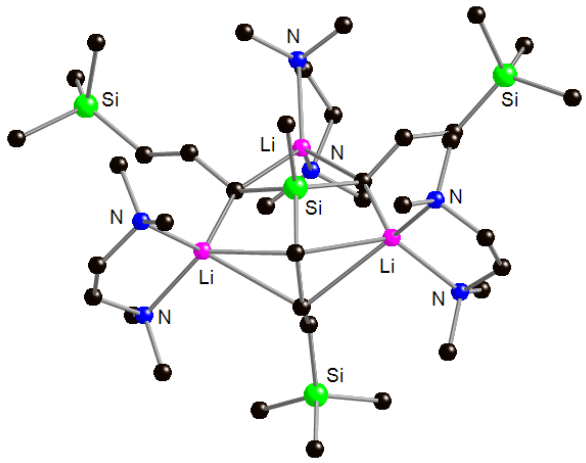

Figure 14: Molecular structure of [MeSi{($C_3H_3SiMe_3$)Li(tmeda)}$_3$] (**1.21**). Hydrogen atoms have been omitted for clarity, carbon = black, silicon = green, nitrogen = blue, lithium = pink. Reproduced from ref. 30

This is the first crystallographically characterised example of such stereochemistry within a s-block silyl-allyl complex, and it is likely that this stereochemistry is favoured to minimise steric clashes between the three trimethylsilyl groups and the tmeda co-ligand. Another contrast to previously reported lithium complexes is the manner in which the allyl ligand coordinates to the lithium cation. Figure 14, above, shows that the ligand is in a mixed coordination mode of (μ:η^1:η^1)$_2$(μ:η^2:η^2) and the Li–C bond distances; 2.258(7), 2.289(6), 2.283(5) and 2.696(6) Å, show that the coordination in the μ:η^2 bridge is highly unsymmetrical. The structure of **1.16** is preserved in a benzene solution; however there is a slight chemical inequivalence of the three [$C_3H_3SiMe_3$] units, which is evident from the presence of nine allyl hydrogen resonances and three resonances for the trimethylsilyl groups.

1.1.2b Alkali Earth Metal Allyl Complexes

There are several examples of magnesium complexes with the [C_3H_5]$^-$ ligand,[31,32] as well as lanthanide/magnesium mixed metal systems,[33,34] that have been

crystallographically characterised. The first crystallographically characterised allylmagnesium complex was $[Mg(\eta^1\text{-}C_3H_5)(tmeda)(\mu\text{-}Cl)_2]_2$ (**1.22**),[31] where addition of one equivalent of tmeda to allylmagnesium chloride allowed **1.22** to crystallise. The Mg−C σ-bond (2.179(3) Å) in **1.22** is typical of that found in allylmagnesium complexes. Until recently, allylmagnesium complexes have been synthesised with harder ligands, such as chloride,[31] β-diketiminates[32,34] or ethers.[34] The parent allyl complex '$[Mg(C_3H_5)_2]$' (**1.23**) is only soluble in polar solvents, and as a result the coordination mode of the allyl ligand is unknown. However, this property infers a polymeric structure.[35] Recent work by Hanusa on the silyl-allyl complex $[Mg\{C_3H_3(SiMe_3)_2\}_2]_2$ (**1.24**) shows that the allyl ligand adopts the unusual μ:η^3:η^1 binding modes (Scheme 5).[36]

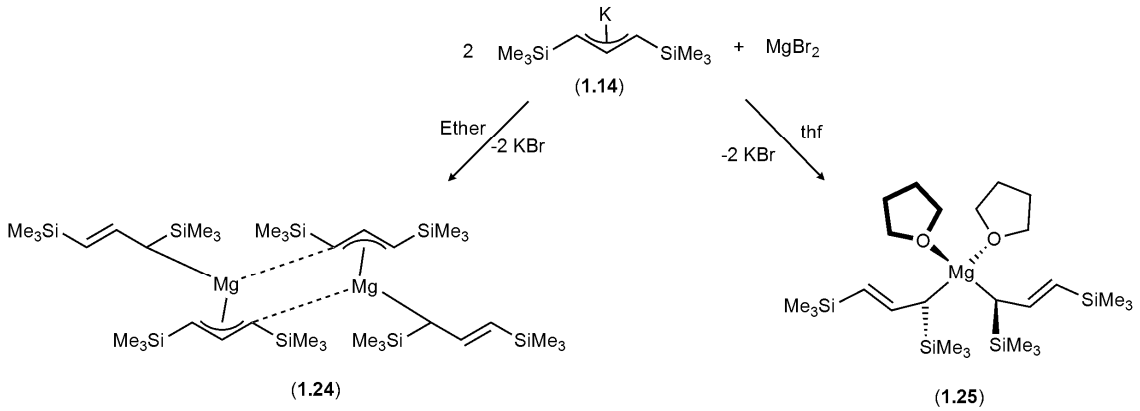

Scheme 5

The dimeric complex **1.24** is a product of the reaction of potassium *bis*-silyl(allyl) with magnesium bromide in diethyl ether. If the same reagents are combined in thf, the product is then the σ-bound complex **1.25**, because, unlike the diethyl ether, the thf cannot be removed from the magnesium coordination environment under vacuum (Scheme 5). However, the difference in allyl C−C bond lengths of 0.12 Å is significant, and implies localised single and double bonds. Therefore the coordination of the bridging allyl is described as a cation-π interaction, which is thought to be the first of its type with magnesium. A DFT study on **1.24** showed that there was an energy minimum

for the symmetric structure with η^3-coordination of the allyl ligands, with allyl C−C bond lengths of 1.389 and 1.412 Å (as quoted). The study also showed that the mono- and *bis*-thf adducts of **1.24** resulted in slippage of one, then both, allyl ligands from η^3 to η^1 coordination to give $[Mg(\eta^3\text{-}C_3H_5)(\eta^1\text{-}C_3H_5)(thf)]$ and $[Mg(\eta^1\text{-}C_3H_5)_2(thf)]$ respectively, which corresponds to the silyl-analogue **1.25**.

Until recently there was only one structurally characterised allylcalcium complex, which was the silyl-allyl calcium complex $[Ca\{\eta^3\text{-}C_3H_3(SiMe_3)_2\}_2(thf)_2]$ (**1.26**) (Figure 15).[37] The silyl-allyl ligands are coordinated in an η^3 manner to the calcium cation, and are in a eclipsed arrangement, with the two thf molecules also coordinated to the Ca^+ cation. The allyl C−C bond lengths, 1.387(4) and 1.402(4) Å, suggest nearly complete delocalisation of the negative charge. The $Ca-C_{allyl}$ bond distances range between 2.648(3)-2.662(3) Å and are similar to the average of Ca−C distance of 2.691 Å found in calcium cyclopentadienyl complexes.[38]

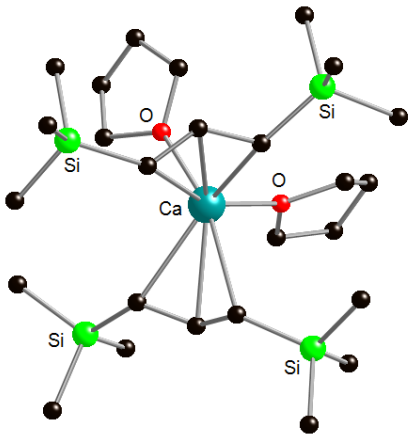

Figure 15: Molecular structure of $[Ca\{\eta^3\text{-}C_3H_3(SiMe_3)_2\}_2(thf)_2]$ (**1.26**). Hydrogen atoms have been omitted for clarity, carbon = black, silicon = green, oxygen = red, calcium = sea blue. Reproduced from ref. 37

Since complex **1.26** was reported, an un-substituted allylcalcium complex has been structurally characterised; $[Ca(\eta^3\text{-}C_3H_5)_2(triglyme\text{-}\kappa^4)]$ (**1.27**).[39] Complex **1.27** was synthesised *via* the reaction of CaI_2 and two equivalents of $K(C_3H_5)$ (**1.7**) in thf, the addition of one equivalent of triglyme produced block-like crystals suitable for X-ray crystallography.

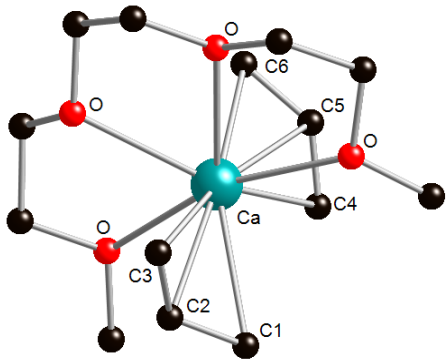

Figure 16 Molecular structure of [Ca(η^3-C_3H_5)$_2$(triglyme-κ^4)] (**1.27**). Hydrogen atoms have been omitted for clarity, carbon = black, oxygen = red, calcium = sea blue. Reproduced from ref. 39

The coordination geometry of the calcium cation is pentagonal bipyramidal; the oxygen atoms of the triglyme occupy four of the equatorial sites, with one remaining vacant, and the allyl ligands are in the apical positions, in a *trans* arrangement. The allyl bond lengths of C(1)−C(2), C(2)−C(3), C(4)−C(5), and C(5)−C(6) are 1.3886(18), 1.369(2), 1.314(3) and 1.373(3) Å respectively. These bond lengths show that the allyl ligands are coordinated in a η^3 fashion with the Ca−C bond lengths ranging from 2.6385(14) to 2.8459(14) Å. DFT studies show that there is good agreement between the experimental and the computed structure and bond lengths. NMR spectroscopy shows that, in thf-d_8, the solution-state structure is that of free triglyme and Ca(C_3H_5), however in pyridine-d_5 an η^1 bonding mode of the allyl is observed.[39]

In the 1970's *bis*(allyl)beryllium and several of its adducts were reported; di(allyl)beryllium, prepared from diethylberyllium and tri(allyl)boron, is insoluble in hydrocarbons and melts at temperatures above 200 °C, indicating a polymeric structure, however it is soluble in thf and is thought to form [Be(C_3H_5)$_2$(thf)$_2$] (**1.28**).[40] Hanusa reported the first structurally characterised beryllium,[41] then strontium and barium,[42] silyl-allyl complexes; [Be{C_3H_3(SiMe$_3$)$_2$}$_2$(Et_2O)] (**1.29**), [Sr{C_3H_3(SiMe$_3$)$_2$}$_2$(thf)$_2$] (**1.30**) and [K(thf)Ba$_2$\{C_3H_3(SiMe$_3$)$_2$\}$_5$] (**1.31**). The silyl-allyl analogue of the parent complex was synthesised from two equivalents of [K{C_3H_3(SiMe$_3$)$_2$}] and $BeCl_2$ in diethyl ether. The product, unlike the parent complex, was soluble in a range of

solvents, both hydrocarbons and ethers. Complex **1.29** is highly air- and moisture-sensitive, and single crystals were grown from hexane, to give the structure shown in Figure 17.

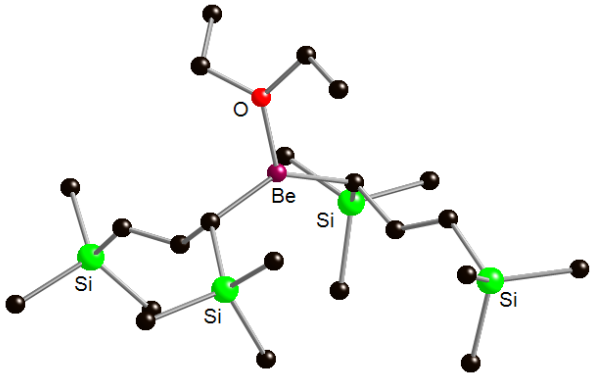

Figure 17: Molecular structure of [Be{$C_3H_3(SiMe_3)_2$}$_2$(Et_2O)] (**1.29**). Hydrogen atoms have been omitted for clarity, carbon = black, silicon = green, oxygen = red, beryllium = deep purple. Reproduced from ref. 41

The beryllium cation is coordinated by two η^1 silyl-allyl ligands and the oxygen from the diethyl ether solvent, in a trigonal planar environment, with the sum of the angles around the metal centre being 360°. The C−C bond lengths of the two allyl moieties are 1.479(4) and 1.343(4), and 1.484(3) and 1.336(4) which is representative of distinct single and double bonds in the allyl ligands, confirming the η^1 coordination mode. DFT studies on beryllium allyl complexes showed that [Be(C_3H_5)H] with the allyl η^3- and η^1-bound represent minima on the potential energy surface, however the π-bonded structure is 3.3 kcal mol^{-1} more stable than the σ-bonded structure. The same pattern was seen with [Be(C_3H_5)Br], however in this case the difference in energy is only 1.2 kcal mol^{-1}. Similarly, with [Be{$C_3H_2(SiH_3)$}$_2$] the π-bonded allyl is 4.0 kcal mol^{-1} more stable, nevertheless addition of a diethyl ether solvent molecule, [Be{$C_3H_2(SiH_3)$}$_2$(Et_2O)], resulted in slippage of both allyl ligands to σ-bonding modes, unlike the computational study on '[Mg(C_3H_5)$_2$]' which showed that addition of two thf molecules was required to push both allyl ligands to η^1 coordination.

The strontium silyl-allyl complex $[Sr\{C_3H_3(SiMe_3)_2\}_2(thf)_2]$ (**1.30**) was synthesised by reacting two equivalents of $[K\{C_3H_3(SiMe_3)_2\}_2]$ with SrI_2 in thf, to give the molecular structure shown in Figure 18.

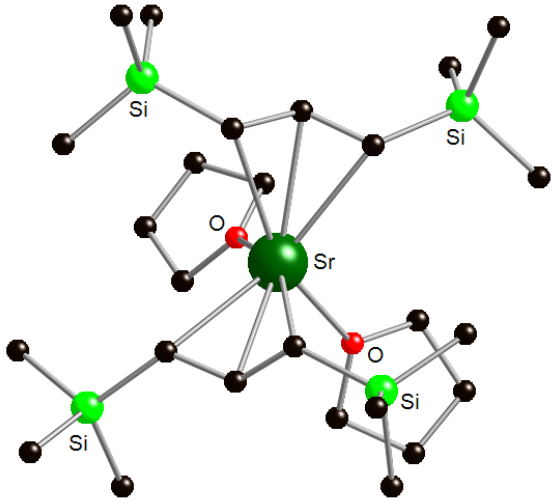

Figure 18: The molecular structure of $[Sr\{C_3H_3(SiMe_3)_2\}_2(thf)_2]$ (**1.30**). Hydrogen atoms have been omitted for clarity, carbon = black, silicon = green, oxygen = red, strontium = dark green. Reproduced from ref. 42

The Sr^{2+} cation lies on a crystallographic two-fold axis, therefore only half of the molecule is unique. The coordination environment of the strontium includes two allyl ligands bound in a η^3 manner, as well as two oxygen atoms from the thf solvent molecules, in a pseudo-tetrahedral arrangement, similar to that of the calcium silyl-allyl complex **1.26**. The Sr−C bond distances in **1.30** range from 2.797(3) to 2.805(3) Å, which are similar to Sr−C distances in strontium cyclopentadienyl complexes such as $[Sr\{1,2,4\text{-}(SiMe_3)_3C_5H_2\}_2]$ (**1.32**) and $[Sr\{1,2,4\text{-}(^tBu)_3C_5H_2\}_2]$ (**1.33**), both of which have bond distances in the range between 2.77-2.85 Å.[43] The C−C bond lengths in **1.30** reflect the η^3 nature of the coordination, ranging from 1.398(5) to 1.406(5) Å.

To synthesise a barium allyl complex, the same procedure that was used for complexes **1.29** and **1.30** was employed; reacting two equivalents of $[K\{C_3H_3(SiMe_3)_2\}_2]$ with BaI_2 in thf. However, this produced the mixed metal species $[K(thf)Ba_2\{C_3H_3(SiMe_3)_2\}_5]$ (**1.31**).

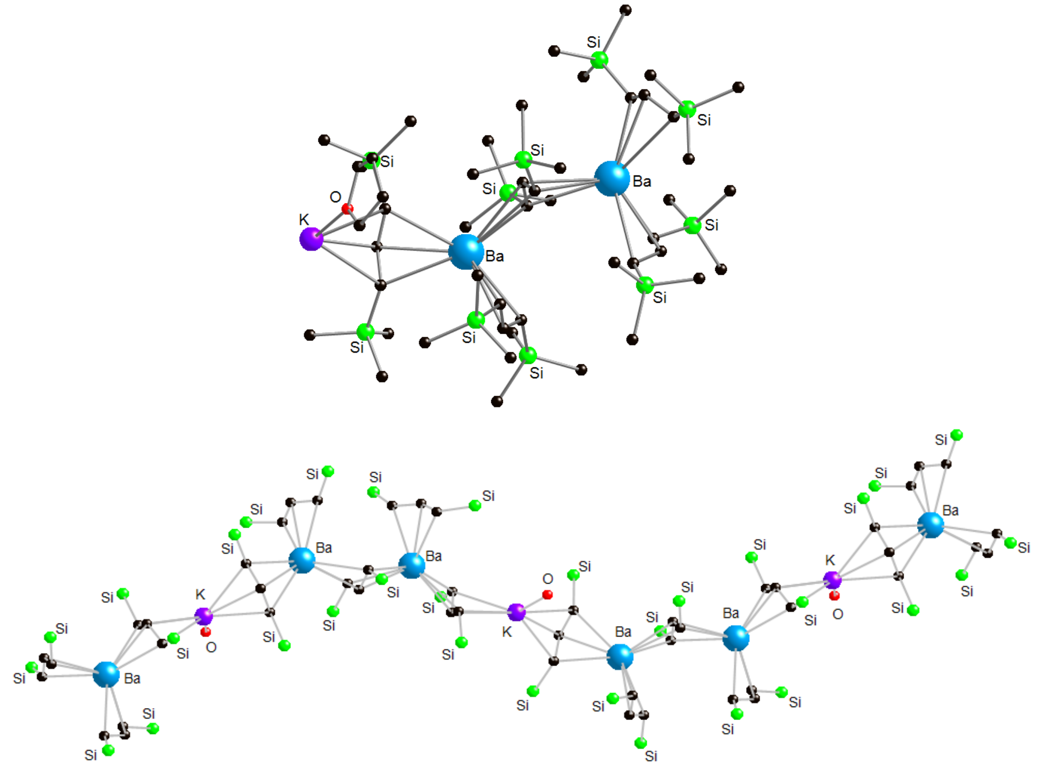

Figure 19: Molecular structure of $[K(thf)Ba_2\{C_3H_3(SiMe_3)_2\}_5]$ (**1.31**). The repeating unit of the polymeric structure (above) and an extended section of the polymeric structure (below). Hydrogen atoms have been omitted for clarity, carbon = black, silicon = green, oxygen = red, potassium = bright purple, barium = bright blue. Reproduced from ref. 42

The complex **1.31** forms polymers parallel to the *c*-axis and the repeat unit includes two Ba^{2+} cations and a K^{+} cation. Each barium is coordinated by one η^3-allyl ligand and two μ:η^3 allyl ligands, and the potassium is coordinated by two bridging allyl ligands and the oxygen from the thf solvent molecule. The Ba−C bonds of the bridging allyl ligands are longer than those of the terminal allyl ligand; $Ba{-}C_{terminal}$ bond distances range from 2.876(4) to 2.969(4) Å, whereas $Ba{-}C_{bridging}$ range from 2.998(3) to 3.141(4) Å, which are similar to the $K{-}C_{bridging}$ bond distances (2.980(4) to 3.157(4) Å). The Ba−C in **1.31** bond distances are similar to the average Ba−C distances reported for $[Ba(C_5Me_5)_2]$ (**1.34**)[44] and $[Ba\{C_5(C_6H_5)_2\}_2]$ (**1.35**)[45] of 2.99(2) and 2.928(6) Å respectively. The K−C bond distances in **1.31** are similar to those seen in $[(thf)_3K_2\{C_3H_3(SiMe_3)_2\}_2]_\infty$ (**1.10**)[21] and $[K_2\{(\eta^3\text{-}C_6H_4SiMe_3\text{-}6)_2SiMe_2\}(thf)_3]_\infty$ (**1.20**),[29] ranging from 2.930(3)-3.116(3) Å and 2.93-3.12 Å (as stated), respectively. ^1H NMR spectroscopy on $[K(thf)Ba_2\{1,3\text{-}C_3H_3(SiMe_3)_2\}_5]$ (**1.31**) shows that the allyl signals were slightly upfield to those of

$[(K\{C_3H_3(SiMe_3)_2\}]_\infty$ (**1.14**), indicating that there is some extent of interaction with the barium cation.

1.1.3 Group 3 and f-Block Metal Allyl Complexes

Unlike transition metal allyl complexes (see Section 1.1.4), lanthanide complexes of the parent allyl $[C_3H_5]^-$ ligand are stable, and several examples have been structurally characterised. Some examples are mixed metal structures with magnesium,[33,34] others are alkali metal/lanthanide systems.[46,47] Lanthanide allyl complexes are important, in part, due to their role as pre-catalysts in the polymerisation of 1,3-butadiene.[48] Another driving force behind lanthanide allyl complex development is the need to develop new/improved catalysts for other polymerisations and to investigate the nature of the active species.

Initial attempts to synthesise homoleptic complexes of general formula $[Ln\{C_3H_3(SiMe_3)_2\}_3]$ *via* salt metathesis reactions of lanthanide (III) halides and pseudo-halides with alkali metal silyl-allyl complexes were not successful. Reactions of LnI_3 with three equivalents of lithium allyls yielded the formation of 'ate complexes $[LnI\{C_3H_3(SiMe_3)_2\}_3][Li(thf)_4]$, and inital reaction of LnI_3 (Ln = Ce, Pr, Nd, Gd, Tb, Dy and Er) with three equivalents of $[K\{C_3H_3(SiMe_3)_2\}]$ gave incompletely substituted 'ate complexes of the type $[K(thf)_4][LnI\{C_3H_3(SiMe_3)_2\}_3]$ for Ln = Ce (**1.36**), Er (**1.37**) and Tb (**1.38**) (Scheme 6).[49]

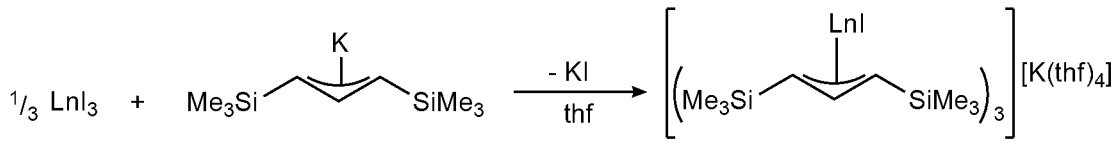

Scheme 6

Each of the crystallographically determined structures of **1.36-1.38** has three η^3 coordinated silyl-allyl ligands, as well as an iodo ligand. The Ln−C bond lengths range

from 2.749(9)-2.810(9) Å (Ce, **1.36**), 2.66(2)-2.71(2) Å (Er, **1.37**) and 2.61(2)-2.64(2) Å (Tb, **1.38**), and the silyl substituents are in the *exo,exo* conformation. The reaction of $[K\{C_3H_3(SiMe_3)_2\}]$ with $[NdI_3(thf)_{3.5}]$ in a 2:1 stoichiometry gave $[NdI_2\{C_3H_3(SiMe_3)_2\}(thf)_{1.25}]$ (**1.39**), however from a concentrated solution, at lower temperatures, the expected product $[NdI\{C_3H_3(SiMe_3)_2\}_2(thf)_2]$ (**1.370**) was formed.[50] The Nd−C bond distances range from 2.672(6) to 2.781(6) Å, as with complexes **1.36**-**1.38** the silyl substituents are in the *exo,exo* conformation. These Nd−C bond distances are similar to those seen in $[\{\eta^3\text{-}C_3H_5\}_2Nd(\mu\text{-}Cl)(thf)_2]_2$ (**1.41**), ranging from 2.674(5) to 2.718(5) Å, showing that the trimethylsilyl groups do not affect the coordination of the allyl.[51] However, the reaction of $[K\{C_3H_3(SiMe_3)_2\}]$ with $[SmI_2(thf)_2]$ in a ratio of 3:1 gave the cyclic complex $[Sm\{\mu\text{-}C_3H_3(SiMe_3)_2\}_2\{C_3H_3SiMe_3\}_2K(thf)_2]_2$ (**1.42**), in which four η^3-silyl-allyl ligands μ-bridge between alternating potassium and samarium cations. Each potassium in **1.42** is also coordinated by two thf molecules, and the samarium cations are also coordinated by a third terminal η^3 allyl ligand.[52] The Sm−C bond distances are longer than those seen in the previously mentioned Ln(allyl) complexes, ranging from 2.743(5) to 2.915(4) Å.

The most reliable route to lanthanide(III) *tris*-(silyl-allyl) complexes is the metathesis of lanthanide(III) triflates with three equivalents of a potassium silyl-allyl complex (Scheme 7).[53,54]

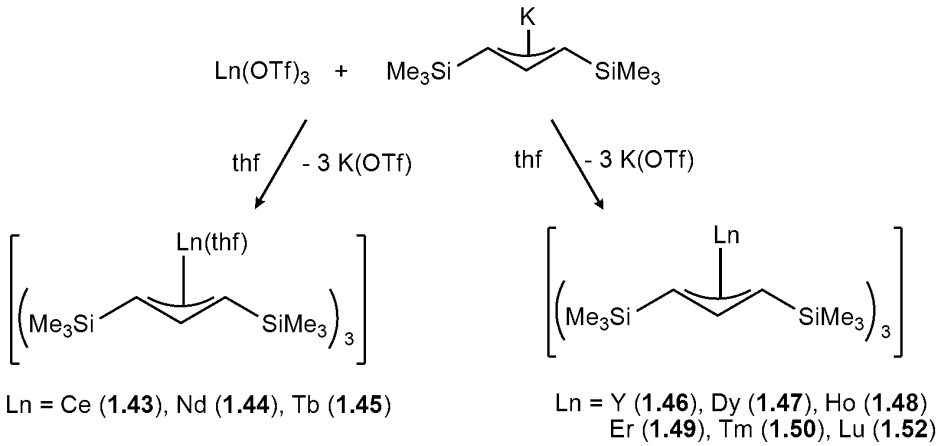

Scheme 7

The structure of the neodymium complex **1.44** is shown in Figure 20; the silyl-allyl ligands are coordinated in an η^3-fashion. The molecular structures of complexes **1.43** and **1.45** are similar to that of complex **1.44**, with the Ln–C bond distances ranging from 2.64 to 2.80 Å (as quoted). Complexes **1.46** to **1.51** do not contain thf solvent molecules as ligands $[Ln\{C_3H_3(SiMe_3)_2\}_3]$; however only the structure of the thulium complex (**1.50**) was crystallographically determined, with data for the other complexes showing that the structures were analogous to that of the Tm complex. As with the complexes **1.43-1.45**, the silyl-allyl ligands in **1.50** are coordinated in an η^3 manner, with the silyl substituents in the *exo,exo* conformation and the Tm–C bond distances ranging from 2.326(2) to 2.606(2) Å.

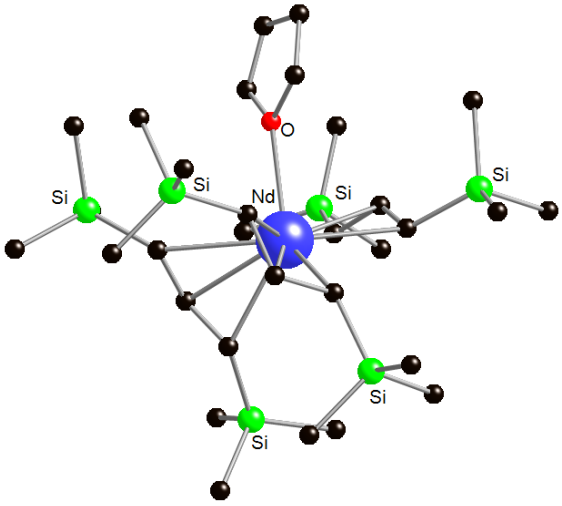

Figure 20: Molecular structure of $[Nd\{C_3H_3(SiMe_3)_2\}_3(thf)]$ (**1.44**). Hydrogen atoms have been omitted for clarity, carbon = black, silicon = green, oxygen = red, neodymium = blue. Reproduced from ref. 42

Such large differences in M–C bond lengths are not uncommon for metal allyl complexes, as seen in complex **1.42**. The structural difference between complexes **1.43-1.45** and **1.46-1.51**, and whether thf coordinates to the metal is apparently a case of the size of the ion, with the cut-off point being between terbium and dysprosium. However, even the smaller lanthanides such as holmium and erbium can accommodate an iodide ligand.[54]

Lanthanide(II) *bis*-(silyl-allyl) complexes of general formula [Ln{C_3H_3-$(SiMe_3)_2$}$_2$$(thf)_2$] with Ln = Sm (**1.53**), Eu (**1.54**) and Yb (**1.55**) are also known, and have been synthesised *via* a simple salt metathesis reactions, according to Scheme 8.[53] Complexes **1.53-1.55** are essentially *iso*-structural monomers with two thf ligands and two η^3-coordinated silyl-allyl ligands. All the trimethylsilyl groups in **1.53-1.55** are in the *exo* position and the Ln–C bond lengths range from 2.741(9)-2.796(6) Å.

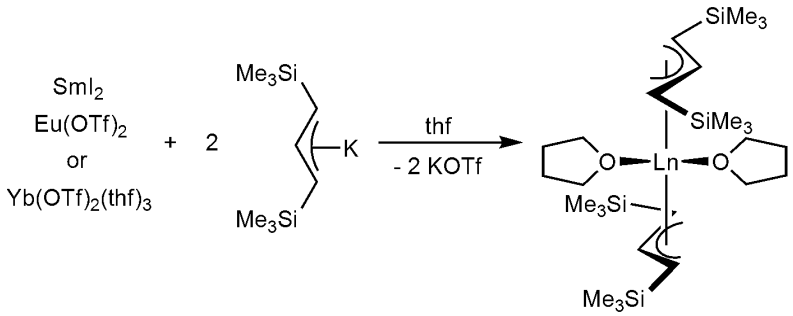

Scheme 8

The reaction of *ansa-bis*(allyl) potassium [K_2{3-(C_3H_3-$SiMe_3)_2$}$_2$$Ph_2Si$] with [{$\eta^5$-$C_5H_3(SiMe_3)_2$}$_2$$Sm(\mu$-$Cl)_2Li(thf)_2$] gives an unusual structure in which the *ansa-bis*(allyl) ligand has substituted a chlorine and a Cp ligand [$SmPh_2Si${3-(C_3H_3-$SiMe_3)_2$}{η^5-$C_5H_3(SiMe_3)_2$}{μ-Cl}$Li(thf)_3$] (**1.56**), see Figure 21 below.[55]

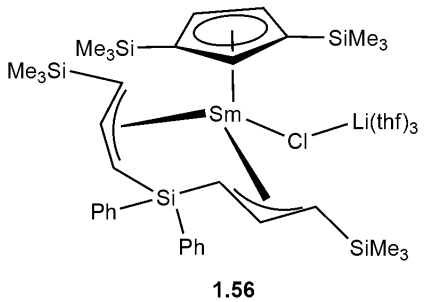

1.56

Figure 21: Structure of [$SmPh_2Si${3-(C_3H_3-$SiMe_3)_2$}{η^5-$C_5H_3(SiMe_3)_2$}{μ-Cl}$Li(thf)_3$]

The silyl substituents of the *ansa-bis*(silyl-allyl) ligand are in an [*endo,exo*][*exo,exo*] arrangement, and coordinated to the samarium in an η^3 manner. The Sm–C bond distances range from 2.681(4)-2.759(4) Å, which is similar to that of the unsubstituted

[{Sm(C_3H_5)$_3$}$_2${μ-C_3H_5}][Mg(thf)$_6$] (**1.57**) and [Sm(C_3H_5)$_4$][Mg(thf)$_6$] (**1.58**) (Scheme 9).[33] Complexes **1.58** and **1.59** have Sm−C bond distances of 2.623(5) to 2.725(5) Å, however the bridging allyl in **1.57** has longer Sm−C bond lengths of 2.762(6) to 2.977(6) Å.

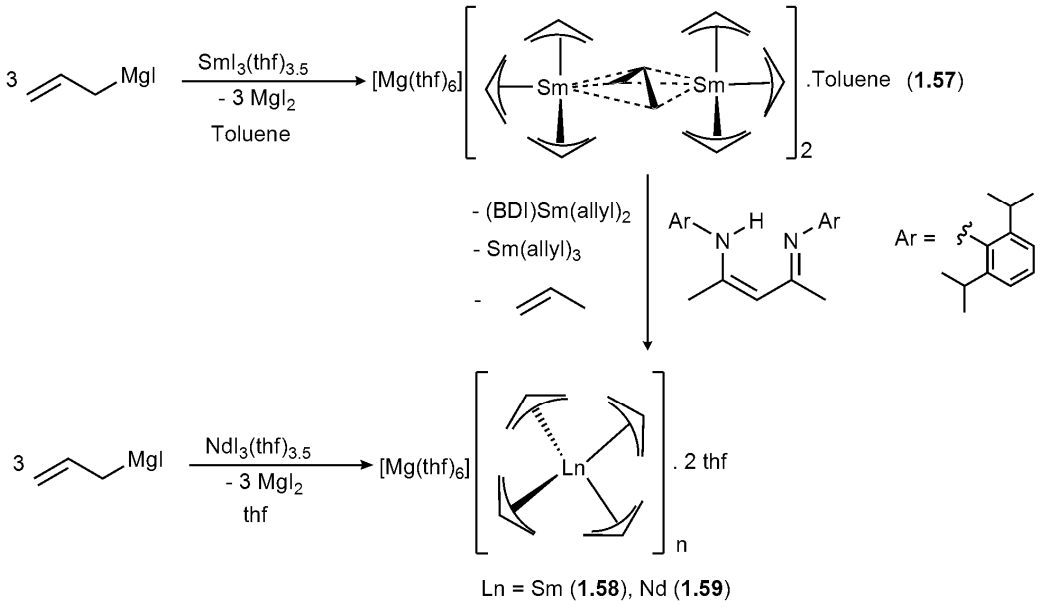

Scheme 9

Bochmann *et al.* have synthesised lanthanide complexes of the *ansa-bis*(silyl-allyl) ligand shown in Scheme 10.[46,56] The structures of **1.60**, and **1.62-1.64** were not confirmed crystallographically, but the structure of **1.61** was solved. The La−C bond lengths in **1.59** ranged from 2.769(3)-2.902(5) Å. However, as with complex **1.56**, the trimethylsilyl substituents on the *ansa-bis*(allyl) ligand in **1.61** are in an *endo,exo* arrangement, with the terminal silyl group *exo*. The bite angles of the C−($SiMe_2$)−C bridge are 112.86° and 113.12°, and hence are much greater than that of the related Zr complex, [Zr{$Me_2Si(C_3H_3SiMe_3)_2$}$_2$], 104.2° (See Section 1.1.4),[28] which can be attributed to the large radius of the lanthanide(III) ion. The structures of complex **1.62-1.64** were shown by NMR spectroscopy to be similar to that of **1.61**.

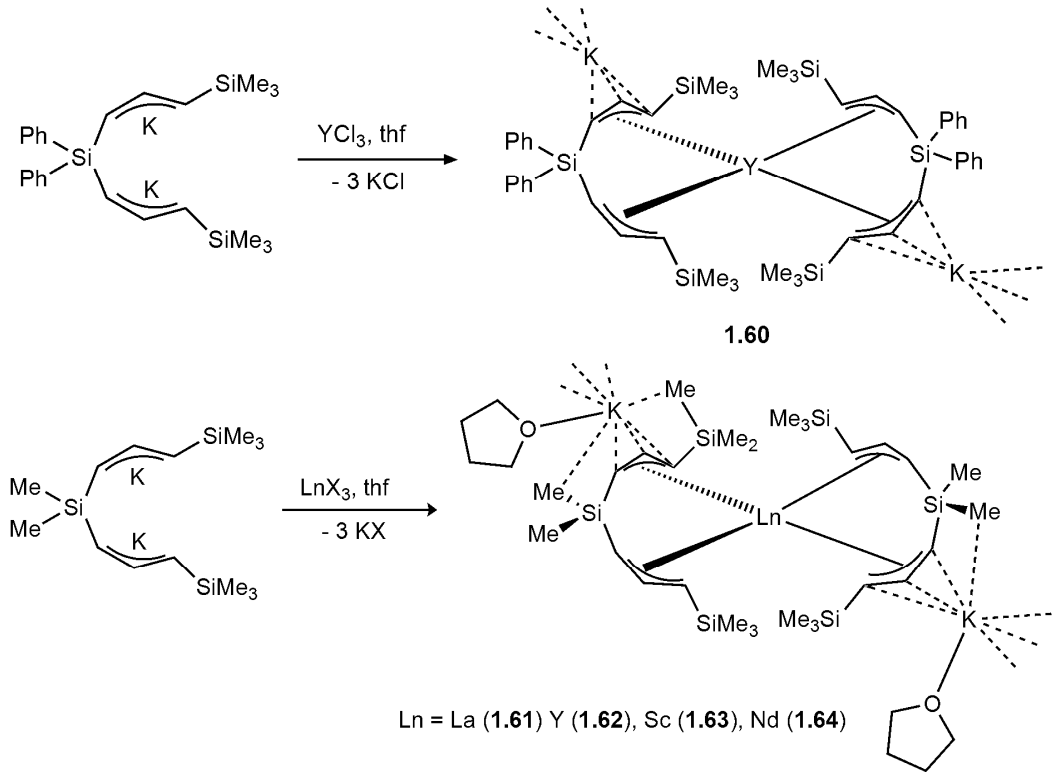

Scheme 10

From Scheme 10, it can be seen that if the alkali metal is potassium the 'ate complexes formed are ion-contact coordination polymers, where the K^+ cation bridges between the lanthanide moieties of the polymer. However, 'ate complexes formed *via* a metathesis reaction of $LnCl_3$ with lithium *ansa-bis*(silyl-allyl), are of the type [Ln{*ansa-bis*(silyl-allyl)}$_2$][Li(ether)$_4$], *i.e.* they are separated ion-pairs; where Ln = Sc (**1.65**), Y (**1.66**), La (**1.67**) and Nd (**1.68**).[52,55]

Another example of the stabilising effects of substituted allyl ligands is seen in the stable thorium allyl complexes [Th{1,3-(SiMe$_3$)$_2$C$_3$H$_3$}]$_4$ (**1.69**) and [Th{3-(SiMe$_3$) C$_3$H$_4$}]$_4$ (**1.70**).[57] Whereas tetra(allyl)thorium, [Th(C$_3$H$_5$)$_4$] (**1.71**), decomposes above 0°C under an N_2 atmosphere, the extra steric bulk of trimethylsilyl(allyl) ligands means that **1.69** is stable at higher temperature (melting point being 122-124°C), indefinitely stable under nitrogen, and only shows signs of decomposition in air after five minutes. In contrast, **1.70** melts with decomposition between 88-90°C, and shows signs of decomposition in air after one minute. Both complexes show a distorted pseudo-

tetrahedral geometry at thorium. The allyl ligands in **1.69** and **1.70** are coordinated η^3 to thorium, with the trimethylsilyl groups in the *exo* configuration, and the Th–C bond distances for complexes **1.69** and **1.70** are 2.679(3)-2.806(3) and 2.617(5)-2.892(5) Å, respectively.

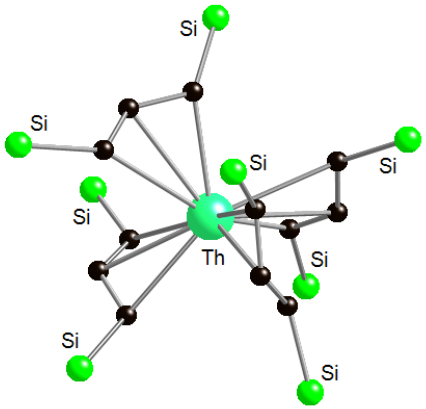

Figure 22: Molecular structure of [Th{1,3-$(SiMe_3)_2C_3H_3$}]$_4$ (**1.69**). Hydrogen atoms and carbon atom on the $SiMe_3$ groups have been omitted for clarity, carbon = black, silicon = green, thorium = pale green. Reproduced from ref. 57

In toluene solution, both **1.69** and **1.70** show fluxional behaviour, consistent with π-σ-π rearrangements of the silyl-allyl ligands. This is similar to the behaviour of the parent complex **1.71**, which suggests that the silyl substituted analogues may be useful models for the unsubstituted allyl complex **1.71**. Complexes **1.69** and **1.70** remain the only known examples of actinide silyl-allyl complexes.

1.1.4 Transition Metal Allyl Complexes

As briefly mentioned in the introduction, homoleptic transition metal allyl ligands are highly unstable and reactive species.[1,2] Pannell and Lappert, in 1976, first recognised the potential ability of trialkyl-silyl and triaryl-silyl substituents to stabilise transition metal allyl complexes. They reported a series of σ- and π-silyl-allyl transition metal complexes of general formula [(silyl-allyl)M$(CO)_xCp_y$], where M = Mn, Fe, Co, Mo and W, or [(silyl-allyl)$MCl]_2$, where silyl-allyl = $C_3H_4(SiMe_3)$ M = Ni and Pd.[58] No

crystallography was carried out on any of the complexes, however using a combination of IR spectroscopy, elemental analysis and mass spectroscopy the bonding modes of the ligands were determined. The most outstanding result was the formation of [Ni{2-($SiMe_3$)C_3H_4}$_2$] (**1.72**) (Scheme 11) which was isolated and characterised by NMR spectroscopy and mass spectrometry. In contrast to the parent allyl complex [Ni(C_3H_5)$_2$] (**1.1**), which is thermally unstable, [Ni{2-($SiMe_3$)C_3H_4}$_2$] (**1.72**), is stable at room temperature in air for prolonged periods.

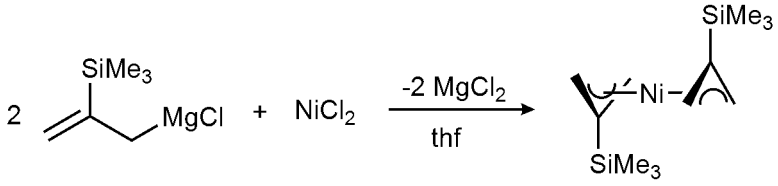

Scheme 11

The synthesis and crystallographic characterisation of complexes of the general formula [M{C_3H_3($SiMe_3$)$_2$}$_2$], M = Cr (**1.73**), Fe (**1.74**), Co (**1.75**) and Ni (**1.76**) were reported by Bochmann[59,60] and by Hanusa[61,62,63,64] between 2001 and 2005. Complexes **1.73-1.76** are all formed *via* metathesis reactions between the metal halide and two equivalents of [K{C_3H_3($SiMe_3$)$_2$}] (Scheme 12).

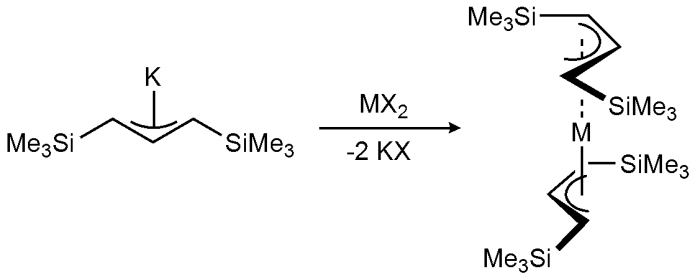

Scheme 12

Complexes **1.73-1.76** are all stable at room temperature despite being electron deficient and having formal electron counts of 12, 14, 15 and 16-electon, respectively. Complex [Ni{C_3H_3($SiMe_3$)$_2$}$_2$] (**1.76**) is sufficiently stable to be isolated and characterised crystallographically, and it is also stable in air for a few days. The parent allyl

complexes $[Cr(C_3H_5)_2]$ and $[Fe(C_3H_5)_2]$ are unknown, and even the base-stabilised analogues such as $[M(C_3H_5)_2(L)]$ (L = tertiary phosphine) still decompose below room-temperature.[65] The silyl-substituted allyl complex $[Cr\{C_3H_3(SiMe_3)_2\}_2]$ (**1.73**) can be heated to reflux in toluene, and melts at 54°C without decomposing, with similar properties seen in $[Fe\{C_3H_3(SiMe_3)_2\}_2]$ (**1.74**).

Complexes **1.73-1.76** are structurally very similar (Figure 23); in all structures the silyl-allyl ligand is coordinated in a η^3 manner, however there is a slight asymmetry of the M−C distances (Table 1).[61-64] Complex **1.73** has M−C distances ranging from 2.193(2)-2.257(2) Å; which is a much wider range than is found in complexes **1.74-1.76**, which range from 1.944(3)-2.096(3) Å.

Table 1: M−C(allyl) bond distances in complexes **1.73-1.76**

Complex	**M−$C_{terminal}$ /Å**	**M−$C_{central}$ /Å**
$[Cr\{C_3H_3(SiMe_3)_2\}_2]$	2.257(2), 2.212(2); 2.255(2), 2.206(2)	2.195(2); 2.193(2)
$[Fe\{C_3H_3(SiMe_3)_2\}_2]$	2.079(2), 2.084(2)	1.998(2)
$[Co\{C_3H_3(SiMe_3)_2\}_2]$	2.091(3), 2.046(3); 2.050(3), 2.096(3)	1.996(3); 2.006(3)
$[Ni\{C_3H_3(SiMe_3)_2\}_2]_{staggered}$	2.070(2), 2.016(2)	1.972(2)
$[Ni\{C_3H_3(SiMe_3)_2\}_2]_{eclipsed}$	2.037(3), 2.029(3)	1.944(3)

In most examples of *mono* silyl-allyl ligands, when coordinated to the metal the ligand is in the *exo,exo* arrangement, however in complexes **1.73-1.76** all the silyl substituents are found in the *exo,endo* formation, most probably due to steric factors. The allyl carbons can be either mutually staggered or eclipsed. In complex **1.73** and **1.75** it is favoured for the allyl ligands to be staggered, however in complex **1.74** it is thermodynamically favoured to be in an eclipsed arrangement. The structure of complex **1.76** was crystallographically determined, showing that both the staggered and eclipsed forms exist at room-temperature, but on heating above 85°C the eclipsed form undergoes an irreversible rearrangement to the staggered form. The chromium (**1.73**)

and iron (**1.74**) compounds did not exhibit any agostic C–H···M interactions, whereas the cobalt (**1.75**) and nickel (**1.76**) compounds did, with terminal *endo* H atoms bent out of the allyl plane by 30° and 27°, respectively.

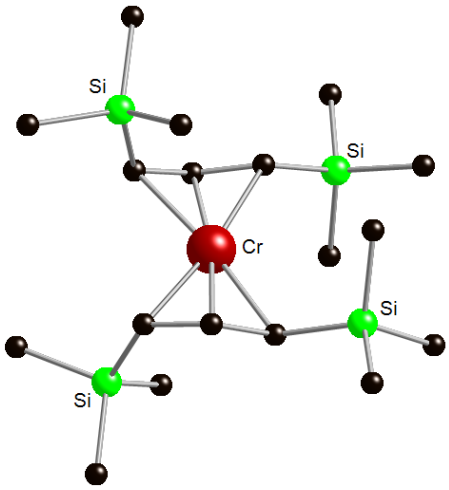

Figure 23: Molecular structure of [Cr{$C_3H_3(SiMe_3)_2$}$_2$] (**1.73**). Hydrogen atoms have been omitted for clarity, carbon = black, silicon = green, chromium = red. Reproduced from ref. 62

DFT studies of complexes **1.73**[61] and **1.76**[64] showed that the steric bulk of the trimethylsilyl group does not affect the η^3-coordination mode of the silyl-allyl ligand. The computed structures for the parent complexes [Cr(C_3H_5)$_2$] (**1.77**) and [Ni(C_3H_5)$_2$] (**1.1**) are the same as the *bis* trimethylsilyl substituted analogues.

If [K{C_3H_4(1-$SiMe_3$)] is reacted with $CrCl_2$, complex [Cr_2{C_3H_4(1-$SiMe_3$)}$_4$] (**1.78**) is formed.[62] Therefore, reducing the steric bulk of the ligand gives the chromium-chromium bonded dimer **1.78**; with a quadruple Cr–Cr bond bridging between two [Cr{C_3H_4(1-$SiMe_3$)}$_2$] units (Figure 24). Complex **1.78** is isostructural with its parent compound [$Cr_2(C_3H_5)_4$] (**1.79**),[66] with a Cr–Cr bond distance of 1.9784(7) Å. Each chromium is coordinated by one silyl-allyl ligand in an η^3 manner, where Cr–C bond distances vary from 2.192(11) to 2.303(5) Å, and then by two other silyl-allyl ligands in a μ:η^1 fashion in which the Cr–C bond distances range from 2.123(6) to 2.164(9) Å.

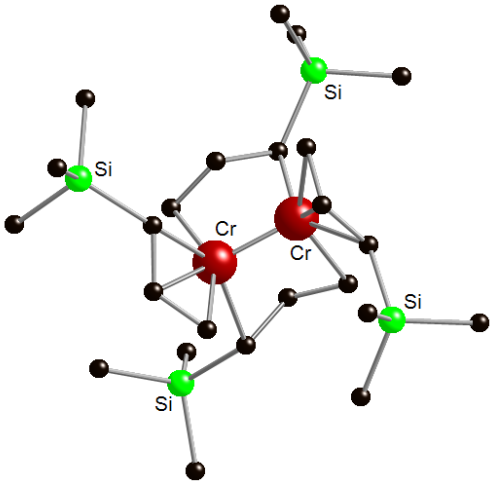

Figure 24: Molecular structure of $[Cr_2\{C_3H_4(1\text{-}SiMe_3)\}_4]$ (**1.78**). Hydrogen atoms have been omitted for clarity, carbon = black, silicon = green, chromium = dark red. Reproduced from ref. 62

Complex $[Ni\{C_3H_3(SiMe_3)_2\}_2]$ (**1.76**) can be used as a precursor to silyl-substituted allyl nickel(II) halides; the reaction of two equivalents of $[Ni\{C_3H_3(SiMe_3)_2\}_2]$ with Br_2 or I_2 yields $[Ni(\mu\text{-}X)\{\eta^3\text{-}C_3H_3(SiMe_3)_2\}]_2$, where X = Br (**1.80**) and I (**1.81**). The solid-state structure of **1.80** was not determined, but the solution-state studies (for both complexes **1.80** and **1.81**) suggests that the complexes occur as a mixture of two diastereomers, with *exo,endo* trimethylsilyl groups. Complex **1.81** crystallises as a halide-bridged dimer, however there are two unique molecules in the unit cell; one with the silyl-allyl ligands in an eclipsed arrangement and the other with the ligands staggered (Figure 25). The Ni−C bond distances range from 1.973(8) to 2.049(7) Å, which are similar to those seen in complex **1.76**. As seen with other transition metal allyl complexes, the trimethylsilyl groups are in the *exo,endo* arrangement, which agrees with the structure determined in solution.

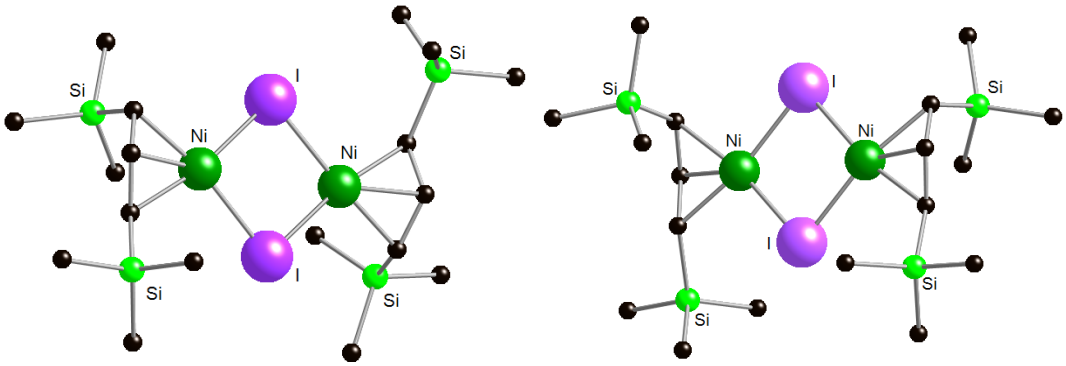

Figure 25: Molecular structure [Ni(μ-I){η^3-$C_3H_3(SiMe_3)_2$}]$_2$ (**1.81**), eclipsed structure (left) and staggered structure (right). Hydrogen atoms have been omitted for clarity, carbon = black, silicon = green, nickel = deep green, iodine = lilac. Reproduced from ref. 64

Bis(1,3-trimethylsilyl)allyl bromide reacts with *bis*-cyclooctadiene nickel(0) to give the *exo,exo* conformation bromide-bridged dimer of [Ni(μ-Br){η^3-$C_3H_3(SiMe_3)_2$}]$_2$ (**1.82**); the molecular structure shows that the silyl-allyl ligands are mutually staggered and the structure is maintained in solution.

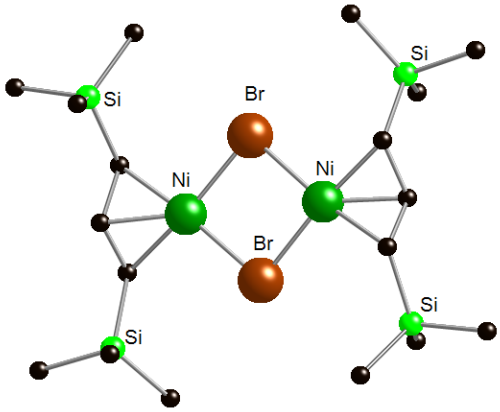

Figure 26: Molecular structure of staggered [Ni(μ-Br){η^3-$C_3H_3(SiMe_3)_2$}]$_2$ (**1.82**). Hydrogen atoms have been omitted for clarity, carbon = black, silicon = green, nickel = deep green, bromine = brown. Reproduced from ref. 64

The first structurally authenticated manganese(II) allyl complex was [Li(thf)$_4$][Mn{η^3-$(SiMe_3)_2C_3H_3$}{η^1-$(SiMe_3)_2C_3H_3$}$_2$] (**1.83**) (Figure 27) obtained by reacting three equivalents of *bis*-1,3-trimethylsilyl(allyl)lithium with $MnCl_2$ in thf.[67] In the anion of complex **1.83** there are allyl ligands in both the η^1- and η^3-coordination mode; one of the allyl ligands coordinates η^3, whereas the other two ligands coordinate η^1. This is the first time σ bonded silyl-allyl ligands have been observed in a transition

metal complex and this is the first time that a mixed hapticity has been observed in any metal allyl complex. However, this is not due to steric crowding around the metal since DFT calculations show that replacing the $SiMe_3$ substituents with H-atoms makes no difference to the hapticities of the ligands.[68] The manganese(II) is unsolvated and resides in a distorted tetrahedral coordination environment with C−Mn−C bond angles ranging from 110.81(14)-131.05(14)°. The Mn−C distances of the η^1-allyl ligands are essentially the same at 2.184(4) and 2.187(4) Å, with the η^3 Mn−C bond lengths being 2.398(4) and 2.470(4) Å for the two terminal allyl carbon atoms, and 2.348(3) Å for the central carbon atom.

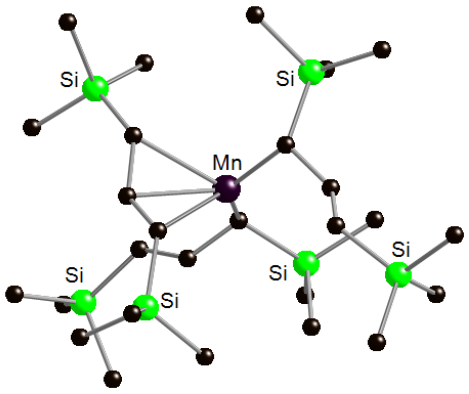

Figure 27: Molecular structure of the anion of $[Li(thf)_4][Mn\{\eta^3\text{-}(SiMe_3)_2C_3H_3\}\{\eta^1\text{-}(SiMe_3)_2C_3H_3\}_2]$ (**1.83**). Hydrogen atoms have been omitted for clarity, carbon = black, silicon = green, manganese = dark purple. Reproduced from ref. 67

Transition metal allyl complexes of 4d metals are rare, but a few examples of group 4 complexes are known. Complexes of group 4 metals, titanium, zirconium and hafnium, are used in homogenous olefin polymerisation, therefore the allyl complexes of these metals and their chemistry are of great relevance. The attempted synthesis of $[(silyl\text{-}allyl)_2MCl_2]$ (M = Ti, Zr), allylic analogues of the metallocene pre-catalysts Cp_2MCl_2, resulted in reduction to Ti(III) and Zr(III) bimetallic complexes $[(silyl\text{-}allyl)_2Ti(\mu\text{-}Cl)_2Li(tmeda)]$ (**1.84**) and $[(silyl\text{-}allyl)_2Zr(\mu\text{-}Cl)_2Li(tmeda)]$ (**1.85**).[69] The (silyl-allyl)lithium precursor is both a reducing reagent and an allylation reagent. Complexes **1.84** and **1.85** are structurally similar; in both complexes the allyl ligands are in a

exo,endo conformation and the allyl ligand appears to be coordinated η^3. However the M−C_{allyl} bond distances are very asymmetric; Ti−C distances range from 2.275(14) to 2.461(11) Å, and Zr−C bond distances range from 2.361(4) to 2.56(12) which suggest σ + π bonding modes. If the allyl is considered to occupy two coordination sites each, with the bridging chloride ligands the metal centres are 6-coordinate. Complexes **1.84** and **1.85** are d^1 species and their magnetic moments in toluene, determined by the Evans method, are μ_{eff} = 1.7 ± 0.7 μ_B and μ_{eff} = 1.5 ± 0.8 μ_B respectively. The corresponding Ti(IV) (**1.86**) and Zr(IV) (**1.87**) complexes were formed, in low yield, *via* controlled oxidation reactions.

Lappert *et al.* synthesised the *ansa-bis*(silyl-allyl) complexes [Zr{Me_2Si-($C_3H_3SiMe_3$)$_2$}$_2$] (**1.88**) and [Hf{$Me_2Si(C_3H_3SiMe_3)_2$}$_2$] (**1.89**) according to Scheme 13.[28]

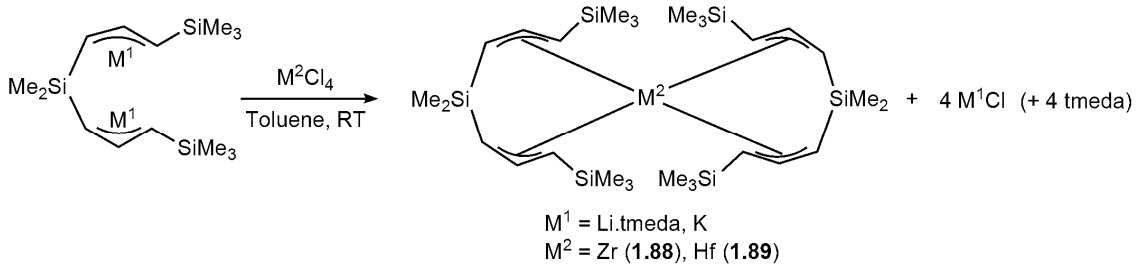

Scheme 13

Complex **1.88** is a mononuclear complex with a crystallographically imposed two-fold rotation axis. Each of the silyl-allyl ligands coordinates in a pincer-like manner, with the allylic carbon coordinating in an η^3-fashion, and the trimethylsilyl substituents in an *exo,exo* arrangement with respect to each other. There is an C−$SiMe_2$−C bite angle of 104.2(2)° and the C−C−C angle is 128.6(6)°, both of which are similar to the analogous angles found in lanthanide allyl complex **1.61**. The C−C bond lengths in **1.88** range from 1.355(2)-1.382(7) Å and the Zr−C bond distances range from 2.462(5) to 2.594(5) Å suggesting complete delocalisation of the allyl negative charge.

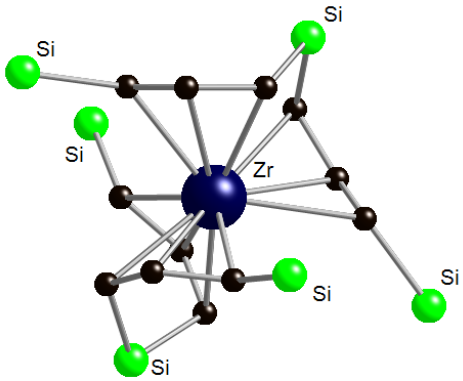

Figure 28: Molecular structure of [Zr{$Me_2Si(C_3H_3SiMe_3)_2$}$_2$] (**1.88**). Hydrogen atoms and Me groups from $SiMe_2$ and $SiMe_3$ groups have been omitted for clarity, carbon = black, silicon = green, zirconium = dark blue. Reproduced from ref. 28

As with the 4d transition metals, 5d allyl metal complexes are also rare. The reaction of the stannyl-substituted allyl pro-ligand $Me_3SiC_3H_3(SiMe_3)(SnMe_3)$ with tantalum(V) chloride yields the product [{η^3-$C_3H_3(SiMe_3)_2$}$TaCl_4$] (**1.90**) (Scheme 14).[59]

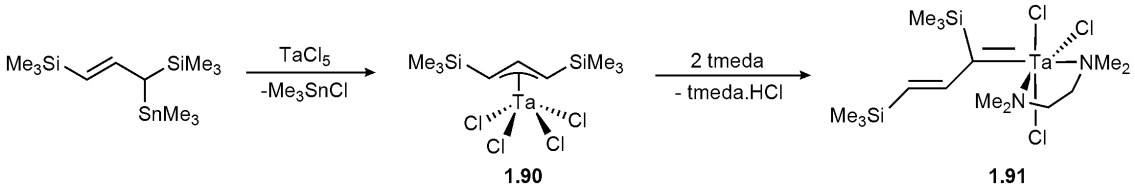

Scheme 14

Crystals of **1.90** suitable for X-ray crystallography were not obtained, but ^{1}H NMR spectroscopy showed the coupling pattern characteristic of the C_3H_3 backbone and elemental analysis confirmed the presence of a 1:1 ratio of allyl to metal. The addition of tmeda to **1.90** results in deprotonation of the allyl to give the tantalum(V) alkylidene (**1.91**), which was characterised by X-ray crystallography. The tantalum(V) is in a distorted octahedral environment with the tmeda ligand in a *cis* arrangement, and C−C bond lengths of 1.320(10) and 1.488(9) Å indicate that the allyl contains a localised double bond, and hence the formation of the vinyl alkylidene structure. The slipped pentadienyl complex [Cp_2Ta{η^3-1,5-$(SiMe_3)_2C_5H_5$}] (**1.92**) is the only other contender for the description of a silyl-allyl complex of a 5d transition metal.[70]

1.1.5 Group 12 and p-Block Complexes

Very few investigations of p-block allyl complexes have been carried out; only two examples of silyl-allyl p-block complexes are known. The first reported structure was the gallium(III) species $[Ga\{C_3H_3(SiMe_3)_2\}_3]$ (**1.83**), which was formed by the reaction of $GaCl_3$ with three equivalents of $[K\{C_3H_3(SiMe_3)_2\}]$ in thf.[71] Complex **1.93** is indefinitely stable under an inert atmosphere, and can survive exposure to air for a few minutes before signs of decomposition. At room temperature the ^1H NMR spectrum shows a singlet for the $SiMe_3$ groups and a triplet for the central allyl proton, suggesting symmetrically coordinated or fluxional allyl ligands, in solution. Variable-temperature ^1H NMR spectroscopic studies confirmed that in solution the complex is fluxional.

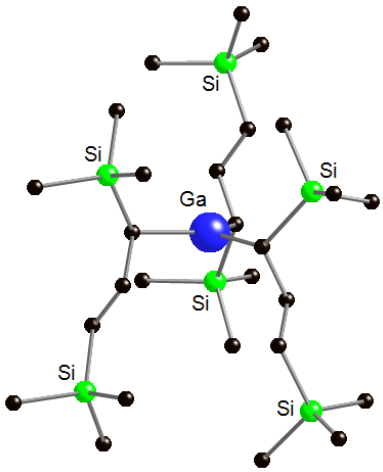

Figure 29: Molecular structure of $[Ga\{C_3H_3(SiMe_3)_2\}_3]$ (**1.93**). Hydrogen atoms have been omitted for clarity, carbon = black, silicon = green, gallium = blue. Reproduced from ref. 71

However, X-ray crystallography shows that the three allyl ligands are σ-bonded to the gallium to generate a trigonal planar coordination environment, with the C−Ga−C angles being 121.46(11), 120.39(11) and 117.89(11)°. The three allyl ligands are perpendicular to the GaC_3 plane and the Ga−C bond lengths average 1.980 Å. One of the ligands is coordinated such that it is orientated in the opposite direction to the other two allyl ligands (Figure 29). The trimethylsilyl substituents are in the *exo,exo*

arrangement, with the C−C−C bond angles being 127.5(3), 127.5(3) and 127.8(3)° and with C−C bond lengths of distinct single and double bond character.

A similar reaction of tin(II) chloride with three equivalents of [K{$C_3H_3(SiMe_3)_2$}] in thf yielded [Sn{$C_3H_3(SiMe_3)_2$}K(thf)] (**1.94**) (Figure 30); the *tris*(silyl-allyl)stannate anion encapsulates the potassium in an η^3 fashion by the *ansa-tris* tin allyl ligand. In the molecular structure a C_3 axis runs through the tin and potassium centres, with the lone pair on the tin resulting in a pyramidal geometry.

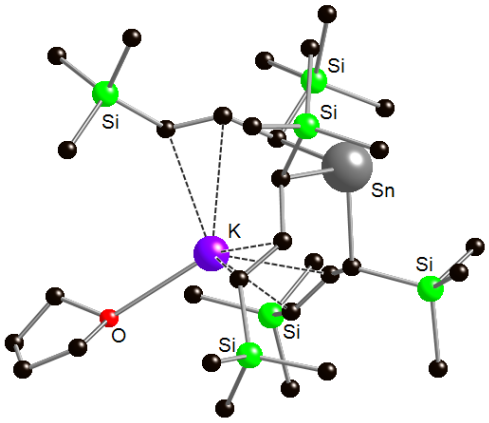

Figure 30 Molecular structure of [Sn{$C_3H_3(SiMe_3)_2$}K(thf)] (**1.94**). Hydrogen atoms have been omitted for clarity, carbon = black, silicon = green, potassium = purple, tin = dark grey. Reproduced from ref. 30

The Sn−C bond lengths average 2.343 Å, with the C−Sn−C bond angles of 96.8(2)°, suggesting the tin lone pair has substantial s-character. The K−C bond distances are 3.159(8) and 3.062(8) Å. The C−C bond lengths 1.499(9) and 1.337(10) Å imply localised single and double bonds within the allyl and confirms the σ-bonding of the silyl-allyl ligand. ^{1}H NMR spectroscopy of **1.94** in benzene-d_6 showed the solid-state structure is maintained in solution with only slight asymmetry, with nine separate resonances for the allyl protons, ^{119}Sn NMR spectroscopy showed a single resonance at $\delta(^{119}Sn) = -132.9$ ppm

Hanusa *et al.* isolated a series of zinc *tris*(silyl-allyl) 'ate complexes of the general formula [Zn{$C_3H_3(SiMe_3)_2$}$_3$M], M = Li (**1.95**), Na (**1.96**), and K (**1.97**) *via* the reaction of zinc triflate with three equivalents of [M{$C_3H_3(SiMe_3)_2$}].[72]

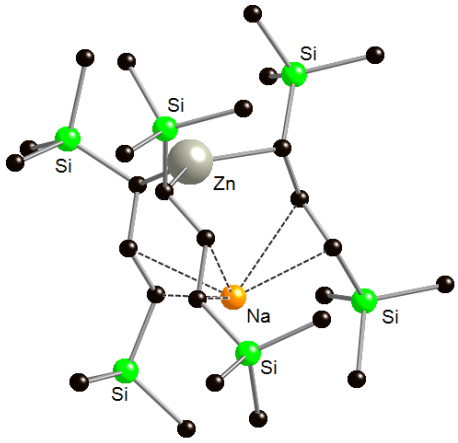

Figure 31: Molecular structure of [Zn{$C_3H_3(SiMe_3)_2$}$_3$Na] (**1.96**). Hydrogen atoms have been omitted for clarity, carbon = black, silicon = green, sodium = pale orange, zinc = light grey. Reproduced from ref. 72

The structures of **1.95-1.97** were determined by X-ray crystallography, and in each case the zinc centre is coordinated by three σ-bound silyl-allyl ligands, which are all orientated in the same perpendicular direction, unlike **1.93**, in which one silyl-allyl is anti-parallel. The alkali metal cation interacts with the C=C double bond electron density. NMR spectroscopy studies in benzene-d_6 showed that the silyl-allyl ligands are fluxional in solution, similar to that of **1.93** but in contrast to **1.94**, which implies that the alkali metal cations do not hold the silyl-allyl ligand rigid, however the chemical shifts of the allyl protons suggest that the cation is still coordinated. It is likely that the structural difference between **1.94** and **1.95-1.97** in solution is a combination of the K−C bond strength and that any rearrangement of the silyl-allyl ligands would involve an inversion of the tin lone pair. However in thf-d_8 all three complexes gave identical ^{1}H NMR spectra, suggesting that there was solvent separation of the alkali metal cation.

Chapter 2

Synthesis of Alkali Metal *Ansa*-*Tris*(Allyl) Complexes

2.1 Introduction to *Ansa-tris*(allyl) Chemistry

As discussed in the previous chapter, a large range of silyl-allyl complexes are known Before this thesis however, there was only one example of an *ansa-tris*(silyl-allyl) complex in the literature.[30] Therefore, my aims are to:

1. Synthesise different *ansa-tris*(silyl-allyl) pro-ligands, with different substituents, to investigate the effect substituents have on structure;
2. Investigate the effect of different alkali metals, and larger ionic radii, on the structure of the allyl complex;
3. Investigate any effect different tertiary amine co-ligands may have on the overall structure of the complex.

2.2 Synthesis of *Ansa-tris*(allyl) Ligands

The *ansa-tris*(allyl) pro-ligands discussed herein are the previously reported $MeSi\{C_3H_4(SiMe_3)\}_3$ ($\mathbf{L^1}H_3$)[30] and the new pro-ligand $PhSi\{C_3H_4(SiMe_3)\}_3$ ($\mathbf{L^2}H_3$).[73] Scheme 15 below shows the synthesis of $\mathbf{L^1}H_3$ and $\mathbf{L^2}H_3$, which were both isolated as oils, colourless and pale yellow, respectively. Both pro-ligands were collected in moderate to high yields, $\mathbf{L^1}H_3$ in 67 % yield and $\mathbf{L^2}H_3$ in 58% yield.

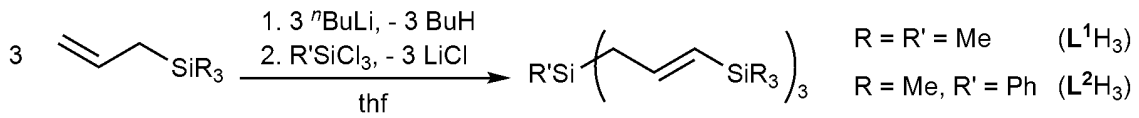

Scheme 15

2.3 Synthesis and Structures of *Ansa-tris*(Allyl) Complexes

Based on the unusual structure and *endo,exo* stereochemistry of the silyl-substituents in the *ansa-tris*(allyl) lithium complex $[MeSi\{(C_3H_3SiMe_3)Li(tmeda)\}_3]$ **1.21** (Chapter 1, Figure 14) a more detailed investigation into the factors that influence the coordination mode of $\mathbf{L^1}$ in complex **1.21** were undertaken. In this section are the results of a

crystallographic and NMR spectroscopic study of a range of *ansa-tris*(allyl) alkali complexes, which have been synthesised. As well as gaining insight from experiment, a computational study was carried out on to look into the relative energies of the $[\mathbf{L^1}]^{3-}$ pristine anion, and its lithium and sodium complexes, which is to be discussed in section 2.4.

2.3.1 [PhSi{($C_3H_3SiMe_3$)Li(tmeda)}$_3$] (2.1)

Firstly, in order to explore the effect of the varying the substituent on the central silicon atom on the structure, complex [PhSi{($C_3H_3SiMe_3$)Li(tmeda)}$_3$], [$\mathbf{L^2}$(Li·tmeda)$_3$] **2.1** was synthesised. Ligand $\mathbf{L^2}H_3$ was treated with three equivalents of ^{n}BuLi at −78 °C, and then treated with three equivalents of tmeda, in hexane (Scheme 16). The solution was filtered, concentrated and left at +5°C to recrystallise, affording yellow-orange plate-like crystals of complex **2.1** (0.41g, 44 %).

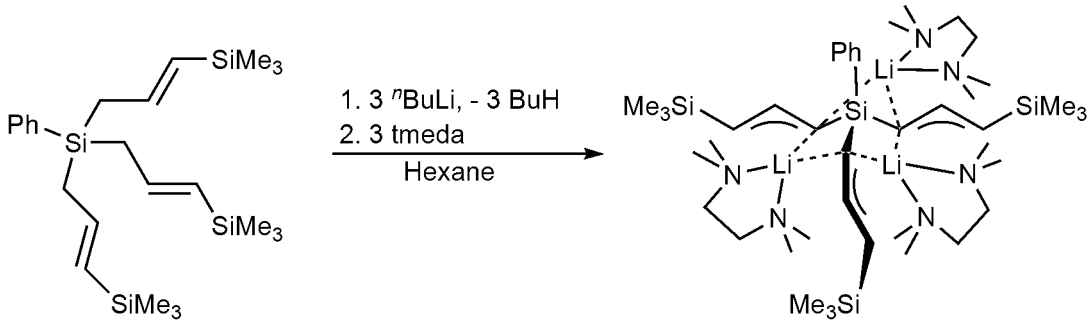

2.1

Scheme 16

Complex **2.1**, is essentially isostructural to complex [MeSi{($C_3H_3SiMe_3$) Li(tmeda)}$_3$] **1.21**; featuring three four-coordinate lithium cations in distorted tetrahedral geometries. The allyl ligands are bridging between the lithium cations, in a mixed coordination mode of $(\mu{:}\eta^2)(\mu{:}\eta^1)_2$, which means one of the allyl ligands is bridging in an η^2 manner and the other two allyl ligands are bridging in an η^1 manner, with Li−C bond distances range from 2.250(5)-2.691(6) Å. The C−C bond lengths in

complex **2.1** range from 1.377(4)-1.428(4) Å, which can be split into a shorter set (av. 1.378 Å) and longer set (av. 1.423 Å), suggesting that the bonding in each allyl unit is only partially delocalised. The trimethylsilyl substituents in complex **2.1** are in [*exo,exo*]$_2$[*endo,exo*] conformations (see Figure 1, **(D)**) with respect to the central silicon atom Si1.

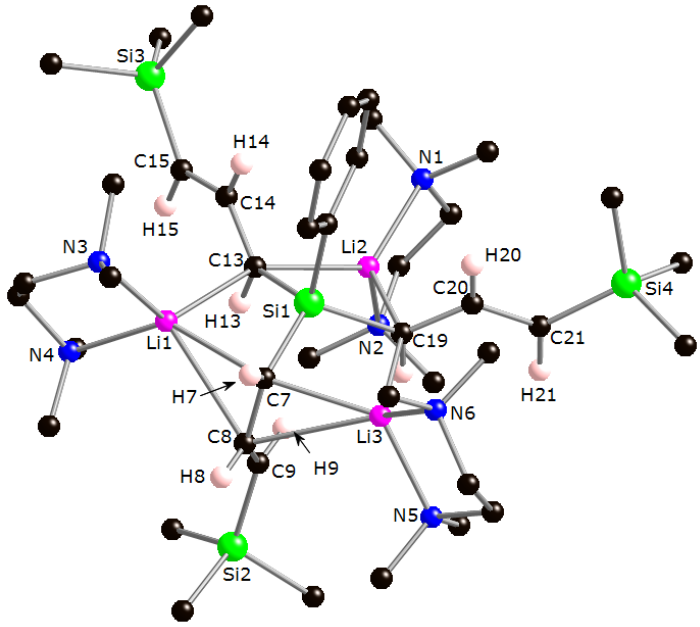

Figure 32: Molecular structure of [**L**^{2}(Li·tmeda)$_3$] (**2.1**), selected bond lengths (Å) and angles (°). Hydrogen atoms have been omitted for clarity, carbon = black, silicon = green, lithium = bright pink, nitrogen = blue: C(7)−C(8) 1.428(4), C(8)−C(9) 1.377(4), C(13)−C(14) 1.418(3), C(14)−C(15) 1.379(3), C(19)−C(20) 1.424(3), C(20)−C(21) 1.377(4), C(9)−C(8)−C(7) 129.5(2), C(15)−C(14)−C(13) 130.7(2), C(21)−C(20)−C(19) 130.5(2), C(13)−C(14)−C(15)−Si(3) 179.9(2), C(19)−C(20)−C(21)−Si(4) 178.2(2), C(7)−C(8)−C(9)−Si(2) 178.8(2), Li(1)−C(7) 2.275(5), Li(1)−C(8) 2678(5), Li(1)−C(13) 2.301(5), Li(2)−C(13) 2.313(5), Li(2)−C(19) 2.250(5), Li(3)−C(7) 2.259(5), Li(3)−C(8) 2.691(6), Li(3)−C(19) 2.267(5).

The ^{1}H and ^{13}C NMR spectra, in benzene-d_6 at room temperature, of **2.1** confirm the [*exo,exo*]$_2$[*endo,exo*] conformations of the allyl groups of **L**^{2}. The ^{1}H NMR spectrum for **2.1** is complicated however; some proton environments can be assigned. The protons H13-H15 and H19-H21 (see Figure 32 for numbering) are in very similar environments and protons H7-H9 are in a different environment owing to the *endo* conformation of the allyl moiety. Protons H15/H21 can be assigned to a multiplet at 3.03 ppm, and the central *exo* protons H14/H20 to a triplet at 6.70 ppm with ^3J = 28.0 Hz. The *endo* proton

H7 is seen as a doublet of doublets at 3.47 with ^{3}J = 24.0 and ^{4}J = 8.0 Hz. Also, the $SiMe_3$ groups are distinguishable within the ^{13}C NMR spectrum; with the two *exo* $SiMe_3$ groups at 0.62 and 0.00 ppm and the *endo* $SiMe_3$ group at -3.71 ppm.

The Li−C bond lengths for complex **1.21** range from 2.088(7)-2.696(6) Å and the C−C bond lengths range from 1.383(7)-1.416(4) Å.[30] These bond lengths are very similar to those seen in complex **2.1**. The bond lengths of the *ansa-bis*(allyl) complex $[Me_2Si\{Li(tmeda)\}_2\{3\text{-}(C_3H_3\text{-}1\text{-}SiMe_3)\}_2]$ (**1.16**) have Li−C bond lengths ranging from 2.202(11)-2.131(10) Å and C−C bond lengths ranging from 1.390(8)-1.395(8) Å. The difference in Li−C and C−C bond lengths between complexes **2.1** and **1.16** can be attributed to the *ansa-tris*(allyl) ligand being more sterically crowded around each of the allyl units, and as a result the Li−C bond lengths have a larger range. The delocalisation of the negative charge, on the allyl units in **2.1**, has become more localised, and this is reflected in the C−C bond lengths.

The proton NMR spectrum shows the central *exo* protons H14/H20 as a triplet at 6.70 ppm with ^{3}J = 28.0 Hz and the *endo* proton H7 as a doublet of doublets at 3.47 ppm with ^{3}J = 24.0 Hz. It is likely that in solution the structure is fluxional with the allyl units having some flexibility, due to some delocalization of the negative charge, and an average coupling for the *endo* and *exo* allyls is seen. It is also common in lithium allyl complexes for structures to be fluxional and rearrangement pathways available, as seen in complex **1.21**[30] and $[(tmeda)Li\{C_3H_3(SiMe_3)_2\}]$ (**1.8**).[19]

2.3.2 $[MeSi\{(C_3H_3SiMe_3)Li(pmdeta)\}_3]$ (2.2)

The influence of a higher denticity co-ligand on the lithium cation was investigated using pmdeta (*N,N,N',N',N''*-pentamethyldiethylenetriamine). The reaction of $\mathbf{L^1}H_3$ with three equivalents of ^{n}BuLi and three equivalents of pmdeta, in hexane, resulted in

the formation of [MeSi{($C_3H_3SiMe_3$)Li(pmdeta)}$_3$], [**L**^{1}(Li·pmdeta)$_3$] **2.2** as red crystals at −5 °C from a small volume of hexane in a 39 % yield (Scheme 17).

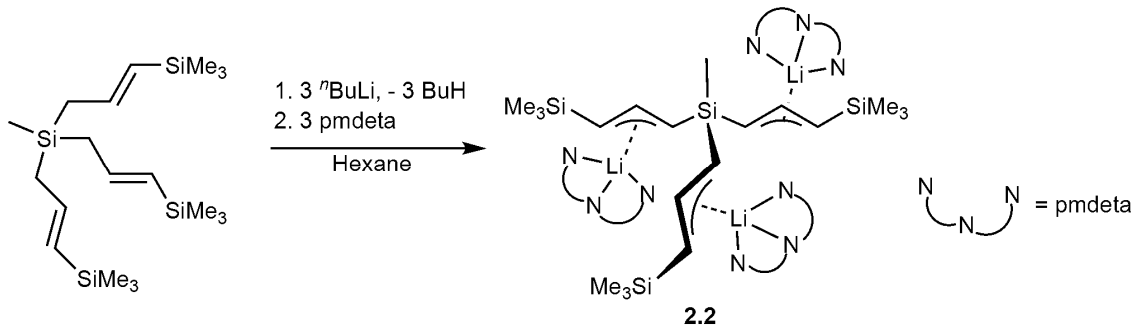

2.2

Scheme 17

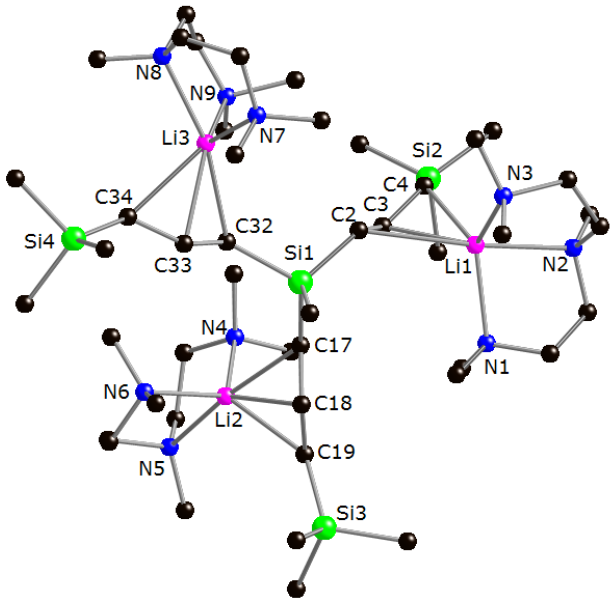

Figure 33: Molecular structure of [**L**^{1}(Li.pmdeta)3] (**2.2**), selected bond lengths (Å) and angles (°). Hydrogen atoms have been omitted for clarity, carbon = black, silicon = green, lithium = bright pink, nitrogen = blue: C(2)−C(3) 1.382(7), C(3)−C(4) 1.426(7), C(17)−C(18) 1.367(7), C(18)−C(19) 1.424(7), C(32)−C(33) 1.379(7), C(33)−C(34) 1.414(8), C(2)−C(3)−C(4) 130.9(5), C(17)−C(18)−C(19) 129.5(5), C(32)−C(33)−C(34) 130.8(5), Li(1)−C(2) 2.655(10), Li(1)−C(3) 2.311(10), Li(1)−C(4) 2.315(10), Li(2)−C(17) 2.400(11), Li(2)−C(18) 2.328(11), Li(2)−C(19) 2.316(11), Li(3)−C(32) 2.377(11), Li(3)−C(33) 2.333(11), Li(3)−C(34) 2.448(11).

In complex **2.2** each lithium cation is coordinated by an allyl unit and a terdentate pmdeta ligand, giving each lithium cation a coordination number of 5. Coordination to the pmdeta is preferential to forming the μ-allyl bridging mode seen in complex **2.1**, due to the interactions between the hard Li^+ cation and the hard nitrogen of the pmdeta co-ligand. The trimethylsilyl substituents in **2.2** are in the [*exo*,*exo*]$_3$ conformation. The

bond lengths for the allyl units can be split into two types, the shorter C−C bond lengths which average 1.376 Å (range 1.367(7)-1.382(7) Å) and the longer C−C bond lengths which average 1.421 Å (range 1.414(8)-1.426(7) Å). The Li−C bond distances range from 2.311(10)-2.655(10) Å. However the lithium cations are each coordinated by the allyl asymmetrically such that each lithium has a "long" Li−C bond and two "short" Li−C bonds, the long Li−C bond lengths are 2.655(10), 2.400(11) and 2.448(11) Å for Li(1)−C(2), Li(2)−C(17) and Li(3)−C(34), respectively.

The ^{1}H NMR spectrum, in benzene-d_6 at room temperature, of **2.2** reveals the allylic protons as a series of overlapping multiplets; the central allyl protons are observed between $\delta(^{1}H)$ = 5.46-5.76, 6.08-6.24, 6.53-6.58 and 7.09 ppm, whereas the terminal allylic protons occur between $\delta(^{1}H)$ = 1.61-1.80 ppm as doublets of doublets. Where it was possible to measure the allyl ^{3}J coupling constants, they were measured at ^{3}J = 7.78 and 15.81 Hz. The $SiMe_3$ substituents at $\delta(^{1}H)$ = 0.14, 0.16, and 0.23 ppm, and the methyl group of the central silicon at $\delta(^{1}H)$ = 0.00 ppm.

The Li−C and C−C bond lengths of complex **2.2** would suggest that the bonding of the allyl is partially localised, similar to that seen by Fraenkel in which the lithium cation is *intra*molecularly solvated, with C−C allyl bond lengths ranging from 1.349(1) to 1.494(7) Å.[83] Another reason for the asymmetry of the allyl coordination may be to reduce steric clashes between the pmdeta ligands. The C−C bond lengths are also similar to those seen in complex **2.1**. Similar bonding of lithium is seen in [(pmdeta)Li(C_3H_5)] (**1.5**), where the terminal Li−C bond distances differ by almost 0.5 Å.[15] From the ^{1}H and ^{13}C NMR spectra, it can be deduced that there are three structurally similar, but not identical, allylic units of '[(pmdeta)Li($C_3H_3SiMe_3$)]', with three unique $SiMe_3$ substituents. The measured proton-proton coupling suggests that both *exo*- and *endo*-orientated silyl groups are present in solution.

2.3.3 [MeSi{($C_3H_3SiMe_3$)Na(tmeda)}$_3$](2.3)

In order to explore the effects of the alkali metal cations with larger ionic radii on the *ansa-tris*(allyl) ligand structure, the sodium complex [MeSi{($C_3H_3SiMe_3$)Na(tmeda)}$_3$], [$\mathbf{L^1}$(Na.tmeda)$_3$] (**2.3**) was prepared. Ligand $\mathbf{L^1}H_3$ was added to a suspension of three equivalents of freshly prepared ^{n}BuNa, in hexane. The resulting mixture was then treated with three equivalents of tmeda. The orange solution was filtered and concentrated and stored at −15 °C to yield a crop of bright orange crystals of **2.3** (0.30g, 38 %).

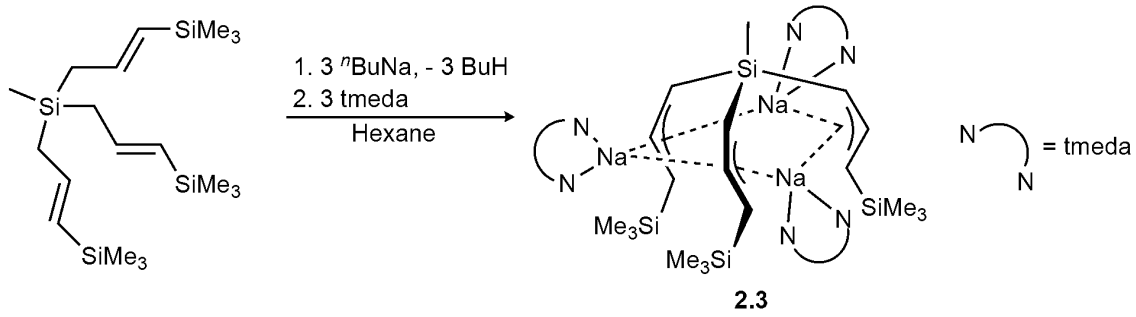

2.3

Scheme 18

In the solid-state structure of [$\mathbf{L^1}$(Na.tmeda)$_3$] **2.3**, allyl units C(2)−C(3)−C(4)−Si(2) and C(14)−C(15)−C(16)−Si(4) have their silyl substituents in the [*endo,exo*] conformation and the allyl ligands C(2)−C(3)−C(4) and C(14)−C(15)−C(16) coordinate in an η^3:η^3-coordination mode to Na(2). The third allyl ligand C(8)−C(9)−C(10) experiences disorder over two sites, resulting in a 51:49 [*endo,exo*]:[*exo,exo*] occupancy. Between Na(1) and Na(3) the allyl bridges in an asymmetric μ:η^2:η^3 bonding mode. The range of Na−C distances within complex **2.3** for Na(1), Na(2) and Na(3) are 2.553(17)-3.016(12), 2.587(7)-3.193(7) and 2.575(7)-2.882(7) Å respectively. The sodium cations are also coordinated by the tmeda co-ligand, which means Na(1), Na(2) and Na(3) have coordination numbers of 6, 6, and 5 respectively.

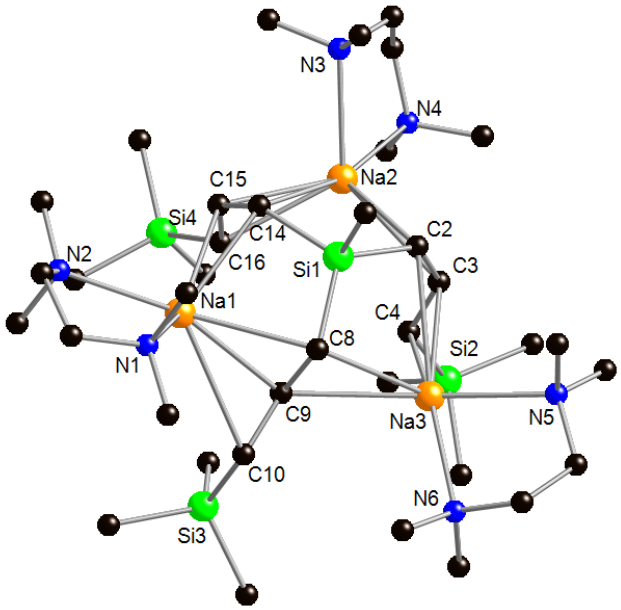

Figure 34: Molecular structure of [L^1(Na.tmeda)$_3$] (**2.3**), in the [*endo*,*exo*]$_2$[*exo*,*exo*] conformation, selected bond lengths (Å) and angles (°). Hydrogen atoms have been omitted for clarity, carbon = black, silicon = green, sodium = pale orange, nitrogen = blue: C(2)−C(3) 1.395(9), C(3)−C(4) 1.368(10), C(8)−C(9) 1.463(13), C(9)−C(10) 1.383(13), C(14)−C(15) 1.391(9), C(15)−C(16) 1.344(9), C(2)−C(3)−C(4) 132.3(7), C(8)−C(9)−C(10) 132.4(12), C(15)−C(15)−C(16) 132.9(8), Na(1)–C(8) 2.718(7), Na(1)–C(9) 2.553(17), Na(1)–C(10) 3.016(12), Na(1)–C(14) 2.614(8), Na(1)–C(15) 2.865(7), Na(2)–C(14) 2.819(7), Na(2)–C(15) 2.652(7), Na(2)–C(16) 2.605(8), Na(2)–C(2) 2.587(7), Na(2)–C(3) 2.762(7), Na(3)–C(2) 2.882(7), Na(3)–C(3) 2.689(7), Na(3)–C(4) 2.677(7), Na(3)–C(8) 2.575(7), Na(3)–C(9) 2.837(16). Selected bond lengths (Å) and angles (°) for the [*endo*,*exo*]$_3$ conformation: C(8)−C(9A) 1.394(13), C(9A)−C(10A) 1.365(14), C(8)−C(9A)−C(10A) 123.4(12), Na(1)–C(9A) 2.655(18), Na(1)–C(10A) 2.615(13), Na(3)-C(9A) 2.903(18).

The ^{1}H NMR spectrum of **2.3**, in benzene-d_6, showed three trimethylsilyl groups and the central SiMe group at $\delta(^1H)$ = −0.01, 0.00, 0.13 and 0.15 ppm, with a broad singlet for each of the two tmeda environments at $\delta(^1H)$ = 2.14 and 1.95 ppm. The allyl proton signals occur as overlapping multiplets (see Experimental Section – Chapter 8). The allyl protons in the region $\delta(^1H)$ = 5.46-5.64 (Figure 35) are mutually coupled to the allyl protons in the region $\delta(^1H)$ = 1.63-1.86 ppm (the signal of which is partially obscured by the tmeda ligand resonance - Figure 35). Another group of mutually coupled resonances due to allylic protons is seen at $\delta(^1H)$ = 2.99, 3.63 and 7.35 ppm.

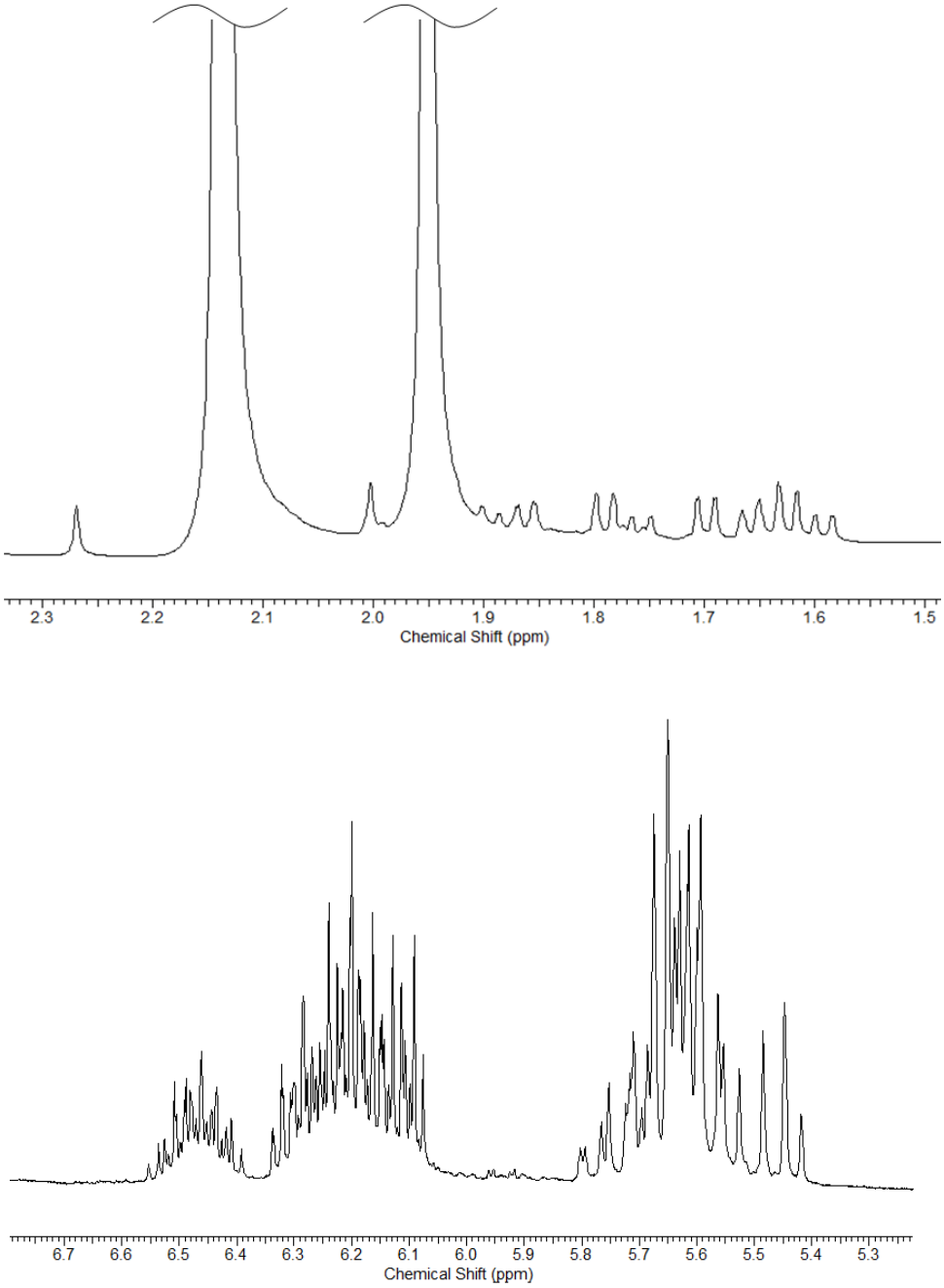

Figure 35: ^{1}H NMR spectrum of **2.3** recorded in benzene-d_6 at 300 K. Allyl region 1.5-2.3ppm with the resonances due to the tmeda at 1.94 and 2.13 ppm, have been truncated (above). Complicated allyl region 5.3-6.5 ppm (below).

The Na−C bond distances in complex **2.3** are asymmetric and reflect those seen in other examples of sodium allyl complexes, such as [(pmdeta)Na(1-PhC$_3$H$_4$)] (**1.17**)[26] and the more recent example of [Na{1,3-(SiMe$_3$)$_2$C$_3$H$_3$}(thf)]$_4$ (**1.18**).[27] In both complexes **1.17** and **1.18** the Na−C bond distances to the allyl ligand consist of two shorter bonds and one longer bond, the asymmetric bonding mode μ:η^2:η^3 between

Na(1) and Na(3) is an extension of this. The longest Na−C bond recorded in the Cambridge Structural Database is currently 3.199 Å,[74] which is significantly shorter than Na(1)–C(16) (3.378 Å) and Na(30)−C(10) (3.735 Å) distances. Therefore rather than the pattern of 'short, short, long' with the Na−C bond distances, in complex **2.3** there are only two short Na−C bonds from allyl units to cations Na(1) and Na(3). The greater ionic radius of the sodium enables the higher coordination numbers in comparison to lithium complexes **2.1** and **2.2**. Another effect of the larger cation radius of sodium is that the silyl-allyl ligands have the *endo,exo* stereochemistry and are orientated in the same direction, whereas for complexes **2.1** and **2.3** they are oriented 'away' from each other.

The ^{1}H and ^{13}C NMR spectra of complex **2.3** suggests that there are several species in solution at 292 K. These species are likely to correspond to the different *endo* and *exo* stereochemistries of the silyl-allyl groups, and their relative orientation in relation to tmeda (Scheme 19).

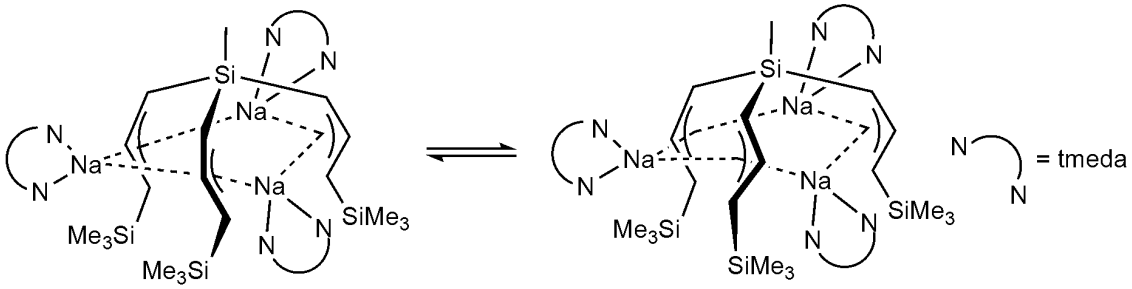

Scheme 19

2.3.4 $[PhSi\{(C_3H_3SiMe_3)Na\}_3]_2$ $[2.4]_2$

Replacement of the methyl substituent on the central silicon atom in $\mathbf{L^1}H_3$ with a phenyl group to give $\mathbf{L^2}H_3$ does not affect the structures the trilithium complexes **1.21** and **2.1**. However, the reaction of $\mathbf{L^2}H_3$ with benzylsodium (BnNa) in the presence of tmeda in hexane, followed by concentrating the solution and storage at −15 °C, gave $[PhSi\{(C_3H_3SiMe_3)Na\}_3\{tmeda\}_2]_2$, **[2.4]$_2$** in a 42% yield (Scheme 20). Complex **[2.4]$_2$**

has a different structure to that of complex **2.3**. In **[2.4]$_2$** there are two [PhSi{($C_3H_3SiMe_3$)Na}$_3$] moieties dimerise to give a hexametallic macrocycle, with two (of the three) sodium cations in the 'monomer' also coordinated by the tmeda nitrogen atoms.

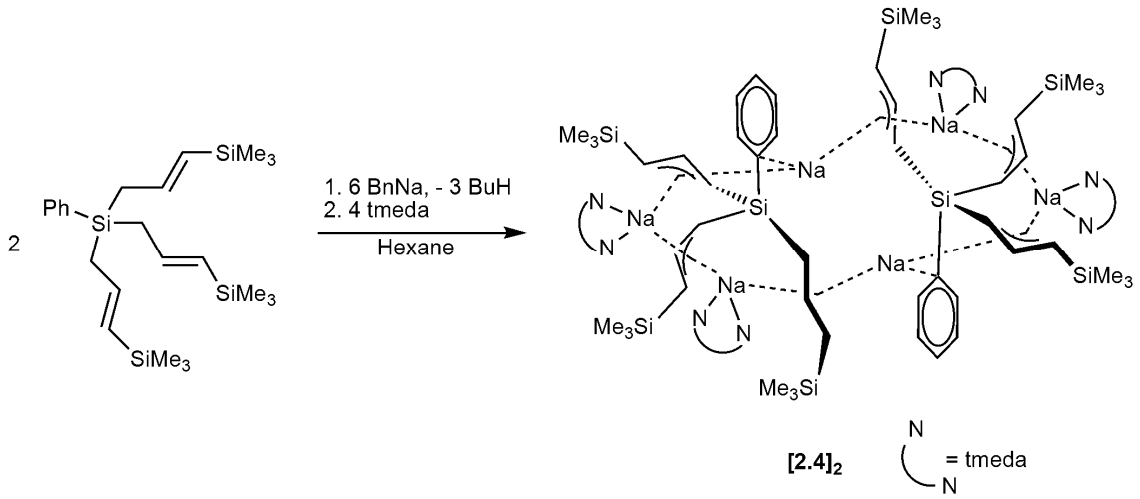

Scheme 20

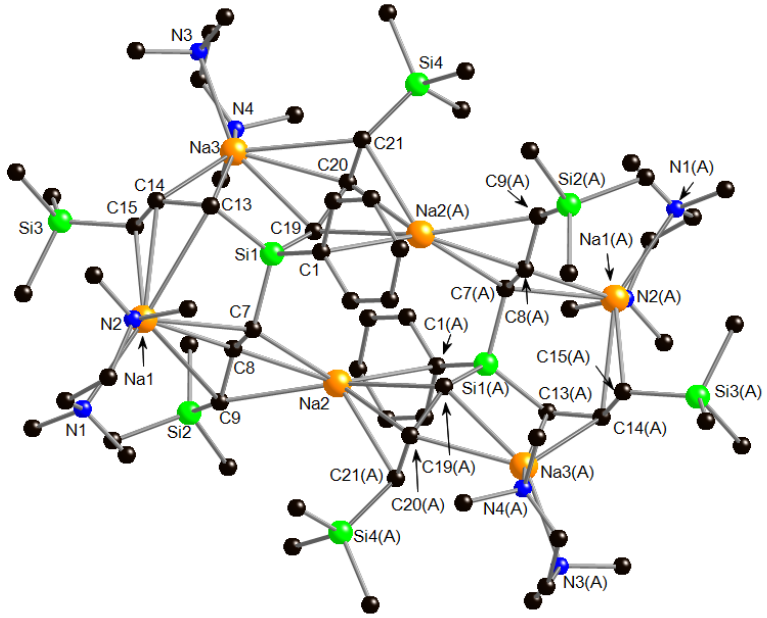

Figure 36: Molecular structure of [PhSi{($C_3H_3SiMe_3$)Na}$_3$]$_2$ [**2.4**]$_2$ selected bond lengths (Å) and angles (°). Hydrogen atoms have been omitted for clarity, carbon = black, silicon = green, sodium = pale orange, nitrogen = blue: C(7)−C(8) 1.415(5), C(8)−C(9) 1.365(6), C(13)−C(14) 1.391(5), C(14)−C(15) 1.401(5), C(19)−C(20) 1.379(6), C(20)−C(21) 1.245(8), C(9)−C(8)−C(7) 133.5(4), C(13)−C(14)−C(15) 131.6(3), C(19)−C(20)−C(21) 136.5(5), Na(1)–C(7) 2.577(3), Na(1)–C(8) 2.831(4), Na(1)–C(9) 3.472(6), Na(1)–C(13) 3.060(4), Na(1)–C(14) 2.768(4), Na(1)–C(15) 2.647(4), Na(2)–C(7) 2.698(4), Na(2)–C(8) 2.831(4), Na(2)–C(9) 2.795(5), Na(2)–C(19) 2.778(4), Na(2)–C(20) 2.549(4), Na(2)–C(21) 2.706(6), Na(2)−C(1) 2.869(3), Na(3)–C(13) 2.637(4), Na(3)–C(14) 2.679(4), Na(3)–C(15) 2.901(5), Na(3)–C(19) 2.628(4), Na(3)–C(20) 2.733(5), Na(3)–C(21) 3.080(6).

Complex **[2.4]$_2$** consists of two sodium cations bridging between two [**L**^{2}]$^{3-}$ anions and another four sodium cations bridging between the allyl moieties of the [**L**^{2}]$^{3-}$ anion to form the dimerised product. The silyl-allyl ligands are all coordinated in an η^3 manner and the trimethylsilyl substituents in **[2.4]$_2$** are in the [*exo,exo*][*endo,exo*]$_2$ stereochemistry, which is presumably to minimise the steric clashes between the ligands in the structure. The Na−C bond distances range from 2.549(4)-3.472(6) Å. The Na(1) and Na(3) cations in complex **[2.4]$_2$** are also coordinated by tmeda co-ligands, however Na(2) cations are not, this is likely to be due to steric crowding from the $SiMe_3$ substituents preventing coordination of the tmeda ligand. There is an additional cation-π interaction between Na(2) and the *ipso* carbon of the phenyl ring C(1).

The ^{1}H NMR spectrum of complex **[2.4]$_2$**, in benzene-d_6, is similar to that of **2.3**. The allyl proton resonances are seen as two series of overlapping multiplets at $\delta(^1H)$ = 2.92-3.81 ppm, which are mutually coupled to multiplets at $\delta(^1H)$ = 7.62-8.40 ppm with a ^3J = 30 Hz. Between $\delta(^1H)$ = 5.60-6.67 ppm are three coupled multiplets, which are also mutually coupled to a multiplet at 1.57-1.73 ppm. Due to the broadened resonances of the ^{1}H NMR spectrum, the integration of peaks was made cautiously.

The Na−C bond distances in complex **[2.4]$_2$** are typical for sodium complexes of π-bonded organo-ligands.[72,74] For example [Zn{$C_3H_3(SiMe_3)_2$}$_3$Na] **1.92**,[72] and [Na{1,3-$(SiMe_3)_2C_3H_3$}(thf)]$_4$ (**1.18**).[27] The additional π-cation interaction seen in **[2.4]$_2$** is common in organosodium complexes containing aromatic rings in close proximity to the sodium cation, and energy of the Na···Ph interaction is up to 25 kcal mol^{-1}.[75] As the cation-π interaction is not possible in the methyl-substituted analogue, complex **2.3**, it is likely that the cation-π interaction between Na(2) and C(1) has a structure-directing influence and may be responsible for the dimeric structure **[2.4]$_2$**.

The ^{1}H NMR spectrum does suggest that the dimeric structure is maintained in solution; however it also suggests the presence of two *ansa-tris*(allyl)sodium species in

a ratio of 3:1, which probably corresponds to the conversion between *exo*-to-*endo*/*endo*-to-*exo* stereochemistry of the silyl substituents.

2.3.5 $[MeSi\{(C_3H_3SiMe_3)_3\}\{K(OEt_2)_2\}_2KLi(\mu_4\text{-}O^tBu)]_2$ $[2.5]_2$

In an attempt to synthesise a potassium *ansa-tris*(allyl) complex, $\mathbf{L^1}H_3$ was treated with ^{n}BuLi, and then transmetallated with KO^{t}Bu in diethyl ether. X-ray crystallography showed that the transmetallation of lithium by potassium had occurred, however the 'by-product' lithium *tert*-butoxide had also been incorporated in the structure of the desired product to give the bimetallic dimer $[MeSi\{(C_3H_3SiMe_3)_3\}\{K(OEt_2)_2\}_2KLi(\mu_4\text{-}O^tBu)]_2$ (**[2.5]$_2$**) in a 10% yield (Scheme 21 and Figure 37). The low yield of this reaction suggests that the isolated product may not be the major product of the reaction, and is likely to be the least soluble product of the reaction.

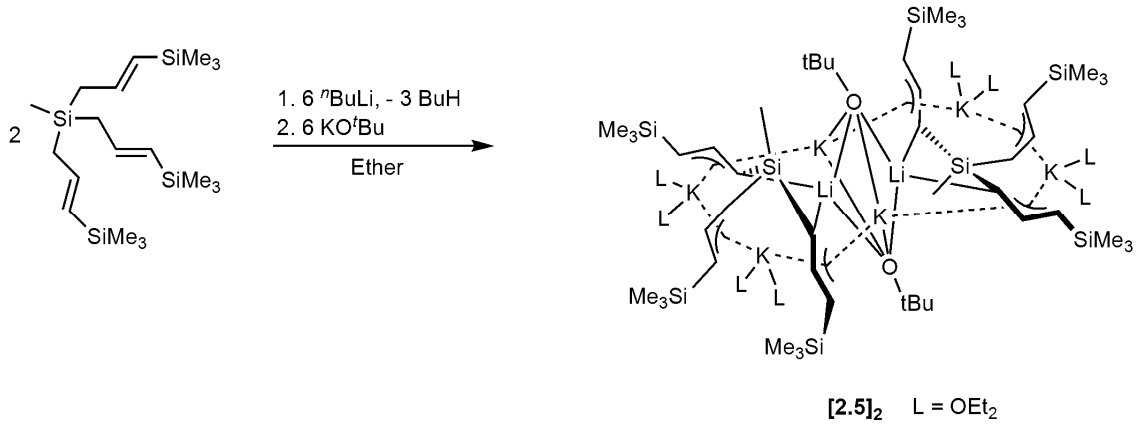

[2.5]$_2$ L = OEt_2

Scheme 21

The structure of **[2.5]$_2$** is similar to that of the sodium allyl **[2.4]$_2$**, the main difference being the orientation of the trimethyl silyl groups. In complex **[2.5]$_2$** the trimethylsilyl groups in one asymmetric unit adopt a [*exo,exo*]$_2$[*endo,exo*] stereochemistry, similar to that in the structures of complexes **1.21** and **2.1**. As with the sodium analogue **[2.4]$_2$**, the dimer **[2.5]$_2$** is centrosymmetric, with K−C distances lie within a broad range of 2.921(6)-3.544(6) Å (average 3.118 Å), which are typical of K−C_{allyl} bond distances.[22,24] Potassium atoms K(1) and K(2) in **[2.5]$_2$** are each solvated by two diethyl ether

molecules, whereas K(3) is between two silyl-allyl groups in the two halves of the dimer, in addition coordinated by the two $[O^tBu]^-$ groups. The silyl-allyl ligands in complex **[2.5]$_2$** bridge between the potassium cations in an η^3 manner, as is seen in all examples of potassium allyl complexes.[21,24]

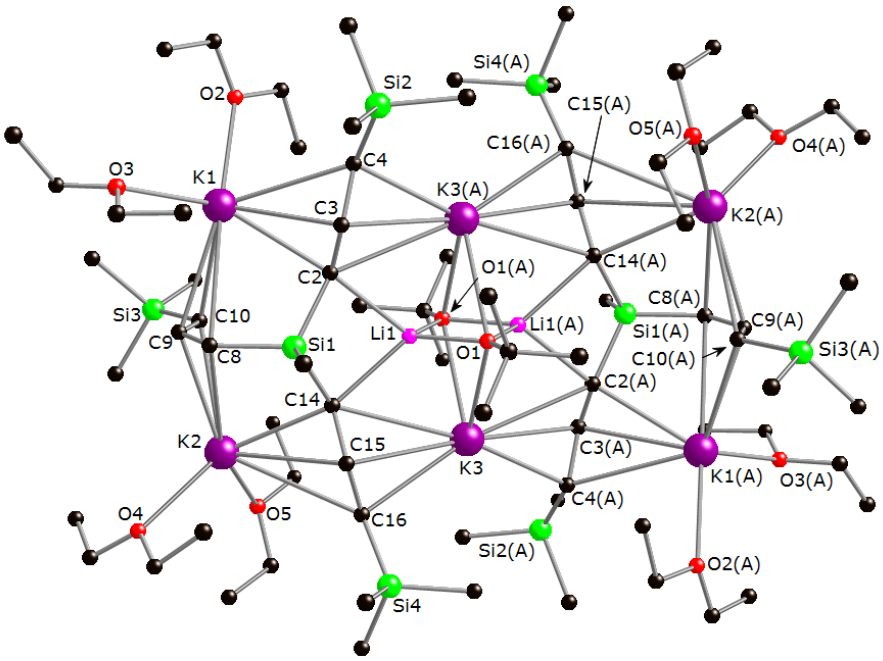

Figure 37: Molecular structure of the $[MeSi\{(C_3H_3SiMe_3)_3\}\{K(OEt_2)_2\}_2KLi(\mu_4\text{-}O^tBu)]_2$ **[2.5]$_2$** selected bond lengths (Å) and angles (°). Hydrogen atoms, ethyl carbons from diethyl ether and methyl carbons from trimethylsilyl groups are omitted for clarity, black = carbon, green = silicon, purple = potassium, red = oxygen, bright pink = lithium: C(2)−C(3) 1.392(8), C(3)−C(4) 1.383(8), C(8)−C(9) 1.363(8), C(9)−C(10) 1.394(8), C(14)−C(15) 1.391(8), C(15)−C(16) 1.397(8), C(4)−C(3)−C(2) 132.5(5), C(8)−C(9)−C(10) 131.3(6), C(14)−C(15)−C(16)132.1(5), K(1)−C(2) 2.921(6), K(1)−C(3) 3.062(5), K(1)−C(4) 3.308(6), K(1)−C(8) 3.196(6), K(1)−C(9) 3.014(6), K(1)−C(10) 3.157(6), K(2)−C(8) 3.069(6), K(2)−C(9) 2.967(6), K(2)−C(10) 3.090(6), K(2)−C(14) 2.930(6), K(2)−C(15) 3.210(6), K(2)−C(16) 3.544(6), K(3)−C(2) 3.252(5), K(3)−C(3) 3.102(5), K(3)−C(4) 3.005(6), K(3)−C(14) 3.309(6), K(3)−C(15) 3.116(6), K(3)−C(16) 3.003(6), K(3)−O(1) 2.829(4), K(3)−O(1A) 2.904(4), Li(1)−C(2) 2.326(11), Li(1)−C(14) 2.334(10), Li(1)−O(1) 1.889(10).

The ^{1}H NMR spectrum of **[2.5]$_2$**, as with the previously mentioned *ansa-tris*(allyl) complexes, is complicated in the allylic region. There is a series of broad overlapping multiplets between $\delta(^1H)$ = 5.25-6.41 ppm coupled with three broad doublets of doublets at $\delta(^1H)$ = 1.44-1.66 ppm that indicate, in benzene-d_6, conformational

fluxionality. The sharp singlet for the *tert*-butoxide protons at $\delta(^1H)$ =1.15 ppm overlaps with allylic resonances, preventing any accurate integration.

The solid-state structure of complex **[2.5]$_2$** is unlike most potassium allyl structures known because potassium allyls tend to have infinite polymeric structures rather than finite aggregates, for example $[K\{C_3H_3(SiMe_3)_2\}]_\infty$ (**1.14**),[21] $[(thf)_3K_2\{C_3H_3(SiMe_3)_2\}]_\infty$ (**1.14**)[24] and $[K_2\{(\eta^3\text{-}C_6H_4SiMe_3\text{-}6)_2SiMe_2\}(thf)_3]_\infty$ (**1.20**).[29] The trapped LiO^tBu in complex **[2.5]$_2$**, can be considered $[LiO^tBu]_2$ dimer with a four-coordinate Li cation being complexed by two of the allylic carbon atoms from the $[\mathbf{L^2}]^{3-}$ ligand. The bimetallic core of **[2.5]$_2$** is similar to that of the cage compound $[Li_4K_4(O^tBu)_8]$ in which the *tert*-butoxide ligands are μ_3- and μ_4-bridged between the cations.[76]

In comparison to the lithium *ansa-tris*(allyl) complexes, which had comparatively simple NMR spectra, the solution phase behaviour of the sodium and potassium complexes is noticeably different. In complexes **2.3**, **[2.4]$_2$** and **[2.5]$_2$**, it is possible owing to the larger size of the Na^+ and K^+ cations, and their higher coordination numbers, that the metal centres have influence over the co-ligands (tmeda or diethyl ether) and trimethylsilyl substituents. This influence may force the co-ligands or silyl substituents into energetically unfavourable interactions. Hence, when in solution, at room temperature there is temporary relief from these interactions. However, this is not seen in the lithium complexes **2.1** and **2.2** in the solution-state because the relatively small lithium cation can be accommodated by the ligand in such a way that steric clashes between tmeda and the trimethylsilyl groups are avoided.

2.4 Computational Studies of *Ansa-tris*(allyl) Complexes

X-ray crystallographic studies and NMR spectroscopic studies revealed that both in the solid-state and solution-state a variety of different structures are possible, with a range of alkali metal cations. Theoretical studies were undertaken to investigate the energy

differences between different conformations, and to see if unusual structures both in solid and solution-state could be explained. To study the structures, stereochemical preferences and relative engeries of alkali metal complexes of *ansa-tris*(allyl) ligands a collaboration with Dr. Jordi Poater and Prof. Miquel Solà (Universitat de Girona, Spain) and Prof. Dr. F. Matthias Bickelhaupt (Department of Theoretical Chemistry and Amsterdam Centre for Multiscale Modeling, Amsterdam) was undertaken to apply Density Functional Theory (DFT) to the pristine trianion $[MeSi\{C_3H_3(SiMe_3)\}_3]^{3-}$, and to complexes $[MeSi\{(C_3H_3SiMe_3)Li(tmeda)\}_3]$ (**1.21**) and $[MeSi\{(C_3H_3SiMe_3)$-$Na(tmeda)\}_3]$ (**2.3**), at various levels of theory. All calculations are based on density functional theory (DFT) and were carried out using the Amsterdam Density Functional (ADF) program, various levels of theory, up to BP86/DZP//BP86/DZP were used. Calculations on the other complexes were not undertaken due to the excessive computational time required. Figure 38 shows the structures of the different stereochemistries the pristine anion/complexes can adopt, this terminology will be used frequently within this section.

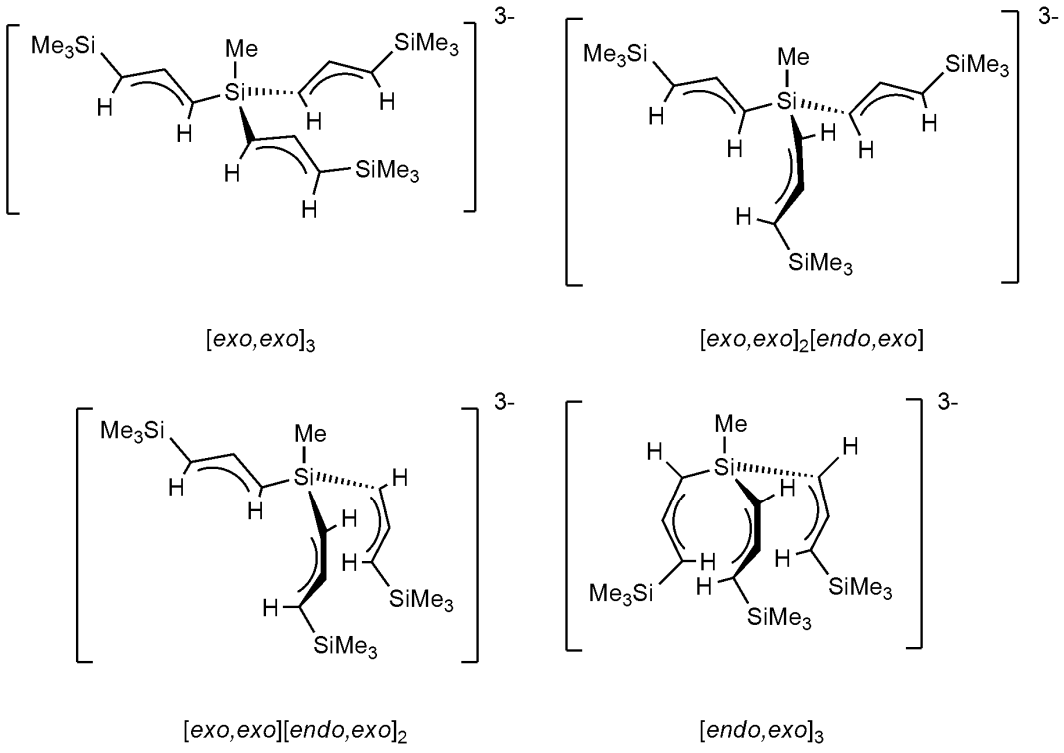

Figure 38: Definition of the *exo* and *endo* terminology used.

2.4.1 The Pristine Trianion, $[L^1]^{3-}$

Various levels of theory were applied to the pristine trianion (VWN/DZP//VWN/DZP, BP86/DPZ/VWN/DZP, BP86/TZ2P//VWN/DZP, BP86/TZ2P//BP86/TZ2P and COSMO-BP86/TZ2P//VWN/DZP (COSMO - COnductor-like Screening MOdel). Regardless of the level of theory applied, the most energetically favourable stereochemistry for the trimethylsilyl substituents in the pristine trianion $[MeSi\{C_3H_3(SiMe_3)\}_3]^{3-}$ is $[exo,exo]_3$. The calculations also show that, with respect to the central SiMe group, the stability of the anion structure decreases with an increasing number of allyl groups in the *endo* stereochemistry, presumably due to steric reasons. (Table 2 and Figure 38).

2.4.2 Complex $[MeSi\{(C_3H_3SiMe_3)Li(tmeda)\}_3]$ (1.21)

Upon coordination to three $[Li(tmeda)]^+$ cations, the pristine trianion $[\mathbf{L^1}]^{3-}$ has a change in the energetically favoured structure from the $[exo,exo]_3$ to $[exo,exo]_2[endo,exo]$ with the VWN/DZP//VWN/DZP method, which is in agreement with experiment (Table 2 and Figure 39). In all levels of theory used, the $[exo,exo]_3$ and $[exo,exo]_2[endo,exo]$ conformations of complex **1.21** are essentially equal in energy and all other levels of theory (except VWN/DZP//VWN/DZP) slightly favour the $[exo,exo]_3$ conformation of complex **1.21**. Therefore revealing the $[exo,exo]_3$ and $[exo,exo]_2[endo,exo]$ forms to be very close in energy. Taking into consideration the fact the $[exo,exo]_3$ and $[exo,exo]_2[endo,exo]$ stereochemistries are so close in energy and there are a variety of different structures available from experiment it is possible to say that the solvent may play a role in determining the preferred stereochemistry of the ligand in the complex.

An estimation of environment effects in water was calculated using COSMO model at the BP86/TZ2P//VWN/DZP level of theory on complex **1.21**. From Table 2, it can be

seen that solvation has very little effect on the outcome of the structure. However, the COSMO model does not take into account specific interactions and only considers the environment as an average, therefore the effects of environment can only be considered a rough estimation. Selected key bond lengths for crystallographically determined and computed structures of **1.21** show good agreement between experiment and theory (Table 3). The VWN-level calculations gave more accurate bond lengths, compared to the BP86/DZP and BP86/TZ2P-levels of theory, for the lithium cation environment, *i.e.* the Li−C, Li−N, allyl C−C and C−Si bond lengths. However, the BP86 level calculations give a better reproduction of the location of the $[Li(tmeda)]^+$ cation.

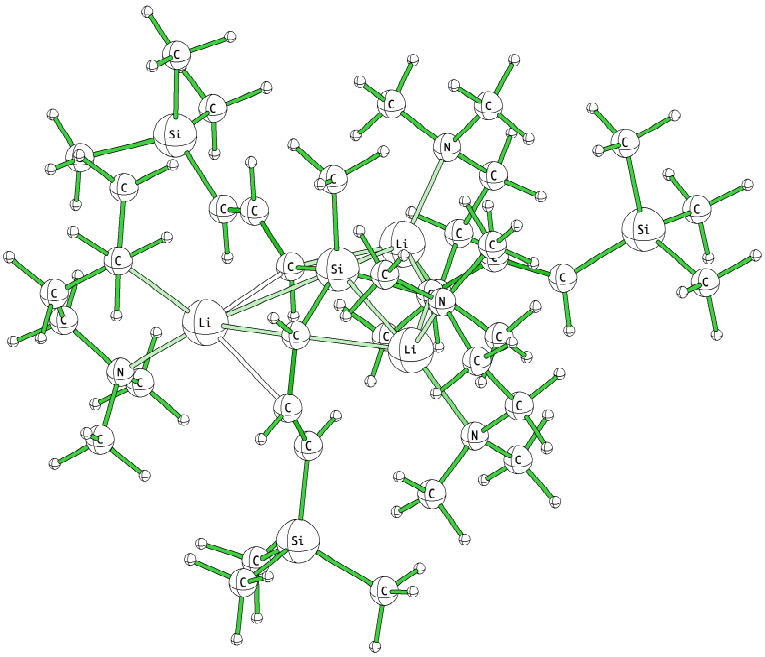

Figure 39: Structure of *exo,exo,endo*-[MeSi{$C_3H_3SiMe_3$}$_3${Li(tmeda)}$_3$] (**1.21**) computed at the BP86/DZP level of theory.

2.4.3 Complex [MeSi{($C_3H_3SiMe_3$)Na(tmeda)}$_3$] (2.3)

For complex **2.3** at all levels of theory (apart from VNW/DZP//VWN/DZP) the [*exo,exo*]$_2$[*endo,exo*] stereochemistry was found to be most stable, with the [*endo,exo*]$_3$ being the least stable configuration by 4.8-6.0 kcal mol^{-1} The [*exo,exo*]$_3$ conformation of complex **2.3** was calculated to be the third highest energy, and the [*exo,exo*][*endo,exo*]$_2$ conformation (one of the disordered forms of complex **2.3** determined by X-ray

crystallography) is the second highest in energy. However if the COSMO method is used to model solvation effects the relative energies of the conformations invert. These results partially contradict experimental observations. The [*exo,exo*][*endo,exo*]$_2$ conformation is quite close to the lowest energy conformation, in agreement with experiment; the [*endo,exo*]$_3$ conformation which should be the most stable form, is higher in energy than both the [*exo,exo*]$_2$[*endo,exo*] and [*exo,exo*][*endo,exo*]$_2$ which is in disagreement with experiment. This disagreement between theory and experiment may be due to the fact that the model systems used do not take into account factors such as van der Waals interactions between neighbouring molecules of **2.3**, and crystallographic disorder effects. However, despite the difference in favoured stereochemistry of the trimethylsilyl substituents there is good agreement with the X-ray data and calculated bond distances (Table 4). The VWN level of theory produces more accurate Na−C and Na−N bond distances compared to the BP86 level of theory, whereas BP86 gives more accurate Si−C and C−C distances than the VWN level of theory.

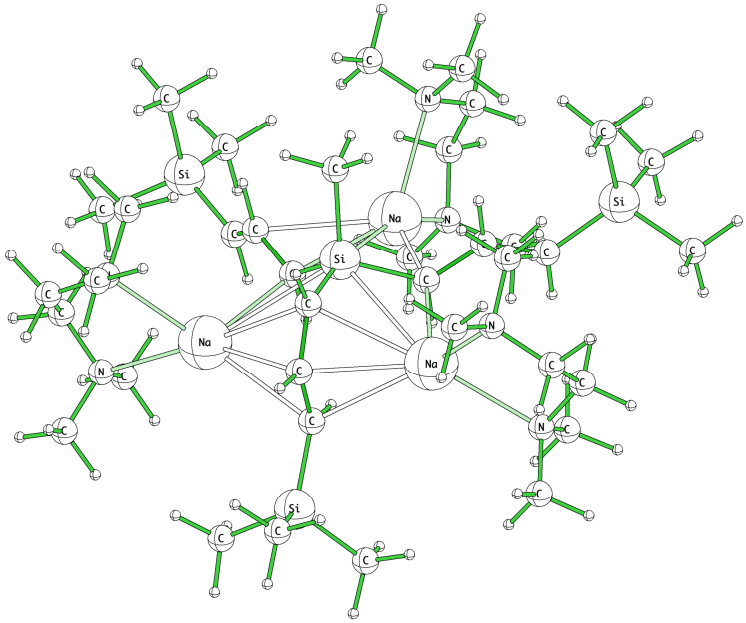

Figure 40: Structure of *exo,exo,endo*-[MeSi{$C_3H_3SiMe_3$}$_3${Na(tmeda)}$_3$] (**2.3**) computed at the BP86/DZP level of theory.

Table 2: Relative energies, ΔE in kcal mol^{-1}, of the structural configurations of the pristine anion $[\mathbf{L^1}]^{3-}$, complex **1.21** and complex **2.3**

[exo,exo]$_n$[endo,exo]$_{3-n}$	**$[L^1]^{3-}$**	**1.21[a]**	**2.3**
VWN/DZP//VWN/DZP			
n = 3	0.0	10.6	11.5
n = 2	2.8	6.2	4.9
n = 1	5.4	6.0	1.4
n = 0	7.6	0.0	0.0
BP86/DZP//VWN/DZP			
n = 3	0.0	0.0	4.6
n = 2	4.2	0.8	0.0
n = 1	8.3	7.3	0.8
n = 0	11.8	7.6	4.8
BP86/TZ2P//VWN/DZP			
n = 3	0.0	0.0	4.8
n = 2	4.6	2.0	0.0
n = 1	9.1	10.0	3.3
n = 0	13.0	11.0	6.8
BP86/DZP//BP86/DZP			
n = 3	0.0	0.0	4.8
n = 2	3.7	0.0	0.0
n = 1	7.3	4.3	1.0
n = 0	10.5	5.0	5.0
BP86/TZ2P// BP86/TZ2P			
n = 3	[b]	0.0	[b]
n = 2	[b]	1.2	[b]
n = 1	[b]	[b]	[b]
n = 0	[b]	[b]	[b]
COSMO-BP86/TZ2P//VWN/DZP			
n = 3	0.0	0.0	1.9
n = 2	2.7	2.4	0.0
n = 1	5.3	10.5	2.8
n = 0	8.1	10.6	7.2

[a] see ref 30 [b] not computed

Table 3: Selected bond distances (Å) for *exo,exo,endo*-[MeSi{$C_3H_3SiMe_3$}$_3${Li(tmeda)}$_3$ (**1.21**)

Distances	**X-Ray[a]**	**VWN/DZP[b]**	**BP86/DZP[b,c]**	**BP86/TZ2P[b,c]**
Si(1)−C(2)	1.851	1.854/1,848	1.869/1.872	1.872/1.875
Si(1)−C(8)	1.858	1.859	1.882	1.884
C(2)−C(3)	1.416	1.400/1.404	1.422/1.421	1.424/1.422
C(3)−C(4)	1.384	1.378/1.376	1.389/1.390	1.392/1.395
C(8)−C(9)	1.401	1.402	1.426	1.425
C(9)−C(10)	1.383	1.392	1.396	1.400
Li(1)−C(2)	2.289	2.206/2.273	2.344/2.307	2.366/2.304
Li(1)−C(8)	2.283	2.190/2.344	2.296/2.286	2.298/2.277
Li(1)−C(9)	2.696	2.619/2.267	2.563/2.738	2.494/2.771
Li(2)−C(2)	2.258	2.223/2.183	2.289/2.313	2.295/2.318
Li(1)−N(1)	2.088	2.105/2.014	2.266/2.240	2.196/2.138
Li(1)−N(2)	2.171	2.157/2.111	2.158/2.127	2.322/2.266
Li(2)−N(3)	2.169	2.069	2.164	2.182
Li(2)−N(4)	2.017	2.024	2.135	2.149

[a] data from ref 30 [b] this work [c] numerical error of *ca*. 0.3 kcal mol^{-1} due to oscillating geometry optimization

Table 4: Selected bond distances (Å) and angles (°) for *exo,exo,endo*-[MeSi{$C_3H_3SiMe_3$}$_3${Na(tmeda)}$_3$ (**2.3**)

Distances & Angles	X-Ray[a]	VWN/DZP[b]	BP86/DZP[b,c]
Si(1)−C(2)	1.874	1.779	1.885
Si(1)−C(8)	1.847	1.965	1.874
Si(1)−C(14)	1.864	1.878	1.888
Na(1)−C(8)	2.718	2.553	2.681
Na(1)−C(9)	2.553	2.724	2.954
Na(1)−C(10)	3.016	3.040	3.409
Na(1)−C(14)	2.614	2.675	2.770
Na(1)−C(15)	2.856	2.612	2.725
Na(2)−C(14)	2.819	2.859	2.855
Na(2)−C(15)	2.652	2.684	2.773
Na(2)−C(16)	2.605	2.680	2.874
Na(2)−C(2)	2.587	2.692	2.737
Na(2)−C(3)	2.762	2.746	2.916
Na(3)−C(2)	2.882	3.000	3.002
Na(3)−C(3)	2.689	2.725	2.770
Na(3)−C(4)	2.677	2.592	2.714
Na(3)−C(8)	2.575	2.545	2.667
Na(3)−C(9)	2.837	3.264	3.339
Na(1)−N(1)	2.501	2.493	2.624
Na(1)−N(2)	2.485	2.469	2.611
Na(2)−N(3)	2.500	2.525	2.669
Na(2)−N(4)	2.500	2.488	2.637
Na(3)−N(5)	2.505	2.482	2.600
Na(4)−N(6)	2.549	2.655	2.668
C(2)−C(3)	1.395	1.366	1.404
C(3)−C(4)	1.368	1.407	1.416
C(8)−C(9)	1.463	1.398	1.415
C(9)−C(10)	1.383	1.391	1.402
C(14)−C(15)	1.391	1.360	1.402
C(15)−C(16)	1.344	1.406	1.416
C(2)−C(3)−C(4)	132.3	131.1	132.4
C(8)−C(9)−C(10)	132.4	129.3	130.4
C(14)−C(15)−C(16)	132.9	128.6	129.9
N(1)−Na(1)−N(2)	72.98	74.9	71.8
N(3)−Na(2)−N(4)	73.63	71.1	69.3
N(5)−Na(3)−N(6)	73.2	73.7	72.6
Na(1)−C(9)−Na(3)	140.8	113.3	114.2
Na(1)−C(15)−Na(2)	129.6	117.8	132.9
Na(2)−C(3)−Na(3)	130.5	121.2	125.4

[a] data from ref 30 [b] this work [c] numerical error of *ca.* 0.3 kcal mol^{-1} due to oscillating geometry optimization

2.5 Summary of *Ansa-tris*(allyl) Complexes

In summary, the lithium, sodium and potassium complexes of the *ansa-tris*(allyl) ligands $\mathbf{L}^1H_3$ and $\mathbf{L}^2H_3$ have been synthesised and characterised by X-ray crystallography and NMR spectroscopy. In the solid-state, complexes **2.1**, **2.2**, **2.3**,

[**2.4**]$_2$ and **[2.5]$_2$** show that a combination of the alkali metal, denticity of the co-ligand (tmeda or pmdeta) and the substituent on the central silicon atom all influence the stereochemistry of the trimethylsilyl groups. Theory calculations at (VWN/DZP//VWN/DZP, BP86/DPZ/VWN/DZP, BP86/TZ2P//VWN/DZP, BP86/TZ2P//BP86/TZ2P and COSMO-BP86/TZ2P//VWN/DZP) levels of theory concluded that the [*exo,exo*]$_3$ and the [*exo,exo*]$_2$[*endo,exo*] conformations of the complexes **1.21** and **2.3** were at similar energies.

2.5 Conclusions

Five new *ansa-tris*(allyl) alkali metal complexes have been synthesised and crystallographically characterised. The crystal structures of complexes **2.1**, **2.2**, **2.4**, **[2.4]$_2$** and **[2.5]$_2$** have shown that in the solid-state the structure is dependent on the combination of alkali metal radius, the denticity of the co-ligand and the substituent on the central silicon atom.

Complex [PhSi{($C_3H_3SiMe_3$)Li(tmeda)}$_3$] **2.1** is iso-structural to complex [MeSi{($C_3H_3SiMe_3$) Li(tmeda)}$_3$] **1.21.**[30] The allyl ligands are in a mixed coordination mode of (μ:η^2)(μ:η^1)$_2$ with the trimethylsilyl substituents in an [*exo,exo*]$_2$[*endo,exo*] conformation. The lithium cation is four-coordinate, and in a distorted tetrahedral geometry. The ^{1}H and ^{13}C NMR spectra confirm the [*exo,exo*]$_2$[*endo,exo*] conformations in benzene-d_6 at room temperature.

The influence of a higher denticity co-ligand was investigated using terdentate pmdeta, in the complex [MeSi{($C_3H_3SiMe_3$)Li(pmdeta)}$_3$] **2.2**. The trimethylsilyl substituents in complex **2.2** are in the more conventional [*exo,exo*]$_3$ conformation. Each lithium cation is coordinated by an allyl in an η^3 manner and is also coordinated by the pmdeta. Coordination of lithium by pmdeta is preferential to forming the μ-allyl bridging mode seen in complex **2.1**. The ^{1}H and ^{13}C NMR spectra in benzene-d_6 at room

temperature, reveals there are three similar allylic environments of [(pmdeta)Li($C_3H_3SiMe_3$)], and three similar $SiMe_3$ substituents.

Replacement of the smaller Li^+ cation with Na^+ resulted in [MeSi{($C_3H_3SiMe_3$)Na(tmeda)}$_3$] **2.3**, in the solid-state two of the three $SiMe_3$ substituents are in the [*endo,exo*] conformation, with the third experiencing disorder resulting in a 51:49 [*endo,exo*]:[*exo,exo*]. The sodium cations are also coordinated by the tmeda co-ligand. The ^{1}H NMR spectrum, in benzene-d_6, showed trimethylsilyl groups, with a broad singlets for the two tmeda environments. The allyl proton signals occur as complicated overlapping which are likely to correspond with there being several species in solution due to the *endo* and *exo* stereochemistries of the silyl-allyl groups, and their relative orientation in relation to tmeda.

Complex [PhSi{($C_3H_3SiMe_3$)Na}$_3$]$_2$ **[2.4]$_2$** is a centrosymmetric dimer in which sodium cations bridge between either the internal silyl-allyl ligands of the [$\mathbf{L^2}$]$^{3-}$ anion or bridging between the two [$\mathbf{L^2}$]$^{3-}$ monomers to form the dimerised product. There is an additional interaction between Na(2) and the *ipso* carbon of the phenyl ring C(1) and it can be assumed this interaction may be a structure-directing influence and responsible for the dimeric structure. The trimethylsilyl substituents are in the [*exo,exo*][*endo,exo*]$_2$ stereochemistry. The ^{1}H NMR spectrum does suggest that the dimeric structure is maintained in solution.

Finally, [MeSi{($C_3H_3SiMe_3$)$_3$}{K(OEt_2)$_2$}$_2$KLi(μ_4-O^{t}Bu)]$_2$ **[2.5]$_2$** is a centro-symmetric dimer, similar to that of the sodium analogue **[2.4]$_2$**, however the trimethylsilyl groups adopt a [*exo,exo*]$_2$[*endo,exo*] stereochemistry. The trapped [LiO^{t}Bu]$_2$ dimer contains a four-coordinate Li cation being complexed by two of the allylic carbon atoms from the [$\mathbf{L^2}$]$^{3-}$ ligand. The ^{1}H NMR spectrum, as with the previously mentioned *ansa-tris*(allyl) complexes, is complicated in the allylic region, as well as the resonances for the diethyl ether and *tert*-butoxide protons.

At the different levels of theory, DFT calculation revealed that for on complexes **1.21** and **2.3** there is little difference in the stability the [*exo,exo*]$_3$ and the [*exo,exo*]$_2$[*endo,exo*] conformations, as well as showing that the [*exo,exo*]$_3$ conformation for the pristine trianion $\mathbf{[L^1]^{3-}}$ is the most stable. Even though DFT calculations revealed that there are some energy differences between the different possible structures, the energy differences aren't large enough to exclude the formation of these structures in experiment.

Chapter 3

Introduction to Donor-functionalised Organometallic Ligands

3.1 An Introduction to Donor-Functionalised Allyl Chemistry

In the complex of a donor-functionalised ligand the metal is *intra*molecularly solvated by an attached Lewis base donor group. This functionality allows control to be exerted over the chemistry of the organometallic compound.[22] Donor-functionalised allyl ligands are uncommon compared to donor-functionalised cyclopentadienyl ligands (Figure 41), which have been investigated since 1970's, with a lot of work being put into a range of donor atoms, particularly *O*-[77] and *N*-donor atoms.[78,79]

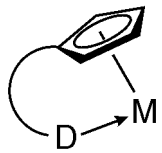

Figure 41: General structure of a donor-functionalised cyclopentadienyl ligand.

3.2 Donor-Functionalised Metal Allyl Complexes

Fraenkel *et al.* have investigated lithium allyl complexes containing *bis*(2-methoxyethyl)amino and related groups. The donor-functionalised allyl complexes can potentially be used in regioselective organic synthesis.[4,80,81] Complex **3.1** (Scheme 22) has been the subject of extensive NMR spectroscopic and crystallographic studies.[7,8,82,83] These studies revealed that the formal negative charge of the allylic anion can be partially localised on one terminal carbon, owing to the pendant donor group holding the cation over one terminal. This partial localisation effect has been called "site-specific electrostatic perturbation of conjugation" (SSEPOC).[9]

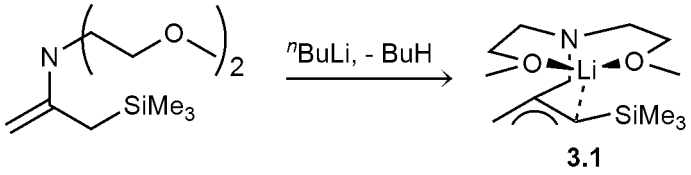

3.1

Scheme 22

An X-ray crystallographic study of [Li{C_3H_2(1,3-$SiMe_3$)$_2$($CH_2N(CH_2CH_2OCH_3)_2$)}] (**3.2**) (Scheme 23) shows that unlike previously discussed lithium allyl complexes (Chapters 1 and 2), the structure is monomeric in the solid-state. The allyl C−C bond lengths of 1.431(3) and 1.351(3) Å[83] are similar to those of the externally solvated [(tmeda)Li{$C_3H_3(SiMe_3)_2$}] (**1.8**), which has C−C bond lengths of 1.423(7) and 1.382(7) Å. The molecular structure of **3.2** also shows that the lithium is coordinated by one terminal carbon of the allyl ligand, which is reflected in the short Li−C_3 bond length 2.186(4) Å and the longer C_2−C_3 bond length of 1.431(3) Å, and terminal carbon.

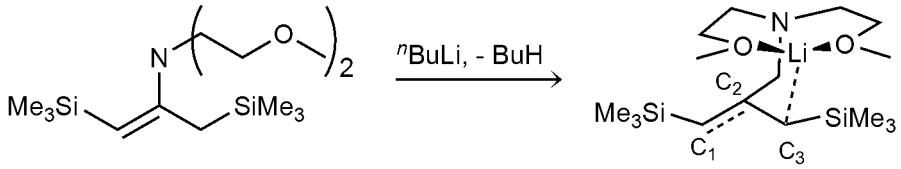

3.2

Scheme 23

Fraenkel *et al.* have also worked with ligands in which the donor group was in a position other than the C_2 (central carbon) atom; the methoxyethyl amino group on a terminal silyl group, for example, showed that the Li^+ cation is held towards one end of the allyl ligand (Figure 42).[84]

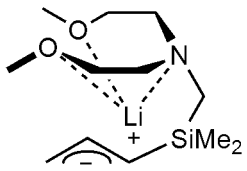

3.3

Figure 42: An example of a allyllithium complex in which the donor-functionalised group is positioned on the silicon atom, rather than the C_2 position of the allyl

The donor-functionalised ligand *N*-piperidinyl allylsilane (**3.4**)$(H)_2$ can be reacted with either one or two equivalents of ^{t}BuLi (Scheme 24) to give two different cyclic structures, [(**3.4**)(H)Li]$_4$ and [(**3.4**)Li_2]$_6$ (Figure 43).[85]

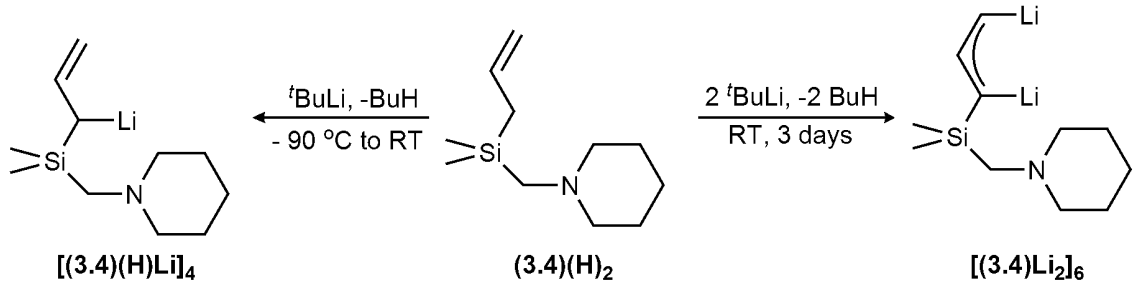

$[(\mathbf{3.4})(H)Li]_4$ $(\mathbf{3.4})(H)_2$ $[(\mathbf{3.4})Li_2]_6$

Scheme 24

The mono-lithiated complex $[(\mathbf{3.4})(H)Li]_4$ is a tetramer in which the allyl ligand bridges between lithium cations forming a Li-allyl 8-membered ring; with one allyl ligand coordinated in an η^3 manner and the other in an η^1 manner, and the piperidinyl nitrogen coordinated to the lithium cation. The Li–C bond distances range from 2.245(5) to 2.338(5) Å. The Li–C bond distances to the carbon in the α-positions, with respect to the silicon, are 2.268(4) and 2.338(5) Å for the η^3-coordinated allyl and the η^1-coordinated allyl, respectively.

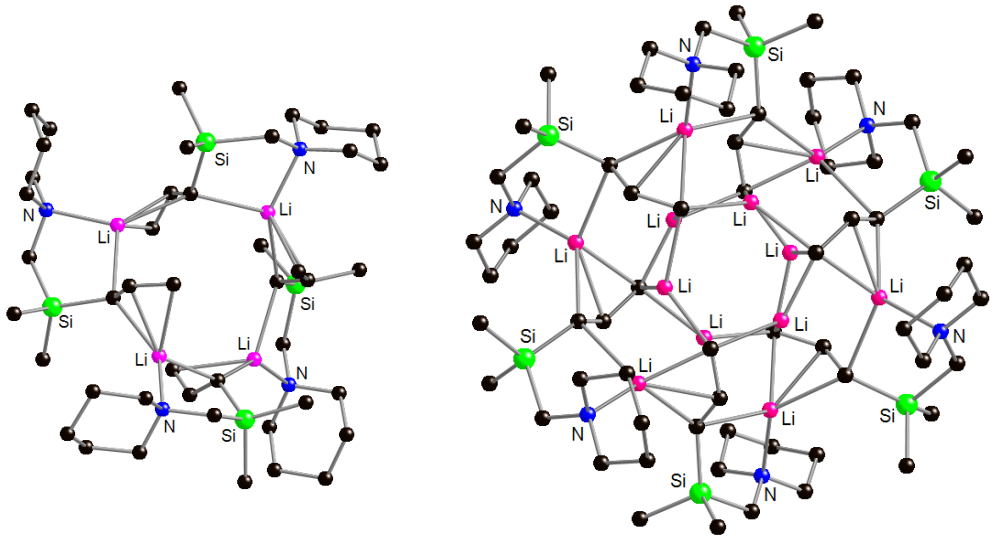

Figure 43: Molecular structures of $[(\mathbf{3.4})(H)Li]_4$ (left) and $[(\mathbf{3.4})Li_2]_6$ (right). Hydrogen atoms have been omitted for clarity, carbon = black, silicon = green, nitrogen = blue, lithium = pink. Reproduced from ref. 85

Complex $[(\mathbf{3.4})Li_2]_6$ can be regarded as an expanded version of complex $[(\mathbf{3.4})(H)Li]_4$, in which the Li cation and allyl units are part of a 12-membered ring. In $[(\mathbf{3.4})Li_2]_6$ the Li–C bond lengths fall into a much broader range of 2.110(7) to 2.372(5) Å; the Li–C

bond distances to the η^3 coordinated allyl are 2.372(5) and 2.163(6) Å to the α and terminal carbon atoms, respectively. In complex [(**3.4**)(H)Li]$_4$ the allyl C−C bond distances are 1.352(4) and 1.424(3) Å, suggesting that the negative charge is more localised. However, in complex [(**3.4**)Li$_2$]$_6$ the C−C allyl bond lengths are 1.400(5) and 1.423(6) Å, which suggest delocalisation of the negative charge across the allyl ligand.

3.3 Donor-Functionalised Cyclopentadienyl Complexes

One of the most important ligand systems in organometallic chemistry is the cyclopentadienyl ligand (C_5H_5, Cp), which forms a vast range of complexes with s-, p-, d- and f-block metals.[86] There are many examples of donor-functionalised Cp complexes in the literature owing to the fact this area of chemistry has been under investigation for 60 years. Several review articles are avalible.[22,77-79,87,88] Therefore a short review focusing on s-block and f-block cyclopentadienyl complexes will be used to explore the extent to which a donor group within the ligand affects the structure of a complex.

3.3.1 Donor-Functionalised s-Block Metal Cyclopentadienyl Complexes

The thf donor-functionalised Cp ligand (**3.5**) was treated with metallic sodium in thf to give the tetrahydrofuranate complex [Na{$C_5H_4(CH_2(C_4H_7O))$}·thf]$_\infty$ (**3.6**) (Scheme 25).[89] The Cp ring of the ligand bridges between two sodium cations in **3.6** in an η^5 manner, the oxygen atom of the internal thf donor group coordinates to the sodium as well as the oxygen atom of the external thf solvent molecule. The C−C bond distances in **3.6** range from 2.697(4) to 2.967(5) Å.

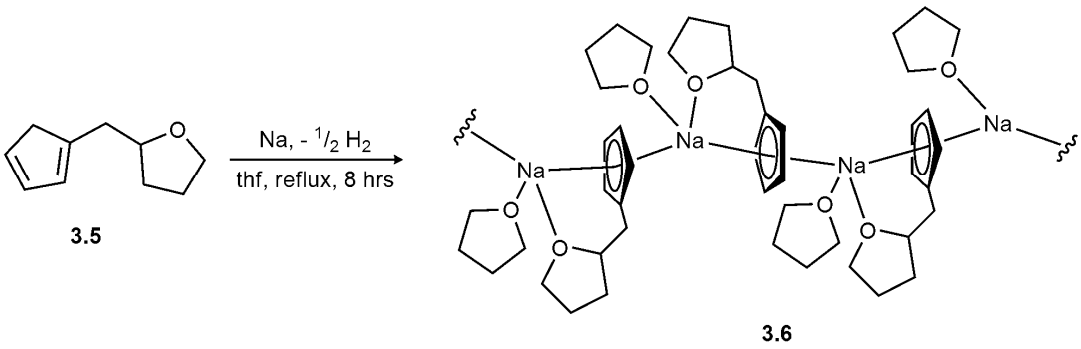

Scheme 25

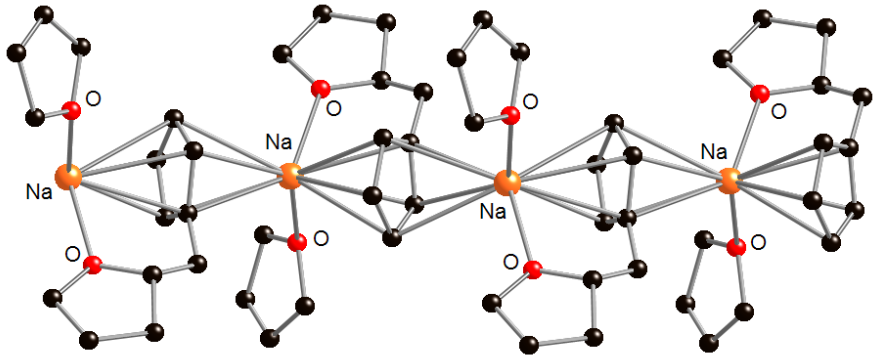

Figure 44: Molecular structure of $[Na\{C_5H_4(CH_2(C_4H_7O))\}\cdot thf]_\infty$ (**3.6**). Hydrogen atoms have been omitted for clarity, carbon = black, sodium = orange, oxygen = red. Reproduced from ref. 89

In the early 1990's Siemeling synthesised a range of *O*-donor functionalised cyclopentadienyl ligands of general formula $C_5HR_4{-}Z{-}(OCH_2CH_2)_nOMe$ (**3.7**), **3.7a**H: R = H, *n* = 2, Z = $SiMe_2$; **3.7b**H: R = H, *n* = 3, Z = $SiMe_2$; **3.7c**H: R = Me, *n* = 2, Z = $SiMe_2$; **3.7d**H: R = Me, *n* = 3, Z = $SiMe_2$; **3.7a**H: R = Me, *n* = 3, Z = $CH_2CH_2CH_2$. All the ligands reacted with potassium, in benzene or toluene, to give the corresponding potassium complexes $[K\{C_5HR_4{-}Z{-}(OCH_2CH_2)_nOMe\}]$ (**3.8**).[90,91] NMR spectroscopic studies showed the complexes to be monomeric, in benzene-d_6, unlike the unfunctionalised counter parts such as CpK and Cp*K which are coordination polymers and are only soluble in ether solvents.

As well as oxygen donor-functionalised Cp ligands there are *N*-donor-functionalised Cp ligands such as **3.9**[92,93] and **3.10**[94] (see Figure 45).

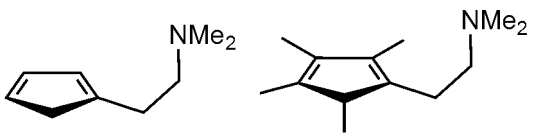

3.9 **3.10**

Figure 45: *N*-donor functionalised Cp and Cp* ligands

Ligands **3.9** and **3.10** were treated with either *n*-butlyllithium or potassium hydride in thf or diethyl ether to give the corresponding Cp complexes: $[Li\{C_5R_4(CH_2CH_2NMe_2)\}]$ where R = H (**3.11**), R = Me (**3.12**), and $[K\{C_5R_4(CH_2CH_2NMe_2)\}]$ where R = H (**3.13**), R = Me (**3.14**). However, on all these compounds the only characterisation was by IR spectroscopy and elemental analysis on complex **3.13**. More recently, a lithium complex of the *N*-donor-functionalised cyclopentadienyl ligand **3.15**$(H)_3$ was synthesised and structurally characterised (Figure 46).[95]

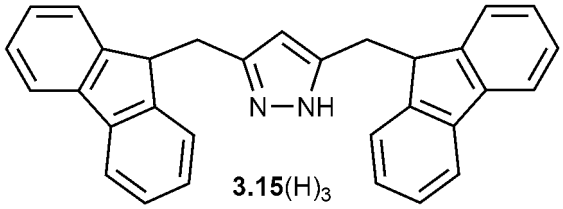

3.15$(H)_3$

Figure 46: Structure of ligand **3.15**$(H)_3$

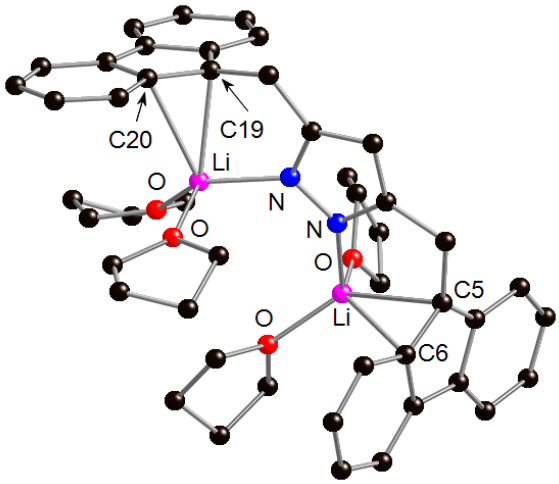

Figure 47: Molecular structure of the anion of $[Li_2(\mathbf{3.15})][Li(thf)_4]\cdot 0.5(thf)$. Hydrogen atoms have been omitted for clarity, carbon = black, oxygen = red, nitrogen = blue, lithium = pink. Reproduced from ref. 95

The complex $[Li_2(\mathbf{3.15})][Li(thf)_4]\cdot 0.5(thf)$ is a solvent-separated ion-pair. Within the anion of the complex each lithium cation is coordinated by the "Cp ring" in an η^2 manner, as well as one *N*-donor atom from the pyrazolate group, and two oxygen atoms from the two thf solvent molecules. The Li−C bond distance to the 5-membered ring are 2.485(7), 2.489(7), 2.412(7) and 2.593(6) Å for Li−C(5), Li−C(6), Li−C(19) and Li−C(20), respectively, with the Li···C distances to the other carbon atoms of the 5-membered ring being in the range of 2.88 to 3.43 Å (as quoted), which is outside the normal bonding range for lithium to carbon bonds.[95]

Unlike group 1 metals, there are several crystallographically characterised examples of group 2 donor-functionalised Cp complexes. In the case of magnesium, ligands **3.9** and **3.10** were reacted with alkyl Grignard reagents to give halogen-bridged dimeric Grignard compounds; $[(Me_2NCH_2CH_2)C_5H_4MgBr]_2$ (**3.16**), $[(Me_2NCH_2CH_2)$-$C_5Me_4MgX]_2$ where X = Cl (**3.17**) and X = Br (**3.18**). Only the structure of complex **3.18** was determined by X-ray crystallography.[96] The Cp ring is η^5-coordinated to the magnesium cation, which is also coordinated by the amino group and the two bridging bromide anions. However, the dimeric structure is broken on addition of excess thf to give the monomeric complex **3.19** (Scheme 26), in which the magnesium cation has a similar coordination environment, where one bromide anion is replaced by a thf ligand.

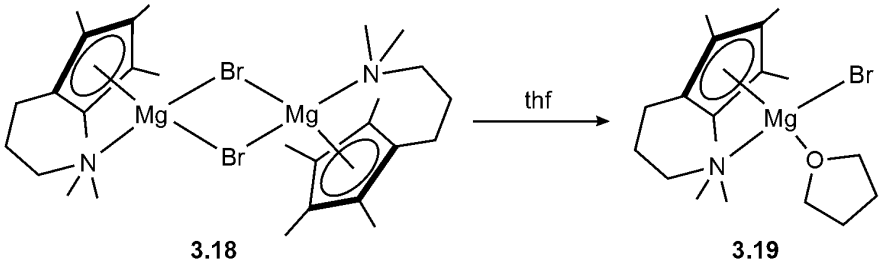

3.18 **3.19**

Scheme 26

The Mg−C bond lengths in complexes **3.18** and **3.19** range from 2.344(5) to 2.432(5) Å and 2.363(5) to 2.484(6) Å, respectively, which are similar to the Mg−C bond lengths in the unfunctionalised magnesocene $[Mg(^tBu\text{-}C_5H_4)_2]$[97] (**3.20**).

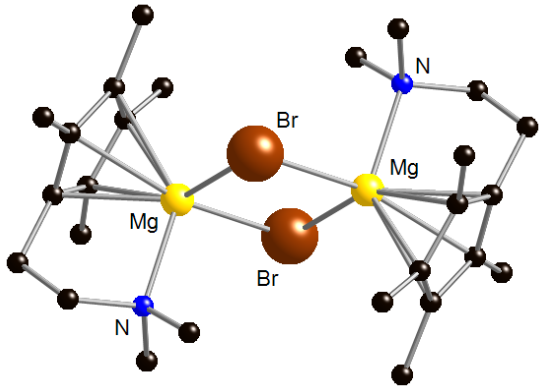

Figure 48: Molecular structure of $[(Me_2NCH_2CH_2)C_5Me_4MgBr]_2$ (**3.18**). Hydrogen atoms have been omitted for clarity, carbon = black, magnesium = yellow, nitrogen = blue, bromine = brown. Reproduced from ref. 96

Donor-functionalised cyclopentadienyl complexes of calcium structures include those seen in Figure 49. Complexes **3.21**[98] and **3.22**[99] possess a bent metallocene geometry, with the calcium in a distorted tetrahedral environment, with the two Cp rings coordinated in an η^5 manner and the two methoxy substituents also coordinated to the metal.

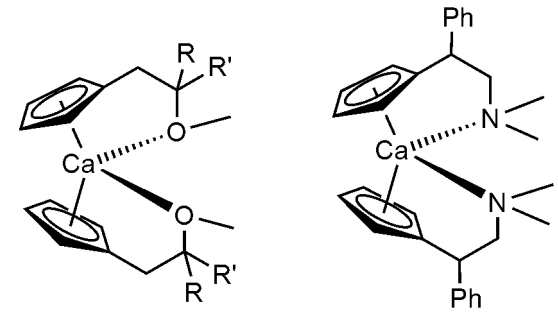

R = H, R' = H (**3.21**)
R = H, R' = Ph (**3.22**)

(**3.23**)

Figure 49: Structures of known calcium donor-functionalised Cp complexes

The Ca−C bond lengths range from 2.622(6)-2.710(6) Å for **3.21** and 2.632(6)-2.703(5) Å for **3.22**. These Ca−C bond lengths are similar to those in $[(MeC_5H_4)_2Ca(dme)]$ (**3.24**)[100] and $[\{(^tBu)C_5H_4\}_2Ca(thf)]$ (**3.25**)[97] which have average Ca−C bond lengths of 2.676(9) Å and 2.733(8) Å, respectively. The amino functionalised complex **3.23** is structurally very similar to that of **3.21** and **3.22**; the coordination environment of the calcium cation consists of two Cp rings coordinated in an η^5 manner and two *N*-donor

atoms from the two amino groups, arranged into a pseudo-tetrahedral geometry.[99] The bond angles around the central Ca^{2+} cation are; Cp−Ca−Cp: 136.6, 139.70 and 137.33° (as quoted) for **3.21**, **3.22** and **3.23**, respectively, and the E−Ca−E (where E = O, N) bond angles are 88.4(1), 102.54 and 101.31° for **3.21**, **3.22** and **3.23**, respectively.

Hanusa *et al.* attempted to synthesise the strontium and barium analogues of **3.21**, and attempts were made to synthesise calcium, strontium and barium complexes of a piperidenyl donor-functionalised Cp ligand. Of these complexes, only one was structurally characterised, $[Sr[\{2\text{-}(2\text{-}C_5H_4N)CH_2C(Me)_2\}C_5H_4]_2]$ (**3.26**).[98] Complex **3.26** crystallises from toluene to give colourless blocks, and, as with the calcium complexes, the strontium centre has a distorted tetrahedral geometry. The Sr−C bond lengths average 2.85(1) Å, which are similar to those of the unfunctionalised strontium complex $[\{(^tBu)C_5H_4\}_2Sr(thf)]$[97] (**3.27**) which has an average Sr−C bond length of 2.845(9) Å.

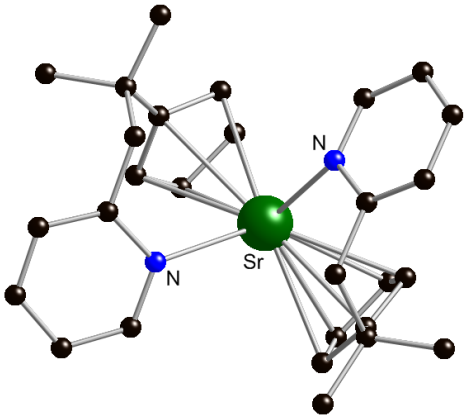

Figure 50: Molecular structure of $[Sr[\{2\text{-}(2\text{-}C_5H_4N)CH_2C(Me)_2\}C_5H_4]_2]$ (**3.26**). Hydrogen atoms have been omitted for clarity, carbon = black, strontium = green, nitrogen = blue. Reproduced from ref. 98

The only other known strontium cyclopentadienyl complex is **3.28** (Figure 51), formed from a one-pot reaction of strontium *bis*(trimethylsilylamide) with acetophenone and 6-methyl-6-phenyl-fulvene in thf.[101] Each strontium cation is coordinated by four oxygen atoms; two from the thf solvent molecules and two from the ligand, as well as the two Cp rings.

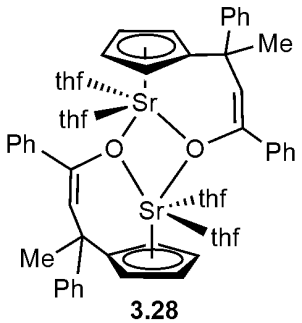

3.28

Figure 51: Structure of strontium complex **3.28**

Attempts have been made to synthesise donor-functionalised Cp complexes of barium. However, of the various functional groups attached to the Cp rings, the only structure that could be determined was the complex $[Ba\{C_5H_4(CH_2CH_2OCH_2CH_2OCH_3)\}_2]$ (**3.29**) (Figure 52).[102]

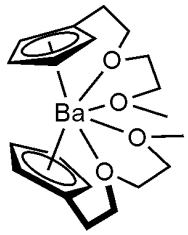

3.29

Figure 52: Structure of barium complex **3.29**

Complex **3.29** is a viscous oil, which is typical of complexes of oligoethylene-glycol-functionalised compounds, and such complexes only crystallize when the flexibility of the functional group is restricted by coordination.[103] The ^{13}C NMR spectrum **3.29** indicated that all the oxygen coordinated to the barium cation.

3.3.2 Donor-Functionalised Group 3 and f-Block Metal Cyclopentadienyl Complexes

There is a large range of donor-functionalised group 3 and lanthanide (Ln) metal cyclopentadienyl complexes.[77] Only a few examples will be discussed here, focusing on *O*-donor functionalised ligands. In the early 1990's, various Cp complexes with the

ligand $C_5H_4(CH_2CH_2OMe)$ were synthesised.[104,105,106] The initial work produced a range of complexes of the type $[LnCl\{C_5H_4(CH_2CH_2OMe)\}_2]_2$ where Ln = La (**3.30**), Nd (**3.31**), Gd (**3.32**), Ho (**3.33**), Er (**3.34**), Yb (**3.35**) and Y (**3.36**); by reacting two equivalents of $[Na\{C_5H_4(CH_2CH_2OMe)\}]$ with $LnCl_3$. However, none of these complexes were structurally characterised, the only characterisation completed was elemental analysis and IR spectroscopy. Coordination of the methoxy functional group to the lanthanide cation was suggested on the basis of IR spectroscopy.

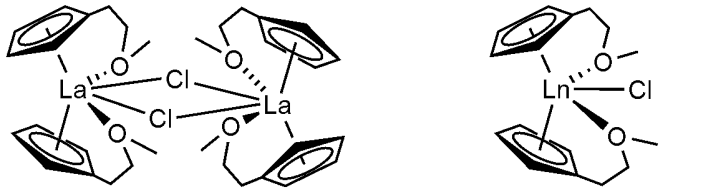

3.37 Ln = Dy (**3.38**), Yb (**3.39**)

Figure 53: Structures of complexes **3.38-3.40**

Complexes **3.37**, **3.38** and **3.39** were structurally characterised.[107] Complex **3.37** is a chloride-bridged dimer, with each lanthanum coordinated by two cyclopentadienyl rings, in an η^5 manner, two oxygen atoms from the ligand and two chlorine atoms. The coordination geometry can be thought of as being distorted octahedral, if the Cp rings are regarded as occupying one vertex.

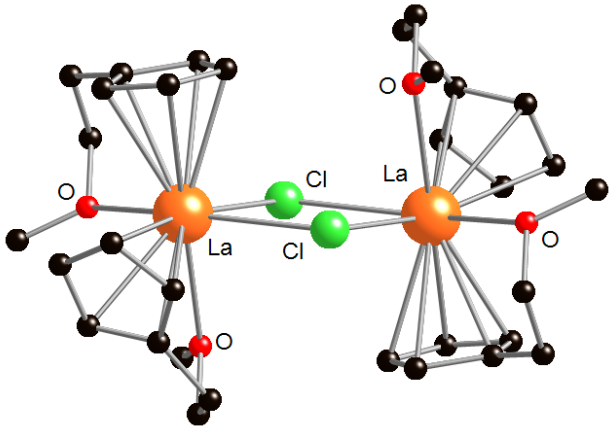

Figure 54: Molecular structure of $[LaCl\{C_5H_4(CH_2CH_2OCH_3)\}_2]_2$ (**3.37**). Hydrogen atoms have been omitted for clarity, carbon = black, lanthanum = orange, oxygen = red, chlorine = green. Reproduced from ref. 107

The La−C bond distances in **3.37** are between 2.778(4)-2.885(3) Å, (average 2.548 Å), which are similar to those seen in [(η^5-C_5H_5)$_3$La(thf)] (**3.40**)[108] and [(η^5-C_5H_5)$_3$La] (**3.41**)[109] which have average La−C bond lengths of 2.575 Å and 2.597 Å, respectively. Complexes **3.38** and **3.39** are isostructural. The dysprosium and ytterbium cations are each coordinated by two Cp rings, two oxygen ligands from the ligand and one chlorine atom, which can be described as a distorted trigonal bipyramidal structure. The Ln−C bond lengths for complexes **3.38** and **3.39** range from 2.462(5) to 2.75(2) and 2.437(7) to 2.70(4) Å, respectively. These Ln−C bond distances are similar to those seen in other dysprosium and ytterbium complexes such as [(C_5H_5)$_2$DyCl]$_n$ (**3.42**)[110] (av. 2.63 Å), [(C_5H_5)$_3$Dy(thf)] (**3.43**)[111] (av. 2.500 Å), [(C_5H_5)$_2$Yb(Me)]$_2$ (**3.44**)[112] (av. 2.613(13) Å), and [{(Me_3Si)$_2$$C_5H_3$}$_2$YbCl]$_2$ (**3.45**)[113] (av. 2.62 Å), Unlike complex **3.37**, complexes **3.38** and **3.39** are monomeric, which shows that the smaller radius of the dysprosium and ytterbium cations compared to the lanthanum, affects the structure.

Other functionalised lanthanide cyclopentadienyl complexes are **3.46**[99] and **3.47**[114] (Figure 55), which have a pendant amino group on the Cp ring.

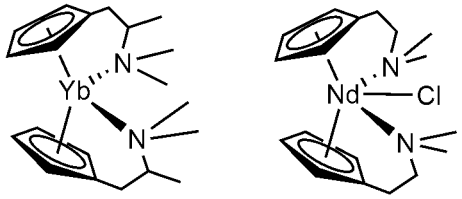

3.46 **3.47**

Figure 55: Structures of *N*-donor functionalised Cp complexes

Complex **3.46** has a distorted tetrahedral geometry around the ytterbium cation, with the coordination environment formed by two Cp rings coordinated in an η^5 manner and the two amino groups from the ligand. The Yb−C bond distances are between 2.665(5) and 2.698(5) Å, which are similar to the *O*-donor functionalised Cp ytterbium complex **3.39**.

In complex **3.47** the neodymium cation is coordinated by two η^5 Cp rings, the two *N*-donor atoms from the ligand and one chlorine atom. The Nd−C bond lengths are

2.731(3) to 2.807(3) Å, which is similar to Nd−C bond lengths seen in other neodymium cyclopentadienyl complexes such as [Nd(C_5H_5)$_3$(thf)] (**3.48**)[115] (av. 2.79(4) Å) and [Nd(C_5H_5)$_3$Py] (**3.49**)[116] (av. 2.085(13) Å). Schumann *et al.*, in the late 1990's structurally characterised donor-functionalised complexes of samarium, thulium and lutetium.[117]

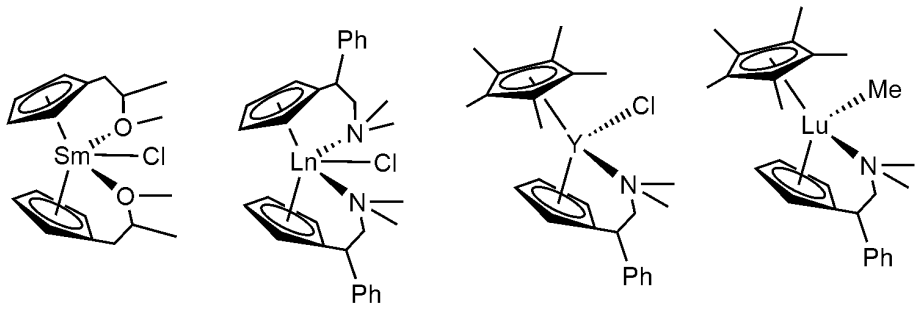

3.50 Ln = Sm **3.51** Ln = Lu **3.52** **3.53** **3.54**

Figure 56: Examples of a range of lanthanide donor-functionalised cyclopentadienyl complexes

In the case of complexes **3.50**-**3.52** the metal is coordinated by two η^5 functionalised Cp rings, two functional groups (methoxy group for **3.50** and amino group for **3.51** and **3.52**) and a chlorine atom. The geometry around the lanthanide is distorted trigonal bipyramidal, with the donor groups in the axial positions and the Cp rings and the chlorine in the equatorial positions. The Ln−C_{Cp} bond distances for complex **3.50**, **3.51** and **3.52** are 2.683(4) to 2.741(3), 2.715(1) to 2.769(1) and 2.605(2) to 2.689(1) Å, respectively, which reflects the lanthanide contraction.

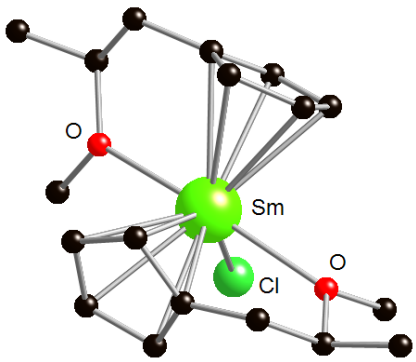

Figure 57: Molecular structure of [SmCl{C_5H_4(CH_2CH(CH_3)OCH_3)}$_2$]$_2$ (**3.51**). Hydrogen atoms have been omitted for clarity, carbon = black, samarium = green, oxygen = red, chlorine = light green. Reproduced from ref. 117

Complexes **3.53** and **3.54** have similar coordination environments (Figure 56). The metal in complexes **3.53** and **3.54** are in a distorted tetrahedral geometry, with Ln−C_{Cp} bond distances of 2.622(5) to 2.666(5) and 2.590(1) to 2.651(1) Å, repectively. The average Ln−E (E = O or N) bond distances for complexes **3.50**, **3.51**, **3.52**, **3.53** and **3.54** are 2.543(9), 2.745(7), 2.71(1), 2.501(4) and 2.454(9) Å.

Schumman *et al.*, attempted to synthesise a range of *ansa-bis*(donor-functionalised) metallocenes: [LnX{C_5H_2(^{t}Bu-3-Me-5)}$SiMe_2${1-C_9H_5($CH_2CH_2NMe_2$-3)}] where X = Cl, Ln = Y (**3.55**), Sm (**3.56**), Lu (**3.57**), X = I, Ln = Tm (**3.58**), [LuCl{1-C_9H_6}$SiMe_2${1-C_9H_5($CH_2CH_2NMe_2$-3)}] (**3.59**) and [Sm(CH_3){C_5H_2(^{t}Bu-3-Me-5)}$SiMe_2${1-C_9H_5($CH_2CH_2NMe_2$-3)}] (**3.60**).[118] Of these complexes, **3.57** and **3.58** were structurally characterised.

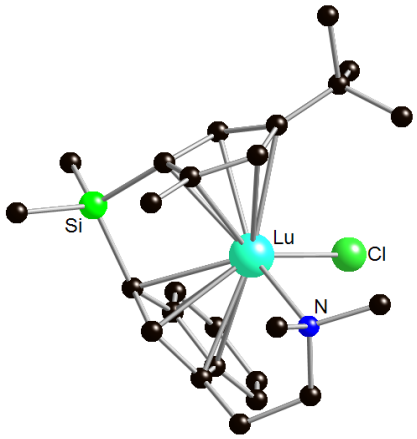

Figure 58: Molecular structure of [LuCl{C_5H_2(^{t}Bu-3-Me-5)}$SiMe_2${1-C_9H_5($CH_2CH_2NMe_2$-3)}] (**3.57**). Hydrogen atoms have been omitted for clarity, carbon = black, lutetium = light blue, nitrogen = dark blue, chlorine = light green, silicon = bright green. Reproduced from ref. 118

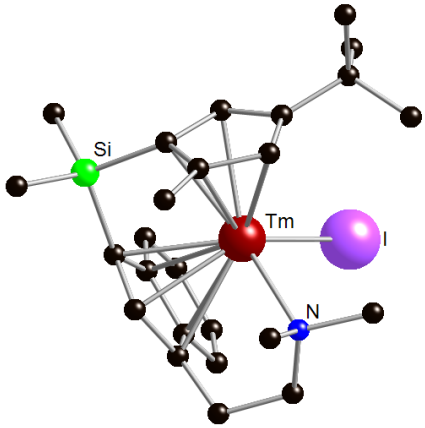

Figure 59: [TmCl{C_5H_2(^{t}Bu-3-Me-5)}$SiMe_2${1-C_9H_5($CH_2CH_2NMe_2$-3)}] (**3.58**). Hydrogen atoms have been omitted for clarity, carbon = black, thulium = deep red, nitrogen = dark blue, iodine = light purple, silicon = bright green. Reproduced from ref. 118

Both **3.57** and **3.58** have the same molecular structure, with a distorted tetrahedral geometry, with the metal being coordinated by the halide atom, the nitrogen atom of the functional group and an η^5-indenyl ring. However, the coordination of the indenyl has a slight tendency to bond η^3 to the metal. The Ln−C_{Cp} bond distances for **3.57** and **3.58** are 2.558(8) to 2.687(8) and 2.648(1) to 2.701(3) Å. Ln−$C_{indenyl}$ bond distances for **3.57** and **3.58** have shorter bonds and longer bonds; for complex **3.57** the shorter bonds range from 2.512(8) to 2.641(8) Å, and the longer bonds are 2.677(8) and 2.746(8) Å; for complex **3.58** the shorter bonds range from 2.545(1) and 2.580(1) Å, and the longer bonds are 2.646(2) and 2.776(2) Å.[118]

3.3.3 Donor-Functionalised d-Block Metal Cyclopentadienyl Complexes

As with the f-block there are many examples of transition metal complexes of donor functionalised cyclopentadienyl ligands,[77,79] and zirconium and titanium in particular have an extensive range of complexes.[119] This section will only briefly mention some examples of complexes that exist.

Some examples of group 4 donor-functionalised cyclopentadienyl complexes include: $[TiCl_2\{\eta^5{:}\eta^1\text{-}C_5H_4CH_2CH_2O\}]_2$ (**3.61**), $[TiCl_2\{\eta^5{:}\eta^1\text{-}C_5H_4CH_2CH_2CH_2O\}]$ (**3.62**),[120] $[ZrCl_2\{\eta^5{:}\eta^1\text{-}C_5H_4CH_2CH_2OMe\}(\mu\text{-}Cl)]_2$ (**3.63**),[121] and *bis*(methoxyethyl)-cyclopentadienyl complex $[ZrCl_3\{C_5H_4(CH_2CH_2OMe)_3]$ (**3.64**).[122] As well as *O*-donor functionalised cyclopentadienyl zirconium complexes, there are *N*-donor complexes known in the literature, for example $[Zr(H)\{C_5Me_5\}\{C_5Me_4(CH_2CH_2N(CH_3)CH_2)\}]$ (**3.65**) $[ZrCl\{C_5Me_5\}\{C_5Me_4(CH_2CH_2N(CH_3)CH_2)\}]$ (**3.66**),[123] $[ZrCl\{\mu\text{-}Cl\}\{C_5H_4(SiMe_2N^tBu)\}]_2$ (**3.67**) and $[ZrCl\{\mu\text{-}Cl\}\{C_5Me_4(SiMe_2N^iPr)\}]_2$ (**3.68**).[124] Studies on *P*-donor-functionalised cyclopentadienyl ligands, include $[(thf)ZrCl_3\{C_5H_4(CH_2CH_2PMe_2)\}]$ (**3.69**), $[ZrCl_2(\mu\text{-}Cl)\{C_5H_4(CH_2CH_2PMe_2)\}]_2$ (**3.70**),

[(thf)$ZrCl_3${$C_5Me_4(CH_2CH_2PMe_2)$}] (**3.71**) and [$ZrCl_2$(μ-Cl){$C_5Me_4(CH_2CH_2PMe_2)$}]$_2$ (**3.72**).[125,126] Functionalised hafnium cyclopentadienyl complexes are less common than those of titanium and zirconium; an example of a hafnium complex is [$HfCl_2(\eta^5{:}\eta^1{:}\eta^1$-$C_5Me_4SiMe_2NCH_2CH_2OCH_3$)] (**3.73**), in which the donor-functionalised ligand has both a *N*- and an *O*-functionality.[127] The solid-state structure of **3.73** was determined by X-ray crystallography (Figure 60).

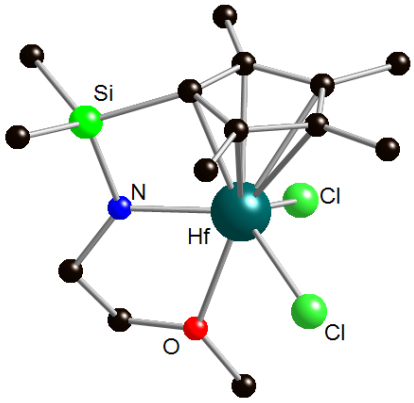

Figure 60: Molecular structure of [$HfCl_2(\eta^5{:}\eta^1{:}\eta^1$-$C_5Me_4SiMe_2NCH_2CH_2OCH_3$)] (**3.73**). Hydrogen atoms have been omitted for clarity, carbon = black, chlorine = light green, oxygen = red, nitrogen = blue, silicon = bright green, hafnium = turquoise. Reproduced from ref. 127

Complex **3.73** adopts a distorted trigonal bipyramidal structure, with the Cp* ring and the methoxy functionality in the axial positions and the chlorides and amino functionality in the equatorial positions.

There are also many examples of non-group 4 metal donor-functionalised cyclopentadienyl complexes, for example the *N*-donor-functionalised [$Mo(CO)_2$I{$C_5H_4(CH_2CH_2NMe_2)$}] (**3.74**)[128] and group 7 *S*-donor-functionalised complex [$Mn(CO)_2${$C_5H_4(C{=}OCH_2SCH_3)$}] (**3.75**) (Figure 61). The manganese in complex **3.75** is in a distorted tetrahedral geometry coordinated by two carbon monoxide groups, the Cp ring and the sulphur atom of the functional group. The average Mn−C bond distance to the Cp ring is 2.133 Å, which is similar to that of [$(C_5H_5)Mn(CO)_3$] which has Mn−bond lengths ranging from 2.120(2) to 2.131(2) Å.[129]

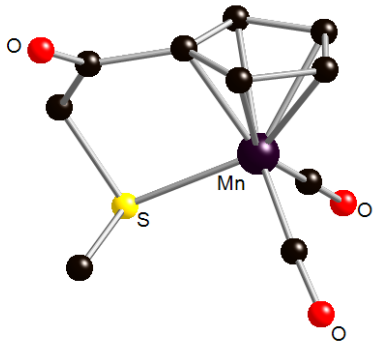

Figure 61: Molecular structure of $[Mn(CO)_2\{C_5H_4(C{=}OCH_2SMe)\}]$ (**3.75**). Hydrogen atoms have been omitted for clarity, carbon = black, oxygen = red, nitrogen = blue, manganese = dark purple, sulphur = yellow. Reproduced from ref. 129

Other examples of structurally characterised donor-functionalised cyclopentadienyl complexes of late transition metals include the cobalt, rhodium and iridium complexes of the ligand $C_5Me_4(CH_2CH_2NMe_2)$ (**3.10**); $[M(I_2)\{C_5Me_4(CH_2CH_2NMe_2)\}]$ where M = Co (**3.76**), Rh (**3.77**) and Ir (**3.78**).[130,131] The attempted synthesis of the group 10 metals, nickel, palladium and platinum with *O*-donor-functionalised Cp ligands resulted in complex $[Ni(\mu\text{-}CO)_2\{C_5Me_4(CH_2CH_2NMe_2)\}]_2$ (**3.79**), in which the nitrogen functional group has not coordinated to the nickel cations.[132] An analogous palladium complex was also synthesised, however attempts to synthesise the platinum analogue failed. Several attempts to synthesise other group 10 metals complexes in which the amino group could coordinate with the metal centre also failed, with only the Cp ring coordinating.[132]

3.3.4 Donor-Functionalised p-Block Metal Cyclopentadienyl Complexes

There are quite a few examples of p-block metal donor-functionalised cyclopentadienyl complexes, focusing mainly on group 13 metals and a few group 14 metal examples.[78,133] Of the p-block complexes known, many contain aluminium (Scheme 27). Complexes **3.80** to **3.84** were isolated as air-sensitive colourless crystals, but the

crystals were not suitable for X-ray crystallography. However, the methylated Cp complexes **3.85** and **3.86** were stable in air and complexes **3.87** to **3.89** were moderately stable in air. Only complexes **3.82**, **3.83** and **3.87** were structurally characterised, with NMR spectroscopy and cryoscopic molecular mass determinations confirming that the monomeric structure is maintained in solution.[78,133]

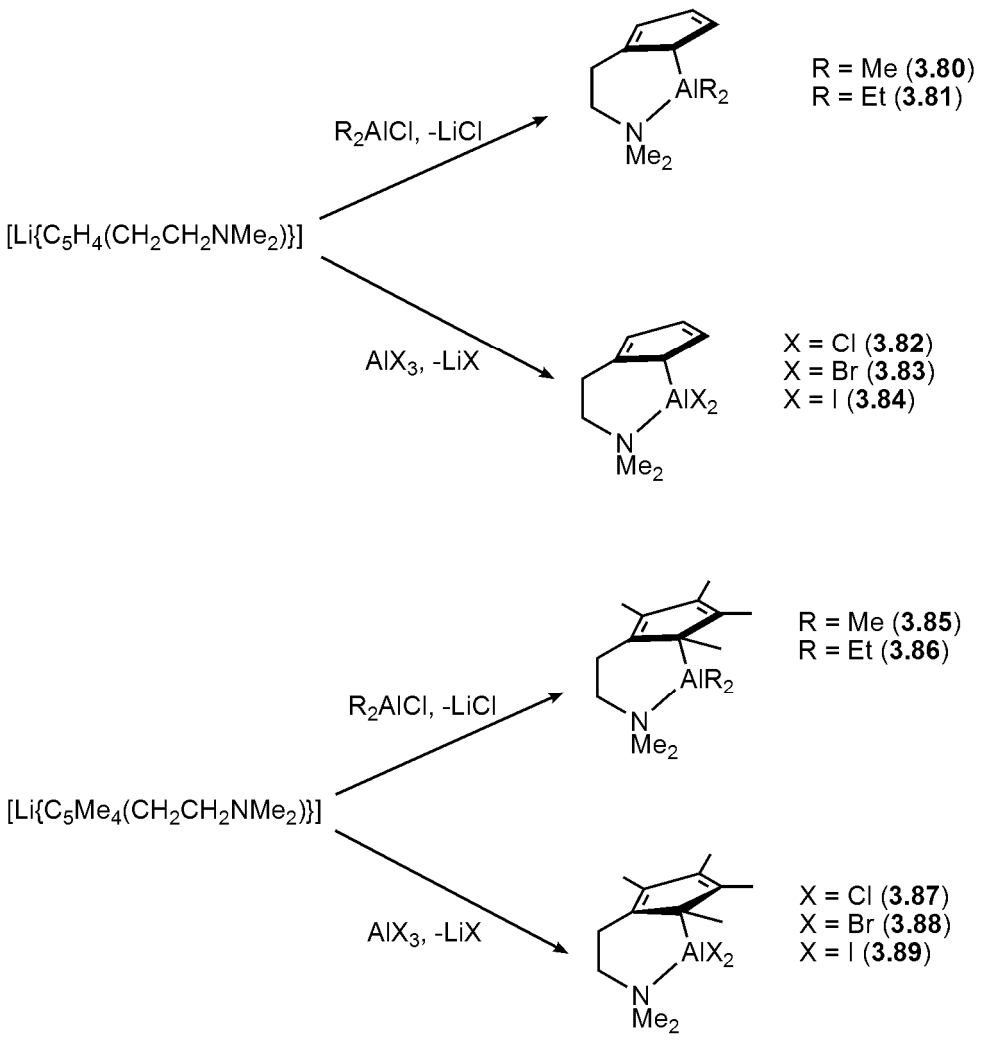

Scheme 27

Complexes **3.82**, **3.83** and **3.87** have similar structures; the aluminium(III) cation is coordinated by two R groups, the nitrogen atom of the functionality and a Cp rings. In complexes **3.82** and **3.83** the Cp ring is coordinated in an η^1 fashion but in complex **3.87** the Cp ring is coordinated between η^2 and η^3 bonding. The Al−C_{Cp} bond lengths for complexes **3.82** and **3.83** are 2.09 and 2.10 Å (as quoted) and for complex **3.87** the bond

lengths are 2.06, 2.51 and 2.32 Å.[78] Normally, Al−C_{Cp} bond lengths are shorter than those seen in complex **3.87**, for example complex $[(\eta^1\text{-}C_5H_5)_2AlO\text{-}^iPr]_2$ (**3.90**)[134] has Al−C_{Cp} bond lengths of 2.003(2) and 2.022(2) Å. The Al−N bond lengths for complexes **3.82**, **3.83** and **3.87** are 2.07, 2.08 and 2.01 Å (as quoted), respectively; which is similar to the Al−N bond distance in $[AlCl_3NMe_2]$ (**3.91**) of 1.96(1) Å.[135]

Complexes of gallium and indium were synthesised to give complexes of general formula $[MCl_2\{C_5R_4(CH_2CH_2NMe_2)\}]$ where M = Ga, R = H (**3.92**), R = Me (**3.93**) and M = In, R = H (**3.94**), R = Me (**3.95**). NMR spectroscopic studies and relative molecular mass measurements confirm a monomeric structure in solution, with the amino group coordinated to the metal. This was confirmed by X-ray crystallography on complexes **3.92**, **3.94** and **3.95** (Figure 62). The M−C_{Cp} bond lengths are 1.99, 2.34 and 2.18 Å (as quoted), respectively; with the M−N bond lengths for the complexes being 2.03, 2.36 and 2.27 Å (as quoted), respectively.[78]

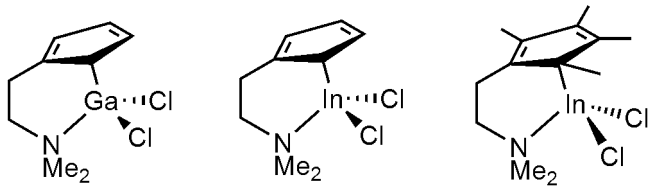

3.92 **3.94** **3.95**

Figure 62: Structures of complexes **3.92**, **3.94** and **3.95**

Attempts have been made to synthesise the thallium donor-functionalised cyclopentadienyl complexes $[Tl\{C_5H_4(CH_2C_4H_7O)\}]$ (**3.96**),[136] $[Tl\{C_5H_4\text{-}(CH_2CH_2NMe_2)\}]$ (**3.97**) and $[Tl\{C_5Me_4\text{-}(CH_2CH_2NMe_2)\}]$ (**3.98**).[78] However none have succeeded in structurally characterising the complexes formed, and there is no conclusive evidence that the donor-functionality is coordinated to the metal.

Attempts have also been made to synthesise germanium, silicon, tin and lead cyclopentadienyl complexes. The only structurally characterised complexes are the

germanium(II) complex [GeCl{$C_5Me_4(CH_2CH_2NMe_2)$}] (**3.99**)[137] and the lead complex [$(C_5H_5)_2$Pb{$C_5H_4(CH_2C_4H_7O)$}Na]·0.5thf (**3.100**).[138]

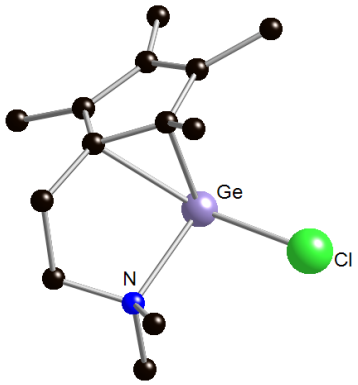

Figure 63: Molecular structure of [GeCl{$C_5Me_4(CH_2CH_2NMe_2)$}] (**3.99**). Hydrogen atoms have been omitted for clarity, carbon = black, nitrogen = blue, chlorine = light green, germanium = light purple. Reproduced from ref. 137

Complex **3.99** is coordinated by the Cp ring in an η^2 fashion, and the nitrogen from the ligand is also coordinated, as well as a chloride anion. The Ge–C bond lengths are 2.180(3) and 2.402(3) Å, typical Ge–C σ-bond lengths range between 1.98 and 2.14 Å.[139] The Ge–N and the Ge–Cl bond lengths are 2.286(3) and 2.369(1) Å, respectively. The Ge–Cl bond is longer than those seen in other germanium complexes such as $GeCl_2$ (**3.101**)[140] (2.183(4) Å) and [GeCl(C_5Me_5)] (**3.102**)[141] (2.258(12) Å). From the longer Ge–C and Ge–Cl bonds it can be seen that the nitrogen donor-functionality is having an effect on the CpGeCl unit. Studies were undertaken to synthesise a complex with an external *N*-donor group, in this case pyridine, which failed.[137]

Complex [$(C_5H_5)_2$Pb{$C_5H_4(CH_2C_4H_7O)$}Na]·0.5thf (**3.100**) was synthesised by reacting Cp_2Pb with [{$C_5H_4(CH_2C_4H_7O)$}Na·thf] in toluene. Complex **3.100** has a complicated polymeric structure, seen in Figure 64. The structure of **3.100** can be considered as Na^+ cation association with the [$(C_5H_5)_2$Pb{$C_5H_4(CH_2C_4H_7O)$}]$^-$ anion. The extended structure of **3.100** forms a honeycomb lattice sheet.

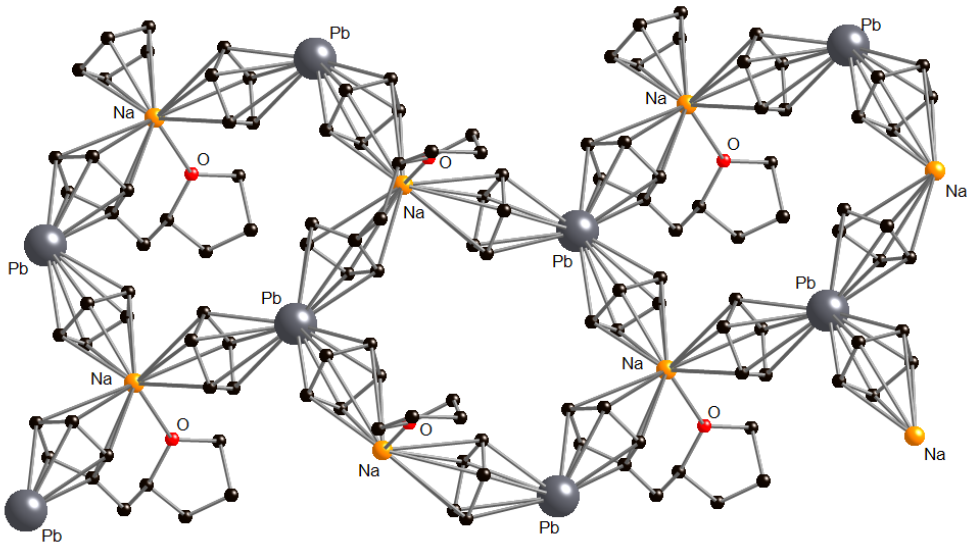

Figure 64: Molecular structure of $[(C_5H_5)_2Pb\{C_5H_4(CH_2C_4H_7O)\}Na]\cdot 0.5thf$ (**3.100**). Hydrogen atoms have been omitted for clarity, carbon = black, oxygen = red, sodium = orange, lead = grey. Reproduced from ref. 138

The Pb−C(Cp) bond distances range from 2.848(9) to 3.00(1) Å, and the Pb−C(Cp^{thf}) (where $Cp^{thf} = C_5H_4\{CH_2C_4H_7O\}$) bond distances range from 2.86(1) to 2.91(1) Å. The lead is coordinated by three Cp rings (including the donor-functionalised Cp ring) in an η^5 manner. The oxygen donor group on the donor-functionalised Cp ligand is coordinated to the Na^+ cation, which is also coordinated by three Cp rings.[138]

Chapter 4

Synthesis of s-Block Metal Donor-Functionalised Allyl Complexes

4.1 Introduction to Donor-functionalised Allyl Chemistry

As discussed in the previous chapter, relatively few donor-functionalised allyl complexes are known. Those that are known have been lithium complexes studied by Fraenkel *et al.*[7,8,82-84] and Strohmann *et al.*[85] Therefore, this is an attractive area to expand into, with a lot of scope for new and novel complexes to be synthesised. Therefore, the aims of this chapter are to:

1. Synthesise different donor-functionalised pro-ligands, with different heteroatom functionalities.
2. Study the coordinating ability of the ligand with different s-block metals.
3. Investigate the effect polarising power of the metal has on the structure of the allyl complex and study the effect on (de)localisation of the allyl ligand.

4.2 Synthesis of Donor-functionalised Ligands

Attempts were made to synthesise a variety of different donor-functionalised allyl pro-ligands; with *O*-, *N*-, and *S*-functional groups incorporated into the allyl backbone (Figure 65).

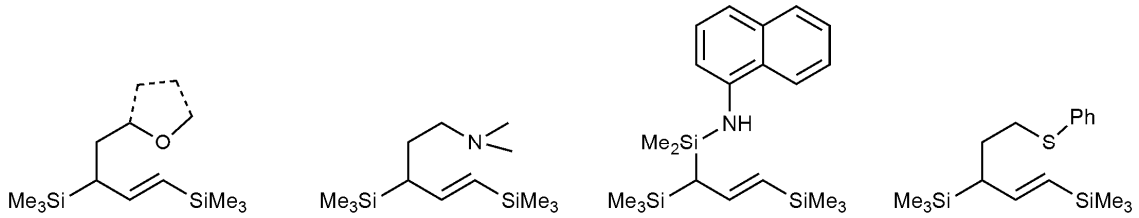

Figure 65: Different types of donor-functionalised pro-ligands

However, only the pro-ligands $\mathbf{L^3}$H and $\mathbf{L^4}$H were successfully synthesised, in yields of 63% and 47%, respectively. In order to synthesise these pro-ligands the appropriate ether-containing tosylate had to be prepared. Tosylchloride was added to a mixture of either pyridine/tetrahydrofurfuryl alcohol or pyridine/2-methoxyethanol and then the

reaction mixtures were worked up using standard procedures (Scheme 28). (Tetrahydrofuran-2-yl)methyl-4-methylbenzenesulfonate (thf-tosylate) was isolated as a cream-coloured solid in a yield of 82%, and the 2-methoxyethyl 4-methylbenzenesulfonate (methoxy-tosylate) was isolated as a colourless oil in a yield of 80%.

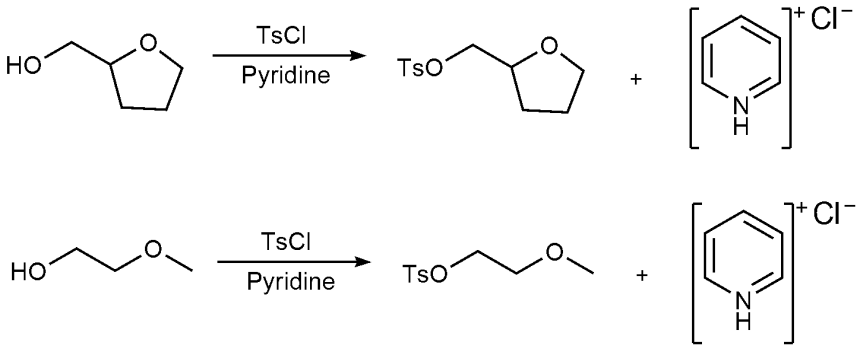

Scheme 28

The donor-functionalised allyl pro-ligands were synthesised by lithiating the 1,3-*bis*(trimethylsilyl)propene[28] with one equivalent of ^{n}butyllithium and then quenching the lithiated allyl with the respective tosylate in slight excess (Scheme 29).

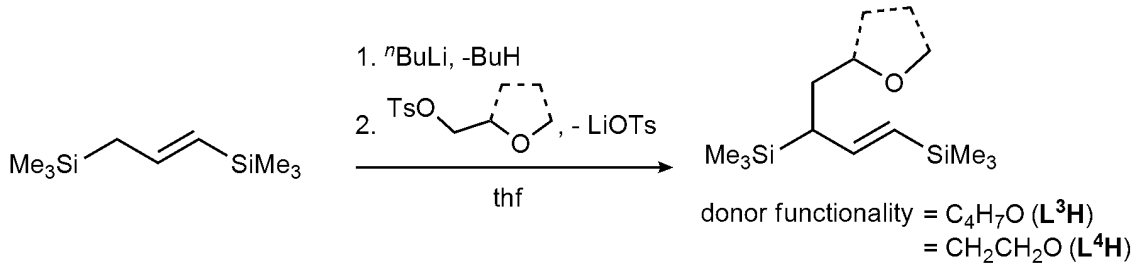

Scheme 29

Both ligands $\mathbf{L}^{3}$H and $\mathbf{L}^{4}$H were isolated as colourless oils and purified by vacuum distillation, with the products distilling at 68-72°C and 58-64°C, respectively. Both ligands were characterised by ^{1}H and ^{13}C NMR spectroscopy, mass spectroscopy and elemental analysis.

4.3 Synthesis and Structures of Donor-Functionalised Allyl Complexes

In this section, the results of a study into the structures of lithium, potassium and magnesium complexes of $\mathbf{L^3}$H and $\mathbf{L^4}$H will be discussed. Both solid-state structures and the solution-state structures were studied for each complex.

4.3.1 Complexes $[Li\{(SiMe_3)_2C_3H_2(CH_2C_4H_7O)\}]_2$ [4.1]$_2$ and $[Li\{(SiMe_3)_2C_3H_2\ (CH_2CH_2OCH_3)\}]_2$ [4.2]$_2$

Ligands $\mathbf{L^3}$H and $\mathbf{L^4}$H were deprotonated with one equivalent of *n*-butyllithium in hexane to afford the corresponding lithium complexes $[Li\{(SiMe_3)_2C_3H_2(CH_2C_4H_7O)\}]_2$ **[4.1]**$_2$ and $[Li\{(SiMe_3)_2C_3H_2(CH_2CH_2OCH_3)\}]_2$ **[4.2]**$_2$ in yields of up to 35% and 24%, respectively (Scheme 30). Both complexes crystallised as dimers, however complex **4.1** crystallised in a racemic mixture of the homochiral dimers (*R,R*)/(*S,S*)-**[4.1]**$_2$ with the *R* and *S* referring to the configuration at C(5) and C(19) (Figure 66), indicated in Scheme 30.

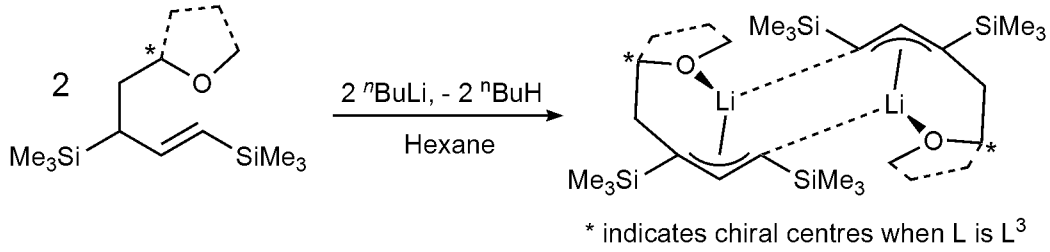

Scheme 30

Both complexes **[4.1]**$_2$ and **[4.2]**$_2$ have similar dimeric structures (Figure 66 and Figure 67). Each lithium cation is coordinated by one allyl component of the ligand in an η^3 manner, as well the *O*-donor functional group of the ligand. Each allyl ligand also coordinates to another lithium cation in an μ:η^1 manner to form the dimer structure.

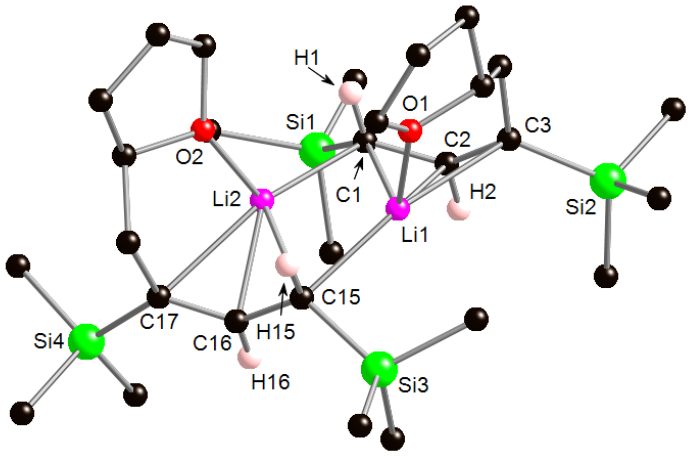

Figure 66: Molecular structure of $[Li\{(SiMe_3)_2C_3H_2(CH_2C_4H_7O)\}]_2$ **[4.1]**$_2$, selected bond lengths (Å) and angles (°). Hydrogen atoms, except those bonded to allylic carbon atoms, are omitted for clarity, black = carbon, green = silicon, bright pink = lithium, red = oxygen, pale pink = hydrogen: C(1)−C(2) 1.431(4), C(2)−C(3) 1.378(4), C(15)−C(16) 1.430(4), C(16)−C(17) 1.382(4), Li(1)−C(1) 2.317(6), Li(1)−C(2) 2.200(5), Li(1)−C(3) 2.495(5), Li(2)−C(15) 2.311(5), Li(2)−C(16) 2.203(5), Li(2)−C(17) 2.471(5), Li(1)−C(15) 2.271(5), Li(2)−C(1) 2.260(7), Li(1)−O(1) 1.871(7), Li(2)−O(2) 1.871(8), C(3)−C(2)−C(1) 132.1(2), C(17)−C(16)−C(15) 131.6(2), Si(1)−C(1)−C(2)−C(3) 150.3(3), Si(2)−C(3)−C(2)−C(1) 178.3(2), Si(4)−C(17)−C(16)−C(15) 178.8(2), Si(3)−C(15)−C(16)−C(17) 150.9(3).

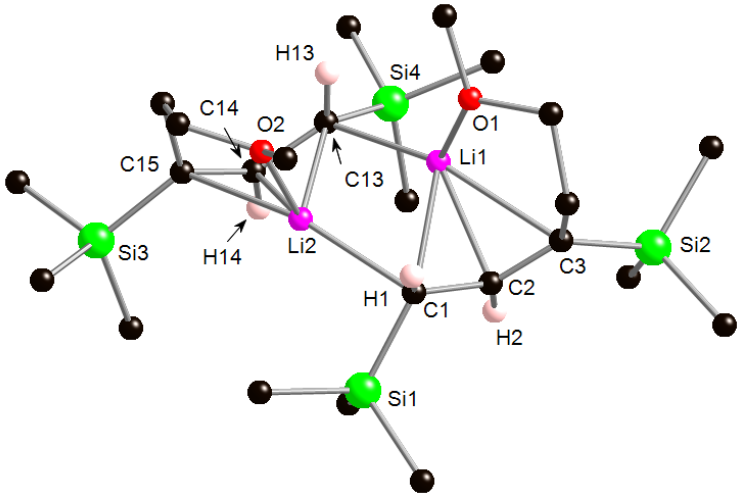

Figure 67: Molecular structure of $[Li\{(SiMe_3)_2C_3H_2(CH_2CH_2OCH_3)\}]_2$ **[4.2]**$_2$, selected bond lengths (Å) and angles (°). Hydrogen atoms, except those bonded to allylic carbon atoms, are omitted for clarity, black = carbon, green = silicon, bright pink = lithium, red = oxygen, pale pink = hydrogen: C(1)−C(2) 1.436(6), C(2)−C(3) 1.383(6), C(13)−C(14) 1.439(6), C(14)−C(15) 1.373(6), Li(1)–C(1) 2.354(9), Li(1)–C(2) 2.180(8), Li(1)–C(3) 2.453(8), Li(2)–C(13) 2.350(4), Li(2)–C(14) 2.157(8), Li(2)–C(15) 2.394(8), Li(1)–C(13) 2.291(8), Li(2)–C(1) 2.261(8), Li(1)−O(1) 1.908(7), Li(2)−O(2) 1.910(7) Si(1)−C(1)−C(2)−C(3) 149.9(4), C(1)−C(2)−C(3)−Si(2) 174.9(3), Si(4)−C(13)−C(14)−C(15) 152.9(4), C(13)−C(14)−C(15)−Si(3) 178.1(3), C(3)−C(2)−C(1) 131.3(4), C(15)−C(14)−C(13) 130.7(4).

Only **[4.2]**$_2$ will be discussed in detail due to the similarity of the structures of the two complexes. In complex **[4.2]**$_2$ the Li(1)−C(1), Li(1)−C(2) and Li(1)−C(3) bond distances are 2.345(9), 2.180(8) and 2.453(8) Å, respectively, and the Li(2)−C(13), Li(2)−C(14) and Li(2)−C(15) bond distances are 2.350(4), 2.157(8) and 2.394(8) Å, respectively. The C−C bond lengths of the allyl components C(1)−C(2) and C(2)−C(3) are 1.436(6) and 1.383(6) Å, respectively, and C(13)−C(14) and C(14)−C(15) are 1.439(6) and 1.373(6) Å, respectively. The shorter C−C bonds between C(2)−C(3) and C(14)−C(15) correspond to the longer Li−C bonds of Li(1)−C(3) and Li(2)−C(15), similarly the longer C−C bonds between C(1)−C(2) and C(13)−C(14) correspond to the shorter Li−C bonds of Li(1)−C(1) and Li(2)−C(13). The torsional angles within the allyl component for Si(2)−C(3)−C(2)−C(1) and Si(3)−C(15)−C(14)−C(13) are 174.9(3) and 178.1(3)°, respectively, whereas for Si(1)−C(1)−C(2)−C(3) and Si(4)−C(13)−C(14)−C(14) are 149.9(4) and 152.9(4)°, respectively. The internal solvation by the *O*-donor produces Li(1)−O(1) and Li(2)−O(2) bond distances of 1.908(7) and 1.910(7) Å, respectively. The near-planar nature of the Si(2)−C(3)−C(2)−C(1) and Si(3)−C(15)−C(14)−C(13) torsional angles combined with the C−C and Li−C bond lengths within the structure of **[4.2]**$_2$ suggests that there is partial localisation of the allyl negative charge, which is in agreement with the findings of by Fraenkel.[7,8,82,83]

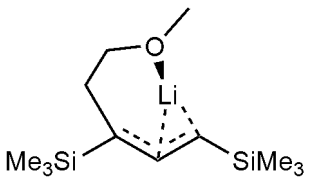

Figure 68: Partially localised bonding in complex **[4.2]**$_2$

For complex **[4.2]**$_2$ the charge is partially localised at C(1) and C(13). The two **4.2** units assemble into the dimer *via* a C_2Li_2 core by means of μ:η^1-bridging interaction to produce Li(1)−C(13) and Li(2)−C(1) bond distances of 2.291(8) and 2.261(8) Å,

respectively. This dimerisation results in the lithium being 4-coordinate, and in a distorted tetrahedral environment.

Complex **[4.1]**$_2$ has a similar structure to that of **[4.2]**$_2$, relevant bond lengths and angles have been summarised in Table 5. The formal negative allyl charge within complex **[4.1]**$_2$ is partially localised over one carbon atom in each allyl ligand (carbons C(1) and C(15)).

Table 5: Selected bond lengths (Å) and angles (°) for complex **[4.1]**$_2$

Parameters for [Li{(SiMe$_3$)$_2$C$_3$H$_2$(CH$_2$C$_4$H$_7$O)}]$_2$			
C(1)−C(2)	1.431(4)	C(15)−C(16)	1.430(4)
C(2)−C(3)	1.378(4)	C(16)−C(17)	1.382(4)
Li(1)−C(1)	2.317(6)	Li(2)−C(15)	2.311(5)
Li(1)−C(2)	2.200(5)	Li(2)−C(16)	2.203(5)
Li(1)−C(3)	2.495(5)	Li(2)−C(17)	2.471(5)
Li(1)−C(15)	2.271(5)	Li(2)−C(1)	2.260(7)
Li(1)−O(1)	1.871(7)	Li(2)–O(2)	1.871(8)
Si(1)−C(1)−C(2)−C(3)	150.3(3)	Si(3)−C(15)−C(16)−C(17)	150.9(3)
Si(2)−C(3)−C(2)−C(1)	178.3(2)	Si(4)−C(17)−C(16)−C(15)	178.8(2)

As discussed previously, Fraenkel *et al.* have reported extensive studies on allyllithium complexes,[83] such as complex **3.2** [Li{C$_3$H$_2$(1,3-SiMe$_3$)$_2$-(CH$_2$N(CH$_2$CH$_2$OCH$_3$)$_2$)}] (Scheme 23, Chapter 3) in which the Li−C bond distances are 1.968(4) and 2.035(4) Å. Other complexes include [Li{C$_3$H$_3$(1-SiMe$_3$)(CH$_2$N(CH$_2$CH$_2$OCH$_3$)$_2$)}] (**4.3**) and [Li{C$_3$H$_3$(CH$_2$N(CH$_2$CH$_2$OCH$_3$)$_2$)}]$_2$ (**4.4**) which have Li−C bond distances of 2.145(5) to 2.375(5) and 2.083(7) to 2.197(7) Å, respectively; which are similar in length to the Li−C bond distances in complex **[4.1]**$_2$ and **[4.2]**$_2$.

NMR spectroscopy revealed that the solution-phase structures of complex **[4.1]**$_2$ and **[4.2]**$_2$, are similar in several respects and therefore can be discussed collectively. NMR properties of lithium allyl complexes have been studied in detail.[17,19] NMR spectroscopy studies on internally solvated lithium allyl complexes have shown that several rearrangement mechanisms are possible in solution; including rotation about

C−C and Si−C bonds, 1,3-sigmatropic shifts (Scheme 31) and inversion at lithium (Scheme 32).[7,8,82,83]

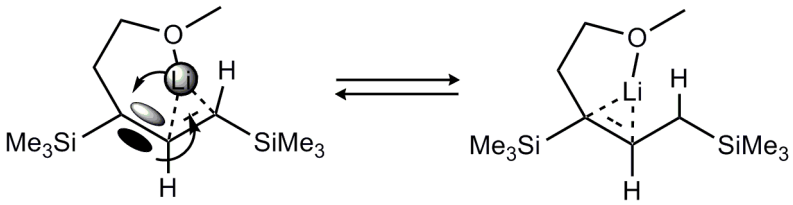

Scheme 31: 1,3-sigmatropic shift.[142]

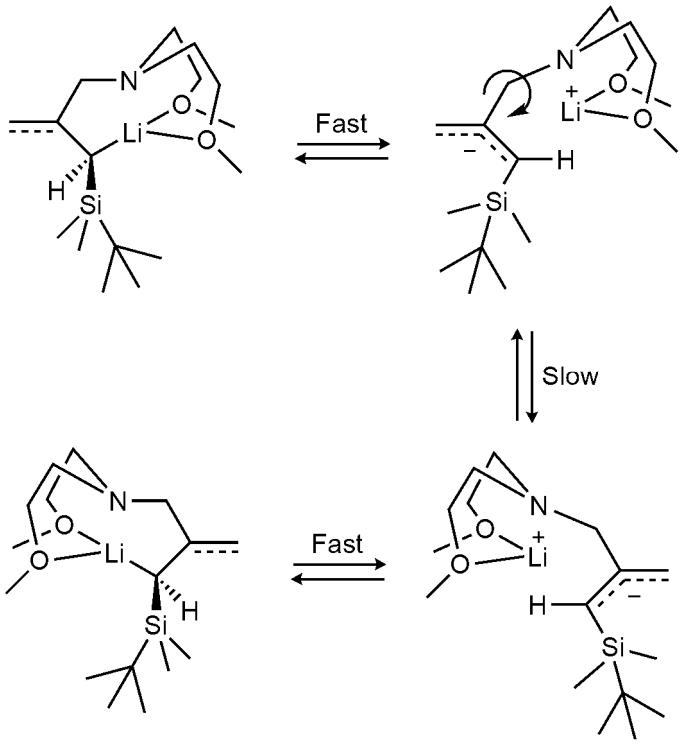

Scheme 32: Proposed mechanism for inversion of allylic lithium compounds, reproduced from ref. 82

As well as potentially having the complicated solution behaviour of donor-functionalised lithium allyls, complex **[4.1]**$_2$ has four pairs of diastereotopic protons in the [$CH_2C_4H_7O$] donor functionality. The ^{1}H NMR spectrum of complex **[4.1]**$_2$ can be seen in Figure 69, Figure 70 and Figure 71. For complex **[4.1]**$_2$, in benzene-d_6 solution, it appears there are two species in solution evident by the four resonances in both ^{1}H NMR (Figure 69) and ^{13}C NMR spectra due to the $SiMe_3$ groups, eight ^{13}C resonances due to CH_2 groups and six ^{13}C resonances for the allylic carbons.

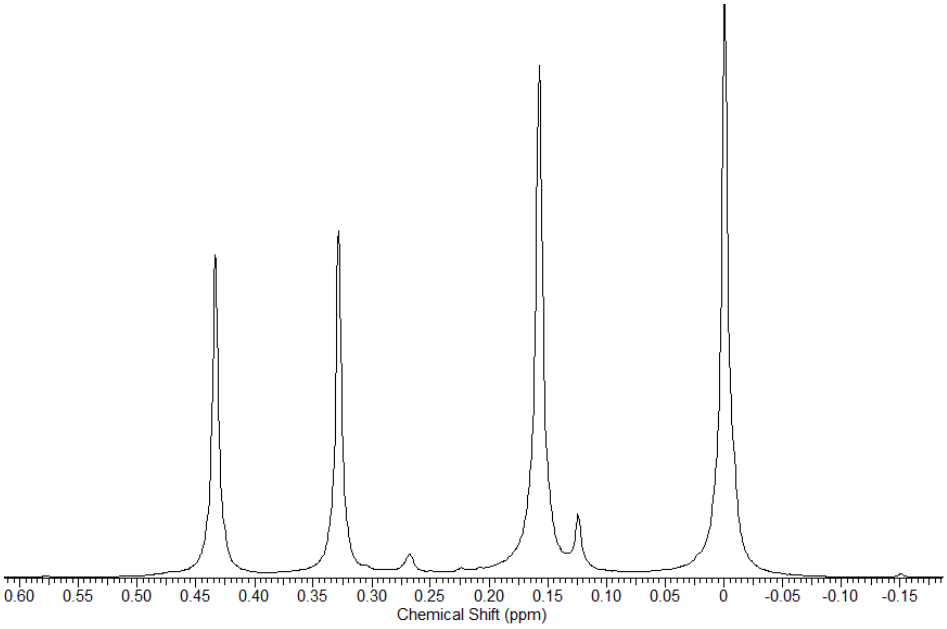

Figure 69: Segment of the ^{1}H NMR spectrum of complex **[4.1]**$_2$, in d_6-benzene, showing the trimethylsilyl region.

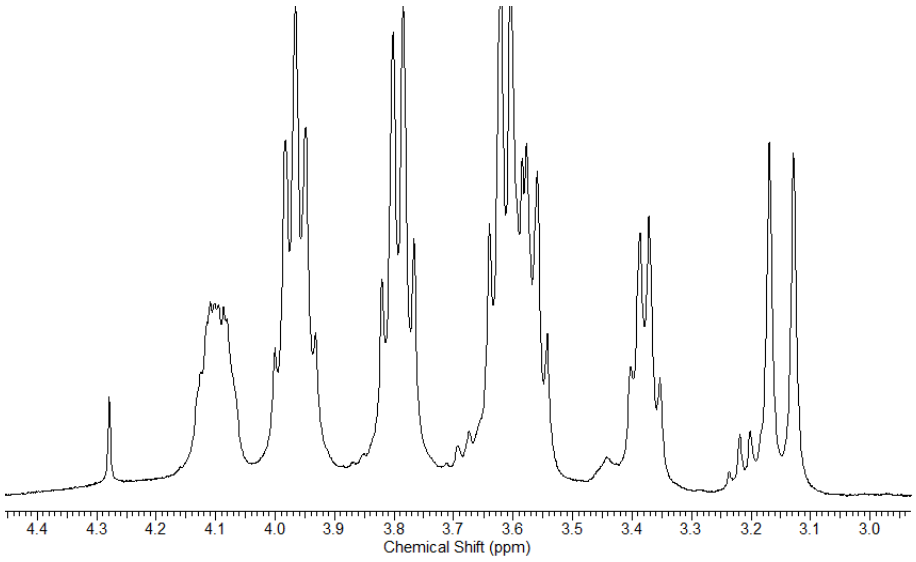

Figure 70: Segments of the ^{1}H NMR spectrum of complex **[4.1]**$_2$, in d_6-benzene.

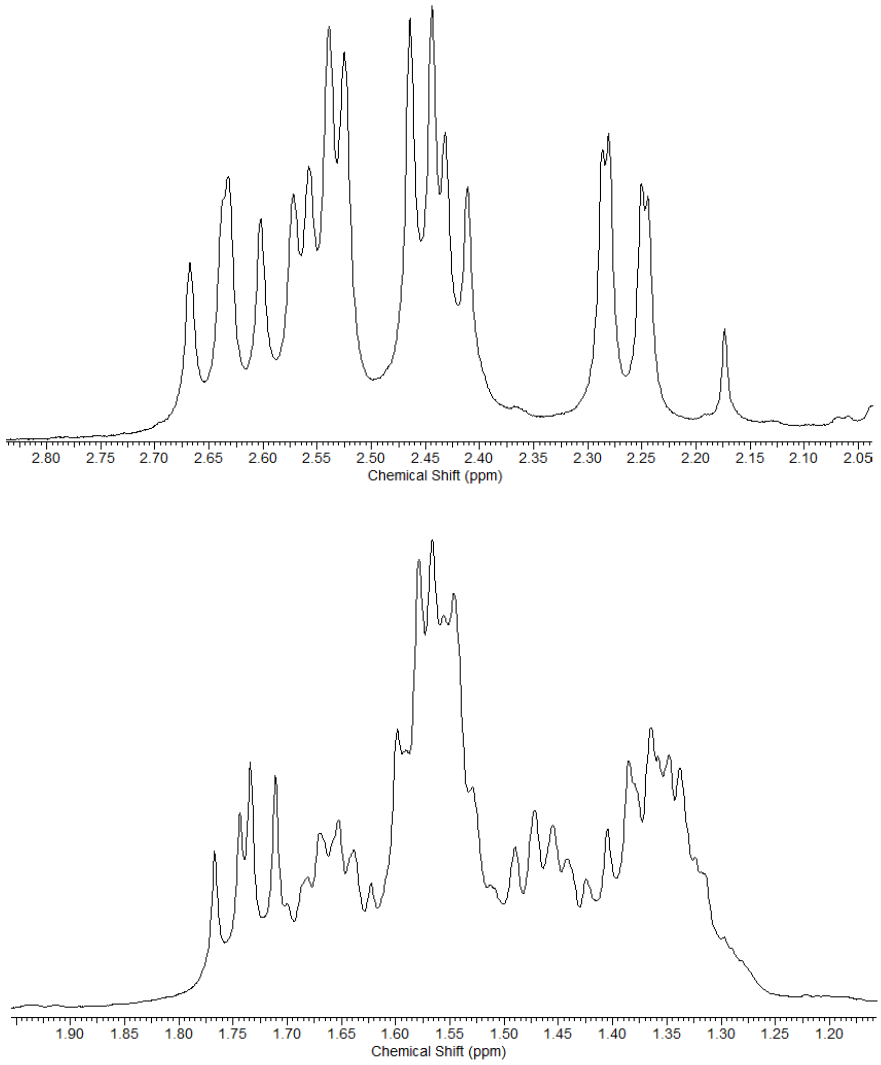

Figure 71: Segments of the ^{1}H NMR spectrum of complex **[4.1]**$_2$, in d_6-benzene.

The rest of the ^{1}H NMR resonances occur as a series of overlapping multiplets. Both ^{1}H and ^{13}C NMR spectra contain resonances that occur in pairs, with very similar chemical shifts, the most likely explanation for these resonances is the presence of two diastereoisomers in solution. The resonances in the ^{1}H and ^{13}C NMR spectra for complex **[4.1]**$_2$ are similar to those of **L**^{3}H ligand in solution; and the resonances of complex **[4.1]**$_2$ in solution are those of the homochiral (*R*,*R*) and (*S*,*S*) enantiomeric pairs and their corresponding heterochiral diastereoisomers (*R*,*S*) and (*S*,*R*), with respect to the tetrahydrofurfuryl methane group.

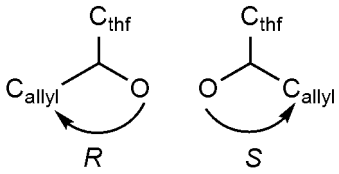

Figure 72: *R* and *S* conformations in the complex **[4.1]$_2$** for L^3

In principle aggregation state equilibria are possible, however the dimeric structure of **[4.1]**$_2$ in solution remains intact. The structure of analogous complex $[Li(C_3H_5)]_2$ also remains a dimer in thf under various conditions.[12]

The ^{1}H NMR spectrum of **[4.2]**$_2$ is similar to that of **[4.1]$_2$**. Similar patterns are seen in the ^{1}H and ^{13}C NMR spectra for complex **[4.2]**$_2$, in both ^{1}H and ^{13}C NMR spectra there are four resonances for the $SiMe_3$, four ^{13}C resonances for the CH_2 groups, however there are only three resonance for the allyl carbon atoms. Due to the fact the donor functionalised ligand in **[4.2]**$_2$ does not contain any chiral carbon atoms the ^{1}H NMR spectrum resonances are clearer and the allyl protons resonances can be identified; a doublet at 5.51ppm for the C*H*SiMe$_3$ protons and a doublet at 7.18ppm for the C*H*CHSiMe$_3$ protons.

4.3.2 Complex [(thf)K{(SiMe$_3$)$_2$C$_3$H$_2$(CH$_2$C$_4$H$_7$O)}]$_\infty$ [4.5]$_\infty$

The potassium complex of $\mathbf{L^3}$H was synthesised by treating potassium *tert*-butoxide (KO^{t}Bu) with freshly prepared $\mathbf{L^3}$Li in hexane to give a viscous solution. Evaporating the hexane afforded a red-brown powder which was re-dissolved in thf and left to recrystallise, affording crystals of [(thf)K{(SiMe$_3$)$_2$C$_3$H$_2$(CH$_2$C$_4$H$_7$O)}]$_\infty$ **[4.5]**$_\infty$ in a 34% yield (Scheme 33 and Figure 73). Complex **[4.5]**$_\infty$ is the first donor-functionalised potassium allyl complex.

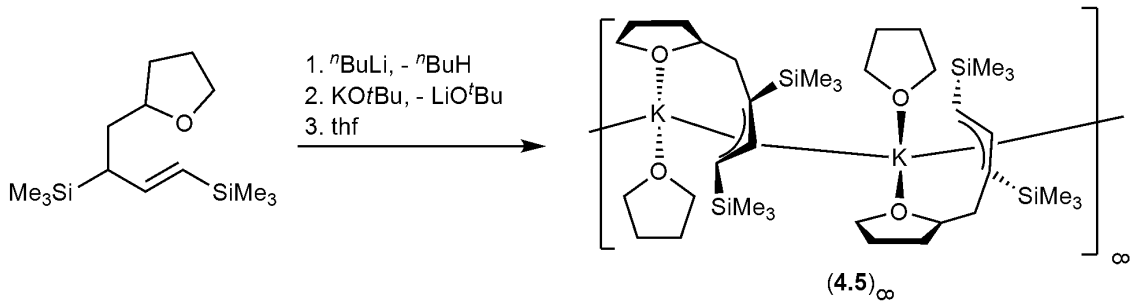

(**4.5**)$_\infty$

Scheme 33

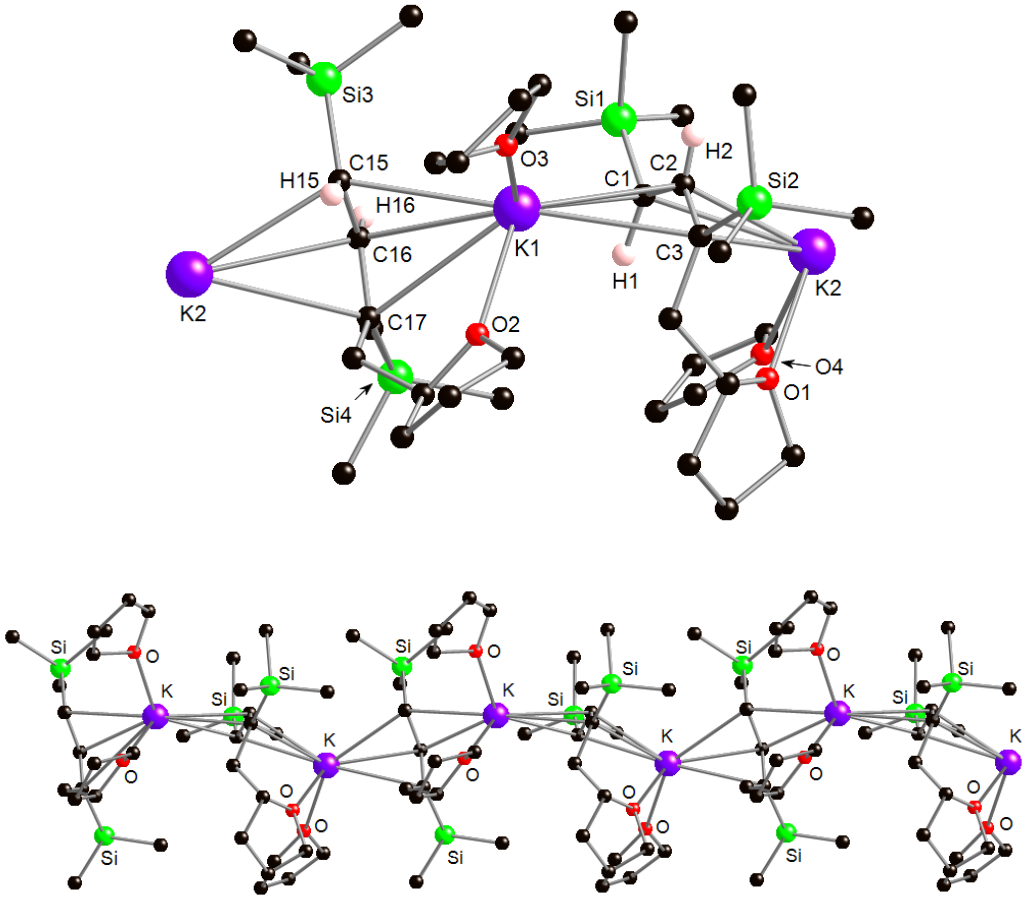

Figure 73: Molecular structure of [(thf)K{(SiMe$_3$)$_2$C$_3$H$_2$(CH$_2$C$_4$H$_7$O)}]$_\infty$ **[4.5]**$_\infty$, detailed structure (upper) and extended segment (lower), selected bond lengths (Å) and angles (°). Hydrogen atoms, except those bonded to allylic carbon atoms, are omitted for clarity, black = carbon, green = silicon, purple = potassium, red = oxygen, pale pink = hydrogen: C(1)−C(2) 1.411(5), C(2)−C(3) 1.395(5), C(15)−C(16) 1.411(5) C(16)−C(17) 1.397(5), K(1)−C(1) 3.119(4), K(1)−C(2) 3.059(4), K(1)−C(3) 3.188(4), K(1)−C(15) 3.103(4), K(1)−C(16) 3.015(3), K(1)−C(17) 3.348(4), K(2)−C(1) 3.085(4), K(2)−C(2) 3.007(4), K(2)−C(3) 3.333(4), K(2)−C(15) 3.074(3), K(2)−C(16) 3.048(3), K(2)−C(17) 3.218(4), K(2)−O(1) 2.659(3), K(1)−O(2) 2.664(3), K(1)−O(3) 2.731(3), K(2)−O(4) 2.727(8) average due to disorder, C(3)−C(2)−C(1) 131.0(3), C(17)−C(16)−C(15) 131.4(3).

Complex **[4.5]**$_\infty$ crystallises as a zig-zag coordination polymer consisting of two unique, repeating molecules of [**L**^{3}K(thf)] in which the configuration at the tetrahydrofurfuryl CH group alternates between *R* and *S* along the polymer. The potassium cation is formally 6-coordinate. Individual molecules of [**L**^{3}K(thf)] aggregate by means of μ:η^3:η^3-allyl interactions, which result in the zig-zag polymer in which K(1) and K(2) alternate generating a K(1)···K(2)···K(1) angle of 141.3°. Each potassium is also coordinated by the *intra*molecular pendant *O*-donor group and one thf ligand. The K−C in complex **[4.5]**$_\infty$ bonds range from 3.009(4) to 3.348(4) Å, with an average length of 3.133 Å. The polymeric structure and the bond lengths of complex **[4.5]**$_\infty$ are typical of potassium allyl complexes, for example complexes [(thf)K{$C_3H_3(SiMe_3)_2$}]$_\infty$ **1.10**, [K{$C_3H_3(SiMe_3)_2$}]$_\infty$ **1.14** and [K_2{(η^3-$C_6H_4SiMe_3$-6)$_2$$SiMe_2$}$(thf)_3$]$_\infty$ **1.20** in which the K−C bond distances are 2.93-3.12 Å (as quoted),[21] 2.87-3.15 Å (as quoted)[24] and 2.932(6)-3.350(7) Å.[29] The C−C bond lengths within the allyl units of complex **[4.5]**$_\infty$ are 1.412(5), 1.394(5), 1.412(5) and 1.397(5) for C(1)−C(2), C(2)−C(3), C(15)−C(16) and C(16)−C(17), respectively, and the Si–C–C−C torsional angles are 174.3(3) to 179.6(3)°. Suggesting that the negative charge is fully delocalised across the allyl unit. Complexes **1.10**, **1.14** and **1.20** have C−C bond lengths and torsional angles of 1.366(4)-1.400(4) Å, 168.8-178.8°; 1.372(1)-1.392(1) Å, 172.2-179.9° and 1.379(5)-1.412(4), 168.2-179.5°, respectively.

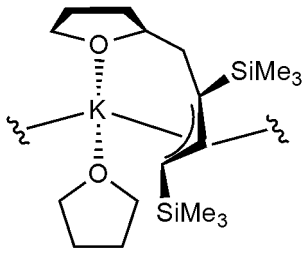

Figure 74: Segment of complex **[4.5]**$_\infty$, delocalisation of the negative charge across the allyl

In addition to the potassium allyls **1.10**, **1.14** and **1.20**, there are the mixed metal complexes [K(thf)Ba_2{$C_3H_3(SiMe_3)_2$}$_5$] (**1.31**)[42] and [Sm{μ-$C_3H_3(SiMe_3)_2$}$_2$-

$\{C_3H_3SiMe_3\}_2K(thf)_2]_2$ (**1.42**)[52] are known, which both exhibit K−C and C−C bond lengths similar to **[4.5]**$_\infty$, as well as similar Si−C−C−C torsional angles.

As with complex **[4.1]**$_2$ the ^{1}H and ^{13}C NMR spectra of complex **[4.5]**$_\infty$ were recorded in benzene-d_6, with the spectra showing evidence of two diastereomeric forms. For example there are four resonances in both the ^{1}H and ^{13}C NMR spectra of complex **[4.5]**$_\infty$ for the $SiMe_3$ at 0.33, 0.29, 0.20 and 0.00ppm. The ^{1}H spectrum is also complicated by the additional thf ligand coordinated to the potassium, however, resonances at 6.83 ppm (a broad dimer, integrating 0.3H) and at 6.01 ppm (multiplet, integrating 1.3H) correspond to the central allyl CH with a ^3J = 16.1 Hz; for the terminal allyl CH there is a very broad multiplet between 1.77-1.15 ppm. The NMR as already stated, suggests the presence of two diastereomeric forms, due to each proton and carbon having two resonances in the NMR spectra.

4.3.3 Complex [Mg{(SiMe$_3$)$_2$C$_3$H$_2$(CH$_2$C$_4$H$_7$O)}$_2$] (4.6)

The magnesium complex of **L**^{3}H [Mg{(SiMe$_3$)$_2$C$_3$H$_2$(CH$_2$C$_4$H$_7$O)}$_2$] (**4.6**) was prepared by treating **L**^{3}H with ^{n}Bu$_2$Mg (dibutylmagnesium) in hexane and heating to reflux for 18hrs. The solution was then allowed to slowly cool to afford colourless needle-like crystals of complex **4.6** in a 15% yield (Scheme 34 and Figure 75).

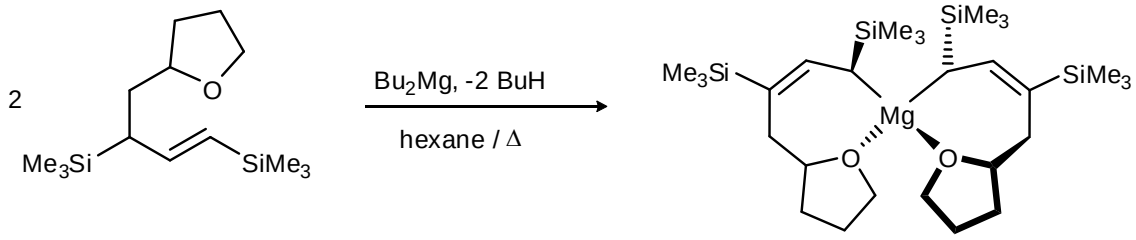

(**4.6**)

Scheme 34

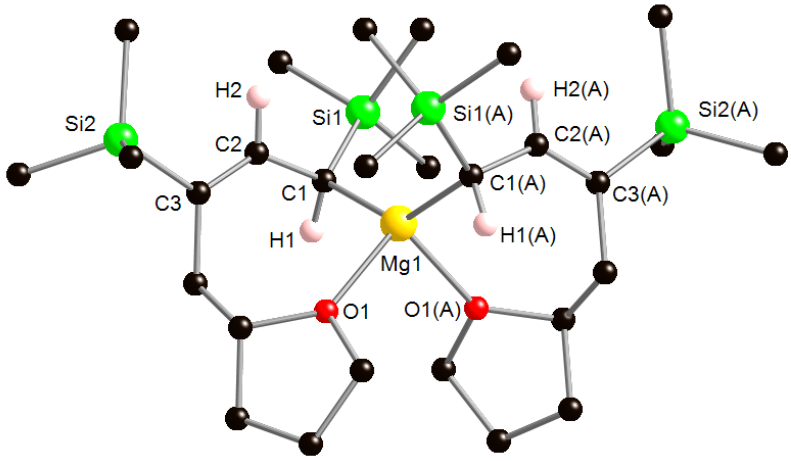

Figure 75: Molecular structure of [Mg{$(SiMe_3)_2C_3H_2(CH_2C_4H_7O)$}$_2$] (**4.6**), selected bond lengths (Å) and angles (°). Hydrogen atoms, except those bonded to allylic carbon atoms, are omitted for clarity, black = carbon, green = silicon, yellow = magnesium, red = oxygen, pale pink = hydrogen: Mg(1)−O(1) 2.063(2), Mg(1)−C(1) 2.172(4), C(1)−C(2) 1.461(5), C(2)−C(3) 1.348(5), C(3)−C(2)−C(1) 132.3(3), C(1)−Mg(1)−O(1) 100.65(12), C(1)−Mg(1)−C(1A) 138.9(2), O(1)−Mg(1)−O(1A) 91.52(13). Symmetry transformations used to generate equivalent atoms (A) = $-x + 3/2, -y + 1/2, z$.

Molecules of **4.6** are C_2-symmetric and the two $\mathbf{L^3}$ ligands coordinate to magnesium by an η^1 bond to the C(1) allyl carbon and by the oxygen atom of the pendant tetrahydrofurfuryl group. The bond angles around the magnesium cation are C(3)−C(2)−C(1) 132.3(3)°, C(1)−Mg(1)−O(1) 100.65(12)°, C(1)−Mg(1)−C(1A) 138.9(2)°, O(1)−Mg(1)−O(1A) 91.52(13)° giving a highly distorted tetrahedral geometry. The Mg(1)−C(1) and Mg(1)−O(1) bond lengths are 2.173(4) and 2.063(2) Å, respectively, which results in the formation of seven-membered chelate rings. The formation of these seven-membered rings suggests that after initial deprotonation there is a 1,3-sigmatropic rearrangement, which is possibly due to steric factors that would not allow a complex to form without the rearrangement. Another possibility for the 1,3-sigmatropic rearrangement is that without it the complex would form strained 5-membered chelate rings to coordinate to the metal. The two chiral carbon atoms, C(1) and C(5), are in the *S* configuration, giving the overall structure of the complex (*R*,*R*)(*S*,*S*)-[Mg{$(SiMe_3)_2C_3H_2(CH_2C_4H_7O)$}$_2$].

Complex **4.6** can be compared with the externally solvated analogue complex **1.25** $[Mg(thf)_2\{(SiMe_3)_2C_3H_3\}_2]$ (Chapter 1), in which the Mg−C bond lengths are 2.197(3) and 2.195(3) Å and the Mg−O bond lengths are 2.057(17) and 2.054(13) Å,[36] which are very similar to those seen in complex **4.6**. The magnesium complex $[Mg(\eta^1\text{-}C_3H_5)(tmeda)(\mu\text{-}Cl)_2]_2$ (**1.22**)[31] has a Mg−C bond length of 2.179(3) Å which is the same (within error) as that seen in complex **4.6**. Also complexes **4.6**, **1.22** and **1.25** have completely localised C−C allyl bond lengths are a result of the magnesium forming a σ-bond to the allyl. The C−C bond lengths are C(1)−C(2) 1.461(5) and C(2)−C(3) 1.348(5) Å for complex **4.6**, and for complex **1.22** and **1.25** C−C bond distances are 1.442(4) and 1.335(4) Å and 1.467(4), 1.352(4), 1.469(4) and 1.355(4) Å, respectively. As discussed in Chapter 1, magnesium allyl complexes have not been studied in as much detail as other s-block metals, and few examples have been crystallographically characterised. Compared to alkali metals and the group 2 metals (except beryllium), magnesium tends to form η^1/σ bonds to allyl ligands. However, for the recently structurally characterised $[Mg\{C_3H_3(SiMe_3)_2\}_2]_2$ **1.24**, the Mg^{2+} cation is bridging between two allyl ligands in a π/η^2 manner which has Mg−C ranging from 2.139(2)-2.464(3) and C−C bond distances ranging from 1.353(3)-1.471(3) and 1.328(3)-1.484(3) for the non-bridging and bridging allyl ligands, repectively.[36] The bond lengths in **1.24** are similar to those seen in **4.6**.

The ^1H and ^{13}C NMR spectra of complex **4.6** were recorded in dmso-d_6 (in benzene-d_6 a gelatinous precipitate forms); the spectra also show evidence of a second diastereomer in addition to the (*R*,*R*) and (*S*,*S*) enantiomeric of the two chiral carbons within each $\mathbf{L^3}$ are (*R*,*S*) or (*S*,*R*). In both the ^1H and ^{13}C NMR spectra there are four resonances for the $SiMe_3$ groups, 0.00, -0.01, -0.05, -0.09 ppm in the ^1H NMR spectrum and 0.02, -0.25, -1.14, -2.80 ppm in the ^{13}C NMR spectrum. In the ^1H NMR spectrum

there is a broad doublet at 2.23 ppm (^3J = 6.7 Hz) corresponding to the terminal allyl CH, however there is no clear resonance for the central allyl CH.

4.4 Conclusion

In summary, four new donor-functionalised allyl complexes were synthesised. Both complexes **[4.1]**$_2$ and **[4.2]**$_2$ have similar dimeric structures, with each lithium cation in a distorted tetrahedral environment. The coordination environment of the lithiums includes one η^3-allyl ligand, as well the *O*-donor-functional group. The lithium cation also bridges across to the second allyl unit and is coordinated by an η^1-allyl ligand. In both lithium complexes **[4.1]**$_2$ and **[4.2]**$_2$ the negative charge is partially localised across the allyl moiety of the ligand.

Complex **[4.5]**$_\infty$ crystallises in a zig-zag coordination polymer consisting of two unique, repeating molecules of [**L**^{3}K(thf)]. The configuration at the tetrahydrofurfuryl CH group alternates between *R* and *S* along the polymer. The potassium cation is formally 6-coordinate; the molecules of [**L**^{3}K(thf)] aggregate *via* μ:η^3:η^3-allyl interactions, which result in the zig-zag polymer, each potassium is also coordinated by the *intra*molecular pendant *O*-donor group and one thf ligand and as with most potassium allyl complexes the negative charge is completely delocalised across the allyl. In this complex, the large radius of the potassium means that despite coordination of the donor group of the ligand, the metal is not held specifically over one end or the other of the allyl, and as a result SSEPOC is not seen and the negative charge is completely delocalised. It is likely that the different aggregation states of the lithium and potassium allyl complexes is also due to the different size of the metal ion radii, with the larger size of K^+ cation allowing for a larger coordination number than lithium.

Complex **4.6** is C_2-symmetric and with two **L**^{3} ligands coordinated to magnesium cation by an η^1 bond to an allyl carbon and by the oxygen atom of the pendant

tetrahydrofurfuryl group, these bonds result in two seven-membered chelate rings, whose formation suggests that after initial deprotonation there is a 1,3-sigmatropic rearrangement. The coordination environment around the magnesium cation is a highly distorted tetrahedral geometry. Also complex **4.6** has completely localised C−C allyl bond lengths are a result of the magnesium forming a σ-bond to the allyl.

The NMR spectroscopy studies showed that for all the donor-functionalised complexes $\mathbf{[4.1]}_2$, $\mathbf{[4.2]}_2$, $\mathbf{[4.5]}_\infty$ the solid-state structure is preserved in solution, however the NMR spectra are complicated by overlapping diastereomers within solution. The ^{1}H and ^{13}C NMR spectroscopy for complex **4.6** was run in dmso-d_6. Therefore, the solid-state structure will not be maintained, and it is likely the dmso will coordinate to the magnesium, and potentially displace a pendant thf group.

Chapter 5

Introduction to Metal Pentadienyl Complexes

5.1 An Introduction to Metal Pentadienyl Chemistry

At the beginning of the 1980's the pentadienyl (Pn) ligand had received very little attention compared to the cyclopentadienyl and allyl ligands. Since Ernst *et al.* began thorough investigations into pentadienyl chemistry the area has expanded significantly, with the major focus being on transition metal complexes.[143,144] Several types of pentadienyl ligand are known, such as **5.1-5.5**. The focus of this discussion will be mainly on ligand types **5.1**, **5.2** and **5.3**. When bonded to a metal the pentadienyl ligand can adopt one of three conformations (Figure 76). Their hapticity can be η^1, η^3 or η^5. The main focus of this literature review will be on the s-block and f-block complexes of pentadienyl ligands, with a brief discussion on d-block complexes of silyl-substituted pentadienyl ligands.

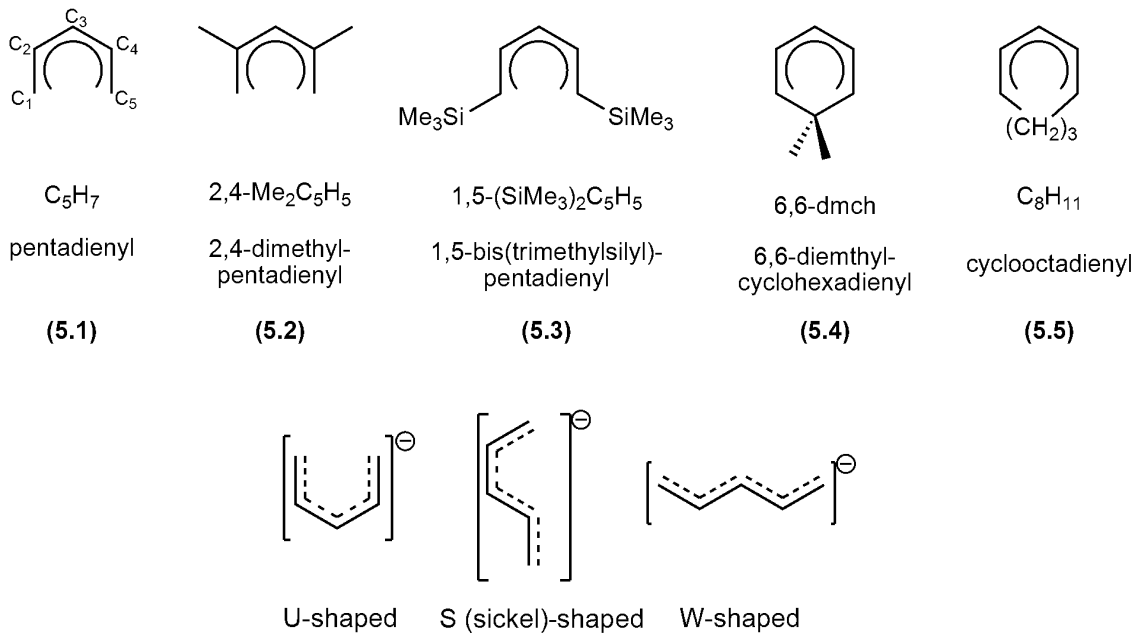

Figure 76: (Above) Examples of pentadienyl ligands. (Below) Different conformations of the pentadienyl anion

5.2 s-Block Metal Pentadienyl Complexes

Very few s-block pentadienyl complexes have been structurally characterised. Most s-block metal pentadienyl complexes are known in solution-state or have been

investigated only theoretically. In the early 1970's, NMR spectroscopic studies and anion trapping reactions were carried out on pentadienyllithium.[145,146] These studies showed that for a range of different pentadienyl anions, the negative charge is predominantly delocalised over the C_1, C_3 and C_5 carbon atoms. The ^{13}C NMR spectrum of various pentadienyl ligands shows that the odd numbered carbons C_1, C_3 and C_5 of the pentadienyl ligand are at higher field (65-99 ppm) compared to the even numbered carbons C_2 and C_4 (127-147 ppm). From this it can be deduced that C_1, C_3 and C_5 have more electron density located around them than C_2 and C_4.[145] From Figure 77 it can be seen that the combination of p-orbitals of the HOMO produces nodes at C_2 and C_4, meaning that the electron density is shared between C_1, C_3 and C_5.[147]

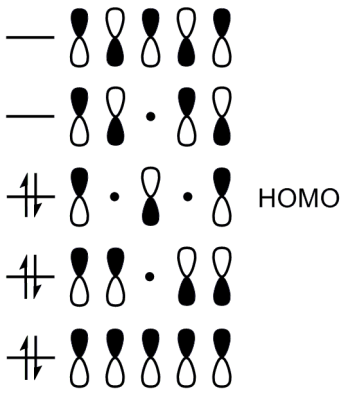

Figure 77: Representation of combinations of p-orbitals of a pentadienyl anion to form molecular orbitals.

The reactions of several alkali metal pentadienyl compounds with alkaline hydrogen peroxide exclusively react at the terminal carbon atoms.[149] Similar conclusions were made in a regioselectivity study, by Nakamura, in which the electrophile reacted at a terminal carbon atom, followed by C_5 then finally at the C_3 position (Scheme 35).[148]

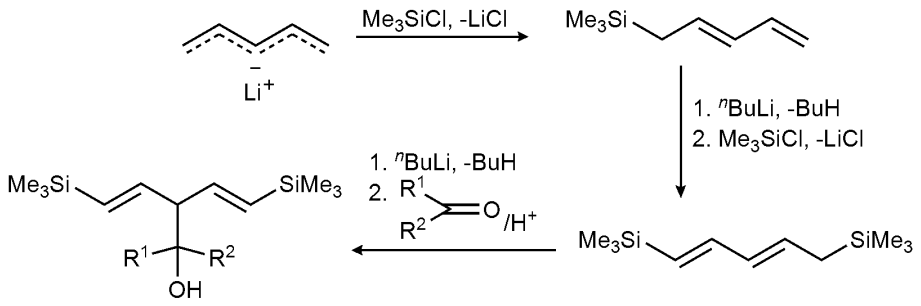

Scheme 35

First Nakamura investigated the addition of aldehydes and ketones to [(*E*)-1-(trimethylsilyl)pentadienyl]lithium, [{(*E*)-1-($SiMe_3$)C_5H_6}Li] (**5.6**). This generally gave a mixture of two regioisomers (**5.8** and **5.9**) (Scheme 36), the yields/ratio of the isomers would depend on the cation and the aldehydes or ketone used.

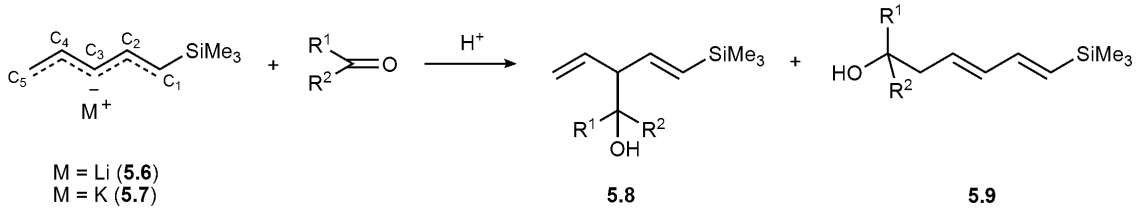

M = Li (**5.6**)
M = K (**5.7**)

5.8 **5.9**

Scheme 36

Regioselectivity in these reactions is poor, however increasing the steric bulk of the R groups increased the selectivity for addition to the C_5 position to avoid steric clashes with the trimethylsilyl group. Substitution at the C_1 position is suppressed by the presence of the trimethylsilyl group. Whether the counter ion is lithium or potassium is thought to make little difference to the selectivity of the reaction. On the other hand, addition of aldehydes and ketones to [{1,5-($SiMe_3$)$_2C_5H_5$}Li] (**5.10**) gave the product **5.11** with high selectivity for the C_3 position (Scheme 37).

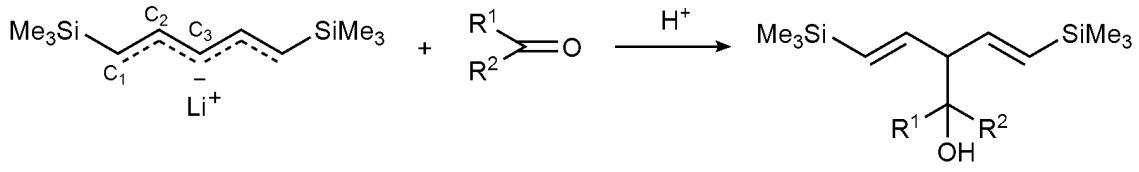

5.10 **5.11**

Scheme 37

More specific solution-state structures have been determined for lithium, potassium, rubidium and caesium pentadienyl complexes; [Li(C_5H_7)] (**5.12**),[146,149] [Li(2-MeC_5H_6)] (**5.13**), [K(C_5H_7)] (**5.14**),[150] [K(2-MeC_5H_6)] (**5.15**), [K(2,4-$Me_2C_5H_5$)] (**5.16**),[149] [Rb(C_5H_7)] (**5.17**) and [Cs(C_5H_7)] (**5.18**).[150] It was shown that the conformation of the pentadienyl anion depended on the cation, solvent and temperature of the solution. Complex **5.12** in ether solutions is in the W conformation, as is complex **5.13**, however

for the larger cations potassium, rubidium and caesium the U-shape conformation is the most stable in ether solutions, as is the U-shape conformation for [Li(2,4-$Me_2C_5H_5$)] (**5.19**). However, trapping reactions with chlorotrimethylsilane have shown that either a hexane suspensions of **5.14** or cooling a thf solution of **5.14** react to form the *trans* product (*E*)-2,4-pentadienyltrimethylsilane, suggesting the W-shaped pentadienyl conformation. It has been shown that pentadienylpotassium complexes are in the W-shaped conformation in liquid ammonia.[150] NMR spectroscopy studies on [Li{1,3,5-($Me_3Si)_3C_5H_4$}] (**5.20**) revealed that the structure of the complex is temperature dependent in solution, and that the limiting structure is the S-shaped conformation of the pentadienyl ligand.[151]

Streitweiser *et al.*[152] and Merino *et al.*[153] undertook computational studies of group 1 metal pentadienyl complexes. These studies investigated a range of group 1 metals (M = Li-Cs) with the pentadienyl anion $[C_5H_7]^-$ and the 2,4-dimethyl-substituted pentadienyl anion $[2,4\text{-}Me_2C_5H_5]^-$. In the gas-phase, it was shown that for all alkali metals, with both pentadienyl anions, that the U-shaped conformation was the most stable. However, for the free pentadienyl anion $[C_5H_7]^-$ the most stable conformation is W-shape, and the U-conformation is 3.4 kcal mol^{-1} higher in energy due to steric interactions between the hydrogen atoms. This is not the case for the $[2,4\text{-}Me_2C_5H_5]^-$ anion, which adopts the U-conformation, in the gas-phase. These findings are in agreement with NMR spectroscopy studies, with the exception of [Li(C_5H_7)] (**5.12**), which was shown to be in the W-conformation in thf. Solvent effects were modelled using COSMO (COnductor-like Screening MOdel), however in a variety of simulated dielectric constants the U-shaped conformation was still the most stable. However, in water the W-shaped conformation is only 0.8 kcal mol^{-1} higher in energy, suggesting that it could exist at room temperature.

The first and only crystallographically characterised group 1 metal pentadienyl complex was reported in 1988 (Figure 78).[154] The complex [(tmeda)K(2,4-$Me_2C_5H_5$)] (**5.21**) was synthesised by treating 2,4-dimethylpentadienyl with metallic potassium in thf in the presence of tmeda at −78 °C. As is seen with both allyl and cyclopentadienyl complexes of potassium, in the solid-state [(tmeda)K(2,4-$Me_2C_5H_5$)] has a polymeric structure in which the two K^+ cations are bridged by a U-shaped η^5 2,4-dimethylpentadienyl anion, each potassium cation is also coordinated by the two nitrogen atoms of the tmeda ligand. The polymer chain has a zig-zag structure to give a K···K···K angle of 120.3° (as quoted).[154] The K−C bond distances range from 3.152(7) to 3.219(8) Å, which is slightly longer than the K−C bond distances in the allyl complexes $[(thf)_3K_2\{C_3H_3(SiMe_3)_2\}_2]_\infty$ (**1.10**) and $[K\{C_3H_3(SiMe_3)_2\}]_\infty$ (**1.14**) are 2.93 to 3.12 Å[21] and 2.87 to 3.15 Å,[24] respectively, (as quoted).

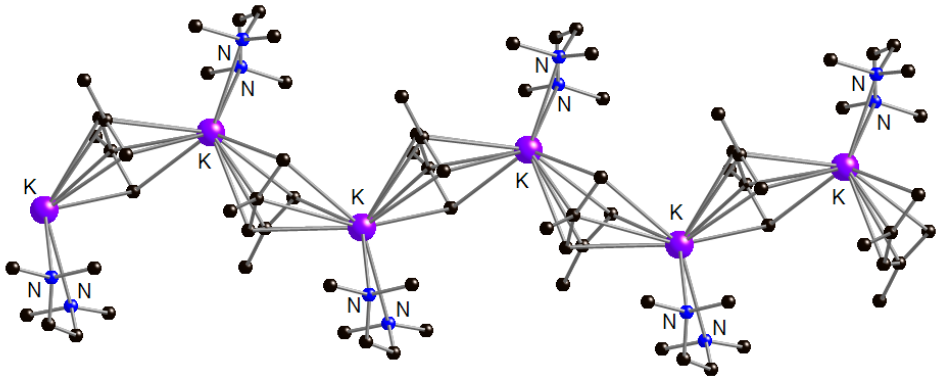

Figure 78: Molecular structure of $[(tmeda)K(2,4\text{-}Me_2C_5H_5)]_\infty$ (**5.21**) Hydrogen atoms have been omitted for clarity, carbon = black, nitrogen = blue, potassium = bright purple. Reproduced from ref. 154

Complex **5.21** is also structurally similar to $[K(C_5H_5)]_\infty$ (**5.22**), which has the same zig-zag polymer structure in the solid-state. The K−C_{Cp} bond lengths are in the range of 2.955(5) to 3.140(6) Å and the K···K···K angle along the polymer is 138.0° (as quoted).[155]

Group 2 metal pentadienyl complexes have been studied less than the group 1 metal pentadienyl complexes. Nakamura *et al.* synthesised a range of magnesium pentadienyl

complexes, and studied their structures using NMR spectroscopy and X-ray crystallography.[156] A range of acyclic pentadienyl complexes of general formula [(tmeda)Mg{Pn}$_2$] were synthesised where Pn = C_5H_7 (**5.23**), 5-MeC_5H_6 (**5.24**), 4-MeC_5H_6 (**5.25**), 3-MeC_5H_6 (**5.26**) and 2,4-$Me_2C_5H_5$ (**5.27**), as well as cyclic pentadienyl complexes [(tmeda)Mg{Pn}$_2$] where Pn = C_7H_9 (**5.28**) and Pn = C_8H_{11} (**5.29**). All the magnesium complexes were synthesised *via* the same route; two equivalents of the potassium pentadienyl complex were treated with one equivalent of anhydrous magnesium halide in thf, and the pure crystalline products were isolated as the tmeda complex. NMR spectroscopy revealed that all acyclic complexes contain a σ-bound, terminal pentadienyl ligand; for the **5.23** to **5.26** the pentadienyl is in the W-shaped conformation in solution. For the cyclic magnesium pentadienyl complexes **5.28** and **5.29** the magnesium is σ-bound to the C_3 central carbon given a 1,4-diene structure.

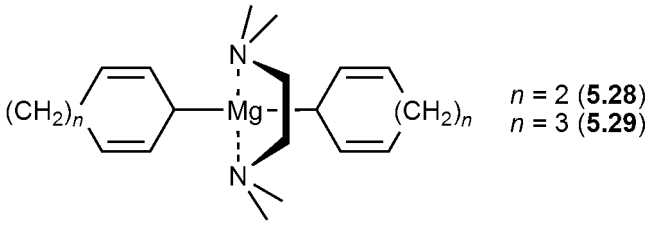

Figure 79: Structures of cyclic magnesium pentadienyl complexes **5.28** and **5.29**

The acyclic pentadienyl complex **5.27**, like the other acyclic pentadienyl complexes, has a 1,3-diene structure in solution and the magnesium cation is σ-bound to the terminal carbon atom, however the 2,4-dimethylpentadienyl ligand is in the U-shape conformation. This unusual U-shaped conformation for complex **5.27** is due to steric repulsion between the two methyl groups, making the W-shaped conformation less favourable (Figure 80).

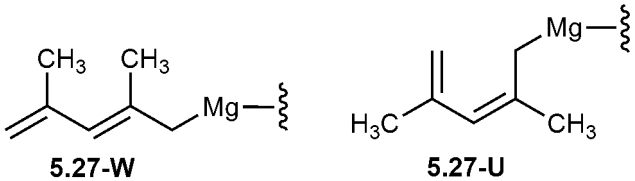

5.27-W **5.27-U**

Figure 80: Part of the structures of the W- and U-conformations for complex **5.27**

Complex **5.27** was analysed by X-ray crystallography. The solid-state structure of complex **5.27** (Figure 81) confirmed the U-shaped conformation of the pentadienyl ligand that was seen in the solution-state. The geometry around the magnesium atom is a distorted tetrahedron; the N−Mg−N′, N′−Mg−C′, N−Mg−C and C−Mg−C bond angles are 84.2(5), 118.0(6), 110.4(6) and 113.1(6)°, respectively. The magnesium in complex **5.27** is coordinated by the terminal carbon atom of the 2,4-dimethylpentadienyl ligand, and the Mg−C bond length of 2.179(15) Å is similar to that in the allyl complex $[Mg(\eta^1\text{-}C_3H_5)(tmeda)(\mu\text{-}Cl)_2]_2$ (**1.19**).[31]

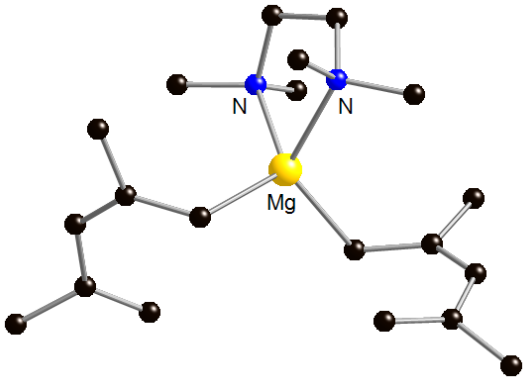

Figure 81: Molecular structure of $[(tmeda)Mg(2,4\text{-}Me_2C_5H_5)_2]$ (**5.27**) Hydrogen atoms have been omitted for clarity, carbon = black, nitrogen = blue, magnesium = yellow. Reproduced from ref. 156

Nakamura *et al.* synthesised a range of beryllium pentadienyl complexes with the general formula $[(tmeda)Be\{Pn\}_2]$ where Pn = C_5H_7 (**5.30**), 3-MeC_5H_6 (**5.31**), 4-MeC_5H_6 (**5.32**), 5-MeC_5H_6 (**5.33**) and 2,4-$Me_2C_5H_5$ (**5.34**).[157] As seen with the magnesium complexes (**5.23** to **5.27**), the beryllium cation in complexes **5.30** to **5.34** is σ-bound to the terminal carbon atom of the pentadienyl ligand. For complex **5.30** two different methods were employed to synthesise the complex, and the structure of the complex is dependent on which method was used. One method to synthesise complex **5.30** is to react two equivalents of potassium pentadienyl with $BeCl_2$ in thf. The other method is to react two equivalents of $[(C_5H_7)MgBr{\cdot}2thf]$ with $BeCl_2$. If complex **5.30** is

prepared *via* the potassium pentadienyl route there is only one product, the W-shape conformation of the pentadienyl terminally σ-bonded to the beryllium. However, NMR spectroscopy and hydrolysis studies on complex **5.30** prepared from the magnesium pentadienyl reveals that there is an 8:1 mixture of the W-shape and S-shape conformations. Complex **5.31** has the methyl substituent on the central carbon atom of the pentadienyl and has the W-shaped pentadienyl ligand σ-bonded to beryllium. Complex **5.32** exists predominantly (95%) in the *bis*[(*E*)-2-methyl-1,3-pentdienyl]beryllium form, and complex **5.33** exist in 4:1 mixture of the *bis*[(*E,E*)-2,4-hexadienyl]beryllium and *bis*[(*E,Z*)-2,4-hexadienyl]beryllium forms. Complex **5.34** in NMR spectroscopy studies showed that there were two sets of resonances in 7:5 ratio, corresponding to a mixture of U-shaped and W-shaped pentadienyl ligand with a terminally σ-bonded beryllium cation.

The only other example of a group 2 pentadienyl complex is the calcium complex [(thf)Ca{2,4-(^{t}Bu)$_2$C$_5$H$_5$}$_2$] (**5.35**) (Figure 82).[158] Complex **5.35** was synthesised by reacting two equivalents of the potassium pentadienyl [K{2,4-(^{t}Bu)$_2$C$_5$H$_5$}] with CaI_2 in thf, and crystals suitable for X-ray crystallography were slowly grown from a saturated hexane solution.

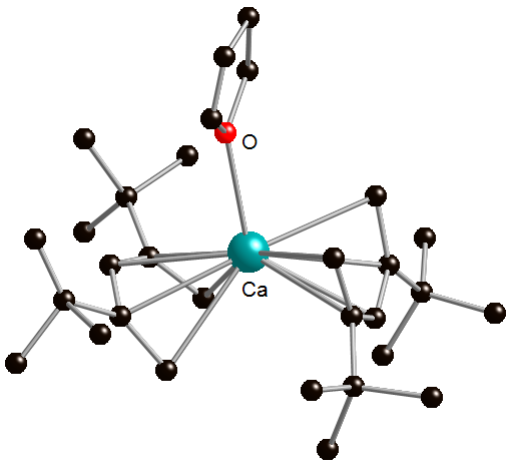

Figure 82: Molecular structure of [(thf)Ca{2,4-(^{t}Bu)$_2$C$_5$H$_5$}$_2$] (**5.35**) Hydrogen atoms have been omitted for clarity, carbon = black, oxygen = red, calcium = blue. Reproduced from ref. 158

Complex **5.35** is monomeric, and unlike its magnesium and beryllium counterparts, the calcium is coordinated by two pentadienyl ligands in the U-conformation, in an η^5 manner, as well as by a thf ligand. The Ca−C bond distances range from 2.74(2) to 2.81(2) Å, and are longer than the Ca−C bond distances seen in the cyclopentadienyl complex [(thf)Ca{1,3-$(SiMe_3)_2C_5H_3$}$_2$] (**5.36**) (2.678(8) Å).[159] The allyl complex [Ca{η^3-$C_3H_3(SiMe_3)_2$}$_2$(thf)$_2$] (**1.23**) (Figure 15, Chapter 1), which has a similar structure to **5.35**, has Ca−C_{allyl} bond distances in the range 2.648(3)-2.662(3) Å.[37]

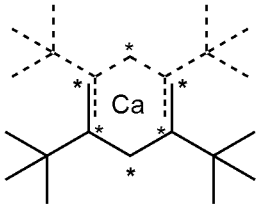

Figure 83: *Anti*-eclipesd structure of complex **5.35**, carbon atoms marked with an asterisk (*) indicate the location of the negative charge on the pentadienyl ligand. Reproduced from ref. 158

The pentadienyl ligands are coordinated to the calcium metal centre in a nearly perfect *anti*-eclipsed conformation (Figure 82 and Figure 83). The *anti*-eclipsed conformation is thought to occur partly to avoid unfavourable steric interactions between the *tert*-butyl groups, but also as a result of the *anti*-eclipsed conformation providing more favourable metal-ligand electrostatic bonding.

The last set of compounds to be discussed are a family of zinc pentadienyl complexes: [ZnCl(C_5H_7)·tmeda] (**5.37**), [Zn(C_5H_7)$_2$·tmeda] (**5.38**), [Zn(3-MeC_5H_6)$_2$·tmeda] (**5.39**), [Zn(4-MeC_5H_6)$_2$·tmeda] (**5.40**), [Zn(5-MeC_5H_6)$_2$·tmeda] (**5.41**) and [Zn(2,4-$Me_2C_5H_5$)$_2$·tmeda] (**5.42**).[157] The pentadienyl ligands are σ-bound to the zinc and are analogous to the beryllium complexes made [(tmeda)Be{Pn}$_2$] **5.30-5.34**, so will not be discussed.[157]

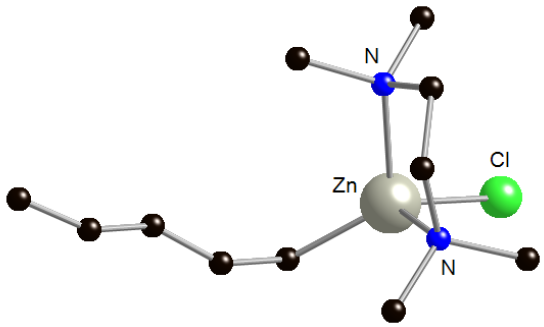

Figure 84: Molecular structure of [ZnCl(C_5H_7)·tmeda] (**5.37**). Hydrogen atoms have been omitted for clarity, carbon = black, chlorine = green, nitrogen = blue and zinc = grey. Reproduced from ref. 157

X-ray crystallography on complex [ZnCl(C_5H_7)·tmeda] (**5.37**) revealed that the zinc cation is in a distorted tetrahedral geometry; coordinated by the pentadienyl ligand *via* a σ-bond to the C_1 atom in the **W**-shape conformation, the two nitrogen atoms of the tmeda ligand and a chlorine atom (Figure 84). The Zn−C bond length is 2.031(12) Å which is similar to the Mg−C bond distance (2.179(15) Å) in the complex [(tmeda)Mg(2,4-$Me_2C_5H_5)_2$] (**5.27**) discussed previously. The C−C bond lengths in complex **5.37** are representative of localised double and single bonds.

5.3 Group 3 and f-Block Metal Pentadienyl Complexes

Very few f-block metal complexes of pentadienyl ligands are known. However their structures are similar to those of the s-block because M-L bonding is ionic. One of the first structurally characterised lanthanide pentadienyl complexes is [Nd(2,4-$Me_2C_5H_5)_3$] (**5.43**).[160] A monomeric structure was confirmed by X-ray crystallography (Figure 85); the neodymium cation is coordinated to three U-shaped η^5-2,4-dimethylpentadienyl ligands.

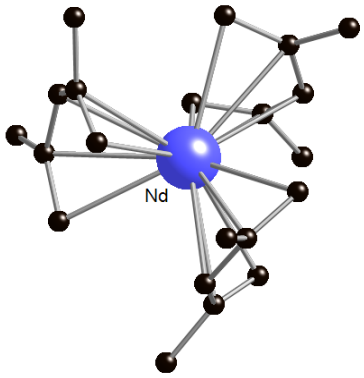

Figure 85: Molecular structure of [Nd(2,4-$Me_2C_5H_5)_3$] (**5.43**) Hydrogen atoms have been omitted for clarity, carbon = black, neodymium = blue. Reproduced from ref. 160

The C−C bond distances within the pentadienyl ligands in **5.43** can be split into two sets; internal bond between C_2−C_3 and C_3−C_4 and external bonds between C_1−C_2 and C_4−C_5 (Figure 85). The internal average C−C bond distance is 1.421(12) Å and the external average C−C bond distance is 1.373(12) Å. There are three resonance forms for the pentadienyl ligand. Resonance forms **(K)** and **(M)** have the negative charge localised on the terminal carbon atoms, and resonance form **(L)** has the negative charge localised on the central carbon atom. From the C−C bond lengths it can be seen that resonance form **(L)** has a higher contribution to the structure than resonance forms **(K)** and **(L)**.[160]

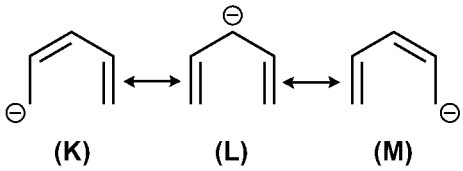

Figure 86: Resonance forms of the pentadienyl anion.

The Nd−C bond distances can also be split into sets; Nd−$C_{(1,5)}$, Nd−$C_{(2,4)}$ and Nd−$C_{(3)}$ for the respective carbon atoms along the pentadienyl carbon chain. The average Nd−$C_{(1,5)}$, Nd−$C_{(2,4)}$ and Nd−$C_{(3)}$ bond distances are 2.801(9), 2.855(8) and 2.749(10) Å respectively. It can be seen that the order of bond length is Nd−$C_{(3)}$ < Nd−$C_{(1,5)}$ < Nd−$C_{(2,4)}$, suggesting that the metal cation is interacting more with the carbon atoms that have an associated negative charge. However the Nd−$C_{(2,4)}$ bond lengths are still

within the range of other Nd−C bond distances such as $[Nd(CH_3C_5H_4)_3]_4$ (**5.44**)[161] (Nd−C bond distances 2.703(7) to 2.886(7) Å). Analogous lanthanide complexes were synthesised with the general formula $[Ln(2,4\text{-}Me_2C_5H_5)_3]$; Ln = Y (**5.45**), Ln = La (**5.46**),[162] Ln = Gd (**5.47**),[163] Ln = Tb (**5.48**)[164] and Ln = Dy (**5.49**) (Table 6).[165]

Table 6: Table of average bond distances (Å) for complexes **5.45**-**5.49**

$[Ln(2,4\text{-}Me_2C_5H_5)_3]$	**Ln = Y**	**Ln = La**	**Ln = Gd**	**Ln = Tb**	**Ln = Dy**
$Ln{-}C_{(1)}$	2.700(4)	2.882(3)	2.73	2.76	2.72
$Ln{-}C_{(2)}$	2.795(4)	2.907(2)	2.82	2.86	2.81
$Ln{-}C_{(3)}$	2.755(4)	2.812(2)	2.76	2.80	2.75
$Ln{-}C_{(4)}$	2.797(4)	2.884(2)	2.83	2.82	2.81
$Ln{-}C_{(5)}$	2.713(4)	2.853(3)	2.74	2.74	2.69
$C_1{-}C_2$	1.378(5)	1.379(4)	1.36	1.44	1.36
$C_4{-}C_5$	1.434(5)	1.427(3)	1.43	1.49	1.42
$C_2{-}C_3$	1.421(5)	1.425(3)	1.41	1.48	1.42
$C_3{-}C_4$	1.379(6)	1.376(3)	1.39	1.41	1.36

In the early 1990's Chen *et al.* synthesised a set of lanthanide pentadienyl complexes of general formula $[(C_8H_8)Ln(2,4\text{-}Me_2C_5H_5)\cdot(thf)]$ where Ln = Sm (**5.50**),[166] Ln = Nd (**5.51**) and Ln = Er (**5.52**).[167] The complexes were synthesised by reacting the anhydrous lanthanide chloride in thf with $K_2C_8H_8$ to give the intermediate $[(C_8H_8)LnCl\cdot 2(thf)]$, which was treated with the potassium pentadienyl $[K(2,4\text{-}Me_2C_5H_5)]$. The three complexes have similar structures, but are not isostructural; in all three complexes the metal cation is coordinated by an η^8-C_8H_8 ligand, a U-shaped η^5-pentadienyl ligand and the oxygen of the thf molecule. The difference between the complexes is the orientation of the pentadienyl ligand to the thf molecule; in complexes **5.50** and **5.51** the pentadienyl ligand is coordinated such that the "open" side is facing away from the thf molecule, however with complex **5.52** the pentadienyl ligand has the "open" side facing towards the thf molecule (Figure 87 and Figure 88).

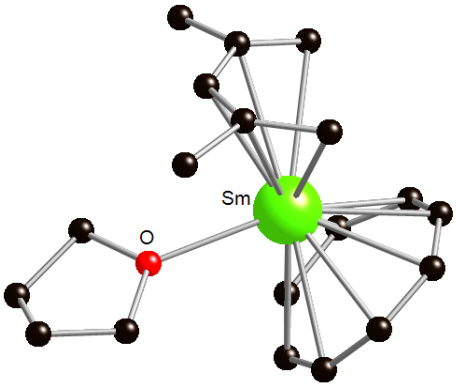

Figure 87: Molecular structure of [(C_8H_8)Sm(2,4-$Me_2C_5H_5$)·(thf)] (**5.50**) Hydrogen atoms have been omitted for clarity, carbon = black, oxygen = red, samarium = green. Reproduced from ref. 166

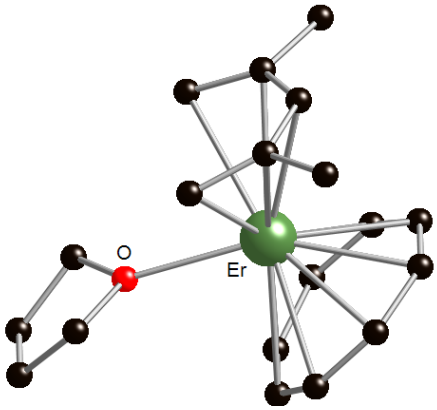

Figure 88: Molecular structure of [(C_8H_8)Er(2,4-$Me_2C_5H_5$)·(thf)] (**5.52**) Hydrogen atoms have been omitted for clarity, carbon = black, oxygen = red, erbium = grey/green. Reproduced from ref. 167

This difference in orientation of the pentadienyl ligand is thought to be due to steric repulsion from the pentadienyl ligand towards the thf molecule; the ionic radii of neodymium and samarium are larger than that of erbium, therefore if complex **5.50** were to have the same structure as complexes **5.50** and **5.51** the ligands would experience steric hindrance.[167] The M−C_{Pn} for complex **5.50**, **5.51** and **5.52** follow the order M−$C_{Pn(3)}$ < M−$C_{Pn(2,4)}$ < M−$C_{Pn(1,5)}$ (see Table 7) and the C−C bond distances within the pentadienyl ligand can be split into two sets, internal and external bonds. As seen with the previous lanthanide examples (**5.43** and **5.45-5.49**), the internal C−C bond distances are longer than those of the external C−C bond distances, suggesting a larger contribution from resonance form **(L)** (Figure 86).

Table 7: Table of bond distances (Å) for complexes **5.50**-**5.52**

[(C_8H_8)Ln(2,4-$Me_2C_5H_5$)·(thf)]	**Ln = Nd**	**Ln = Sm**	**Ln = Er**
Ln−$C_{Pn(1)}$	2.844(15)	2.92(4)	2.736(6)
Ln−$C_{Pn(5)}$	2.927(12)	2.87(4)	-
Ln−$C_{Pn(2)}$	2.814(13)	2.84(3)	2.719(5)
Ln−$C_{Pn(4)}$	2.838(9)	2.84(2)	-
Ln−$C_{Pn(3)}$	2.712(11)	2.70(3)	2.653(7)
C_1−C_2	1.367(18)	1.43(5)	1.379(7)
C_4−C_5	1.387(18)	1.38(3)	-
C_2−C_3	1.475(18)	1.44(3)	1.420(6)
C_3−C_4	1.490(21)	1.44(3)	-

Schumann *et al*. synthesised a *tris*-pentadienyl lutetium complex [Lu(η^5-2,4-$Me_2C_5H_5$)(η^3-2,4-$Me_2C_5H_5$)] (**5.53**), this species is different from those previously reported because one of the pentadienyl ligands is coordinated in the less common η^3 manner.[168] Figure 89 shows the structure of complex **5.53**, and for the purpose of clearly showing the conformation of the pentadienyl ligand the carbon atoms representing the methyl groups have been coloured grey.

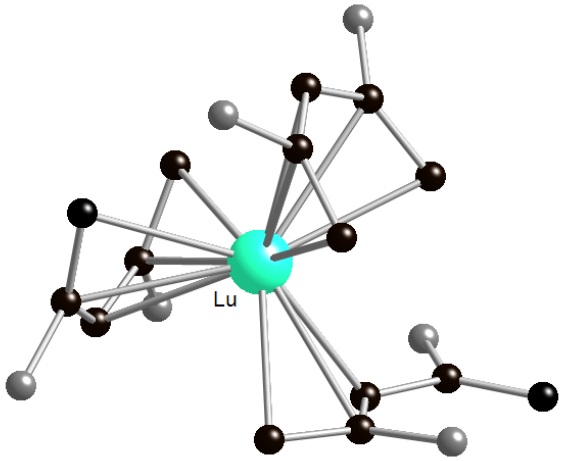

Figure 89: Molecular structure of [Lu(η^5-2,4-$Me_2C_5H_5$)$_2$(η^3-2,4-$Me_2C_5H_5$)] (**5.53**) Hydrogen atoms have been omitted for clarity, carbon = black, methyl group carbon = grey, lutetium = blue. Reproduced from ref. 168

It can be seen that the two pentadienyl ligands coordinated in an η^5 manner are in the U-shape conformation, however the S-shaped pentadienyl ligand is coordinated in an η^3 manner. The Lu−C bond distances for the η^5 coordinated pentadienyl ligands range

from 2.61(1) to 2.70(5) Å, however in this case the shortest bond distances are from the lutetium cation to the $C_{(1,5)}$ pentadienyl carbon atoms, rather than the $C_{(3)}$ carbon atom; the Lu−C bond distance range for the η^3 coordinated pentadienyl ligand is shorter, 2.53(1) to 2.64(1) Å. Again, the η^5 coordinated pentadienyl C−C bond distances can be split into internal and external bond sets, with the internal bonds (av. 1.42 Å) being longer than those of the external (av. 1.39 Å). However, the C−C bond distances of the S-conformation η^3-pentadienyl in complex **5.53** reveal that the vinyl-substituted allyl is a more fitting description for the pentadienyl ligand. The C−C bond distance of the coordinated carbon atoms are 1.40(1) and 1.39(1) Å, similar to that of delocalised allyl ligands; the other C−C bond distances are 1.46(2) and 1.35(2) Å which are more representative of a single and double bond, repetitively.[168]

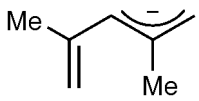

Figure 90: The S-η^3-pentadienyl in **5.53** is better described as a vinyl-substituted allyl

Taube *et al.* synthesised halide-bridged lanthanide pentadienyl complexes of general formula $[Ln_2(\eta^5\text{-}2,4\text{-}Me_2C_5H_5)_4(\mu\text{-}X)_2]$, where Ln = Nd, X = Cl (**5.55**), X = Br (**5.56**), X = I (**5.57**), Ln = La, X = Br (**5.58**), X = I (**5.59**) and Ln = Y, X = Br (**5.60**). Only complexes **5.56**, **5.57** and **5.60** were characterised by X-ray crystallography and all have similar structures.[162] Each lanthanide cation is coordinated by two U-shaped conformation η^5-pentadienyl ligands, and is bridged by two halide atoms. The average Ln−C bond distances have the same pattern as seen in complexes **5.50**-**5.52** $Ln{-}C_{(3)} < Ln{-}C_{(2,4)} < Ln{-}C_{(1,5)}$ and as with all the previously discussed examples of lanthanide pentadienyl complexes the C−C bond lengths can be split into internal and external; with the internal C−C bond lengths being longer (Table 8).[162]

Therefore, the pattern seen in the pentadienyl lanthanide complexes is that in the homoleptic complexes the Ln−C bond distances are in the order of $Ln{-}C_{(3)} < Ln{-}C_{(1,5)}$

< Ln−$C_{(2,4)}$ however in the mixed ligand or halide bridged complexes the order is Ln−$C_{(3)}$ < Ln−$C_{(2,4)}$ < Ln−$C_{(1,5)}$; on the other hand, in all the complexes discussed, the pentadienyl C−C bond distances are in two sets, internal and external, with the internal bond distances longer than those of the external C−C bonds.

Table 8: Table of average bond distances (Å) for complexes **5.56**, **5.57** and **5.60**

$[Ln_2(\eta^5\text{-}2,4\text{-}Me_2C_5H_5)_4(\mu\text{-}X)_2]$	**Ln = Nd X = Br**	**Ln = Nd X = I**	**Ln = Y X = Br**
Ln−$C_{(1)}$	2.763(5)	2.776(4)	2.736(9)
Ln−$C_{(2)}$	2.778(4)	2.781(3)	2.697(6)
Ln−$C_{(3)}$	2.688(4)	2.696(3)	2.611(6)
Ln−$C_{(4)}$	2.785(4)	2.811(3)	2.739(7)
Ln−$C_{(5)}$	2.818(5)	2.819(4)	2.777(8)
C_1−C_2	1.369(7)	1.366(5)	1.360(10)
C_4−C_5	1.414(7)	1.418(5)	1.417(9)
C_2−C_3	1.414(7)	1.433(5)	1.431(9)
C_3−C_4	1.372(7)	1.380(6)	1.358(9)

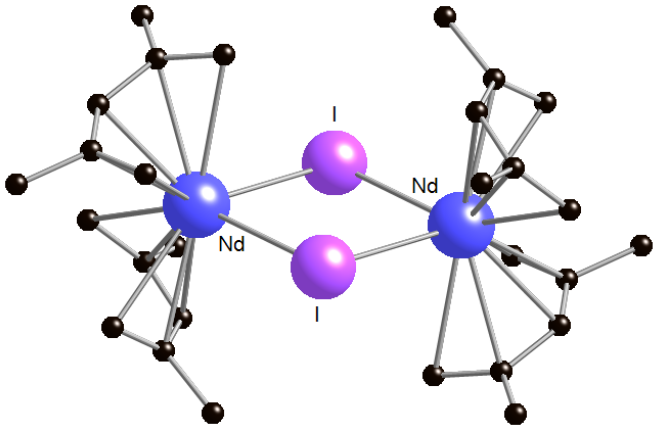

Figure 91: Molecular structure of $[Nd_2(2,4\text{-}Me_2C_5H_5)_4(\mu\text{-}I)_2]$ (**5.57**) Hydrogen atoms have been omitted for clarity, carbon = black, neodymium = blue, iodine = purple. Reproduced from ref. 162

Finally, a range of uranium pentadienyl complexes were synthesised in the 1980's; $[(BH_4)_3U(\eta^5\text{-}2,4\text{-}Me_2C_5H_5)]$ (**5.61**), $[(BH_4)_2U(\eta^5\text{-}2,4\text{-}Me_2C_5H_5)_2]$ (**5.62**), $[(BH_4)_2U(\eta^5\text{-}2,4\text{-}Me_2C_5H_5)_2][K(18\text{-crown-6}]$ (**5.63**), as well as the cyclopentadienyl complex $[(BH_4)_3U(\eta^5\text{-}C_5H_5)]$ (**5.64**).[169] The solid-state structure of complexes **5.61** (Figure 92)

and **5.64** were solved using X-ray crystallography. Unlike the lanthanide complexes of pentadienyl ligands, and transition metal complexes (to be discussed in the next chapter), the uranium complexes of 2,4-dimethylpentadienyl are less stable than the cyclopentadienyl analogues.[169] Addition of *O*-donor ligands, including thf, to complex **5.61** resulted in immediate reduction to the uranium(III) complex and in some cases dimerisation of the pentadienyl ligand occurred. And with complex $[(BH_4)_2U(\eta^5\text{-}2,4\text{-}Me_2C_5H_5)_2]$ (**5.62**) in thf transforms to the uranium(III) complex and $U(BH_4)_3$ while complex $[(BH_4)_2U(C_5H_5)_2]$ (**5.64**) is stable in a thf solution.

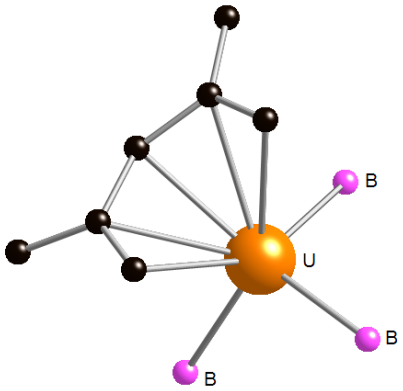

Figure 92: Molecular structure of $[(BH_4)_3U(2,4\text{-}Me_2C_5H_5)]$ (**5.61**). The structure was refined without hydrogen atoms, therefore the U−B bonds are only representative of the position of the BH_4^- group. Carbon = black, uranium = orange, boron = pink. Reproduced from ref. 169

The solid-state structure of complex **5.61** and **5.64** are very similar; the uranium cation is in a distorted tetrahedral environment, coordinated by three BH_4^- ligands and a U-shape conformation η^5 pentadienyl ligand or a η^5 cyclopentadienyl ligand, respectively. The U−C bond distances in complex **5.61** range from 2.63(2) to 2.80(2) Å; the $U-C_{(3)}$ bond length is the shortest at 2.63(2) Å, with the other 4 U−C bond lengths in the range of 2.77(3) to 2.80(2) Å, with the order of bond length being $U-C_{(3)} < U-C_{(1,5)} \approx U-C_{(2,4)}$. This suggests that there is a degree of ionic character between the uranium and pentadienyl ligand, which has a large contribution from the **(L)** (Figure 86, pg 126) resonance form. Comparing the U−C bond distances in the pentadienyl complex **5.61** with the cyclopentadienyl complex **5.64** it can be seen that in complex **5.64** the bond

lengths are shorter, in the range of 2.60(3) to 2.72(2) Å, confirming what was shown in the solution-state, that the cyclopentadienyl ligand is more strongly bound than the pentadienyl ligand. The C−C bond lengths for complex **5.61** within the pentadienyl ligand follows the same pattern as seen in the lanthanide pentadienyl complexes, that the bonds can be split into internal and external, and the internal bonds are longer (av. 1.44(4) Å) than the external bonds (av. 1.35(3) Å). This is in agreement with the U−C bond lengths for complex **5.61** which suggest the resonance form **(L)** is contributing most to the pentadienyl ligand.

5.4 d-Block Metal Pentadienyl Complexes

There is a large volume of literature on transition metal pentadienyl complexes.[22,77-79,88,119,170,171,172] This section will only briefly mention the various types of transition metal pentadienyl complexes. The main focus will be on homoleptic/silyl-substituted pentadienyl complexes. As well as the complexes mentioned in this thesis, there are also "half-open sandwich" complexes, which consist of a cyclopentadienyl ligand and pentadienyl ligand, however they will not be discussed.

5.4.1 Homoleptic d-Block Metal Pentadienyl Complexes

A selection of complexes available in the literature is summarised in Table 9. As with unsubstituted allyl complexes, unsubstituted pentadienyl complexes are usually thermally unstable at room temperature, and as a result there are few transition metal complexes known of the pentadienyl ligand/anion $[C_5H_7]^-$. However, some examples are known *i.e.* $[Ni_2(C_5H_7)_2]$ (**5.65**)[189,190] and $[Fe(C_5H_7)_2]$ (**5.66**).[179,180] Both complexes **5.65** and **5.66** have been characterised by IR, ^{1}H and ^{13}C NMR spectroscopy.

Complex **5.65** is also unusual in the fact that the pentadienyl is in the **W**-shape conformation and is coordinated in an η^3 manner to the nickel cation, which is similar to

that seen in allyl complexes [Ni(C_3H_5)$_2$] (**1.1**) and [Ni{C_3H_3($SiMe_3$)$_2$}$_2$] (**1.72**). The bonding within the complex **5.65** are shown in Figure 93, it can be seen that the bonds between Ni−C_1, Ni−C_2, Ni−C_4 and Ni−C_5 are much shorter than those between Ni−C_3, The reason for this difference may be that the C_3 atom protrudes out of the pentadienyl mean plane by 0.23 Å.

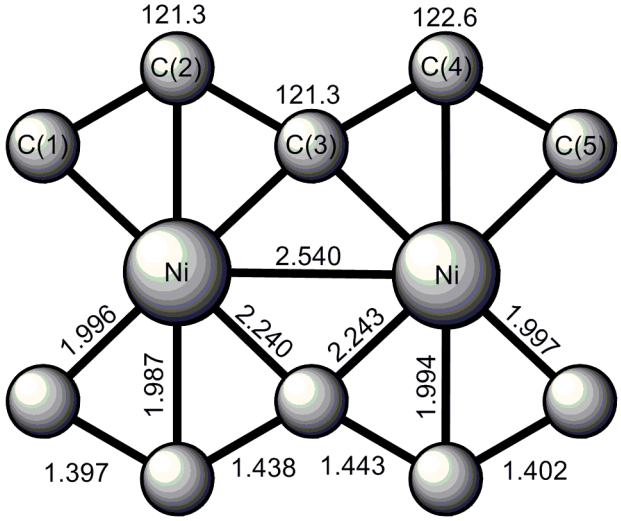

Figure 93: Diagram to represent the molecular structure of [$Ni_2(C_5H_7)_2$] (**5.65**), with selected bond lengths (Å) and bond angles (°), with maximum errors of ±0.006 Å and ±0.4 °, respectively. Reproduced from ref. 190

Ernst *et al.* synthesised a range of methyl substituted *bis*(pentadienyl) iron complexes; [Fe(2-MeC_5H_6)$_2$] (**5.67**), [Fe(3-MeC_5H_6)$_2$] (**5.68**), [Fe(2,4-$Me_2C_5H_5$)$_2$] (**5.69**),[179,180] [Fe(2,3-$Me_2C_5H_5$)$_2$] (**5.70**)[180] and [Fe(2,3,4-$Me_3C_5H_4$)$_2$] (**5.71**).[181,182] For complexes **5.69** and **5.71**, the two pentadienyl ligands are in the *gauche*-eclipsed conformation, in the solid-state.

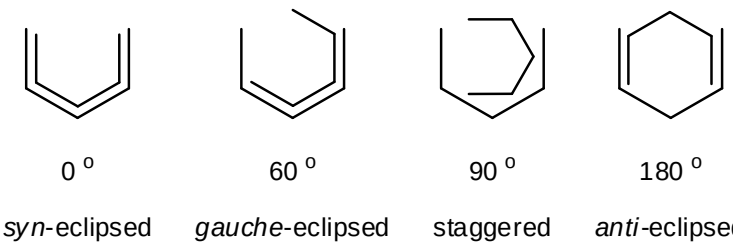

Figure 94: Possible conformations of the two pentadienyl ligands in a homoleptic complex.

Table 9: Examples of transition metal complexes of various pentadienyl ligands, complexes in **bold** have been crystallographically characterised.

	C_5H_7	2-MeC_5H_6	3-MeC_5H_6	2,4-$Me_2C_5H_5$	3,4-$Me_2C_5H_5$	2,3,4-$Me_3C_5H_4$	1,5-$(SiMe_3)_2C_5H_5$	Other
Ti				$[TiL_2]$[173]			**$[TiL_2]$**[174]	
Zr							**$[ZrL_2]$**[174]	
V				**$[VL_2]$**[174,175,176]			$[VL_2]$[177]	
Nb	$[NbCp(\eta^5L)(\eta^3L)]$[178]			$[NbCp(\eta^5L)(\eta^3L)]$[178] $[Nb(MeC_5H_4)(\eta^5L)(\eta^3L)]$[178]				
Ta					**$[TaCp_2(\eta^3L)]$**[178]		**$[TaCp_2(\eta^3L)]$**[178]	
Cr				**$[CrL_2]$**[175,176,] **$[CrCpL]$**[177]			**$[CrL_2]$**[177]	
Mn			**$[Mn_3L_4]$**[175]					
Fe	$[FeL_2]$[179,180]	$[FeL_2]$[179,180]	$[FeL_2]$[179,180]	**$[FeL_2]$**[179,180]	$[FeL_2]$[180]	**$[FeL_2]$**[181,182]		**$[Fe(1\text{-}SiMe_3\text{-}3\text{-}MeC_5H_5)_2]$**[183]
Ru				**$[RuL_2]$**,[184,185] **$[RuCp^*L]$**[186]		$[RuL_2]$[184]		
Os				**$[OsL_2]$**[181]				
Co				**$[CoCpL][BF_4]$**[187]				
Rh				**$[RhCp^*L][BF_4]$**[186]				
Ir				**$[CoCpL][BF_4]$**[188]				
Ni	**$[Ni_2L_2]$**[189,190]							
Zn·tmeda	$[ZnL_2]$[157] **$[ZnLCl]$**[157]	$[ZnL_2]$[157]	$[ZnL_2]$[157]	$[ZnL_2]$[157]				$[Zn(5\text{-}MeC_5H_6)_2]$[157]

Figure 94 shows the possible ligand conformations in a transition metal *bis*pentadienyl complex. When discussing the conformation of the complex, the conformation angle, χ, is defined as 0° for *syn*-eclipsed, 60° for *gauche*-eclipsed, 90° for staggered and 180 ° for *anti*-eclipsed. The conformational angle is the angle between two planes in the complex; the plane is defined by the metal atom, the carbon atom in position 3 (C(3) or C(11)) and the mid-point between carbon atoms in position 1 (C(1) or C(9)) and 5 (C(5) and C(13)).[180] The conformational angle for complexes **5.69** and **5.71** are 59.7° and 55.1°, respectively.

Complex [Fe(1-$SiMe_3$-3-Me-C_5H_5)$_2$] (**5.72**)[183] is a *bis*(pentadienyl)iron complex of an unsymmetrical pentadienyl ligand, 1-$SiMe_3$-3-Me-C_5H_5. Due to the asymmetric nature of the ligand, two isomers are possible (Figure 95).

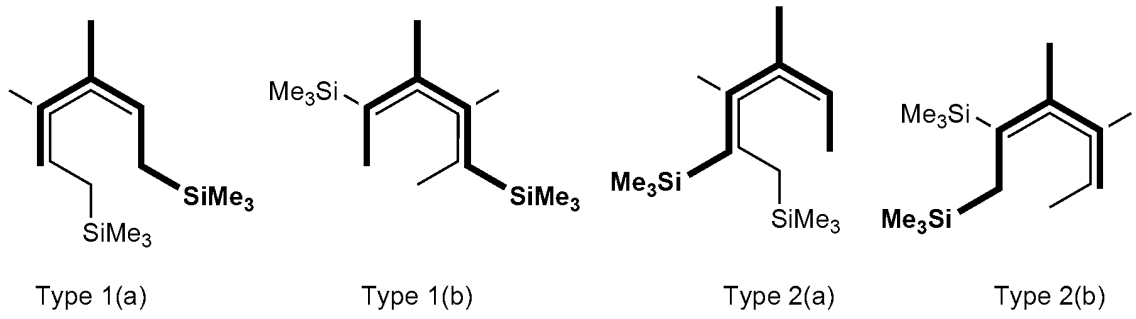

Figure 95: Possible *gauche*-eclipsed conformations for complex **5.72**, reproduced from ref. 183

The solid-state structure of complex **5.72** was determined by X-ray crystallography, showing the *gauche*-eclipsed conformation 1a (Figure 95), with a conformational angle of 45.4°. The average Fe−C bond distances for $C_{1,5}$, $C_{2,4}$ and C_3 are 2.129(4), 2.062(4) and 2.106(6) Å, respectively, with an overall average of 2.097(3), which is similar to both complexes **5.69** and **5.71**[183] and the average Fe−C bond distance in ferrocene is 2.064(3) Å.[191] The methyl substituents in **5.72** tilt out of the pentadienyl plane and towards the iron cation. It is thought that the tilt seen in substituents, of pentadienyl ligands, toward the metal cation is to increase metal-ligand orbital overlap (Figure 96).[143,144,177,183]

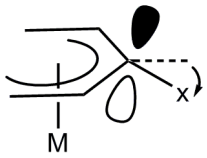

Figure 96: Metal-ligand orbital overlap.

Other first row transition metal *bis*(silyl-pentadienyl) complexes include complexes [Ti{1,5-$(SiMe_3)_2C_5H_5$}$_2$] (**5.73**),[174] [V{1,5-$(SiMe_3)_2C_5H_5$}$_2$] (**5.74**) and [Cr{1,5-$(SiMe_3)_2C_5H_5$}$_2$] (**5.75**)[177] Only complexes [Ti{1,5-$(SiMe_3)_2C_5H_5$}$_2$] (**5.73**) and [Cr{1,5-$(SiMe_3)_2C_5H_5$}$_2$] (**5.75**) were characterised crystallographically, with both revealing staggered ligand conformations, with conformation angles of 82.5 and 78.7 °, respectively. Both angles, especially that of complex **5.75**, are much smaller than the ideal angle of 90°, which is thought to be due to the ligands attempting to minimise $SiMe_3\cdots SiMe_3$ interactions, which is more pronounced in the chromium complex due to the smaller radius of the chromium.

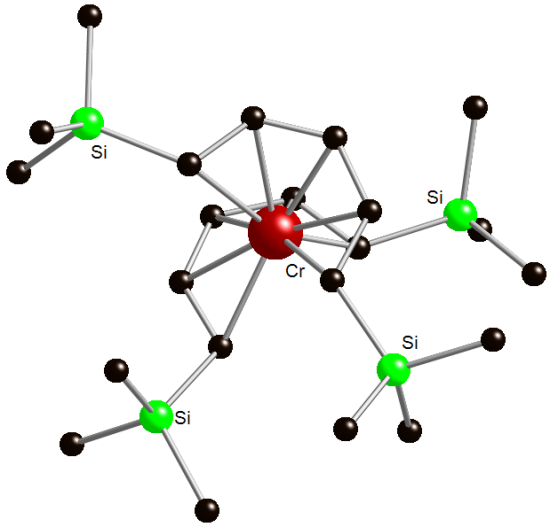

Figure 97 Molecular structure of [Cr{1,5$(SiMe_3)_2C_5H_5$}$_2$] (**5.75**). Hydrogen atoms have been omitted for clarity, carbon = black, silicon = green, chromium = deep red. Reproduced from ref.177

Other effects of the sterically bulky $SiMe_3$ substituents are seen in the M−C bond distances; in complex [Ti{1,5-$(SiMe_3)_2C_5H_5$}$_2$] (**5.73**) the average Ti−C bond length is 2.275(3) Å. The Ti−C_5 bond distance is 2.315(5) Å, this long Ti−C_5 bond is thought to

be due to $SiMe_3\cdots SiMe_3$ interactions. Ligand interactions also lead to a distortion of the complex $[Cr\{1,5\text{-}(SiMe_3)_2C_5H_5\}_2]$ (**5.75**), in which one ligand is closer to the chromium cation than the other. The average $Cr-C_n$ and $Cr-C_{n'}$ bond distances are 2.224 and 2.199 Å, respectively.

Complex $[Zr\{1,5(SiMe_3)_2C_5H_5\}_2]$ (**5.76**)[174] was synthesised from $ZrCl_4$ and four equivalents of $[K\{1,5(SiMe_3)_2C_5H_5\}]$. Reduction of Zr(IV) to Zr(II) is notable and highlights the preference of the pentadienyl ligand for metals in low oxidation states. Complex **5.76** is in the staggered conformation, with a conformation angle of 82.2° which is quite departed from the ideal of 90°, as with the titanium analogue $[Ti\{1,5\text{-}(SiMe_3)_2C_5H_5\}_2]$ (**5.73**) (82.5°) discussed previously. The overall average Zr–C bond length is 2.369(4) Å, with the average $Zr-C_{1,5}$, $Zr-C_{2,4}$ and $Zr-C_3$ bond lengths being 2.38, 2.400(5) and 2.421(7) Å, respectively, unlike the titanium complex **5.73** the $Zr-C_3$ bond lengths are longest.

Complex $[(C_5H_5)_2Ta\{\eta^3\text{-}1,5\text{-}(SiMe_3)_2C_5H_5\}]$ (**5.77**)[178] was formed in an attempt to synthesise the half-open sandwich complex. Complex **5.77** was characterised by X-ray crystallography and isolated as the *bis*(cyclopentadienyl) complex.

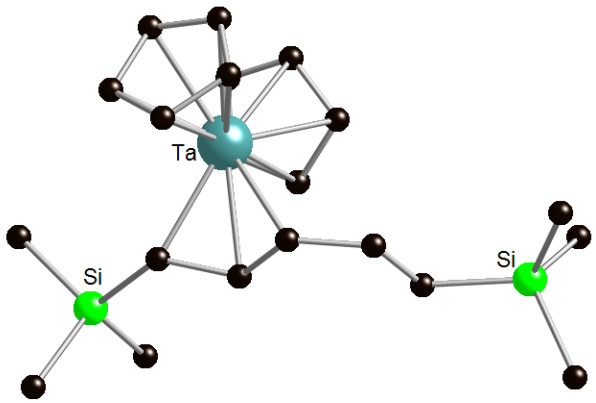

Figure 98: Molecular structure of $[(C_5H_5)_2Ta\{1,5\text{-}(SiMe_3)_2C_5H_5\}]$ (**5.77**). Hydrogen atoms have been omitted for clarity, carbon = black, silicon = green, tantalum = light blue. Reproduced from ref.178

However the 1,5-*bis*(silyl) substituted pentadienyl ligand is η^3-coordinated mode, in the less common the **S**-shape conformation. It is thought that the trimethylsilyl groups

destabilise the C_1, C_2 and C_5 coordination, hence the pentadienyl complex **5.77** coordinating in an η^3 allylic manner.[178] The Ta−C_1, Ta−C_2 and Ta−C_3 bond lengths are 2.297(10), 2.2304(9) and 2.306(9) Å, respectively. The C−C bond lengths between C_1−C_2 and C_2−C_3 are 1.433(15) and 1.431(14) Å suggesting delocalisation of the negative charge across C_1 and C_3 positions and the C−C bond lengths between C_3−C_4 and C_4−C_5 are 1.483(13) and 1.332(14) Å suggesting localised single and double bonds. These C−C bond lengths reveal that the pentadienyl is more accurately coordinated to the tantalum as a vinyl-substituted allyl.

Chapter 6

Alkali Metal Pentadienyl Complexes – Results and Discussion

6.1 Introduction to Donor-functionalised Pentadienyl Chemistry

As shown in the previous chapter, no donor-functionalised pentadienyl complexes are known, therefore there is a lot of potential for developing donor-functionalised pentadienyl chemistry. My aims are to:

1. Synthesise donor-functionalised pentadienyl pro-ligands
2. Study the coordinating ability of the ligand with different alkali metals.
3. Investigate the effect of metal radii, on the structure of the allyl complex and study the effect on (de)localisation of the pentadienyl ligand.

6.2 Synthesis of Donor-functionalised Pentadienyl Ligands

Attempts were made to make a variety of different donor-functionalised pentadienyl pro-ligands with an *O*-functional group incorporated into the pentadienyl backbone (Figure 99).

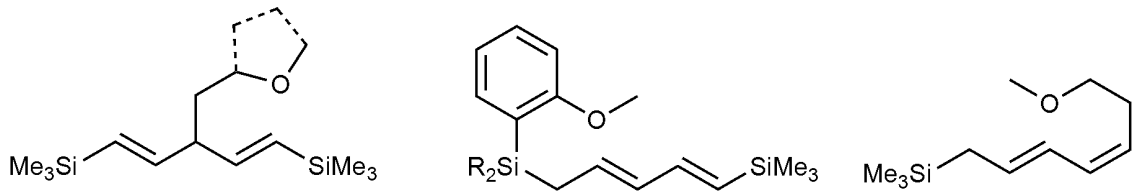

Pn-thf = **L**^{8}H
Pn-OMe = **L**^{9}H

R = Me (**L**^{10}H)
R = Ph (**L**^{11}H)

L^{12}H

Figure 99: Different types of donor-functionalised pentadienyl pro-ligands

Ligands **L**^{8}H to **L**^{12}H were successfully synthesised, with the exception of **L**^{11}H which was extremely difficult to purify. The ligands were isolated in yields of 70%, 60%, 65% and 43% for **L**^{8}H, **L**^{9}H, **L**^{10}H and **L**^{12}H, respectively. Only pro-ligands **L**^{8}H and **L**^{9}H were successfully coordinated to an alkali metal, therefore only the synthesis of pro-ligands **L**^{8}H and **L**^{9}H will be discussed.

To synthesise the donor functionalised pentadienyl pro-ligands, 1-(trimethylsilyl)pentadiene and 1,5-(trimethylsilyl)pentadiene were synthesised according to literature procedures.[151,192] *Bis*-1,5-(trimethylsilyl)penta-1,3-diene, was then lithiated with one equivalent of *n*-butyllithium in thf, then quenched with the respective tosylate, in slight excess (Scheme 38).

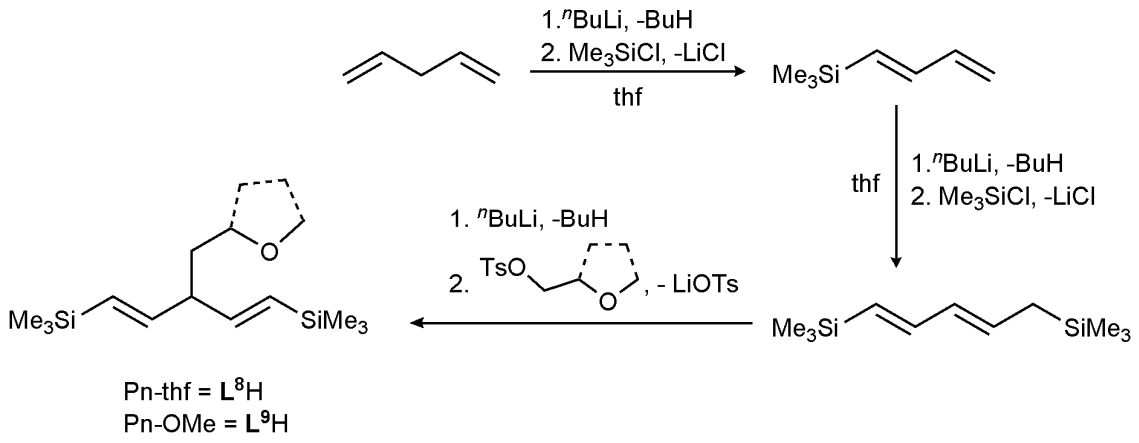

Scheme 38

Both ligands $\mathbf{L^8}$H and $\mathbf{L^9}$H were isolated as colourless oils and purified by vacuum distillation, with the products distilling at 75-80°C and 45-50°C, respectively. Both ligands were characterised by ^{1}H and ^{13}C NMR spectrometry, mass spectroscopy and elemental analysis.

6.3 Synthesis and Structures of Donor-functionalised Pentadienyl Complexes

Both pro-ligands, $\mathbf{L^8}$H and $\mathbf{L^9}$H, were treated with *n*-butyllithium in hexane, at −78 °C, followed by adding one equivalent of tmeda, which resulted in the formation of a bright orange solution. The solution was then filtered, concentrated, and left at room temperature to afford orange crystals of [(tmeda)Li{$(SiMe_3)_2C_5H_4(CH_2C_4H_7O)$]] **6.1** and [(tmeda)Li{$(SiMe_3)_2C_5H_4(CH_2CH_2OCH_3)$]] **6.2** in 39% and 21% yields, respectively, (Scheme 39).

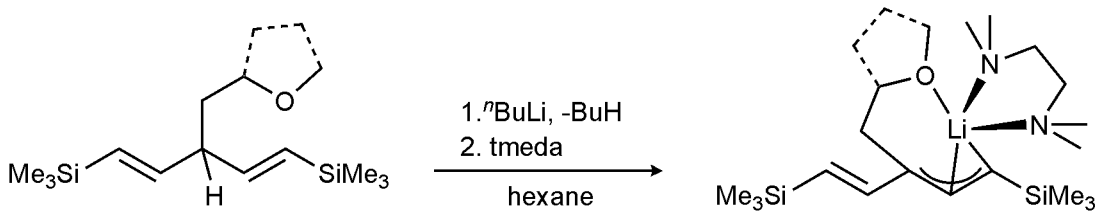

Pn-thf = L^8H
Pn-OMe = L^9H

Pn-thf = **6.1**
Pn-OMe = **6.2**

Scheme 39

Both complexes **6.1** and **6.2** crystallise in the $P2_1/c$ space group, and complex **6.2** has two unique molecules in the unit cell (**6.2a** and **6.2b**). Complexes **6.1**, **6.2a** and **6.2b** all have very similar structures, and only **6.2a** will be discussed in detail, see Table 10 for a comparison of selected bond lengths and angles. An illustration of **6.2b** is shown in Chapter 8 (Experimental Section 8.4.4, Figure 116).

6.3.1 Solid-state Structures of [(tmeda)Li(L^8)] (6.1) and [(tmeda)Li(L^9)] (6.2)

The structure of complex **6.2a** shows that the pentadienyl ligand is in the W-conformation, and both trimethylsilyl groups are in the *exo* stereochemistry, therefore the formula of this complex is abbreviated to (*exo*,*exo*)-W-**6.2**. From Figure 101 it can be seen that the ligand is coordinated to the lithium in an η^2 manner, the Li(1)−C(1) and Li(1)−C(2) bond lengths are 2.368(4) and 2.446(4) Å, respectively, and the Li(1)···C(3) distance is 2.843 Å, which is too long to be considered a Li−C bond.[38] The lithium cation is also coordinated by the oxygen of the pendant donor group, and the two nitrogen atoms of the tmeda, with Li(1)−O(1), Li(1)−N(1) and Li(1)−N(2) bond distances of 1.986(4), 2.132(5) and 2.192(4) Å, respectively. The geometry around the lithium cation is that of a distorted tetrahedron. The Pn C−C bond distances are 1.400(4), 1.400(3), 1.430(3) and 1.360(3) Å for C(1)−C(2), C(2)−C(3), C(3)−C(4) and C(4)−C(5), respectively. These bond lengths suggest that the complex should be

considered a vinyl-substituted allyl rather than a fully delocalised pentadienyl complex (Figure 100).

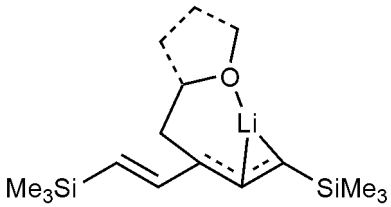

Figure 100: The vinyl-substituted allyl of complexes **6.1** and **6.2**

The Si(1)−C(1)−C(2)−C(3) and Si(2)−C(5)−C(4)−C(3) torsional angles of 169.1(2) and 179.09(19)°, respectively, support the proposed vinyl-allyl structure. Similar bond lengths and torsional angles can be seen for **6.1** and **6.2b** in Table 10.

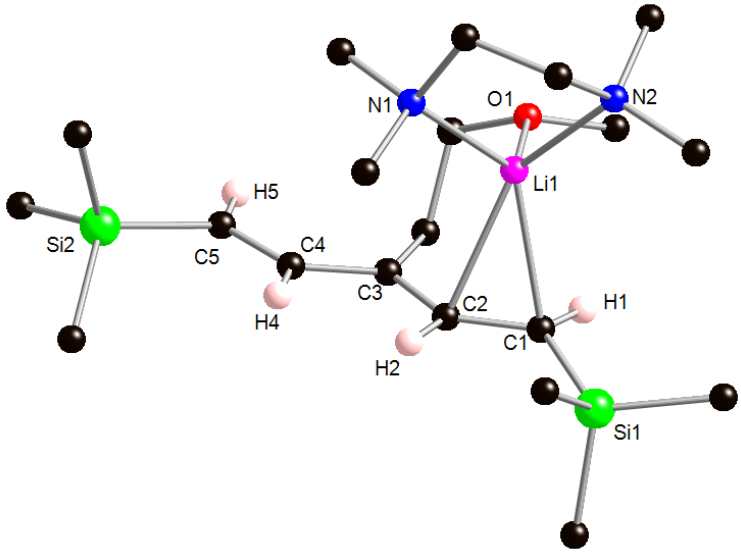

Figure 101: Molecular structure [(tmeda)Li{($SiMe_3$)C_5H_4($CH_2CH_2OCH_3$)}] (**6.2a**). Hydrogen atoms have been omitted for clarity apart from pentadienyl hydrogen atoms, carbon = black, silicon = bright green, oxygen = red, nitrogen = blue and hydrogen = light pink. C(1)−C(2) 1.400(3), C(2)−C(3) 1.400(3), C(3)−C(4) 1.430(3), C(4)−C(5) 1.360(3), Li(1)−C(1) 2.368(4), Li(1)−C(2) 2.446(4), Li(1)···C(3) 2.843, Li(1)−O(1) 1.986(4), Li(1)−N(1) 2.132(5), Li(1)−N(2) 2.192(4), C(1)−C(2)−C(3) 132.43(19), C(2)−C(3)−C(4) 119.38(19), C(3)−C(4)−C(5) 130.5(2).

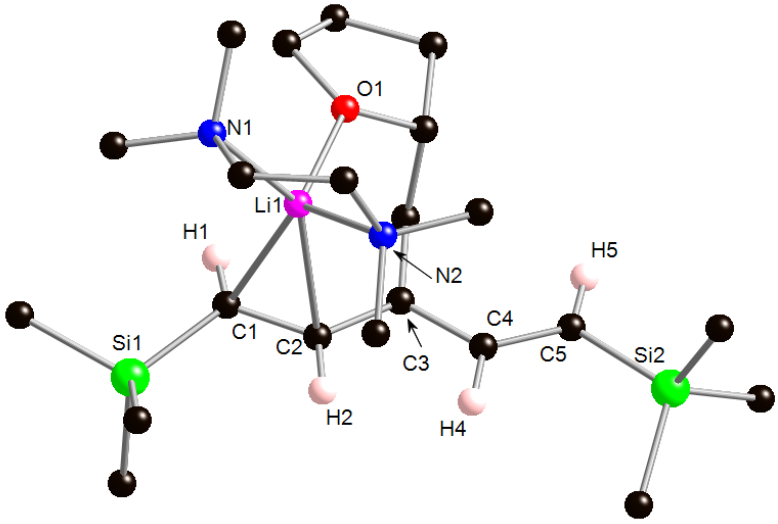

Figure 102: Molecular structure of [(tmeda)Li{$(SiMe_3)C_5H_4(CH_2C_4H_7O)$}] (**6.1**) with selected bond lengths (Å) and angles (°). Hydrogen atoms have been omitted for clarity apart from pentadienyl hydrogen atoms, carbon = black, silicon = bright green, oxygen = red, nitrogen = blue and hydrogen = light pink. C(1)−C(2) 1.400(3), C(2)−C(3) 1.394(3), C(3)−C(4) 1.429(3), C(4)−C(5) 1.352(3), Li(1)−C(1) 2.391(4), Li(1)−C(2) 2.445(4), Li(1)···C(3) 2.819, Li(1)−O(1) 1.958(4), Li(1)−N(1) 2.168(5), Li(1)−N(2) 2.138(4), C(1)−C(2)−C(3) 132.9(2), C(2)−C(3)−C(4) 118.9(2), C(3)−C(4)−C(5) 130.8(2).

Table 10: Selected bond lengths (Å) and angles (°) for the experimental structures of **6.1**, **6.2a** and **6.2b** and for the calculated structures of **6.1**.

	6.1	**6.2a**	**6.2b**[a]	**BP86/ TZ2P**[b]	**BP86/ TZ2P**[c]	**BP86/ QZ4P**[b]
C(1)–C(2)	1.400(3)	1.400(3)	1.393(3)	1.408	1.406	1.410
C(2)–C(3)	1.394(3)	1.400(3)	1.403(3)	1.406	1.408	1.405
C(3)–C(4)	1.429(3)	1.430(3)	1.423(3)	1.433	1.432	1.435
C(4)–C(5)	1.352(3)	1.360(2)	1.365(3)	1.375	1.378	1.374
C(1)–Li(1)	2.391(4)	2.368(4)	2.399(4)	2.346	2.396	2.309
C(2)–Li(1)	2.445(4)	2.446(4)	2.427(5)	2.400	2.471	2.409
C(3)···Li(1)	2.819	2.843	2.810	2.769	2.857	2.821
O(1)–Li(1)	1.958(4)	1.986(4)	1.990(4)	2.061	2.048	2.033
N(1)–Li(1)	2.168(4)	2.132(5)	2.159(4)	2.241	2.220	2.203
N(2)–Li(1)	2.138(4)	2.192(4)	2.161(4)	2.315	2.269	2.299
C(2) –C(1) –Si(1)	122.04(18)	120.89(15)	121.41(15)	123.0	123.3	122.0
C(1) –C(2) –C(3)	132.9(2)	132.43(19)	132.04(19)	131.0	131.0	131.6
C(2) –C(3) –C(4)	118.9(2)	119.38(19)	119.48(18)	119.6	119.5	119.4
C(3) –C(4) –C(5)	130.8(2)	130.5(2)	131.15(19)	129.5	129.6	129.6
C(4) –C(5) –Si(2)	125.3(2)	123.0(3)	122.94(16)	125.9	125.9	125.9

a. The bond lengths and angles listed for **6.2b** are the equivalents of those in **6.2a**, although the actual atom labels used in the structure of **6.2b** are different (see Experimental).

b. Gas-phase.

c. COSMO simulation in toluene.

Complexes **6.1** and **6.2** are the first crystallographically characterised lithium pentadienyl complexes, as well as the first structurally authenticated examples of donor-functionalised pentadienyl complexes of any metal. The only other structurally characterised pentadienyl s-block complexes are $[(tmeda)K(2,4\text{-}Me_2C_5H_5)]_\infty$ **5.9**[154] and $[(tmeda)Mg(2,4\text{-}Me_2C_5H_5)_2]$ **5.14**[156] (see Chapter 5). Complex **5.9** is a zig-zag polymer structure in which the pentadienyl complex is in the U-conformation bridging between the potassium cations in an η^5 manner. Complex **5.14** has the magnesium coordinated by a σ-bond to the terminal carbon atom of a pentadienyl in the **U**-conformation. Previously, structures of s-block pentadienyl complexes have been determined by NMR spectroscopy, or by inference from the stereochemistry of products from electrophile quenching reactions.[148,150,151,192,193,194,195]

Ab initio calculations performed by Streitweiser[152] and a DFT study by Merino[153] have provided insight into the gas-phase structure of pentadienyllithium $[Li(C_5H_7)]$ (**5.1**). The calculations show that, in the gas-phase, the lowest energy structure is the U-shape conformation for the pentadienyl ligand and, irrespective of the level of theory, the U-shape conformation is the lowest energy structure and features three or more Li–C bonds. The inclusion of solvent effects using the COSMO model did not change the preference for the U-conformation, however the W-conformation is only 0.8 kcal mol^{-1} less stable in the simulated aqueous environment. The key difference between the calculated structure of **5.1** and **6.1** and **6.2** is that complexes **6.1** and **6.2** are best described as vinyl substituted-allyl complexes, rather than pentadienyl complexes, which is in good agreement with Streitweiser's gas-phase calculations on complex **5.1**.

Other examples of structurally characterised trimethylsilyl-substituted pentadienyl complexes include complexes $[Fe(1\text{-}SiMe_3\text{-}3\text{-}Me\text{-}C_5H_5)_2]$ (**5.72**),[183] $[Ti\{1,5\text{-}(SiMe_3)_2C_5H_5\}_2]$ (**5.73**),[174] $[V\{1,5\text{-}(SiMe_3)_2C_5H_5\}_2]$ (**5.74**),[177] $[Cr\{1,5\text{-}(SiMe_3)_2C_5H_5\}_2]$ (**5.75**),[177] $[Zr\{1,5(SiMe_3)_2C_5H_5\}_2]$ (**5.76**)[174] and $[(C_5H_5)_2Ta\{\eta^3\text{-}1,5\text{-}(SiMe_3)_2C_5H_5\}]$

(**5.77**).[178] Complexes **5.72-5.76** all exhibit U-η^5-coordination by the pentadienyl ligand, however all these complexes are of transition metals. It is unlikely that the smaller lithium cation could be within bonding distance of all five pentadienyl carbon atoms and hence is only coordinated by the ligand in an η^3 manner. In complex **5.77**, however, the tantalum cation is coordinated by an η^3-pentadienyl ligand. The C−C bond lengths in **5.77** are 1.433(15) and 1.431(14) Å between C_1−C_2 and C_2−C_3 suggesting delocalisation of the negative charge across C_1 and C_3 positions. The C_3−C_4 and C_4−C_5 bond lengths are 1.483(13) and 1.332(14) Å, respectively, suggesting localised single and double bonds. The C−C bond lengths for complex **5.77** are similar to those seen in **6.2**, and in both complexes the pentadienyl ligand is more accurately described as a vinyl-substituted allyl ligand.

6.3.2 Computational Studies of [(tmeda)Li(L^9)] (6.2)

Due to the fact that complexes **6.1** and **6.2** are the first donor-functionalised pentadienyl complexes, and the first examples of solid-state structures of lithium pentadienyl complexes, there is no experimental data to compare to the structures of complexes **6.1** and **6.2**. As with the *ansa-tris*(allyl) complexes, a collaboration with Dr. Jordi Poater, Prof. Miquel Solà and Prof. Dr. F. Matthias Bickelhaupt was undertaken to use DFT to calculate the structures and the relative energies of the pentadienyl anion, $[C_5H_7]^-$ (**6.3**), pentadienyllithium, $[Li(C_5H_7)]$ (**5.1**); the 1,5-*bis*(trimethylsilyl)pentadienyl anion, $[1,5\text{-}(SiMe_3)_2C_5H_5]^-$ (**6.4**); 1,5-*bis*(trimethylsilyl)pentadienyllithium, $[Li\{1,5\text{-}(SiMe_3)_2C_5H_5\}]$ (**6.5**); the lithium complex of the methoxy-functionalized pentadienyl ligand, $[Li\{1,5\text{-}(SiMe_3)_2C_5H_4(CH_2CH_2OCH_3)\}]$ (**6.6**); and the full complex **6.2**. We have also calculated the model complex $[(pmdeta)Li\{1,5\text{-}(Me_3Si)_2C_5H_5\}]$ (**6.7**) (pmdeta = *N*,*N*′,*N*′′,*N*′′-pentamethyldiethylenetriamine), in which the coordination environment of lithium is similar to that in **6.2**, but in which the internal *O*-donor has

been replaced by an *N*-donor atom from a terdentate pmdeta ligand. Although computational studies of the pentadienyl anion **6.3** and pentadienyllithium **5.1** have already been completed, these were re-calculated to check the consistency of our own calculations. However, the calculation performed on silyl-substituted pentadienyl complexes are the first of their type. Calculations were carried out at the BP86/TZ2P level of theory but, for comparison, selected systems were also calculated at the BP86/QZ4P level. In addition, all minima were confirmed by means of frequency calculations at the same level of theory. The Amsterdam Density Functional (ADF) software was used in all cases. Calculations on **5.1** under toluene solvation conditions used the COSMO model.

The pentadienyl anion **6.3** was calculated to be most stable in the W-conformation, with S-**6.3** and U-**6.3** being higher in energy by +2.7 and +3.0 kcal mol^{-1}, respectively, at both levels of theory employed (Figure 103).

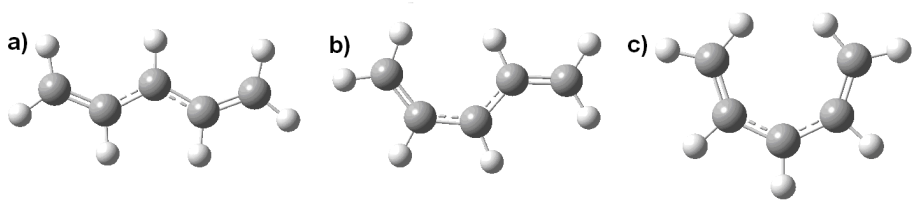

Figure 103: DFT calculated structures of pentadienyl anion $[C_5H_7]^-$ (**6.3**) with energies stated in kcal mol^{-1}: W-**6.3** 0.0 (a), S-**6.3** + 2.7 (b) and U-**6.3** + 3.0 (c). Carbon = grey and hydrogen = white.

Pentadienyllithium (**5.1**) was calculated to be most stable as U-**5.1** with the ligand adopting an η^5-bonding mode, whereas an η^3-bonded W-**5.1** complex is less stable by +10.4 kcal mol^{-1}. There are two coordination modes for S-**5.1**, which are +8.6 and +12.7 kcal mol^{-1} less stable than the lowest energy form (Figure 104). The energies of the different forms of **5.1** obtained at the BP86/TZ2P level of theory agree well with Merino's DFT study.[153]

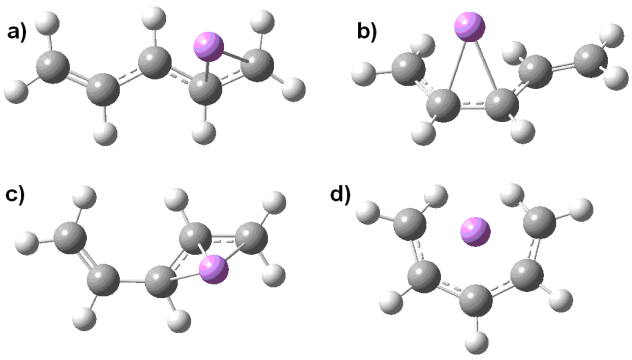

Figure 104: DFT calculated structures of pentadienyllithium [Li(C_5H_7)] (**5.1**) with energies stated in kcal mol^{-1}: W-**5.1** 10.4 (a), S-**5.1** 8.6, 12.7 (b, c) and U-**5.1** 0.0 (d). Calculated at the BP86/TZ2P level of theory. Carbon = grey, hydrogen = white, lithium = pink.

Computational studies of the 1,5-*bis*(trimethylsilyl)pentadienyl anion (**6.4**) and its lithium complexes (**6.5**) have not previously been reported. In **6.4**, the introduction of trimethylsilyl groups causes no changes to the trend in stability calculated for the pentadienyl anion (Figure 105). Therefore, the W-conformation with both trimethylsilyl groups in *exo*- positions, (*exo*,*exo*)-W-**6.4**, is the most stable (Figure 110a), (*exo*,*exo*)-U-**6.4** is the least stable by +4.6 kcal mol^{-1}, and the two S-conformations, (*exo*,*endo*)-S-**6.4** and (*exo*,*exo*)-S-**6.4**, are of intermediate stability, being less stable by +3.9 and +2.9 kcal mol^{-1}, respectively. In the structure of (*exo*,*exo*)-W-**6.4** the C–C bond lengths are essentially equal, being 1.393 and 1.406 Å, respectively, indicating full delocalization of the pentadienyl negative charge.

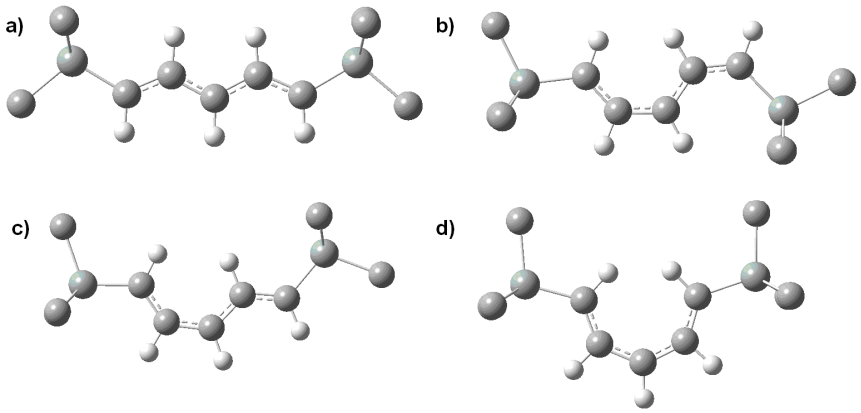

Figure 105: DFT calculated structures of 1,5-*bis*(trimethylsilyl)pentadienyl anion $[(SiMe_3)_2C_5H_5)]^-$ (**6.4**) with energies stated in kcal mol^{-1}: (*exo*,*exo*)-W-**6.4** 0.0 (a), (*exo*,*exo*)-S-**6.4** +2.9 (b), (*exo*,*endo*)-S-**6.4** +3.9 (c) and (*exo*,*exo*)-U-**6.4** +4.6 (d). Calculated at the BP86/TZ2P level of theory. Only the pentadienyl hydrogen atoms are shown. Carbon = grey, hydrogen = white, silicon = grey/green.

The stability of the isomers of 1,5-*bis*(trimethylsilyl)pentadienyllithium (**6.5**) reflect those found for **5.1**, with (*exo*,*exo*)-**U**-**6.5** being the lowest in energy (Figure 110b), (*exo*,*exo*)-W-**6.5** being +8.6 kcal mol^{-1} less stable, and the three S-conformations, (*exo*,*endo*)-S-**6.5**, (*exo*,*exo*)-S-**6.5** and (*exo*,*exo*)-S′-**6.5**, being +8.2, +7.1 and +10.9 kcal mol^{-1} less stable, respectively.

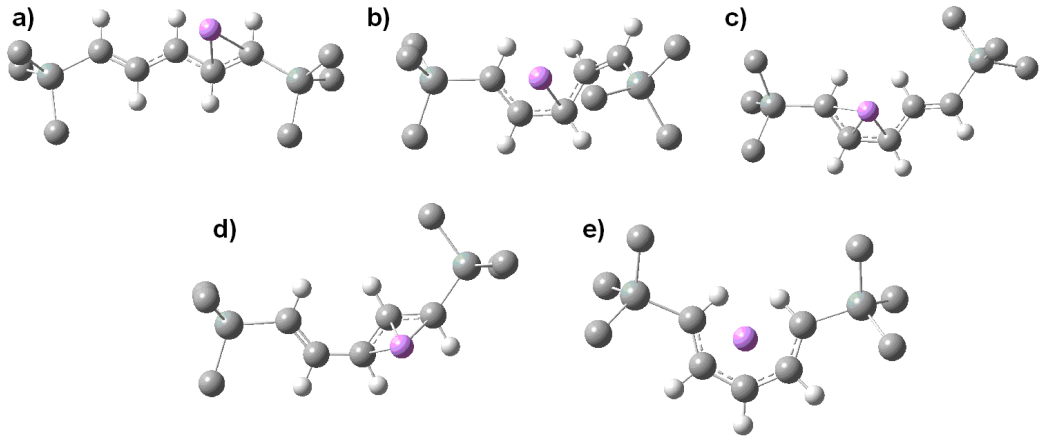

Figure 106: DFT calculated structures of 1,5-*bis*(trimethylsilyl)pentadienyllithium [Li{(1,5-$SiMe_3)_2C_5H_5$}] (**6.5**) with energies stated in kcal mol^{-1}: (*exo*,*exo*)-W-**6.5** +8.6 (a), (*exo*,*endo*)-S-**6.5** +8.2 (b), (*exo*,*exo*)-S-**6.5** +7.1 (c), (*exo*,*exo*)-S′-**6.5** +10.9 (d) and (*exo*,*exo*)-U-**6.5** 0.0 (e). Calculated at the BP86/TZ2P level of theory. Only the pentadienyl hydrogen atoms are shown. Carbon = grey, hydrogen = white, silicon = grey/green, lithium = pink.

Figure 107 shows the calculated structures of the methoxy-functionalized complex [Li{1,5-$(Me_3Si)_2C_5H_4CH_2CH_2OMe$}] (**6.6**), without tmeda, which resulted in a change in the order of stability compared to the unfunctionalised complexes **6.5** and **5.1**. The lowest energy form is (*exo*,*exo*)-W-**6.6**, with the pentadienyl ligand η^3-bonded to the lithium cation in addition to the methoxy oxygen (Figure 110c). However, (*exo*,*exo*)-U-**6.6** is only +0.4 kcal mol^{-1} less stable. The three possible S-conformations, (*exo*,*endo*)-S-**6.6**, (*exo*,*exo*)-S-**6.6** and (*exo*,*exo*)-S′-**6.6**, are higher in energy by +9.3, +2.0 and +6.3 kcal mol^{-1}, respectively. The substantial increase in the stability of the W-conformation of **6.6** is presumably due to the hard-hard interaction between the lithium cation and the oxygen donor, which also results in a reduction of the hapticity of the pentadienyl group for steric reasons from η^5 in **5.1** to η^3 in **6.5**.

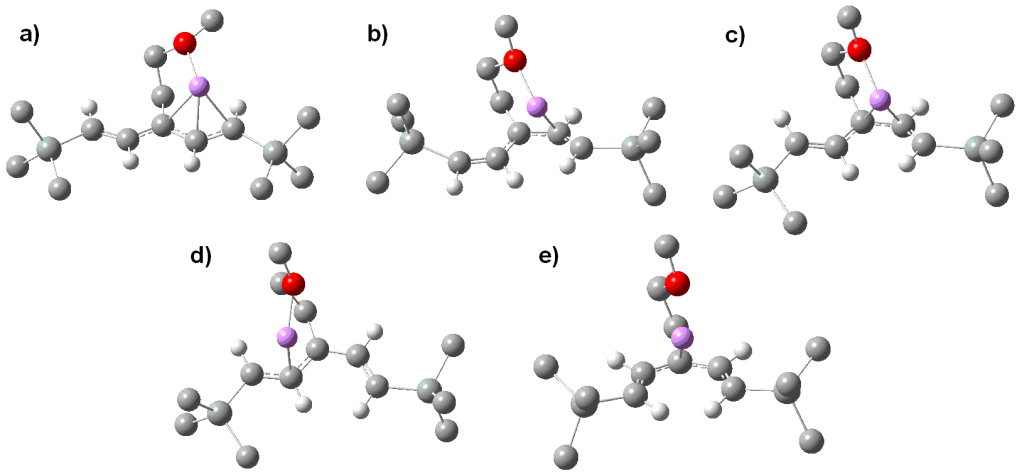

Figure 107: DFT calculated structures of the methoxy-functionalised pentadienyllithium [Li{(1,5-$SiMe_3$)$_2$$C_5H_4$($CH_2CH_2OCH_3$)}] (**6.6**) with energies stated in kcal mol^{-1}: (*exo*,*exo*)-W-**6.6** 0.0 (a), (*exo*,*endo*)-S-**6.6** +9.3 (b), (*exo*,*exo*)-S-**6.6** +2.0 (c), (*exo*,*exo*)-S′-**6.6** +6.3 (d) and (*exo*,*exo*)-U-**6.6** +0.4 (e). Calculated at the BP86/TZ2P level of theory. Only the pentadienyl hydrogen atoms are shown. Carbon = grey, hydrogen = white, silicon = grey/green, oxygen = red, lithium = pink.

For the full complex **6.2**, calculations were carried out at the BP86/TZ2P and the BP86/QZ4P levels of theory and the results can be seen in Figure 108. The geometric parameters in the calculated structures generally agree very well with the experimental data at both levels of theory, except the Li–N distances to the tmeda ligand, which are slightly longer than those seen in experiment (Table 10). The optimized structure of **6.2** is shown in Figure 110d. The coordination of tmeda to lithium in (*exo*,*exo*)-W-**6.6** forms (*exo*,*exo*)-W-**6.2** and gives an association energy of −17.0 kcal mol^{-1} (Scheme 40).

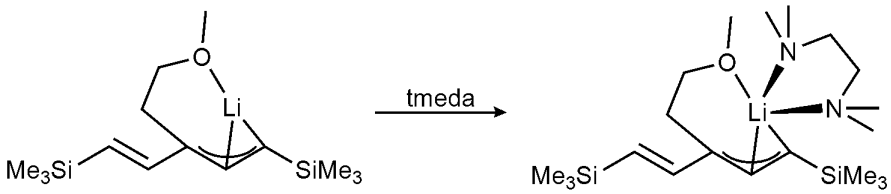

Scheme 40

Complex (*exo*,*exo*)-W-**6.2** is the lowest energy form, with (*exo*,*endo*)-S-**6.2**, (*exo*,*exo*)-S-**6.2**, and (*exo*,*exo*)-U-**6.2** being +10.4, +3.1 and +5.3 kcal mol^{-1} less stable. The addition of tmeda causes only one noteworthy structural change, on formation of (*exo*,*exo*)-W-**6.2** from (*exo*,*exo*)-W-**6.6** the coordination of the pentadienyl slips from η^3

to η^2 coordination. The effects of toluene solvation result in only very small changes to the relative stabilities of the isomers of **6.2**, thus (*exo*,*exo*)-W-**6.2** remains the most stable and (*exo*,*endo*)-S-**6.2**, (*exo*,*exo*)-S-**6.2**, and (*exo*,*exo*)-U-**6.2** are less stable by +10.1, +3.4 and +5.1 kcal mol^{-1}, respectively.

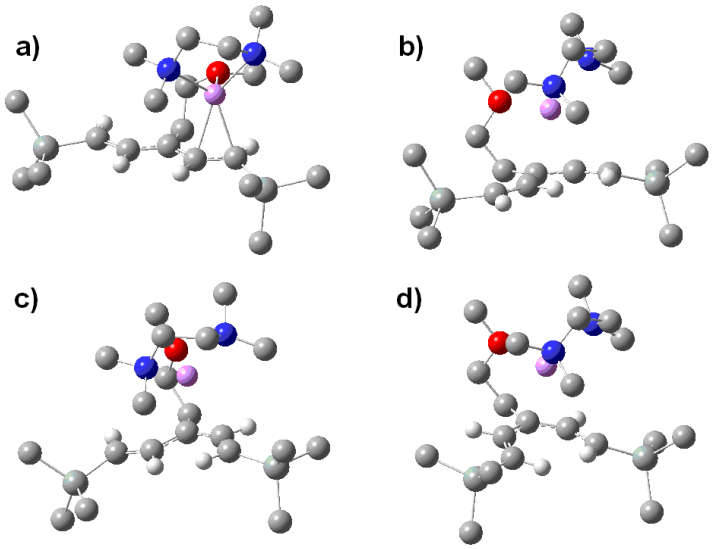

Figure 108: DFT calculated structures of [(tmeda)Li{(1,5-$SiMe_3)_2C_5H_4(CH_2CH_2OCH_3)$}] (**6.2**) with energies stated in kcal mol^{-1}: (*exo*,*exo*)-W-**6.2** 0.0 (a), (*exo*,*exo*)-S-**6.2** +3.1 (b), (*exo*,*endo*)-S-**6.2** +10.4 (c) and (*exo*,*exo*)-U-**6.2** +5.3 (d). Calculated at the BP86/TZ2P level of theory. Only the pentadienyl hydrogen atoms are shown. Carbon = grey, hydrogen = white, silicon = grey/green, oxygen = red, nitrogen = blue, lithium = pink.

Finally, the calculations on complex **6.2** were used to calculate the relative stabilities of different conformations of the complex [(pmdeta)Li{1,5-$(SiMe_3)_2C_5H_5$}] (**6.7**). The trend in stability for model complex **6.7** is the same as that calculated for **6.2**, *i.e.* the (*exo*,*exo*)-W-**6.7** is the most stable and (*exo*,*endo*)-S-**6.7**, (*exo*,*exo*)-S-**6.7** and (*exo*,*exo*)-U-**6.7** are +5.9, + 1.5 and +4.7 kcal mol^{-1} less stable, respectively (Figure 109). The structure of (*exo*,*exo*)-W-**6.7** (Figure 110e) is similar to that of the crystallographically determined structures of **6.1** and **6.2**, in which there is a W-shaped pentadienyl group and a four-coordinate lithium cation. The structures of **6.1** and **6.2** show the pentadienyl ligands to be η^2-coordinated to lithium, however the calculated gas-phase structure of (*exo*,*exo*)-W-**6.7** shows an η^3-bonded pentadienyl ligand with Li–C distances in the range 2.325-2.515 Å (average 2.401 Å). The pentadienyl C–C distances in (*exo*,*exo*)-W-

6.7 are similar to those found in the experimental structure of complex **6.2**, indicating a vinyl-substituted allyl structure and partial localization of the negative charge. The pentadienyl C–C distances in the gas-phase structure of lithium-free model complex **6.4** are equal in length, partial localization of the pentadienyl negative charge in (*exo*,*exo*)-W-**6.2** and (*exo*,*exo*)-W-**6.7** must be intrinsic to the pentadienyllithium unit and stems from the polarizing nature of the Li^+ cation.

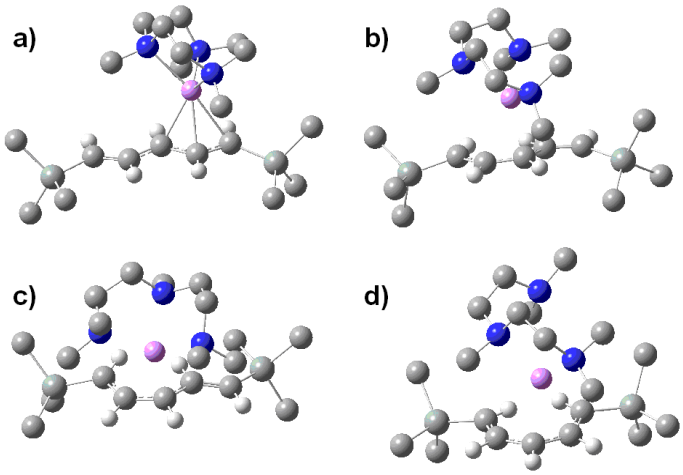

Figure 109: DFT calculated structures of [(pmdeta)Li{(1,5-$SiMe_3$)$_2$$C_5H_5$}] (**6.7**) with energies stated in kcal mol^{-1}: (*exo*,*exo*)-W-**6.7** 0.0 (a), (*exo*,*endo*)-S-**6.7** +5.9 (b), (*exo*,*exo*)-S-**6.7** +1.5 (c) and (*exo*,*exo*)-U-**6.7** +4.7 (d). Calculated at the BP86/TZ2P level of theory. Only the pentadienyl hydrogen atoms are shown. Carbon = grey, hydrogen = white, silicon = grey/green, nitrogen = blue, lithium = pink.

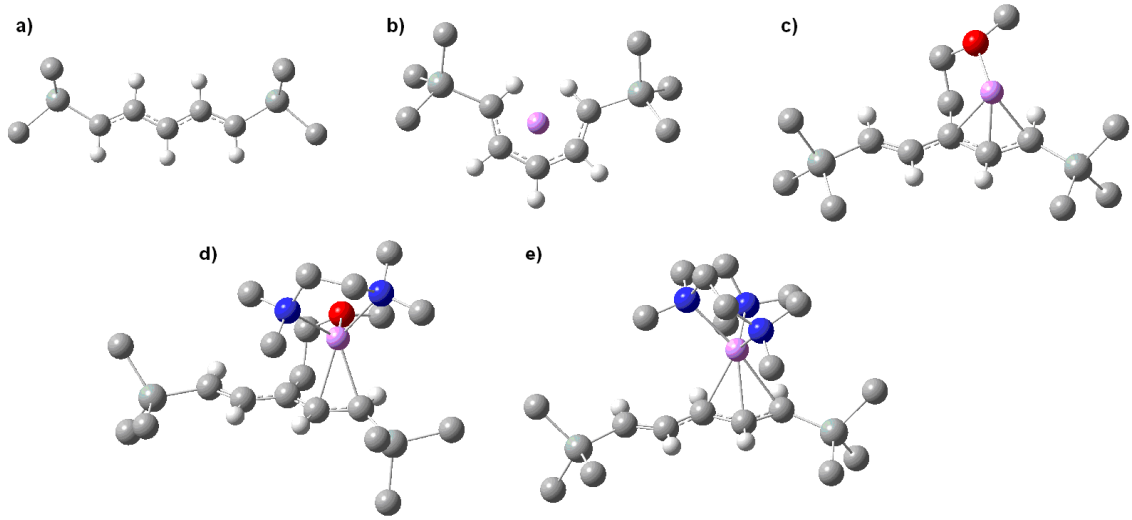

Figure 110: DFT calculated structures of the lowest-energy forms of **6.4** (a), **6.5** (b), **6.6** (c), **6.2** (d) and **6.7** (e). Calculated at the BP86/TZ2P level of theory. Only the pentadienyl hydrogen atoms are shown. Carbon = grey, hydrogen = white, silicon = grey/green, oxygen = red, nitrogen = blue, lithium = pink.

In the crystallographically determined complexes **6.1** and **6.2**, and in the calculated structures of the pentadienyl species **6.2** several factors contribute towards their stability: the σ-/π-bonding in the pentadienyl anion; the minimum steric repulsion between the various organic groups; and the strongest bonding interactions between the lithium cation and the donor atoms. Each of these three factors will compete such that the observed experimental structures of complexes **6.1** and **6.2** are the lowest energy forms of each calculated species that provides the most favourable energetic balance. However, the calculations show that higher energy forms of a particular pentadienyl species are only slightly higher in energy. Therefore such structures could be attainable in an experimental situation. This is true in the case of the calculated structures of **6.2** in a simulated toluene solvent environment, which prompted an investigation into complex **6.2** by variable-temperature ^{1}H NMR spectroscopy.

6.3.3 Solution-phase NMR Spectroscopy of [(tmeda)Li(L^{8})] 6.1 and [(tmeda)Li(L^{9})] 6.2

The ^{1}H NMR spectrum of **6.2** in benzene-d_6 at 300 K consists of eight resonances due to **6.2**: a singlet at δ = 0.38 ppm due to the trimethylsilyl group; a singlet at δ = 2.81 ppm and two mutually coupled triplets at δ = 2.77 and 3.49 ppm due to the $CH_2CH_2OCH_3$ group; two mutually coupled doublets at δ = 3.77 and 6.92 ppm with ^{3}J = 17.5 Hz, which indicate *trans* stereochemistry of the pentadienyl protons, *i.e.* C(1/5)−H and C(2/4)−H; finally the singlets at δ = 1.86 and 1.61 ppm are due to the tmeda CH_3 and CH_2 groups, respectively. An HSQC (Heteronuclear Single-Quantum Correlation) NMR experiment allowed the ^{13}C NMR spectrum to be fully assigned for complex **6.2** (see Chapter 7 - Experimental Section). The NMR spectra of complex **6.2** suggest an element of symmetry in the solution-phase structure, which can be explained by rapidly equilibrating W- or S-shaped conformations of the pentadienyl unit or by the

pentadienyl carbon atoms adopting a U-shape conformation at 300 K. The two small resonances at −0.18 and 0.22 ppm are due to hydrolysis, however their contribution to the NMR spectrum is less than two percent.

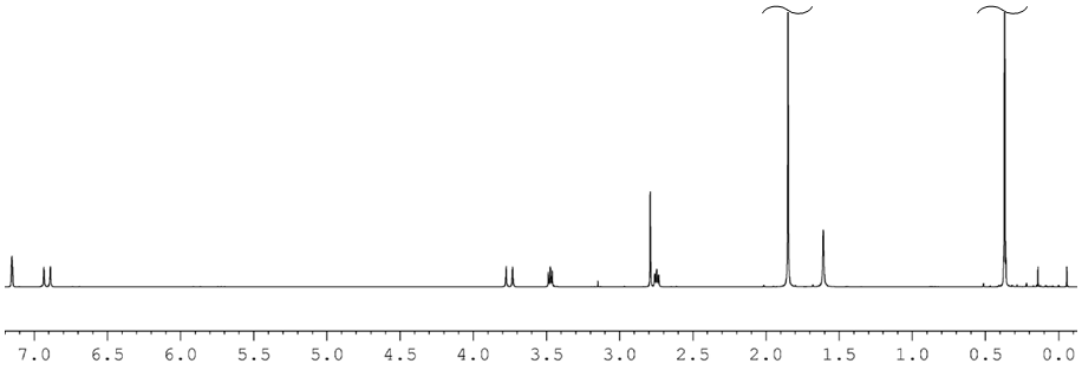

Figure 111: ^{1}H NMR spectrum of **6.2** recorded in benzene-d_6 at 300 K. The resonances due to the tmeda and trimethylsilyl groups at 1.86 and 0.38 ppm, respectively, have been truncated.

Complex **6.1** has a pendant tetrahydrofurfuryl donor group, which produces a complicated ^{1}H NMR spectrum with overlapping multiplets, therefore owing to the simpler structure of the $CH_2CH_2OCH_3$ donor group of complex **6.2** this complex was chosen for a variable temperature ^{1}H NMR study.

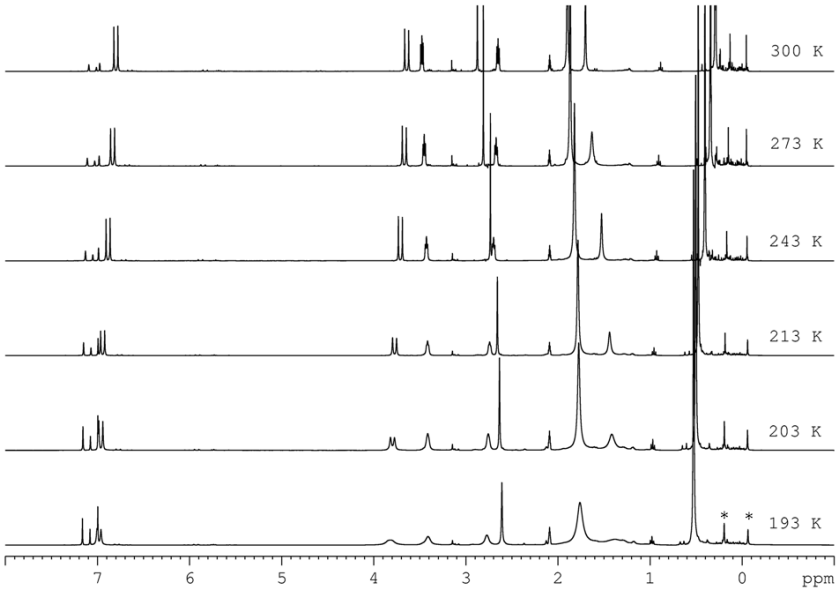

Figure 112: VT ^{1}H NMR spectra of complex **6.2** from 193 K to 300 K, resonances at −0.18 and 0.22 ppm are hydrolysis products*.

In toluene-d_8, the temperature was lowered to 273 K, then down to 193 K in invervals of 20 K. There were no changes in the ^{1}H NMR spectrum of complex **6.2**, except slight changes in chemical shift due to the effects of the low temperature (Figure 112). At the lower limit of 193 K all resonances experienced line-broadening due to the increased viscosity of the toluene as it neared its freezing point.

It is well known that pentadienyl complexes of alkali metals are conformationally flexible.[145,146,193,196] Nakamura found that, in thf, pentadienyl carbon atoms in 1-(trimethylsilyl)pentadienyllithium, [Li{1-($SiMe_3$)C_5H_6] (**6.8**) and 1,5-*bis*(trimethyl-silyl)pentadienyllithium, [Li{1,5-($SiMe_3$)$_2C_5H_5$] (**6.5**) adopt the W-conformation in between temperatures of 203-322 K. However, 1,3,5-*tris*(trimethylsilyl)-pentadienyllithium, [Li{1,3,5-($SiMe_3$)$_3C_5H_4$] (**5.20**) is fluxional in thf, which was revealed by a low-temperature experiment, in which the fluxionality was suppressed at 203 K, revealing that **5.20** does adopt the relatively rare S-conformation.[151]

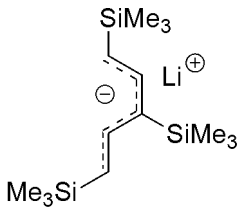

S-5.20

Figure 113: S-conformation of the complex [Li{1,3,5-($SiMe_3$)$_3C_5H_4$] (**5.20**)

Insight into the solution-phase structure of **6.2** can be obtained by comparing the ^{1}H NMR spectra of **6.2** with those of **5.20** at approximately room-temperature and at low-temperatures. The room-temperature ^{1}H NMR spectra of **6.2** and **5.20** exhibit two doublets assignable to the pentadienyl protons. Cooling the solutions to 203 K, the two doublets in the spectrum of **5.20** split into two doublets each, whereas those in the spectrum of **6.2** stay unchanged down to 213 K. This suggests that, in toluene, complex **6.2** either exists as (*exo,exo*)-U-**6.2** or that a fluxional process with an extremely low activation barrier involving the other possible conformations is taking place.

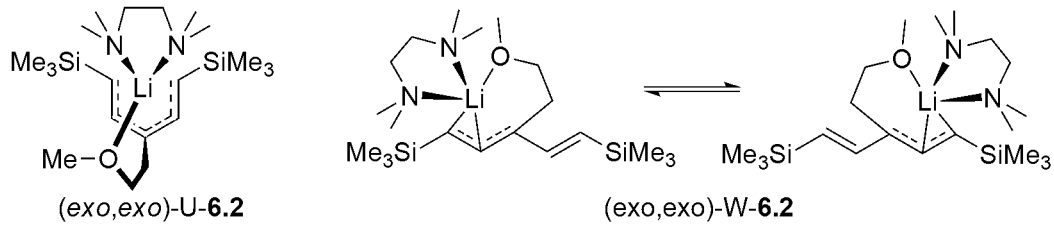

(*exo*,*exo*)-U-**6.2** (exo,exo)-W-**6.2**

Scheme 41

Complex [Li(C_5H_7)] **5.12**[146,149] and complex [Li(2-MeC_5H_6)] **5.13**,[150] are in the W-conformation in ether solutions, therefore it is possible that the solid-state structure is maintained in solution. However, for complex [Li(2,4-$Me_2C_5H_5$)] (**5.19**) the U-shape conformation is found in ether solutions, but the U-shape conformation has been found to be the most favoured conformation of the 2,4-diemthylpentadeinyl ligand.

Although there is no direct evidence for the crystallographic structure of (*exo*,*exo*)-W-**6.2** in solution, the data from experiment and computational studies suggest that a fluxional version of this conformation should be possible in a toluene solution (Scheme 41). However, it has been shown that small environment changes can eventually determine the actual structure, the small energy differences between the calculated structures of **6.2** also allow for fluxionality involving the W-, S- and U-conformations.

The ^{1}H and ^{13}C NMR spectra of complex **6.1**, at room temperature, are qualitatively similar to those of **6.2**, and display resonances that can be assigned to the trimethylsilyl group and the tmeda environments. The tetrahydrofurfuryl group has complicated overlapping resonances, and as a result few could be unquestionably assigned. The trimethylsilyl resonance in the ^{1}H NMR spectrum is a broad singlet at 0.35 ppm, and in the ^{13}C NMR appears as a broad doublet at 1.9 ppm. This suggests that at room temperature there may be an equilibrium between the two (*exo*,*exo*)-W-**6.1** conformations, which is more evident in complex **6.1** than **6.2** due to the larger donor-functionalised group. Only one pentadienyl resonance of complex **6.1** appears in the ^{1}H NMR, as a doublet at $\delta = 6.90$, with a $^3J = 20.0$ Hz.

6.4 Conclusion

In summary, two new donor-functionalised pentadienyl ligands have been synthesised, along with their lithium complexes **6.1** and **6.2**. Complexes **6.1** and **6.2**, are the first lithium pentadienyl complexes to be crystallographically characterised, and are the first donor-functionalised pentadienyl complexes of any metal to be structurally authenticated. The solid-state structures of complexes **6.1** and **6.2** show that the 1,5-*bis*(trimethylsilyl)pentadienyl anion exists as the (*exo,exo*)-W-conformation, and is η^2-coordinated to the lithium cation. The C−C bond distances of the two structures suggest that the anion is best regarded as a vinyl-substituted allyl, rather than a fully delocalised pentadienyl species.

A DFT study of the 1,5-*bis*(trimethylsilyl)pentadienyl anion (**6.4**) showed that the (*exo,exo*)-W-conformation is the most stable, however for its lithium complex (**6.5**) the (*exo,exo*)-U-**6.5** conformation was found to be the most stable form. The internal donor functionality in the functionality of complex [Li{1,5-$(Me_3Si)_2C_5H_4CH_2CH_2OMe$}] (**6.6**) resulted in the (*exo,exo*)-W- and (*exo,exo*)-U-conformations having essentially the same energy, but complexation of tmeda to **6.6** to form **6.2** gave (*exo,exo*)-W-**6.2** as the most stable form, both in the gas-phase and in toluene. The DFT study of the model complex [(pmdeta)Li{1,5-$(SiMe_3)_2C_5H_5$}] (**6.7**) showed that (*exo,exo*)-W-**6.7** was the most stable conformation and revealed a pattern of pentadienyl C–C distances similar to those in the experimental structure of **6.2**. This suggests that the partial localization of the pentadienyl negative charge arises from the polarizing ability of the Li^+ cation and not from the influence of the donor functionality. This conclusion was corroborated by comparing the C–C distances in **6.7** to those in metal-free **6.4**, which are essentially of equal length. The ^{1}H NMR spectrum of **6.2** in the temperature range 193-300 K, in light of the computational results, suggested that this complex can either exist as (*exo,exo*)-U-**6.2** or that a fluxional process involving other conformations is possible.

Chapter 7

Future Work

7.1 Future Work

In the literature, there are many examples of *mono* silyl-allyl complexes of s-, d- and f-block, and a few examples of *ansa-bis*(allyl) complexes. However there are no examples of *ansa-tris*(allyl) complexes of d-block metals. The *ansa-tris*(allyl) ligand may be able to encapsulate transition metals, leaving only one vacant coordination site, and as such potentially be used for regioselective and stereoselective catalysis. For example, the vacant coordination site may be able to distinguish between an *R* and an *S* face of a chiral molecule, and therefore potentially be stereoselective.

The donor-functionalised allyl complexes synthesised in this report and in the literature are only of s-block metals, therefore there is a large scope for potential complexes of f- and d-block metals. Similarly there is a large number of potential donor-functionalised ligands, by varying the length of the carbon chain of the pendant group and varying the size and the heteroatom of the donor group. One direction that is of interest is that of *ansa-bis* donor-functionalised allyl ligands. It is unlikely that this could be extended to *ansa-tris* donor-functionalised allyl ligands, as there would be too much steric crowding to substitute a third donor group. However *ansa-bis* donor-functionalised allyl ligands could be used to encapsulate metal cations, and if ligands were synthesised with a soft and a hard donor, which would bind to the metal more or less strongly, it could allow for an open coordination site for polymerisation catalysis.

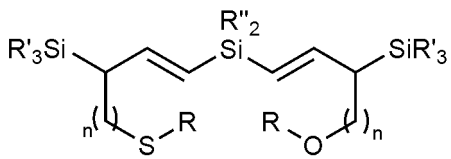

Figure 114: Potential structure for *ansa-bis* donor-functionalised allyl

Finally the area of donor-functionalised pentadienyl ligands is completely unexplored and therefore holds a lot of promise for investigating the nature of the donor-functionalionality and how it interacts with different metals. However, only

lithium complexes have been investigated so far. To truly understand the bonding nature of donor-functionalised pentadienyl ligands it is necessary to synthesise complexes with other metals, such as sodium and potassium or magnesium and calcium. It was shown that for group two metals beryllium and magnesium form σ-bonds to pentadienyl ligands, however calcium behaves for like a transition metal, it will be interesting to see if this still holds true for a donor-functionalised pentadienyl ligand.

As seen from complexes **6.1** and **6.2**, and to a certain extent allyl complexes [**4.1**]$_2$ and [**4.2**]$_2$, the donor-functional group is capable of holding the lithium cation over specific carbon atoms of a pentadienyl ligand. This would have a lot of potential within organic synthesis in which the donor-functionalised ligand may provide a route to selective substitution. To investigate this further donor-functionalised pentadienyl pro-ligands in which the functional group is on the terminal carbon could be synthesised and coordinated to lithium or potassium. Maximising the yields and purity of pro-ligands **L**^{10}H to **L**^{12}H could lead to substitution on the C_1 or C_2 position.

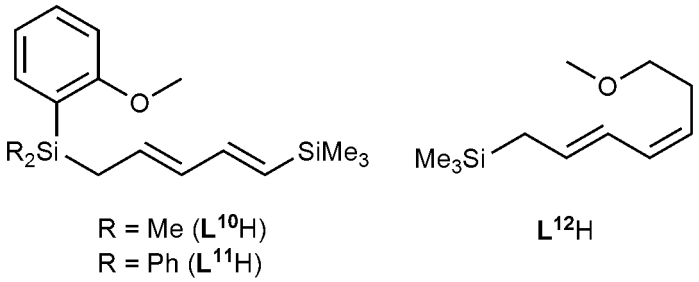

R = Me (**L**^{10}H)
R = Ph (**L**^{11}H)

L^{12}H

Figure 115: Potential donor-functionalised pentadienyl ligands

Another area that is unexplored is that of *ansa-bis* and *ansa-tris* pentadienyl ligands. It would be interesting to see, if like the *ansa-bis*(allyl) ligands, the *ansa-bis*(pentadienyl) ligands would behave as two separate "free" ligands, and if like the *ansa-tris*(allyl) ligands the overall complex is affected by different substituents on the ligand and cation size. It would also be fascinating to see if the pentadienyl ligand can adopt the preferred **U**-shape conformation in such *ansa-bis* and *ansa-tris* complexes.

Chapter 8

Experimental Section

8.1 General Considerations

All syntheses were carried out using conventional Schlenk techniques. A dual-manifold vacuum/inert gas line and a glove-box were used to keep reactions under an inert atmosphere, dinitrogen (N_2) was the inert gas used on the dual-manifold line and for the glove box. The glove box used was the MBRAUN Labstar (1200/780). All reactions solvents were pre-dried over sodium wire before being rigorously dried by refluxing over sodium (diethyl ether) or potassium (hexane and thf) under an N_2 atmosphere. Also under an N_2 atmosphere, NMR solvents benzene-d_6 and toluene-d_8 were dried by stirring over sodium-potassium alloy before being distilled from the alloy, and then stored over activated 4 Å molecular sieves. Synthesis of 1,3-*bis*(trimethylsilyl)propene,[28] *ansa*-*tris*(allyl) pro-ligand $\mathbf{L^1}H_3$,[30] 1-(trimethylsilyl)-2,4-pentadiene[192] and 1,5-*bis*(trimethylsilyl)-1,3-pentadiene[151] were prepared according to literature procedures and all other reagents were obtained from commercial suppliers. More specifically the organometallic reagents, *n*butyllithium, sodium *tert*-butoxide, potassium *tert*-butoxide and dibutylmagnesium, were purchased from Sigma-Aldrich. The *n*butyllthium was bought as a 1.6M solution in hexanes and the dibutylmagnesium was bought as a 1.0M solution in heptanes, both reagents were used as 1.6M solution and a 1.0M solution, respectively. NMR spectra were recorded on a Bruker DPX 300 MHz spectrometer, a Bruker Avance III 400 MHz spectrometer, and a Bruker Avance II+ 500 MHz spectrometer. For the ^{7}Li NMR spectroscopy a 9.7 M solution of lithium chloride (LiCl) in D_2O is used as a reference, and assigned at 0.0ppm, to calibrate the spectra. Mass spectra were recorded on a Mircomass Trio 2000 platform. Elemental analysis was carried out on a Carlo ERBA Instrument CHNS-O EA1108-Elemental Analyser, at London Metropolitan University. Crystallographic studies were carried out using an Oxford Diffraction XCaliber 2 instrument (all compounds, excluding **2.4** and $\mathbf{[4.5]}_\infty$), an Bruker AXS Diffractometer (compound $\mathbf{[4.5]}_\infty$) and an Bruker-Nonius

APEXII Diffractometer (compound **2.4**) at the Daresbury laboratories using the synchrotron source.

8.2 Synthesis of *Ansa-tris*(Allyl) Ligands and Complexes

8.2.1 Synthesis of *ansa-tris*(allyl) ligand L^2H_3

A solution of allyl-trimethylsilane (15.67g, 21.8ml, 0.137 mol), in thf (80ml) was treated dropwise, over 15 mins, with ^{n}BuLi (85.5ml, 0.137 mol, 1.6 M) at −78ºC, with stirring. The solution was stirred for 30 mins, then allowed to return to room temperature, and stirred for 18 hrs resulting in a red/orange solution. Trichlorophenylsilane (10.57g, 8.0ml, 0.050 mol) was added dropwise over 10 mins, at −10ºC. The orange/red colour was discharged. The mixture was left to stir for 19 hrs after which a white precipitate formed. The thf was removed in *vacuo* and replaced with diethyl ether (80ml) and the solution filtered (P3, Celite). This resulted in a pale yellow solution which was run through a silica column (hexane elute) and one fraction collected, the hexane was removed in *vacuo* to produce a viscous yellow oil (11.76g, 0.027mol, 58% yield). Anal. calc. for $C_{24}Si_4H_{44}$; C 64.86, H 9.90; found C 64.63, H 10.12 %. **^{1}H NMR** (δ/ppm, 500.13 MHz, $CDCl_3$, 294.3 K, *J*/Hz): 0.03, 27H, s, 3 × Si$\underline{Me}_3$; 1.95, 6H, dd, ^3J = 8.0, ^4J = 1.0, C$\underline{H}_2$CHCH; 5.52, 3H, d, ^3J = 20.0, $CH_2CHC\underline{H}$; 6.01, 3H, dt, ^3J = 16.0, ^4J = 8.0, $CH_2C\underline{H}CH$; 7.36, 3H, m, *m*-C_6H_5-Si/*p*-C_6H_5-Si; 7.48, 2H, dd, ^3J = 8.0, ^4J = 1.0 *o*-C_6H_5-Si. **^{13}C NMR** (δ/ppm, 125.76 MHz, $CDCl_3$, 295.8 K): −1.09, Si$\underline{Me}_3$; 24.43, PhSi-$\underline{C}H_2$; 127.58, 129.25, *m*-$\underline{C}_6H_5$Si/*p*-$\underline{C}_6H_5$Si; 130.17, Me_3Si-$C\underline{H}$=CH-CH_2; 134.30, *o*-$\underline{C}_6H_5$Si; 135.34, *ipso*-$\underline{C}_6H_5$Si; 142.00, CH=$\underline{C}$H-CH. **MS** ES/CI (m/z); 445 molecular mass + Cl^+, 331 loss of one allyl trimethylsilane, 72 phenyl ring.

8.2.2 Synthesis of *ansa-tris*(allyl) complex 2.1 [L^2(Li.tmeda)$_3$]

A solution of $\mathbf{L^2}H_3$ (0.506g, 1.14mmol) in hexane (10ml) was treated with ^{n}BuLi (1.6M, 2.14ml, 3.42mmol) at −78ºC, with stirring; the solution left to stir for 30 mins, and then allowed to warm to room temperature and left stirring for 18 hrs, affording a pale yellow solution. The solution was treated with tmeda (0.51ml, 0.40g, 3.42mmol), and left to stir for 20 hrs, producing an orange coloured solution. The solution was filtered (P3, Celite), and the solution was concentrated, in *vacuo*, to ~2ml, and left to recrystallise at +5°C affording large flat orange/yellow crystals of **2.1** (0.41g, 44 %). Anal. calc. for $C_{45}H_{96}Li_3N_6Si_4$; C 62.16, H 11.08, N 10.36; found C 60.78, H 11.23, N 9.11%. **^{1}H NMR** (δ/ppm, 400.23 MHz, C_6D_6, 294.3 K, *J*/Hz): 0.00, 0.23, 0.39, 27H, s, 3 × $SiMe_3$; 1.4-2.4 very broad, 48H, overlapping multiplet, 3 × tmeda protons; 3.03, 2H, m, 2 × *exo*- $Me_3SiC\underline{H}CH$; 3.14, 1H, m; 3.47, 1H dd, ^3J = 24.0 and ^4J = 8.0, *endo*-$PhSiC\underline{H}$; 5.85, 1H, m; 6.39, 1H, m; 6.70, 2H, t, ^3J = 28.0, *exo*-central allyl $CHC\underline{H}CH$; 7.14-7.39, broad, 5H, overlapping multiplet, SiPh protons; 7.89, 2H, large, overlapping multiplets. **^{13}C NMR** (δ/ppm, 100.65 MHz, C_6D_6, 295.8 K): -3.7, *endo*-$Si\underline{Me}_3$; 0.0, 0.6, 2 × *exo*-$Si\underline{Me}_3$; 44.0, broad, 4 × $N(\underline{C}H_3)_2$; 55.1 broad, 2 × $N\underline{C}H_2\underline{C}H_2N$; 74.4, *endo*-$CH\underline{C}HSiMe_3$; 122.3, 124.6, 125.3, $\underline{C}_6H_5Si$; 133.3; 134.2; 151.2, 154.1, 2 × *exo*-$CH\underline{C}HSiMe_3$.

8.2.3 Synthesis of *ansa-tris*(allyl) complex 2.2 [L^1(Li.pmdeta)$_3$]

A mixture of $\mathbf{L^1}H_3$ (0.38g, 1.0mmol) and hexane (20ml) was cooled to –78 °C and ^{n}BuLi (1.9ml, 3.0mmol, 1.6 M) was added dropwise. The reaction mixture was slowly warmed to room temperature and stirred for 4 hrs. Upon addition of pmdeta (0.64ml, 3.0mmol) a faintly turbid yellow solution was formed, which, on stirring overnight, became orange-red in colour. Filtration of the solution (Celite, P3) followed by concentration of the filtrate to ca. 2ml and storage at –15 °C for 2-3 days afforded

orange crystals of **2.2** (0.36g, 39 %). $C_{46}H_{108}Li_3N_9Si_4$: calcd. C 60.02, H 11.82, N 13.69; found C 60.07, H 11.75, N 13.69%. **^{1}H NMR** (400.23 MHz, C_6D_6, 294.3 K): δ = 0.00, 0.14, 0.16, 0.23, s, 30H, 3 × Si<u>Me</u>$_3$, Si<u>Me</u>; 1.61, 1.64, 1.71, 1.80, dd, ^3J = 7.78, ^5J = 1.25 Hz, 4H, allyl CH-CH-C<u>H</u>SiMe and C<u>H</u>-CH-CHSiMe; 2.13, s, 36H, pmdeta N<u>Me</u>$_2$, 2.20, s, 9H, pmdeta N<u>Me</u>; 2.38 and 2.51, t, ^3J = 6.78 Hz, 24H, pmdeta C<u>H</u>$_2$C<u>H</u>$_2$; 5.46, 5.50, 5.60, 5.62, 5.65, 5.67, 5.71, 5.76, overlapping m, allyl C<u>H</u>-CHSiMe; 6.08–6.24, overlapping m, allyl C*H*-CHSiMe; 6.53, 6.58, overlapping, ^3J = 7.78 Hz, allyl C<u>H</u>-CHSiMe; 7.09, t, ^3J = 15.81 Hz, allyl C<u>H</u>-CHSiMe *exo,exo*. **^{13}C NMR** (100.65 MHz, C_6D_6, 295.8 K): δ = –1.44, –0.34, 0.03, 3.18 3 × Si<u>Me</u>$_3$, Si<u>Me</u>; 25.67, 26.78, 29.29, 30.92, terminal allyl carbon atoms; 43.69, pmdeta N<u>Me</u>; 46.54, pmdeta N<u>Me</u>$_2$; 57.45 and 58.87, pmdeta <u>C</u>H$_2$<u>C</u>H$_2$; 124.98, 126.72, 130.01, 143.53, 144.13, 147.82, central allyl carbon atoms; **^{7}Li NMR** (155.54 MHz, C_6D_6, 295.2 K): δ = –0.34, –0.17, 0.08, 3 × Li.

8.2.4 Synthesis of *ansa-tris*(allyl) complex 2.3 [L^1(Na.tmeda)$_3$]

A suspension of ^{n}BuNa, freshly prepared from sodium *tert*-butoxide (0.29g, 3.0mmol) and ^{n}BuLi (1.9ml, 3.0mmol, 1.6 M), in hexane (20ml) was cooled to –78 °C and **L^1**H$_3$ (0.39g, 1.0mmol) was added dropwise over 1 min. The reaction mixture was then slowly warmed to room temperature and stirred for 1 hr. On re-cooling to –78 °C, tmeda (0.35g, 0.46ml, 3.0mmol) was added to the pale yellow reaction mixture, which was stirred for 15 min and then warmed to room temperature. Stirring for 18 hrs produced a bright orange solution that was filtered (Celite, P3) and concentrated to ca. 4ml. Storage of the concentrated solution at –15 °C for several days produced large, orange block-like crystals of compound **2.3** (0.30g, 38% isolated yield). $C_{37}H_{87}N_6Na_3Si_4$: calcd. C 55.73, H 11.00, N 10.54; found C 55.01, H 10.25, N 9.98%. **^{1}H NMR** (400.23 MHz, benzene-d_6, 294.3 K): δ = –0.01, 0.00, 0.15, 0.13, 30 H, s, Si<u>Me</u>$_3$ and Si<u>Me;</u> 1.63, 1.70,

1.79, 1.86, overlapping d, allyl H; 1.95, 12 H, s, tmeda C$\underline{H}_2$; 2.14, 36 H, s, tmeda C$\underline{H}_3$; 2.99, broad d, allyl H; 3.63, broad m, allyl H; 5.64, overlapping m, allyl H; 6.20, overlapping m, allyl H; 6.46, overlapping m, allyl H; 7.35, broad m, allyl H. **^{13}C NMR** (100.65 MHz, benzene-d_6, 295.8 K): δ = –4.42, –2.27, –1.20, 2.77, Si$\underline{Me}_3$ and Si$\underline{Me}$; 27.85, allyl C; 56.72, tmeda $\underline{C}H_2$; 45.38, tmeda $\underline{C}H_3$; 73.38, allyl C; 76.61, allyl C; 129.02, allyl C; 145.68, allyl C; 151.12.

8.2.5 Synthesis of *ansa-tris*(allyl) complex [2.4]$_2$

[L^2(Na.tmeda)$_2$Na]$_2$

A suspension of benzylsodium (0.17g, 1.5mmol) in hexane (20ml) was cooled to –78 °C and tmeda (0.18g, 0.23ml, 1.5mmol) was added. The solution was stirred for 5 min and **L^2**H$_3$ (0.223g, 0.5mmol) was added dropwise, then the reaction mixture was stirred at –78 °C for 30 min before being warmed to room temperature. Stirring for a further 48 h afforded a dark yellow solution and a precipitate, which re-dissolved on gentle heating. The resulting solution was filtered whilst hot (Celite, P3), and hexane (5ml) was added. Storage of the solution at +5 °C for several days produced a crop of orange, plate-like crystals of [**2.4**]$_2$ (0.31g, 42 %). $C_{72}H_{146}N_8Na_6Si_8$: calcd. C 58.17, H 9.90, N 7.54; found C 58.05, H 9.93, N 7.47%. **^{1}H NMR** (400.23 MHz, benzene-d_6, 294.3 K): δ = –0.10, –0.06, 0.00, 0.12, 0.25, 0.32, 0.39, 0.41, overlapping s, Si$\underline{Me}_3$; 1.57–1.73, broad m, allyl C$\underline{H}$; 1.85, broad s, tmeda C$\underline{H}_2$; 2.10, broad s, tmeda C$\underline{H}_3$; 2.92–3.81, broad overlapping m, allyl C$\underline{H}$; 5.60–5.99, 6.14–6.42, 6.51–6.67, broad overlapping m, allyl C$\underline{H}$; 7.22–7.62, broad overlapping m, 10 H, C$_6\underline{H}_5$; 8.10–8.47, allyl C$\underline{H}$. **^{13}C NMR** (100.65 MHz, benzene-d_6, 295.8 K): δ = –0.01, 1.01, 4.45, 4.60, 5.00, 5.21, Si$\underline{Me}_3$; 47.73, tmeda $\underline{C}H_3$; 58.98, tmeda $\underline{C}H_2$; 133.12, 134.93, allyl CH-CH-CH. Resonances due to other allyl carbon atoms were too low in intensity to be distinguished from background noise.

8.2.5 Synthesis of *ansa-tris*(allyl) complex 2.5 $[L^1(K.OEt_2)_2KLi\text{-}(O^tBu)]_2$

A solution of $MeSi(CH_2CHCHSiMe_3)_3$ (0.389g, 1.01mmol), in diethyl ether (10ml), was treated dropwise, with ^{n}BuLi (1.91ml, 3.06mmol, 1.6 M), at −78ºC with stirring, then left to stir for 30 mins, then allowed to warm to room temperature, and left to stir for 20hrs, to produce a yellow-orange solution. The reaction mixture was treated with a solution of KO^tBu (0.351g, 3.13mmol) in diethyl ether (10ml) to give an orange solution which was filtered (P3, Celite) and then solution was concentrated, in *vacuo*, to ~2ml, and left to recrystallise at −5°C. Small deep orange crystals were isolated (0.051g, 0.10mmol, 10% yield). Anal. calc. for $C_{78}H_{176}K_6Li_2O_{10}Si_8$; C 45.90, H 7.92; found C 46.45, H 8.13 %. **^{1}H NMR** (δ/ppm, 400.23 MHz, benzene-d_6, 294.3 K, *J*/Hz): 0.00-0.45, 30H, broad, overlapping multiplet, 3 × Si<u>Me</u>$_3$, Si<u>Me</u>; 1.09, 18H, s, $LiO^tC(C\underline{H}_3)_3$; 3.24, 2 × $(CH_3C\underline{H}_2)_2O$; 6.07-6.34, broad, overlapping multiplet, 9H, C<u>H</u>C<u>H</u>C<u>H</u>. **^{13}C NMR** (δ/ppm, 100.65 MHz, benzene-d_6, 295.8 K, very weak spectrum): -3.2, Si<u>Me</u>; 0.0, 1.15, 4.8, 3 ×$SiMe_3$; 17.4, $LiO^t\underline{C}(CH_3)_3$; 67.7, 69.8 2 × $(CH_3\underline{C}H_2)_2O$; 145.5, 147.9, 148.1, allyl carbon atoms.

8.3 Synthesis of Donor-Functionalised Allyl Ligands and Complexes

8.3.1 Synthesis of thf-tosylate precursor

para-Tosylchloride (57.2g, 0.30 mol) was ground up and added, with stirring, to a mixture of pyridine (34.0ml, 33.2g, 0.42 mol) and tetrahydrofurfuryl alcohol (29ml, 30.6g, 0.30 mol) in an ice bath. The mixture was left in the ice bath for 1 hour, then placed in the fridge to set. The resulting solid was dissolved in diethyl ether (150ml) and water (150ml) and the organic and aqueous layers separated. The aqueous layer was

washed with diethyl ether (150ml) and the organic layer was washed with an acid solution (100ml water, 10ml conc. HCl, 2 x 50ml). The aqueous layer was collected and the organic layer washed with water (100ml). The organic layers were combined and dried over $MgSO_4$ overnight. The organic layer was then filtered and the solvent removed *in vacuo* to afford a cream/white solid (77g, 82%) Anal. calc. for $C_{12}H_{16}O_4S$, C 56.23, H 6.29; found C 56.24, H 6.43 %. **^{1}H NMR** (δ/ppm, 500.13 MHz, $CDCl_3$, 294.3 K, *J*/Hz): 1.59, 1H, m, tetrahydrofurfuryl OCHCHH; 1.79, 2H, qd, ^3J = 35.0, ^4J = 5.0, tetrahydrofurfuryl OCH_2CH_2; 1.89, 1H, m, tetrahydrofurfuryl OCHCHH; 3.68, 2H, m, tetrahydrofurfuryl OCH_2; 3.93, 2H, m, CH_2; 4.01, 1H, q, ^3J = 25.0, tetrahydrofurfuryl OCH; 7.27, 2H, d, ^3J = 8.2, phenyl S-CCHCHC-CH_3; 7.72, 2H, d, ^3J = 8.4, phenyl S-CCHCHC-CH_3. **^{13}C NMR** (δ/ppm, 125.76 MHz, $CDCl_3$, 295.8 K): 21.6, CH_3; 25.5, tetrahydrofurfuryl OCH_2CH_2; 27.8, tetrahydrofurfuryl $OCHCH_2$; 68.5, tetrahydrofurfuryl OCH_2; 71.4, CH_2; 75.9, tetrahydrofurfuryl OCH; 127.9, phenyl S-CCHCHC-CH_3; 129.8, phenyl S-CCHCHC-CH_3; 133.0, phenyl S-CCHCHC-CH_3; 144.7, phenyl S-CCHCHC-CH_3. **MS** ES/CI (m/z); 257 molecular mass + H^+.

8.3.2 Synthesis of methoxy-tosylate precursor

para-tosylchloride (57.2g, 0.30 mol) was ground up and added, with stirring, to a mixture of pyridine (34.0ml, 33.2g, 0.42 mol) and 2-methoxyethanol (23.8ml, 22.8g, 0.30 mol) in an ice bath. The mixture was left in the ice bath for 1 hour, and then placed in the fridge to set. The resulting solid was dissolved in diethyl ether (150ml) and water (150ml) and the organic and aqueous layers separated. The aqueous layer was washed with diethyl ether (150ml) and the organic layer was washed with an acid solution (100ml water, 10ml conc. HCl, 2 x 50ml). The aqueous layer was collected and the organic layer washed with water (100ml). The organic layers were combined and dried over $MgSO_4$ overnight. The organic layer was then filtered and the solvent removed *in*

vacuo to afford a colourless oil (42.5g, 62%). Anal. calc. for $C_{10}H_{14}O_4S$, C 52.16, H 6.13; found C 52.39, H 6.47 %. **^{1}H NMR** (δ/ppm, 500.13 MHz, $CDCl_3$, 294.3 K, *J*/Hz): 2.45, 3H, s, C_6H_4–C<u>H</u>$_3$; 3.31, 3H, s, OC<u>H</u>$_3$; 3.58, 2H, t, ^3J = 10.0, $CH_3OCH_2C\underline{H}_2$; 3.16, 2H, t, ^3J = 10.0, $CH_3OC\underline{H}_2CH_2$; 7.35, 2H, d, ^3J = 10.0, phenyl S-CCHC<u>H</u>C-CH_3; 7.81, 2H, d, ^3J = 10.0, phenyl S-CC<u>H</u>CHC-CH_3. **^{13}C NMR** (δ/ppm, 125.76 MHz, $CDCl_3$, 295.8 K): 21.6, C_6H_4–<u>C</u>H$_3$; 58.9, OC<u>H</u>$_3$; 69.0, $CH_3O\underline{C}H_2CH_2$; 9.9, $CH_3OCH_2\underline{C}H_2$; 71.4, <u>C</u>H$_2$; 127.9, phenyl S-C<u>C</u>HCHC-CH_3; 129.8, phenyl S-CCH<u>C</u>HC-CH_3; 133.0, phenyl S-<u>C</u>CHCHC-CH_3; 144.8, phenyl S-CCHCH<u>C</u>-CH_3. **MS** ES/CI (m/z); 231 molecular mass + H^+.

8.3.3 Synthesis of thf-donor-functionalised pro-ligand, L^{3}H

A solution of tetrahydrofurfuryl tosylate (5.63g, 22.0mmol) in thf (30ml) was added to a freshly prepared solution of 1,3-*bis*(trimethylsilyl)allyl lithium (20.0mmol) in thf (30ml) at -78°C. Warming the reaction to room-temperature and stirring for 48 hours afforded a colourless solution and a white precipitate. The thf solvent was removed, in *vacuo*, and replaced with hexane (60ml) and the mixture filtered (P3, Celite). The hexane was removed in *vacuo* to afford a pale yellow oil. Distillation under reduced pressure (68-72°C, 12 mmHg) afforded **L^3**H (3.41g, 13mmol, 63%) as a colourless oil. Anal. calc. for $C_{14}H_{30}OSi_2$, C 62.15, H 11.18; found C 61.98, H 11.25 %. **^{1}H NMR** (δ/ppm, 500.13 MHz, $CDCl_3$, 294.3 K, *J*/Hz): 5.98, 0.1H, dt, ^3J = 7.7 and 18.4, CH–C<u>H</u>=CHSi minor diastereomer; 0.9H, ^3J = 7.7 and 18.4, CH–C<u>H</u>=CHSi major diastereomer; 5.42 (major diastereomer) and 5.40 (minor diastereomer), 1H, 2 × dd, ^3J = 18.4 and 18.4, ^4J = 0.9 and 0.9, C<u>H</u>–CH=CHSi; 3.85-3.74, 2H, 2 × m, tetrahydrofurfuryl C<u>H</u>O and C<u>H</u>HO; 3.70-3.63, 1H, m, tetrahydrofurfuryl CH<u>H</u>O; 1.95, 1H, m, tetrahydrofurfuryl C<u>H</u>HCHO; 1.82, 2H, m, tetrahydrofurfuryl C<u>H</u>$_2$CH$_2$O; 1.59, 1H, m, C<u>H</u>–CH=CH; 1.36, m, 1H, tetrahydrofurfuryl CH<u>H</u>CHO. **^{13}C NMR** (δ/ppm, 125.76 MHz, $CDCl_3$, 295.8 K): 149.23

and 148.68, CH=CHSi; 127.83 and 127.74, CH=CHSi; 79.71 and 79.63, tetrahydrofurfuryl CHO; 68.64, 68.17 tetrahydrofurfuryl CH_2O; 36.16 and 36.07, CH–CH=CHSi; 35.51 and 35.07; tetrahydrofurfuryl CH_2CHO; 32.86 and 31.39, CH_2CH–CH=; 26.83 and 26.58, tetrahydrofurfuryl CH_2CH_2O; 0.02, 0.01, 2.42 and -2.47, $Si(CH_3)_3$. **MS** ES/CI (m/z); 271 molecular mass + H^+.

8.3.4 Synthesis of methoxy-donor-functionalised pro-ligand, L^4H

A solution of 2-methoxyethyl tosylate (7.60g, 33.0mmol) in thf (40ml) was added to a freshly prepared solution of 1,3-*bis*(trimethylsilyl)allyl lithium (30.0mmol) in thf (30ml) at -78°C. Warming the reaction to room-temperature and stirring for 48 hours afforded a colourless solution and a white precipitate. The thf solvent was removed, in *vacuo*, and replaced with hexane (100ml) and the mixture filtered (P3, Celite). The hexane was removed in *vacuo* to afford a pale yellow oil. Distillation under reduced pressure (58-64°C, 12 mmHg) afforded $\mathbf{L^4}H$ (3.50g, 14mmol, 47%) as a colourless oil. Anal. calc. for $C_{12}H_{28}OSi_2$, C 58.9, H 11.54; found C 59.06, H 11.38%. **^{1}H NMR** (δ/ppm, 500.13 MHz, $CDCl_3$, 294.3 K, *J*/Hz): -0.03, 3H, s, CH=CH $SiMe_3$; 0.04, 3H, s, $SiMe_3CH$−CH; 1.68, 2H, q, ^3J = 25.0, CH_2CH_2O; 1.76, 1H, qd, ^3J = 25.0 and 5.0, $SiMe_3CH$−CH; 3.28, 1H, m, $CH_3OCHHCH_2$; 3.32, 3H, s, OCH_3; 3.40, 1H, m, $CH_3OCHHCH_2$; 5.44, 1H, d, ^3J = 15.0, CH=$CHSiMe_3$; 5.86, 1H, dd, ^3J = 15.0 and 5.0, CH=$CHSiMe_3$; **^{13}C NMR** (δ/ppm, 125.76 MHz, $CDCl_3$, 295.8 K): -2.4, Me_3SiCH−CH; 0.0, CH=$CHSiMe_3$; 29.0 $CH_3OCH_2CH_2$; 35.2, Me_3SiCH−CH; 59.4, OCH_3; 73.4, $CH_3OCH_2CH_2$; 128.0, CH=$CHSiMe_3$; 148.6, CH=$CHSiMe_3$. **MS** ES/CI (m/z); 245 molecular mass + H^+.

8.3.5 Synthesis of donor-functionalised complex, $[4.1]_2$ $[L^3Li]_2$

A solution of L^3H (0.54g, 2.0mmol) in hexane (20ml) was treated dropwise with ^{n}BuLi in hexanes (1.6M, 1.25ml, 2.0mmol), at −78°C, with stirring. Slowly warming the

reaction to room-temperature and stirring for 16 hours afforded a yellow solution and a precipitate. Gently heating the precipitate afforded a yellow solution which, on storage at room-temperature overnight, resulted in the formation of large colourless blocks of [**4.1**]$_2$, (0.20g, 35% isolated yield). Anal. calc. for $C_{14}H_{29}LiOSi_2$, C 60.81, H 10.57; found C 60.27, H 10.25 %. **^{1}H NMR** (δ/ppm, 400.23 MHz, benzene-d_6, 294.3 K, *J*/Hz, non-integer integrals are due to presence of two diastereomers): 0.43, 0.33, 0.16, 0.00, 36H, 4 × s, 4 × Si<u>Me</u>$_3$; 1.55, 8H, v broad m, tetrahydrofurfuryl (C<u>H</u>$_2$)$_2$–CH$_2$–O; 2.27, broad dd, 0.7H, ^3J = 14.6, ^4J = 2.3, terminal allyl C<u>H</u>; 2.49, 3H, broad m, tetrahydrofurfuryl SiC–C<u>H</u>$_2$–CH; 2.64, 1H, broad m, tetrahydrofurfuryl SiC–C<u>H</u>$_2$–CH; 3.15, 0.7H broad d, 0.7H, ^3J = 16.0, terminal allyl C<u>H</u>; 3.38, 0.7H, broad m, tetrahydrofurfuryl CH$_2$O; 3.59, 2H, broad m, tetrahydrofurfuryl CH$_2$O; 3.79, 1.3H, broad q, tetrahydrofurfuryl CH$_2$O; 3.97, 1.3H broad quintet, tetrahydrofurfuryl CH; 4.10, 0.7H, broad m, tetrahydrofurfuryl CH; 6.00, 1.3H, broad m, central allyl CH; 7.18, d, integration not possible due to overlap with solvent peak, central allyl C<u>H</u>. **^{13}C NMR** (δ/ppm, 100.65 MHz, benzene-d_6, 295.8 K): 3.23, 1.70, 0.03, -1.25, 4 × Si<u>Me</u>$_3$; 37.69, 35.73, 31.87, 31.45, 26.97, 26.05, 21.61, tetrahydrofurfuryl CH$_2$; 57.90, terminal allyl CH; 68.64, tetrahydrofurfuryl CH$_2$O; 80.36, tetrahydrofurfuryl CH; 82.33, allyl C; 89.27, tetrahydrofurfuryl CH; 134.80, allyl C; 139.45, central allyl CH; 151.20, central allyl CH.

8.3.6 Synthesis of donor-functionalised complex, [4.2]$_2$ [L^{4}Li]$_2$

A solution of **L^4**H (0.2g, 1.0mmol) in hexane (10ml) was treated dropwise with ^{n}BuLi in hexanes (1.6M, 0.63ml, 1.0mmol), at -78°C, with stirring. Slowly warming the reaction to room-temperature and stirring for 16 hours afforded a yellow solution, the solution was concentrated, in *vacuo*, until a precipitate formed. Gently heating the precipitate back into solution and on storage at room-temperature overnight resulted in

the formation of large colourless blocks of [**4.2**]$_2$, (0.060g, 24% isolated yield). Anal. calc. for $C_{12}H_{27}LiOSi_2$, C 57.5, H 10.8; found C 57.42, H 10.79 %. **^{1}H NMR** (δ/ppm, 400.23 MHz, benzene-d_6, 294.3 K, *J*/Hz): 0.00, 0.14, 0.30, 0.41, 36H, 4 × s, 4 × Si<u>Me</u>$_3$; 2.55, 4H, t, ^3J = 16.0, 2 × $CH_3C\underline{H}_2CH_2$; 2.83, 3H, s, $OC\underline{H}_3$; 3.14, 3H, s, $OC\underline{H}_3$; 3.32, 4H, t, 16.0, 2 × $CH_3C\underline{H}_2CH_2$; 5.51, 2H, d, ^3J = 15, 2 × CHC<u>H</u>SiMe$_3$; 7.18, 2H, d, ^3J = 15, 2 × C<u>H</u>CHSiMe$_3$. **^{13}C NMR** (δ/ppm, 100.65 MHz, benzene-d_6, 295.8 K): -1.10, 0.32, 1.81, 3.31, 4 × Si<u>Me</u>$_3$; 21.3, 31.4, 2 × $CH_3OCH_2\underline{C}H_2$; 60.12, 60.25, 2 × O<u>C</u>H$_3$; 74.3, 81.0, 2 × $CH_3O\underline{C}H_2CH_2$; 132.2 Me$_3$Si<u>C</u>CHCH; 140.68, CH<u>C</u>HSiMe$_3$; 152.8, Me$_3$SiC<u>C</u>HCH.

8.3.7 Synthesis of donor-functionalised complex, [4.5]$_\infty$ [L^{3}K·thf]$_\infty$

A solution of [**4.1**]$_2$ was freshly prepared from **L^3**H (0.55g, 2.02mmol) and ^{n}BuLi (1.27ml, 2.03mmol, 1.6 M) and was added drop-wise to a stirred suspension of KO^{t}Bu (0.27g, 2.02mmol) in hexane (20ml) at room-temperature. A viscous red-brown solution was obtained on stirring for 8 hrs and evaporation of the hexane solvent afforded a powder, which upon dissolution in thf (2ml) and storage at +5°C for 2 days afforded amber crystals of **[4.5]**$_\infty$ (0.26g, 34% isolated yield). Anal. calc. for $C_{18}H_{37}KO_2Si_2$, C 56.78, H 9.79; found C, 55.90, H 9.59 %. **^{1}H NMR** (δ/ppm, 400.23 MHz, benzene-d_6, 294.3 K, *J*/Hz, non integer integrals are due to presence of two diastereomers): 0.33, 0.29, 0.20, 0.00, 4 × s, 36H, SiMe$_3$; 1.41, 4H, broad m, thf $C\underline{H}_2CH_2O$; 1.77-1.15, accurate integration not possible, very broad m, tetrahydrofurfuryl $CHC\underline{H}_2C\underline{H}_2$; 2.48 and 2.45, 2H, 2 × overlapping d, terminal allyl CH; 2.56, 2H broad m, tetrahydrofurfuryl SiC–C<u>H</u>$_2$–CH; 2.78, 0.3H, broad d, ^3J = 16.1, terminal allyl CH; 3.56, 4H, broad m, thf CH_2O; 3.84, 3H, broad m, tetrahydrofurfuryl CH and CH_2O; 6.01, 1.3H, m, central allyl CH; 6.83, 0.3H, broad d, ^3J = 16.1, central allyl CH. **^{13}C NMR** (δ/ppm, 100.65 MHz, benzene-d_6, 295.8 K): 3.21, 1.88, 0.03, -1.26, Si<u>Me</u>$_3$;

15.36, terminal allyl CH; 21.40, thf $\underline{C}H_2CH_2O$; 26.27, 26.12, $CHCH_2\underline{C}H_2CH_2O$; 32.07, 32.02, tetrahydrofurfuryl $CH\underline{C}H_2CH_2CH_2O$; 36.08, 35.96, $C\underline{C}H_2CHO$; 38.82, terminal allyl CH; 67.93, 67.89, tetrahydrofurfuryl CH_2O; 68.18, thf CH_2O; 79.94, 79.79, tetrahydrofurfuryl CH; 135.48, allyl C; 136.78, central allyl CH; 138.69, central allyl CH; 139.75, allyl C.

8.3.8 Synthesis of donor-functionalised complex, 4.6 [L^3_2Mg]

A mixture of Bu_2Mg (1.0 M, 1.02ml, 1.02mmol) and L^3H (0.55g, 2.03mmol) in hexane (20ml) was heated under reflux for 16 hours and cooled to room-temperature. The solvent was evaporated *in vacuo* until approximately 2ml remained, affording a faintly cloudy solution, which was heated briefly to reflux using an oil bath and cooled very slowly to room-temperature in the oil to result in the formation of colourless crystals of **4.6** (0.09g, 15 % isolated yield). Anal. calc. for $C_{28}H_{58}MgO_2Si_4$, C 60.81, H 10.57; found C 60.27, H 10.25 %. **^{1}H NMR** (δ/ppm, 400.23 MHz, dmso-d_6, 294.3 K, *J*/Hz): 0.00, -0.01, -0.05, -0.09, 36H, 4 × s, $Si\underline{Me}_3$. 1.73, 1.57, 1.35, 8H, v broad m, tetrahydrofurfuryl $CHC\underline{H}_2C\underline{H}_2CH_2O$; 2.23, 1H, broad d, ^3J = 6.7, =CH–C<u>H</u>Si; 3.71, 3.63, 3.53, v broad m, 6H, tetrahydrofurfuryl CH and CH_2O. **^{13}C NMR** (δ/ppm, 100.65 MHz, dmsod_6, 295.8 K): 0.02, -0.25, -1.14, -2.80, 4 × $Si\underline{Me}_3$; 25.93, 25.69, $CHCH_2\underline{C}H_2CH_2O$; 31.98, 31.36, tetrahydrofurfuryl $CH\underline{C}H_2CH_2CH_2O$; 35.37, 34.96, $C\underline{C}H_2CHO$; 35.24, allyl CH; 68.43, 68.03, tetrahydrofurfuryl CH_2O; 79.10 and 78.24, tetrahydrofurfuryl CH; 126.34 allyl CH; 134.65, allyl C; 138.49, allyl CH; 148.96, allyl C; 149.33, allyl CH.

8.4 Synthesis of Donor-Functionalised Pentadienyl Ligands and Complexes

8.4.1 Synthesis of donor-functionalised pentadienyl pro-ligand, L^8H

1,5-*bis*(trimethylsilyl)-1,3-pentadiene (12.38mmol, 2.63g) in thf (30ml) was treated with ^{n}BuLi (12.38mmol, 7.7ml, 1.6M solution) at ¯78 °C, to give a yellow solution and left to stir for 15 mins, then allowed to warm to room temperature give an orange solution, and left to stir for 2.5 hours. The solution was then treated with 2-(tosylmethyl)tetrahydrofuran (12.50ml, 3.20g) in thf (15ml) dropwise at −10 °C and the solution darkened to dark orange/brown, and left to stir for 5 mins; on warming to room temperature the solution became a dark green/yellow colour and was left to stir for 18 hours to give a pale green solution and white precipitate. The thf/hexane was removed under vacuum, keeping the flask cool at −10 °C, to give a yellow oil and white precipitate. The oil was redissolved in pentane (160ml) to give a suspension of the white precipitate, the solid was filtered (P3, celite) to give a colourless solution. Pentane (~ 60ml) was removed under vacuum, and the solution was left in the freezer for 18 hours to give a white solid. White tosylate crystals form and the solution is filtered off. The rest of the pentane was removed under vacuum, to give a colourless oil. The oil was distilled under a vacuum (75-80 °C); with a −78 °C cardice/acetone ice bath trap, to give a colourless oil (2.57, 70.0% yield), Anal. Calc. for $C_{16}H_{32}OSi_2$; C 64.79, H 10.87; found C 64.73, H 10.88 %. **^{1}H NMR** (δ/ppm, 400.13 MHz, $CDCl_3$, 300.0 K, *J*/Hz): 0.05, 0.06, 18H, 2 × s, 2 × $\underline{Me}_3Si{-}CH{=}CH$; 1.43-1.96, 6H, m, thf $C\underline{H}_2{-}C\underline{H}_2{-}C\underline{H}_2$; 2.89, 1H, quintet (overlapping tt), ^3J = 12.0, ^4J = 8.0, CH–*C*$\underline{H}$−CH; 3.79-3.84, 3H, m, thf *C*$\underline{H}$−O−*C*$\underline{H}_2$; 5.64, 2H, 2 × t, $Me_3Si{-}C\underline{H}{=}CH$; 5.86, 5.97, 2H, 2 × dd, ^3J = 16.0, ^4J = 8.0 $Me_3Si{-}CH{=}C\underline{H}$. **^{13}C NMR** (δ/ppm, 100.61 MHz, $CDCl_3$, 300.0 K): ¯1.16, ¯1.13, 2 ×

$\underline{Me}_3Si$; 25.74, thf O−CH_2−$\underline{C}H_2$; 31.48, thf O−CH−$\underline{C}H_2$; 40.07, CH=CH−CH−$\underline{C}H_2$; 50.11, CH=CH−$\underline{C}$H−CH_2; 67.44, thf O−$\underline{C}H_2$−CH_2; 77.01, thf O−$\underline{C}$H−CH_2; 129.28, 130.12, 2 × Me_3Si−$\underline{C}$H=CH; 148.21, 148.67, 2 × Me_3Si−CH=$\underline{C}$H. **MS** APCI (m/z); 295 molecular mass – H^+.

8.4.2 Synthesis of donor-functionalised pentadienyl pro-ligand, L^9H

1,5-*bis*(trimethylsilyl)-1,3-pentadiene (11.95mmol, 2.54g) in thf (30ml) was treated with ^{n}BuLi (11.95mmol, 7.5ml, 1.6 M) at −78 °C, to give a yellow solution and left to stir for 15 mins, then allowed to warm to room temperature give an orange solution, and left to stir for 2.5 hrs. The solution was then treated with 1-(2-methoxyethylsulfonyl)-4-methylbenzene (12.90mmol, 2.99g) in thf (15ml) dropwise at −10 °C and the solution darkened to dark orange/brown, and left to stir for 5 mins; on warming to room temperature the solution became a dark grey/blue colour and was left to stir for 18 hrs to give a grey solution and white precipitate. The thf/hexane was removed under vacuum, keeping the flask cool at −10 °C, to give an oil and white precipitate. The oil was redissolved in pentane (120ml) to give a suspension of the white precipitate, the solid was filtered (P3, celite) to give a colourless solution. The pentane was removed under vacuum, to give a colourless oil. The oil was distilled under a vacuum (45-50 °C); with a −78 °C cardice/acetone ice bath trap, to give a colourless oil (1.93g, 60.0% yield). Anal. Calc. for $C_{14}H_{30}OSi_2$; C 62.15, H 11.18; found C 62.02, H 11.07 %. **^{1}H NMR** (δ/ppm, 400.13 MHz, $CDCl_3$, 300.0 K, *J*/Hz): 0.06, 18H, s, 2 × Si$\underline{Me}_3$; 1.68, 2H, quartet, ^3J = 8.0, CH=CH−CH−C$\underline{H}_2$; 2.87, 1H, quintet, ^3J = 8.0, Me_3Si−CH=CH−C$\underline{H}$; 3.32, 3H, s, OC$\underline{H}_3$; 3.35, 2H, t, ^3J = 8.0, CH_3O−C$\underline{H}_2$; 5.68, 2H, d, ^3J = 20.0, Me_3Si−C$\underline{H}$=CH; 5.94, 2H, dd, ^3J = 20.0, ^4J = 8.0, Me_3Si−CH=C$\underline{H}$. **^{13}C NMR** (δ/ppm, 100.61 MHz, $CDCl_3$, 300.0 K): ¯1.16, Si$\underline{Me}_3$; 33.66, CH=CH−CH−$\underline{C}H_2$; 49.46,

CH=CH−CH−CH_2; 58.51, OCH_3; 70.52, CH_3O− CH_2; 129.96, Me_3Si−CH=CH; 148.19, Me_3Si−CH=CH. **MS** APCI (m/z); 269 molecular mass – H^+.

8.4.3 Synthesis of (2-methoxyphenyl)lithium precursor

Bromoanisole (104mmol, 19.5g) in hexane (20ml) was treated with ^{n}BuLi (104mmol, 65.0ml) dropwise at 0°C, to give a white precipitate. The suspension was left to stir at 0°C for 1.5hrs. The solid was filtered and collected (P4) and washed with hexane (3 × 20ml) and left to dry for 3hrs. The white powered was isolated (10.4g, 88%) and stored under an inert atmosphere. Anal. Calc. for C_7H_7LiO; C 73.70, H 6.19; found C 73.88, H 6.26%. **^{1}H NMR** (δ/ppm, 400.13 MHz, $CDCl_3$, 300.0 K, *J*/Hz): 3.02, 3H, s, OCH_3; 6.55, 1H, d, ^3J = 8.0, CH_3O-*ortho*-C_6H_4; 7.16, 1H, t, ^3J = 8.0, CH_3O-*ortho*-C_6H_4; 7.31, 1H, td, ^3J = 8.0, 1.6, CH_3O-*para*-C_6H_4; 7.97, 1H, dd, ^3J = 8.0, 1.6 CH_3O-*meta*-C_6H_4. **^{13}C NMR** (δ/ppm, 100.61 MHz, $CDCl_3$, 300.0 K): 54.7 OCH_3; 107.6, CH_3O-*ortho*-C_6H_4; 123.4 LiC-*para*-C_6H_4; 128.1 CH_3O-*para*-C_6H_4; 141.5, CH_3O-*meta*-C_6H_4; 156.6 LiC-*ipso*-C_6H_4; 170.2, CH_3O-*ipso*-C_6H_4.

8.4.4 Synthesis of chloro(2-methoxyphenyl)dimethylsilane precursor

(2-methoxyphenyl)lithium (90.6mmol, 10.3g) in thf (100ml) at 0°C, was added *via* cannula, to a solution of dichlorodimethyl silane (99.6mmol, 12.9g, 12.0ml) at −10°C and left to stir for 15 mins, then allowed to warm to room temperature. The solution was left to stir at room temperature for 2.5hrs. The thf was removed under vacuum, while keeping the flask cool at 0°C to give an oil and a white precipitate. Allow the oil to warm to room temperature as the product may freeze at 0°C. The oil was re-dissolved in hexane (160ml) to give a suspension of the white solid. The solid was removed by filtration (P3, celite) to give a colourless solution. The hexane was removed under

vacuum to give a cream coloured solid/oil. The solid dissolved into the oil on warming. The oil was purified by vacuum distillation, heating slowly to 45°C to give a colourless oil (10.9g, 60%). Anal. Calc. for $C_9H_{13}ClOSi$; C 53.85, H 6.53; found C 53.74, H 6.42%. **^{1}H NMR** (δ/ppm, 400.13 MHz, $CDCl_3$, 300.0 K, *J*/Hz): 0.67, 6H, s, Si$\underline{Me}_2$; 3.85, 3H, s, O$\underline{CH}_3$; 6.88, 1H, d, ^3J = 8.0, Me_2ClSi-*meta*-$C_6\underline{H}_4$; 7.03, 1H, td, ^3J = 8.0, 1.0, Me_2ClSi-*para*-$C_6\underline{H}_4$; 7.44, 1H, td, ^3J = 8.0, 4.0, CH_3O-*para*-$C_6\underline{H}_4$; 7.65, 1H, dd, ^3J = 8.0, 4.0, CH_3O-*meta*-$C_6\underline{H}_4$. **^{13}C NMR** (δ/ppm, 100.61 MHz, $CDCl_3$, 300.0 K): 2.86, Si$\underline{Me}_2$; 52.2 O$\underline{C}H_3$; 109.7, Me_2ClSi-*meta*-$\underline{C}_6H_4$; 120.8, Me_2ClSi-*para*-$\underline{C}_6H_4$; 123.8, Me_2ClSi-*ipso*-$\underline{C}_6H_4$; 132.5, CH_3O-*para*-$\underline{C}_6H_4$; 135.5, CH_3O-*meta*-$\underline{C}_6H_4$; 163.8, CH_3O-*ipso*-$\underline{C}_6H_4$. **MS** GC/MS (m/z); 200 molecular ion.

8.4.5 Synthesis of donor-functionalised pentadienyl pro-ligand, $L^{10}H$

1-(trimethylsilyl)-2,4-pentadiene (prepared by literature procedure 192) (6.38mmol, 0.90g) in thf (20ml) was treated with ^{n}BuLi (6.38mmol, 4.0ml) at −78°C to give a yellow solution and left to stir for 15mins. Allowed to warm to room temperature and left to stir for 1 hr to give an orange solution. The orange solution was treated, *via* cannula, with a solution of chloro(2-methoxyphenyl)dimethylsilane (6.38mmol, 1.28g) in thf (80ml) at 0°C, the solution was left to stir at 0°C for 15 mins, then allowed to warm to room temperature, and left to stir for 18 hrs to give a yellow solution. The thf/hexane is removed under vacuum to give an oil and a white precipitate. The oil was re-dissolved in hexane (100ml) to give a suspension of the solid, the solid is filtered (P3, celite) to give a yellow solution. The hexane is removed under vacuum to give a viscous yellow/orange oil. The oil was purified by vacuum distillation (48-52°C) to give a pale yellow oil (1.26g, 65%). For future synthesis of this pro-ligand, distillation without the vigreux column would improve the distillation procedure. Anal. Calc. for $C_{17}H_{28}OSi_2$; C

67.04, H 9.27; found C 66.95, H 9.21%. **^{1}H NMR** (δ/ppm, 400.13 MHz, $CDCl_3$, 300.0 K, *J*/Hz): 0.00, 9H, s, Si$\underline{Me}_3$; 0.20, 6H, s, Si$\underline{Me}_2$; 1.80, 2H, d, ^{3}J = 16.00, $Me_2Si-C\underline{H}_2$; 3.75, 3H, s, $OC\underline{H}_3$; 5.52, 1H, d ^{3}J = 16.00, $Me_3Si-C\underline{H}=CH$; 5.70, 1H, overlapping dt, ^{3}J = 16.00, 8.00, $Me_2Si-CH_2-C\underline{H}$; 5.90, 1H, overlapping dd, ^{3}J = 16.00, 8.00, $CH_2-CH=C\underline{H}$; 6.40, 1H, dd, ^{3}J = 16.00, 8.00, $Me_3Si-CH=C\underline{H}$; 6.80, 1H, m, Me_2Si-*meta*-$C_6\underline{H}_4$; 6.90, 1H, m, Me_2Si-*para*-$C_6\underline{H}_4$; 7.30, 2H, overlapping m, CH_3O-*para/meta*-$C_6\underline{H}_4$. **^{13}C NMR** (δ/ppm, 100.61 MHz, $CDCl_3$, 300.0 K): −3.03, Si$\underline{Me}_2$; −1.16, Si$\underline{Me}_3$; 22.41, $Me_2Si-\underline{C}H_2-CH$; 54.97 $O\underline{C}H_3$; 99.99; 109.47, Me_2Si-*meta*-$\underline{C}_6H_4$; 120.43, Me_2Si-*para*-$\underline{C}_6H_4$; 128.41, $Me_3Si-\underline{C}H=CH$; 130.99, CH_3O-*para/meta*-$\underline{C}_6H_4$; 132.48; 133.09; 135.24, CH_3O-*para/meta*-$\underline{C}_6H_4$; 144.94, $Me_3Si-CH=C\underline{H}$. **MS** GC/MS (m/z); 303 molecular ion.

8.4.6 Synthesis of donor-functionalised pentadienyl pro-ligand, L^{12}H

A mixture of ^{n}BuLi (18.0mmol, 11.3ml) and thf (100ml) was treated with a solution of 1-(trimethylsilyl)-2,4-pentadiene (prepared by literature procedure 192) (18.0mmol, 2.53g) in thf (20ml) at −78°C, the mixture was left to stir for 15mins then allowed to warm to room temperature to give an orange solution. The orange solution was left to stir at room temperature for 1.5 hrs and then treated with a solution of 1-(2-methoxyethylsulfonyl)-4-methylbenzene (18.2mmol, 4.19g) in thf (30ml) at −10°C to give the following colour changes: orange → dark orange → orange → yellow. The solution was left to stir for 15 mins, then allowed to warm to room temperature and left to stir for 18 hrs. The thf/hexane is removed under vacuum, keeping the flask cool at 0°C, to give an oil and a white precipitate. The oil was re-dissolved in hexane (140ml) to give a suspension of the solid, the solid is filtered (P3, celite) to give a colourless solution. The hexane is removed under vacuum, keeping the flask cool at 0°C, to give a

pale yellow oil. The oil was purified by vacuum distillation (30°C) to give a colourless oil (1.55g, 43%). Anal. Calc. for $C_{11}H_{22}OSi$; C 66.60, H 11.18; found C 66.43, H 11.07%. **^{1}H NMR** (δ/ppm, 400.13 MHz, $CDCl_3$, 300.0 K, *J*/Hz): 0.06, 9H, s, $Si\underline{Me}_3$; 1.69, 2H, quartet of doublets, ^3J = 8.00, 4.00, $H_3COCH_2C\underline{H}_2$; 2.87, 1H, quintet (overlapping dt), ^3J = 8.00, $OCH_2CH_2C\underline{H}$; 3.32, 3H, s, $OC\underline{H}_3$; 3.37, 2H, t, ^3J = 8.00, $H_3COC\underline{H}_2CH_2$; 5.01/5.04, 2 × 1H, doublet of quartets/quintet, ^3J = 4.00, $Me_3Si{-}C\underline{H}_2{-}CH{=}CH$; 5.57/5.71, 2 × 1H, overlapping dd/dd, ^3J = 16.00, 4.00, and ^3J = 20.00, 8.00, $Me_3Si{-}CH_2{-}CH{=}C\underline{H}{-}C\underline{H}$; 5.89, 1H, dd, ^3J = 20.00, 8.00, $Me_3Si{-}CH_2{-}C\underline{H}{=}CH$. **^{13}C NMR** (δ/ppm, 100.61 MHz, $CDCl_3$, 300.0 K): −1.19, $Si\underline{Me}_3$; 33.74, $H_3COCH_2\underline{C}H_2$; 46.88, $OCH_2CH_2\underline{C}H$; 58.53, $O\underline{C}H_3$; 70.47, $H_3CO\underline{C}H_2CH_2$; 114.52, $Me_3Si{-}\underline{C}H_2{-}CH{=}CH$; 130.01, 140.65, $Me_3Si{-}CH_2{-}CH{=}\underline{C}H{-}\underline{C}H$; 148.17, $Me_3Si{-}CH_2{-}C\underline{H}{=}CH$. **MS** GC/MS (m/z); 199 molecular ion + H^+.

8.4.7 Synthesis of donor-functionalised pentadienyl complex 6.1, [(tmeda)Li(L^8)]

A solution of **L^8**H (1.0 mmol, 0.297 g) in hexane (20 ml) was treated with ^{n}BuLi (1.0 mmol, 0.63 ml, 1.6 M) at −78 °C and left to stir for 15mins, then allowed to warm to room temperature, then left to stir for 1 hr to give a suspension of a yellow precipitate. The suspension was treated with tmeda (1.0mmol, 0.116g, 0.15ml) at room temperature to give an orange solution, and left to stir for 18 hrs. Volume reduced until precipitate crashes out of solution, the precipitate is heated back into solution and left to recrystallise at room temperature over 18 hrs, to give orange block crystals of **6.1** (0.16g, 38.5% yield). Anal. Calc. for $C_{22}H_{47}N_2OSi_2Li$, C 61.17, H 11.55, N 7.13; found C 61.05, H 11.37, N 7.08 %.**^{1}H NMR** spectrum (δ/ppm, 400.13 MHz, toluene-d_8, 300.0 K, *J*/Hz): −0.8, 0.15, hydrolysis product; 0.35, 18H, broad s, 2 × $SiMe_3$; 1.30, 2H, m; 1.50, 2H, m; 1.65, 4H, s, tmeda CH_2; 1.90, 12H, s, tmeda CH_3; 2.65, 2H, t; 3.05, 1H, q;

3.35, 2H, q; 4.45, 2H, q; 6.90, 2H, d, ^{3}J = 20 Hz, $Me_3SiCHC\underline{H}$. **^{13}C NMR** spectrum (δ/ppm, 100.61 MHz, toluene-d_8, 300.0 K, *J*/Hz): −1.59, 0.88, hydrolysis product; 1.93, broad d, $SiMe_3$; 25.81; 31.55; 33.89; 45.87 tmeda CH_3; 57.00 tmeda CH_2; 68.17; 82.18; 99.93, $Me_3SiCHC\underline{H}$; 151.19, broad d, $Me_3SiC\underline{H}CH$. **^{7}Li NMR** spectrum (δ/ppm, 155.51 MHz, toluene-d_8, 300.0 K): –0.64 ppm.

8.4.8 Synthesis of donor-functionalised pentadienyl complex 6.2, [(tmeda)Li(L^{9})]

A solution of **L^{9}**H (2.0mmol, 0.541g) in hexane (20ml) treated with ^{n}BuLi (2.0mmol, 1.25ml) at −78 °C and left to stir for 15 mins, then allowed to warm to room temperature, then left to stir for 1 hr to give a suspension of a yellow precipitate. The suspension was treated with tmeda (2.0mmol, 0.232g, 0.30ml) at room temperature to give an orange solution, and left to stir for 2 hrs. Solution filtered (P3, celite) and concentrated until precipitate crashes out of solution, the precipitate is heated back into solution and left to recrystallise at room temperature over 18 hrs, to afford orange block crystals of **6.2** (0.165g, 21.0% yield). Anal. Calc. for $C_{20}H_{45}N_2OSi_2Li$, C 63.10, H 11.31, N 6.69; found C 62.95, H 11.19, N 6.51 %. **^{1}H NMR** spectrum (δ/ppm, 400.13 MHz, toluene-d_8, 300.0 K, *J*/Hz): δ = 0.29, 18H, s, 2 × $SiMe_3$; 1.70, 4H, s, tmeda CH_2; 1.90, 12H, s, tmeda CH_3; 2.65, 2H, t, ^{3}J = 5.6, $C\underline{H}_2CH_2OMe$; 2.89, 3H, s, $OC\underline{H}_3$; 3.48, 2H, t, ^{3}J = 5.6, $CH_2C\underline{H}_2OMe$; 3.64, 2H, d, ^{3}J = 17.5, $Me_3SiC\underline{H}CH$; 6.80, 2H, d, ^{3}J = 17.5, $Me_3SiCHC\underline{H}$. **^{13}C NMR** spectrum (δ/ppm, 100.61 MHz, toluene-d_8, 300.0 K, *J*/Hz): 1.84, $SiMe_3$; 45.92 tmeda CH_3; 57.09 tmeda CH_2; 58.54 $O\underline{C}H_3$; 75.06, $\underline{C}H_2OMe$; 76.82 $Me_3Si\underline{C}H$; 99.45, $Me_3SiCHCH\underline{C}$; 150.99, $Me_3SiCH\underline{C}H$. **^{7}Li NMR** spectrum (δ/ppm, 155.51 MHz, toluene-d_8, 300.0 K): –0.77.

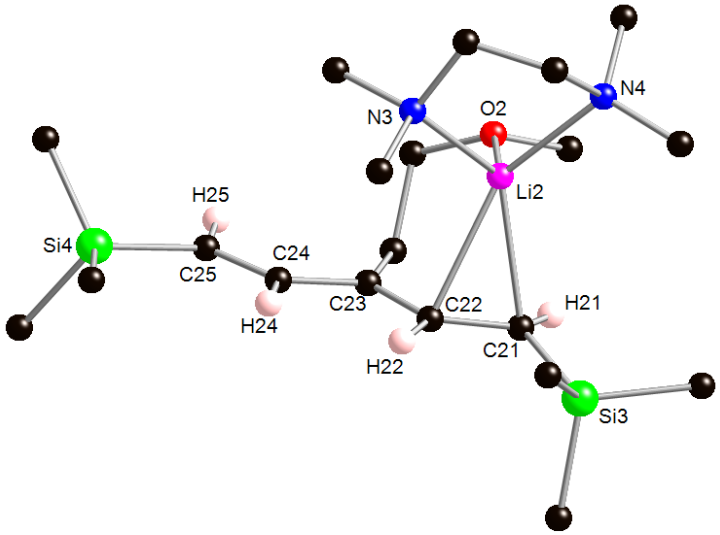

Figure 116: Molecular structure [(tmeda)Li{($SiMe_3$)C_5H_4($CH_2CH_2OCH_3$)}] (**6.2b**). Hydrogen atoms have been omitted for clarity apart from pentadienyl hydrogen atoms, carbon = black, silicon = bright green, oxygen = red, nitrogen = blue and hydrogen = light pink. C(21)−C(22) 1.393(3), C(22)−C(23) 1.403(3), C(23)−C(24) 1.423(3), C(24)−C(25) 1.365(3), Li(2)−C(21) 2.399(4), Li(2)−C(22) 2.427(5), Li(2)···C(23) 2.810, Li(2)−O(2) 1.990(4), Li(2)−N(3) 2.159(4), Li(2)−N(4) 2.161(4), C(21)−C(22)−C(23) 132.04(19), C(22)−C(23)−C(24) 119.48(18), C(23)−C(24)−C(25) 131.15(19).

8.5 Crystallographic details for compounds

Crystals were mounted on thin glass fibers using perfluoropolyether oil and frozen in situ in a flow of cold nitrogen gas from a Cryostream instrument. Data were collected using an Oxford Diffraction XCaliber 2 instrument (all compounds except **2.4** and **[4.5]**$_\infty$) or a Bruker AXS Diffractometer (compound **[4.5]**$_\infty$) using monochromated Mo Kα radiation (λ = 0.71073 Å) and Bruker-Nonius APEXII Diffractometer (compound **2.4**) at the Daresbury laboratories using the synchrotron source. Structures were solved using direct methods and refined on *F*2 using SHELXTL-97.[197] All non-hydrogen atoms were refined anisotropically for all structures. For **2.1**, [**4.1**]$_2$, [**4.2**]$_2$, [**4.5]**$_\infty$ and **4.6** the allylic hydrogen atoms were located directly in the electron peak difference maps and were allowed to refine freely. Also for complexes **6.1** and **6.2** the pentadienyl hydrogen atoms were located directly in the electron peak difference maps and were allowed to refine freely.

Crystal data and structure refinement for complex 2.1

Identification code	oral1	
Empirical formula	$C_{45}H_{96}Li_3N_6Si_4$	
Formula weight	854.46	
Temperature	100(2) K	
Wavelength	0.71069 Å	
Crystal system	Triclinic	
Space group	*P*-1	
Unit cell dimensions	a = 12.025(5) Å	α = 78.384(5)°.
	b = 14.431(5) Å	β = 87.499(5)°.
	c = 18.953(5) Å	γ = 65.960(5)°.
Volume	2939.5(18) $Å^3$	
Z	2	
Density (calculated)	0.965 Mg/m^3	
Absorption coefficient	0.132 mm^{-1}	
F(000)	946	
Crystal size	0.5 x 0.3 x 0.3 mm^3	
Theta range for data collection	3.71 to 28.28°.	
Index ranges	$-16 \leq h \leq 15$, $-19 \leq k \leq 19$, $-25 \leq l \leq 25$	
Reflections collected	37261	
Independent reflections	14095 [*R*(int) = 0.0281]	
Completeness to theta = 28.28°	96.7 %	
Absorption correction	Semi-empirical from equivalents	
Max. and min. transmission	1.00000 and 0.87959	
Refinement method	Full-matrix least-squares on F^2	
Data / restraints / parameters	14095 / 22 / 581	
Goodness-of-fit on F^2	1.067	
Final *R* indices [*I*>2sigma(*I*)]	*R*1 = 0.0656, *wR*2 = 0.1697	
R indices (all data)	*R*1 = 0.1131, *wR*2 = 0.2211	
Largest diff. peak and hole	1.379 and -0.554 e.$Å^{-3}$	

Crystal data and structure refinement for complex 2.2

Identification code	oral7tw	
Empirical formula	$C_{46}H_{108}Li_3N_9Si_4$	
Formula weight	920.59	
Temperature	100(2) K	
Wavelength	0.71073 Å	
Crystal system	Triclinic	
Space group	P-1	
Unit cell dimensions	a = 16.0060(8) Å	α = 86.404(4)°.
	b = 16.1880(9) Å	β = 86.051(4)°.
	c = 24.1430(12) Å	γ = 78.898(5)°.
Volume	6116.1(5) $Å^3$	
Z	4	
Density (calculated)	1.000 Mg/m^3	
Absorption coefficient	0.132 mm^{-1}	
F(000)	2048	
Crystal size	0.80 x 0.40 x 0.35 mm^3	
Theta range for data collection	3.74 to 25.03°.	
Index ranges	$-18 \leq h \leq 19$, $-19 \leq k \leq 19$, $-28 \leq l \leq 28$	
Reflections collected	21473	
Independent reflections	21473 [*R*(int) = 0.0000]	
Completeness to theta = 25.03°	99.3 %	
Absorption correction	Semi-empirical from equivalents	
Max. and min. transmission	1.00000 and 0.78158	
Refinement method	Full-matrix least-squares on F^2	
Data / restraints / parameters	21473 / 0 / 1186	
Goodness-of-fit on F^2	1.114	
Final R indices [*I*>2sigma(*I*)]	*R*1 = 0.0934, *wR*2 = 0.2341	
R indices (all data)	*R*1 = 0.1167, *wR*2 = 0.2451	
Largest diff. peak and hole	0.760 and -0.538 e.$Å^{-3}$	

Crystal data and structure refinement for complex 2.3

Identification code	oral30	
Empirical formula	C37 H87 N6 Na3 Si4	
Formula weight	797.46	
Temperature	100(2) K	
Wavelength	0.71069 Å	
Crystal system	Monoclinic	
Space group	P2(1)/n	
Unit cell dimensions	a = 11.352(5) Å	α = 90.000(5)°.
	b = 41.690(5) Å	β = 105.088(5)°.
	c = 11.407(5) Å	γ = 90.000(5)°.
Volume	5212(3) $Å^3$	
Z	4	
Density (calculated)	1.016 Mg/m^3	
Absorption coefficient	0.168 mm^{-1}	
F(000)	1760	
Crystal size	0.30 x 0.20 x 0.20 mm^3	
Theta range for data collection	3.72 to 23.25°.	
Index ranges	-10<=h<=12, -33<=k<=46, -12<=l<=9	
Reflections collected	14309	
Independent reflections	7448 [R(int) = 0.0832]	
Completeness to theta = 23.25°	99.5 %	
Absorption correction	Semi-empirical from equivalents	
Max. and min. transmission	0.9672 and 0.9514	
Refinement method	Full-matrix least-squares on F^2	
Data / restraints / parameters	7448 / 153 / 519	
Goodness-of-fit on F^2	1.102	
Final R indices [I>2sigma(I)]	R1 = 0.1038, wR2 = 0.1833	
R indices (all data)	R1 = 0.1638, wR2 = 0.1986	
Extinction coefficient	0.0009(3)	
Largest diff. peak and hole	0.541 and -0.331 $e.Å^{-3}$	

Crystal data and structure refinement for complex $[2.4]_2$

Identification code	p21n	
Empirical formula	$C_{72}H_{146}N_8Na_6Si_8$	
Formula weight	1486.63	
Temperature	296(2) K	
Wavelength	0.69420 Å	
Crystal system	Monoclinic	
Space group	*P2*(1)/*n*	
Unit cell dimensions	a = 12.8897(8) Å	α = 90°.
	b = 15.1365(9) Å	β = 94.1500(10)°.
	c = 24.2992(14) Å	γ = 90°.
Volume	4728.5(5) $Å^3$	
Z	2	
Density (calculated)	1.044 Mg/m^3	
Absorption coefficient	0.180 mm^{-1}	
F(000)	1624	
Crystal size	0.13 x 0.13 x 0.05 mm^3	
Theta range for data collection	3.51 to 25.00°.	
Index ranges	$-15 \leq h \leq 15$, $-18 \leq k \leq 18$, $-29 \leq l \leq 29$	
Reflections collected	37930	
Independent reflections	8876 [*R*(int) = 0.0545]	
Completeness to theta = 25.00°	99.1 %	
Absorption correction	Semi-empirical from equivalents	
Max. and min. transmission	0.9911 and 0.9770	
Refinement method	Full-matrix least-squares on F^2	
Data / restraints / parameters	8876 / 12 / 470	
Goodness-of-fit on F^2	1.100	
Final R indices [*I*>2sigma(*I*)]	*R*1 = 0.0867, *wR*2 = 0.2362	
R indices (all data)	*R*1 = 0.1085, *wR*2 = 0.2524	
Largest diff. peak and hole	1.408 and -0.770 e.$Å^{-3}$	

Crystal data and structure refinement for complex $[2.5]_2$

Identification code	oral5	
Empirical formula	$C_{78}H_{176}K_6Li_2O_{10}Si_8$	
Formula weight	1747.39	
Temperature	100(2) K	
Wavelength	0.71073 Å	
Crystal system	Monclinic	
Space group	*P2*(1)*/n*	
Unit cell dimensions	a = 10.4657(17) Å	α = 90°.
	b = 30.656(4) Å	β = 101.553(13)°.
	c = 17.2525(19) Å	γ = 90°.
Volume	5423.1(12) $Å^3$	
Z	2	
Density (calculated)	1.070 Mg/m^3	
Absorption coefficient	0.373 mm^{-1}	
F(000)	1912	
Crystal size	0.20 x 0.10 x 0.10 mm^3	
Theta range for data collection	4.11 to 25.35°.	
Index ranges	$-12 \le h \le 12$, $-36 \le k \le 31$, $-20 \le l \le 20$	
Reflections collected	31107	
Independent reflections	9856 [*R*(int) = 0.0629]	
Completeness to theta = 25.35°	99.2 %	
Max. and min. transmission	0.9636 and 0.9291	
Refinement method	Full-matrix least-squares on F^2	
Data / restraints / parameters	9856 / 0 / 523	
Goodness-of-fit on F^2	1.305	
Final *R* indices [*I*>2sigma(*I*)]	*R*1 = 0.0996, *wR*2 = 0.1855	
R indices (all data)	*R*1 = 0.1307, *wR*2 = 0.1952	
Largest diff. peak and hole	1.027 and -0.563 $e.Å^{-3}$	

Crystal data and structure refinement for complex $[4.1]_2$

Identification code	oral3	
Empirical formula	$C_{28}H_{58}Li_2O_2Si_4$	
Formula weight	552.98	
Temperature	100(2) K	
Wavelength	0.71073 Å	
Crystal system	Triclinic	
Space group	P-1	
Unit cell dimensions	a = 10.1331(8) Å	α = 77.614(7)°.
	b = 10.8060(9) Å	β = 89.490(6)°.
	c = 18.5116(14) Å	γ = 65.099(8)°.
Volume	1788.2(2) $Å^3$	
Z	2	
Density (calculated)	1.027 Mg/m^3	
Absorption coefficient	0.187 mm^{-1}	
F(000)	608	
Crystal size	0.70 x 0.70 x 0.50 mm^3	
Theta range for data collection	2.72 to 28.35°.	
Index ranges	$-13 \leq h \leq 13$, $-13 \leq k \leq 13$, $-24 \leq l \leq 23$	
Reflections collected	15193	
Independent reflections	7883 [*R*(int) = 0.0378]	
Completeness to theta = 28.35°	88.1 %	
Absorption correction	Semi-empirical from equivalents	
Max. and min. transmission	0.9125 and 0.8805	
Refinement method	Full-matrix least-squares on F^2	
Data / restraints / parameters	7883 / 0 / 353	
Goodness-of-fit on F^2	1.036	
Final *R* indices [*I*>2sigma(*I*)]	*R*1 = 0.0599, *wR*2 = 0.1542	
R indices (all data)	*R*1 = 0.0992, *wR*2 = 0.1893	
Extinction coefficient	0	
Largest diff. peak and hole	0.894 and -0.487 e.$Å^{-3}$	

Crystal data and structure refinement for complex $[4.2]_2$

Identification code	p-1(13)	
Empirical formula	$C_{24}H_{54}Li_2O_2Si_4$	
Formula weight	500.91	
Temperature	100(2) K	
Wavelength	0.71073 Å	
Crystal system	Triclinic	
Space group	*P -1*	
Unit cell dimensions	a = 9.3990(11) Å	α = 102.277(17)°.
	b = 10.934(2) Å	β = 91.521(13)°.
	c = 18.150(4) Å	γ = 112.784(15)°.
Volume	1668.1(5) $Å^3$	
Z	2	
Density (calculated)	0.997 Mg/m^3	
Absorption coefficient	0.194 mm^{-1}	
F(000)	552	
Crystal size	0.60 x 0.60 x 0.60 mm^3	
Theta range for data collection	3.73 to 26.37°.	
Index ranges	$-11 \leq h \leq 11$, $-13 \leq k \leq 13$, $-22 \leq l \leq 21$	
Reflections collected	14579	
Independent reflections	6784 [*R*(int) = 0.0332]	
Completeness to theta = 26.37°	99.5 %	
Absorption correction	Semi-empirical from equivalents	
Max. and min. transmission	0.8924 and 0.8924	
Refinement method	Full-matrix least-squares on F^2	
Data / restraints / parameters	6784 / 0 / 315	
Goodness-of-fit on F^2	1.115	
Final *R* indices [*I*>2sigma(*I*)]	*R*1 = 0.0761, *wR*2 = 0.2177	
R indices (all data)	*R*1 = 0.0964, *wR*2 = 0.2264	
Extinction coefficient	0	
Largest diff. peak and hole	1.555 and -0.413 e.$Å^{-3}$	

Crystal data and structure refinement for complex [4.5·thf]$_\infty$

Identification code	bral1abs	
Empirical formula	$C_{36}H_{74}K_2O_4Si_4$	
Formula weight	761.51	
Temperature	100(2) K	
Wavelength	0.71073 Å	
Crystal system	Monoclinic	
Space group	*P2*(1)	
Unit cell dimensions	a = 10.9205(18) Å	α = 90°.
	b = 18.729(3) Å	β = 97.988(3)°.
	c = 11.2860(18) Å	γ = 90°.
Volume	2285.9(6) Å^3	
Z	2	
Density (calculated)	1.106 Mg/m^3	
Absorption coefficient	0.344 mm^{-1}	
F(000)	832	
Crystal size	1.00 x 0.20 x 0.20 mm^3	
Theta range for data collection	1.82 to 28.30°.	
Index ranges	$-14 \le h \le 14$, $-21 \le k \le 24$, $-14 \le l \le 14$	
Reflections collected	14374	
Independent reflections	8085 [*R*(int) = 0.0285]	
Completeness to theta = 28.30°	93.8 %	
Absorption correction	Semi-empirical from equivalents	
Max. and min. transmission	0.9344 and 0.7249	
Refinement method	Full-matrix least-squares on F^2	
Data / restraints / parameters	8085 / 81 / 471	
Goodness-of-fit on F^2	1.036	
Final *R* indices [*I*>2sigma(*I*)]	*R*1 = 0.0501, *wR*2 = 0.1176	
R indices (all data)	*R*1 = 0.0615, *wR*2 = 0.1239	
Absolute structure parameter	0.04(4)	
Largest diff. peak and hole	0.633 and -0.528 e.Å^{-3}	

Crystal data and structure refinement for complex 4.6

Identification code	test	
Empirical formula	$C_{28}H_{58}MgO_2Si_4$	
Formula weight	563.41	
Temperature	100(2) K	
Wavelength	0.71069 Å	
Crystal system	Orthorhombic	
Space group	*P c c n*	
Unit cell dimensions	a = 12.043(5) Å	α = 90.000(5)°.
	b = 15.161(5) Å	β = 90.000(5)°.
	c = 19.417(5) Å	γ = 90.000(5)°.
Volume	3545(2) $Å^3$	
Z	4	
Density (calculated)	1.056 Mg/m^3	
Absorption coefficient	0.206 mm^{-1}	
F(000)	1240	
Crystal size	0.8 x 0.1 x 0.1 mm^3	
Theta range for data collection	4.20 to 25.02°.	
Index ranges	$-14 \leq h \leq 13, -17 \leq k \leq 17, -23 \leq l \leq 14$	
Reflections collected	11758	
Independent reflections	3117 [*R*(int) = 0.1088]	
Completeness to theta = 25.02°	99.4 %	
Absorption correction	Semi-empirical from equivalents	
Max. and min. transmission	1.00000 and 0.75442	
Refinement method	Full-matrix least-squares on F^2	
Data / restraints / parameters	3117 / 0 / 171	
Goodness-of-fit on F^2	0.915	
Final *R* indices [*I*>2sigma(*I*)]	*R*1 = 0.0570, *wR*2 = 0.0878	
R indices (all data)	*R*1 = 0.1346, *wR*2 = 0.1104	
Extinction coefficient	0	
Largest diff. peak and hole	0.352 and -0.283 e.$Å^{-3}$	

Crystal data and structure refinement for complex 6.1

Identification code	oral84	
Empirical formula	C22 H47 Li N2 O Si2	
Formula weight	418.74	
Temperature	100(2) K	
Wavelength	0.71073 Å	
Crystal system	Monoclinic	
Space group	P2(1)/n	
Unit cell dimensions	a = 8.6480(6) Å	α = 90°.
	b = 17.1486(11) Å	β = 102.973(7)°.
	c = 19.0524(13) Å	γ = 90°.
Volume	2753.4(3) $Å^3$	
Z	4	
Density (calculated)	1.010 Mg/m^3	
Absorption coefficient	0.142 mm^{-1}	
F(000)	928	
Crystal size	0.40 x 0.10 x 0.05 mm^3	
Theta range for data collection	3.11 to 26.37°.	
Index ranges	-10<=h<=10, -21<=k<=16, -23<=l<=23	
Reflections collected	18716	
Independent reflections	5613 [R(int) = 0.0931]	
Completeness to theta = 26.37°	99.8 %	
Absorption correction	Semi-empirical from equivalents	
Max. and min. transmission	0.9929 and 0.9454	
Refinement method	Full-matrix least-squares on F^2	
Data / restraints / parameters	5613 / 0 / 441	
Goodness-of-fit on F^2	0.665	
Final R indices [I>2sigma(I)]	R1 = 0.0429, wR2 = 0.0773	
R indices (all data)	R1 = 0.1209, wR2 = 0.0940	
Largest diff. peak and hole	0.257 and -0.223 $e.Å^{-3}$	

Crystal data and structure refinement for complex 6.2

Identification code	oral88	
Empirical formula	C20 H45 Li N2 O Si2	
Formula weight	392.70	
Temperature	100(2) K	
Wavelength	0.71073 Å	
Crystal system	Monoclinic	
Space group	P2(1)/c	
Unit cell dimensions	a = 17.4496(6) Å	α = 90 deg.
	b = 17.7496(11) Å	β = 101.374(4) deg.
	c = 17.2174(7) Å	γ = 90 deg.
Volume	5227.9(4) $Å^3$	
Z	8	
Density (calculated)	0.998 Mg/m^3	
Absorption coefficient	0.146 mm^{-1}	
F(000)	1744	
Crystal size	0.50 x 0.15 x 0.15 mm^3	
Theta range for data collection	3.04 to 28.42°.	
Index ranges	-22<=h<=21, -17<=k<=23, 21<=l<=22	
Reflections collected	22053	
Independent reflections	11675 [R(int) = 0.0535]	
Completeness to theta = 27.00°	99.8 %	
Absorption correction	Semi-empirical from equivalents	
Max. and min. transmission	0.9784 and 0.9305	
Refinement method	Full-matrix least-squares on F^2	
Data / restraints / parameters	11675 / 30 / 513	
Goodness-of-fit on F^2	1.061	
Final R indices [I>2sigma(I)]	R1 = 0.0634, wR2 = 0.1613	
R indices (all data)	R1 = 0.0820, wR2 = 0.1788	
Largest diff. peak and hole	1.411 and -0.585 $e.Å^{-3}$	

References

[1] G. Wilke, *Angew. Chem. Int. Ed. Engl.*, **1963**, *2*, 105

[2] G. Wilke, B. Bogdanovis, P. Hardt, P. Heimbach, W. Keim, M. Kröner, W. Oberkirch, K. Tanaka, E. Steinrücke, D. Walter and H. Zimmerman, *Angew. Chem. Int. Ed. Engl.*, **1966**, *5*, 151

[3] Y. Yamamoto and N Asao, *Chem. Rev.* **1993**, 2207

[4] L. Chabaub, P. James and Y. Landais, *Eur. J. Org. Chem.*, **2004**, 3173

[5] S. A. Solomon and R. A. Layfield, *Dalton Trans.*, **2010**, *39*, 2469

[6] S. C. Chmely and T. P. Hanusa, *Eur. J. Inorg. Chem.*, **2010**, 1321

[7] G. Fraenkel and F. Qiu, *J. Am. Chem. Soc.*, **1996**, *118*, 5828

[8] G. Fraenkel and F. Qiu, *J. Am. Chem. Soc.*, **1997**, *119*, 3571

[9] G. Fraenkel, X. Chen, J. Gallucci and Y. Ren, *J. Am. Chem. Soc.*, **2008**, *130*, 4140

[10] T. Clark, C. Rohde and P. von R.Schleyer, *Organometallics*, **1983**, *2*, 1344

[11] N. J. R. van E. Hommes, M. Bühl and P. von R. Schleyer, *J.Organomet. Chem.* **1991**, *409*, 307

[12] W. R. Winchester, W. Bauer and P. von R. Schleyer, *J. Chem. Soc. Chem. Commun.*, **1987**, 177

[13] H. Koester and E. Weiss, *Chem. Ber.*, **1982**, *115*, 3422

[14] G. Boche, H. Etzrodt, M. Marsch, W. Massa, G.Baum, H. Dietrich and W. Mahdi, *Angew. Chem. Int. Ed. Engl.*, **1986**, *25*, 104

[15] U. Schümann and E. Weiss, *J. Organomet. Chem.*, **1987**, *322*, 299

[16] G. Fraenkel and W. R. Winchester, *Organometallics*, **1990**, *9*, 1314

[17] G. Fraenkel, A. Chow and W. R. Winchester, *J. Am. Chem. Soc.*, **1990**, *112*, 1382

[18] G. Fraenkel, A. Chow and W. R. Winchester, *J. Am. Chem. Soc.*, **1990**, *112*, 2582

[19] G. Boche, G. Fraenkel, J. Cabral, K. Harms, N. J. R. van E. Hommes, J. Lohrenz, M. Marsch and P. von R. Schleyer, *J. Am. Chem. Soc.*, **1992**, *114*, 1562

[20] C. Präsang, Y. Sahin, M. Hofmann, G. Geiseler, W. Massa and A. Berndt, *Eur. J. Inorg. Chem.*, **2004**, 3063

[21] K. T. Quisenberry, C. K. Gren, R. E. White, T. P. Hanusa, and W. W. Brennessel, *Organometallics*, **2007**, *26*, 4354

[22] P. Jutzi and N. Burford, *Chem. Rev.*, **1999**, *99*, 969

[23] C. K. Simpson, R. E. White, C. N. Carlson, D. A. Wrobleski, C. J. Kuehl, T. A Croce, I. M. Steele, B. L. Scott, V. G. Young, Jr., T. P. Hanusa, A. P. Sattelberger and K. D. John, *Organometallics*, **2005**, *24*, 3685

[24] C. K. Gren, T. P. Hanusa and A. L. Rheingold, *Main Group Chemistry*, **2009**, *8*, 225

[25] H. Bock, K. Ruppert, Z. Havlas and D. Fenske, *Angew. Chem. Int., Ed. Engl.*, **1990**, *29*, 1042

[26] S. Corbelin, J. Kopf, N. P. Lorenzen and E. Weiss, *Angew. Chem. Int. Ed. Engl.*, **1991**, *30*, 825

[27] C. H. McMillen, C. K. Gren, T. P. Hanusa and A. L. Rheingold, *Inorg. Chim. Acta.*, **2010**, *364*, 61

[28] R. Fernández-Galán, P. B. Hitchcock, M. F. Lappert, A. Antiñolo and A. M. Rodríguez, *J. Chem. Soc., Dalton Trans.*, **2000**, 1743

[29] P. B. Hitchcock, M. F. Lappert, W.-P. Leung, D.-S. Liu, T. C. W. Mak and Z.-X. Wang, *J. Chem. Soc., Dalton Trans.*, **1999**, 1257
[30] R. A. Layfield, F. García, J. Hannauer, and S. M. Humphrey, *Chem. Commun.*, **2007**, 5081
[31] M. Marsch, K. Harms, W. Massa and G. Boche, *Angew. Chem. Int. Ed. Engl.*, **1987**, *26*, 696
[32] P. J. Bailey, S. T. Liddle, C. A. Morrison and S. Parsons, *Angew, Chem. Int. Ed. Engl.*, **2001**, *40*, 4463
[33] L. F. Sánchez-Barba, D. L. Hughes, S. M. Humphrey and M. Bochmann, *Organometallics*, **2005**, *24*, 5329
[34] L. F. Sánchez-Barba, D. L. Hughes, S. M. Humphrey and M. Bochmann, *Organometallics*, **2006**, *25*, 1012
[35] H. E. Zieger and J. D. Roberts, *J. Org. Chem.*, **1969**, *34*, 1976
[36] S. C. Chmely, C. N. Carlson, T. P. Hanusa and A. L Rheingold, *J. Am. Chem. Soc.*, **2009**, *131*, 6344
[37] M. J. Harvey, T. P. Hanusa and V. G. Young, Jr., *Angew. Chem. Int. Ed.*, **1999**, *38*, 217
[38] F. H. Allan, *Acta. Crystallogr., Sect B: Struct. Sci*., **2002**, *58*, 380
[39] P. Jochmann, T. S. Dols, T. P. Spaniol, L. Perrin, L. Maron and J. Okuda, *Angew. Chem. Int. Ed.*, **2009**, *48*, 5715
[40] W.G. Wiegand and K.-H.Thiele, *Z. Anorg. Allg. Chem.*, **1974**, *405*, 101
[41] S. C. Chmely, T. P. Hanusa and W. W. Brennessel, *Angew. Chem. Int. Ed.*, **2010**, *49*, 5870
[42] K. T. Quisenberry, R. E. White, T. P. Hanusa and W. W. Brennessel, *New J. Chem.*, **2010**, *34*, 1579
[43] M. J. Harvey, K. T. Quisenberry, T. P. Hanusa and V. G. Young, Jr., *Eur. J. Inorg. Chem.*, **2003**, 3383
[44] R. A. Williams, T. P. Hanusa and J. C. Huffman, *Organometallics*, **1990**, *9*, 1128
[45] G. B. Deacon, C. M. Forsyth, F. Jaroschik, P. C. Junk, D. L. Kay, T. Maschmeyer, A. F. Masters, J. Wang and L. D. Field, *Organometallics*, **2008**, *27*, 4772
[46] T. J. Woodman, M. Schormann, D. L. Hughes and M. Bochmann, *Organometallics*, **2004**, *23*, 2972
[47] R. Taube, H. Windisch, S. Maiwald, H.Hemling and H. Schumann, *J. Organomet. Chem.*, **1996**, *14*, 49
[48] R. Taube, H. Windisch and S. Maiwald, *Macromol. Symp.*, **1995**, *89*, 393
[49] C. J. Kuehl, C. K. Simpson, K. D. John, A. P. Sattelberger, C. N. Carlson and T. P. Hanusa, *J. Organomet. Chem*, **2003**, *683*, 149
[50] T. J. Woodman, M. Schormann andM. Bochmann, *Isr. J. Chem.*, **2002**, *42*, 283
[51] S. Maiwald, R. Taube, H. Hemling and H. Schumann, *J. Organomet. Chem.*, **1998**, *552*, 195
[52] T. J. Woodmann, M. Schormann, D. L. Hughes and M. Bochmann, *Organometallics*, **2003**, *22*, 3028
[53] C. K. Simpson, R. E. White, C. N. Carlson, D. A. Wrobleski, C. J. Kuehl, T.A. Croce, I. M. Steel, B. L. Scott, V. G. Young, Jr., T. P. Hanusa, A. P. Sattelberger and K. D. John, *Organometallics*, **2005**, *24*, 3685

[54] R. E. White, T. P. Hanusa and B. E. Kucera, *J. Organomet. Chem.*, **2007**, *692*, 3479
[55] T. J. Woodman, M. Schormann, D. L. Hughes and M. Bochmann, *Organometallics,* **2004**, *23*, 2972
[56] T. J. Woodman, M. Schormann and M. Bochmann, *Organometallics,* **2003**, *22*, 2938
[57] C. N. Carlson, T. P. Hanusa and W. W. Brennessel, *J. Am. Chem. Soc.*, 2004, **126**, 10550
[58] K.H. Pannell, M. F. Lappert and K. Stanley, *J. Organomet. Chem.*, **1976**, *112*, 37
[59] M. Schormann, S. Garratt and M. Bochmann, *Organometallics.*, **2005**, *24*, 1718
[60] T. J. Woodman, Y. Sarazin, S. Garratt, G. Fink and M. Bochmann, *J. Mol. Catal. A: Chem.*, **2005**, *235*, 88
[61] J. D. Smith, T. P. Hanusa an V. G. Young, Jr., *J. Am. Chem. Soc.*, **2001**, *123,* 6455
[62] C. N. Carlson, J. D. Smith, T. P. Hanusa, W. W. Brennessel and V. G. Young, Jr., *J. Organomet. Chem.*, **2003**, *683*, 191
[63] J. D. Smith, K. T. Quisenberry, T. P. Hanusa and W. W. Brennessel, *Acta. Cryst.*, **2004**, *C60*, m507
[64] K. T. Quisenberry, J. D. Smith, M. Voehler, D. F. Stec, T. P. Hanusa and W. W. Brennessel, *J. Am. Chem. Soc.,* **2005**, *127,* 4376
[65] P. W. Jolly, C. Krueger and U. Zakrewski, *J. Organomet. Chem*, **1991**, *412*, 317
[66] T. P. Hanusa and C. N. Carlson, in *Encylopedia of Inorganic Chemistry II*, (ed.), Wiley, New York, **2005**, *9*, 5690
[67] R. A. Layfield and S. M. Humphrey, *Angew. Chem. Int. Ed. Engl*, **2004**, *43*, 3067.
[68] R. A. Layfield, M. Bühl and J. M. Rawson, *Organometallics,* **2006**, *25*, 3570.
[69] B. Ray, G. Neyroud, M. Kapon, Y. Eichen and M. S. Eisen, *Organometallics,* **2001**, *20*, 3044
[70] A. M. Arif, R. D. Ernst, E. Meléndez, A. L. Rheingold and T. E. Waldman, *Organometallics*, **1995**, *14*, 1761
[71] C. K. Gren, T. P. Hanusa and W. W. Brennessek, *Polyhedron*, **2006**, *25*, 286
[72] C. K. Gren, T. P. Hanusa and A. L. Rheingold, *Organometallics,* **2007**, *26*, 1643
[73] S. A. Sulway, R. Girshfeld, S. A. Solomon, C. A. Muryn, J. Poater, M. Solà, F. M. Bickelhaupt and R. A. Layfield, *Eur. J. Inorg. Chem.*, **2009**, 4157
[74] F. H. Allen, *Acta Crystallogr., Sect. B*, **2002**, *58*, 380
[75] J. C. Amicangello and P. B. Armentrout, *J. Phys. Chem. A.*, **2000**, *104*, 11420
[76] W. Clegg, A. M. Drummond, S. T. Liddle, R. E. Mulvey and A. Robertson, *Chem. Commun.*, **1999**, 1569
[77] U. Siemeling, *Chem. Rev.*, **2000**, *100*, 1495
[78] P. Jutzi and J. Dahlhaus, *Coord. Chem. Rev.*, **1994**, *137*, 179
[79] P. Jutzi and U. Siemeling, *J. Organomet. Chem.*, **1995**, *500*, 175
[80] M. Schlosser and F. Franzini, *Synthesis*, **1998**, 707
[81] T. H. Chan and D. Labrecque, *Tetrahedron*, **1992**, *33*, 7997
[82] G. Fraenkel, J. H. Duncan and J. Wang, *J. Am. Chem. Soc.*, **1999**, *121*, 432
[83] G. Fraenkel, A. Chow, R. Fleischer and H. Liu, *J. Am. Chem. Soc.*, **2004**, *126*, 3983
[84] G. Fraenkel and J. A. Cabral, *J. Am. Chem. Soc.*, **1993**, *115*, 1551
[85] C Strohmann, H. Lehman and S. Dilsky, *J. Am. Chem. Soc.*, **2006**, *128*, 8102
[86] N. J. Long, Metallocenes, Blackwell Science, Inc., Malden, MA, 1998
[87] A. L. McKnight and R. M. Waymouth, *Chem. Rev.*, **1998**, *98*, 2587

[88] G. Erker, G. Kehr and R. Fröhlich, *Organometallics*, **2008**, *27*, 3

[89] S. Zhang and J. Liu, *Polyhedron*, **1993**, *12*, 2771

[90] U. Siemeling, *J. Chem. Soc., Chem. Commun.*, **1992**, 1335

[91] U. Siemeling, B Neumann and H.-G. Stammler, *Chem. Ber*, **1993**, *126*, 1335

[92] T.-F. Wang, T.-Y. Lee, J.-W. Chou and C.-W Ong, *J. Organomet. Chem.*, **1992**, *423*, 31

[93] W. A. Herrmann, R. Anwander, F. F. Munck and W. Scherer, *Chem. Ber*, **1993**, *126*, 331

[94] R. G. Pearson, *J. Am. Chem. Soc.*, **1963**, *85*, 3533

[95] J. C. Röder, F. Meyer and H. Pritzkow, *Organometallics*, **2001**, *20*, 811

[96] P. Jutzi, J. Kleimeier, T. Redeker H.-G. Stammler and B. Neumann, *J. Orgnomet. Chem.*, **1995**, *498*, 85

[97] M. G. Gardiner and C. L. Raston, *Organometallics*, **1991**, *10*, 3680

[98] M. L. Hays, T. P. Hanusa, and T. A. Nile, *J. Organomet. Chem*, **1996**, *514*, 73

[99] G. A. Molander, H. Schumann, E. C. E. Rosenthak and J. Demtschuk, *Organometallis*, **1996**, *15*, 3817

[100] A. Hammel, W. Schwarz and J. Weidlein, *J. Organomet. Chem.* **1989**, *378*, 347

[101] M. Westerhausen, M. Hartmenn, N. Makropoulos, B. Wieneke, M. Wieneke, W. Schwarz and D. Stalke, *Z. Naturforsch., B.*, **1998**, *53*, 117

[102] W. R. Rees, Jr., U. W. Lay and K. A. Dippel, *J. Organomet. Chem.*, **1994**, *438*, 27

[103] U. Siemeling, *Polyhedron*, **1997**, *16*, 1513

[104] D. Deng, B. Li and C. Qian, *Polyhedron*, **1990**, *9*, 1453

[105] D. Deng, X. Zheng, C. Qian, J. Sun, A. Dormond, D. Baudry and M. Visseaux, *J. Chem. Soc., Dalton Trans.*, **1994**, 1664

[106] D. Deng, C. Qian, F. Song, Z. Wang, G. Wu and P. Zheng, *J. Organomet. Chem.*, **1993**, *443*, 79

[107] C. Qian, B. Wang, D. Deng, J. Hu, J. Chen, G. Wu and P. Zheng, *Inorg Chem*, **1994**, *33*, 3382

[108] R. D. Rogers, J. L. Atwood, A. Emad, D. J. Sikora and M. D. Rausch, *J. Organomet. Chem.*, **1981**, *216*, 383

[109] S. H. Eggers, J. Kopf and R. D. Fischer, *Organometallics*, **1986**, *5*, 383

[110] W. Lamberts and H. Lueken, *Inorg. Chim. Acta.*, **1987**, *132*, 119

[111] Z. Ye, S. Wang and Y. Yu, *Inorg. Chim. Acta.*, **1990**, *177*, 97

[112] J. Holton, M. F. Lappert, D. G. H. Ballard, R. Pearce, J. L. Atwood and W. E. Hunter, *J. Chem. Soc., Dalton Trans.*, **1979**, 54

[113] C. Qian, C. Ye, H. Lu, Y. Li and Y. Huang, *J. Organomet*. Chem., **1984**, *263*, 333

[114] W. A. Herrmann, R. Anwander, F. C. Munck and W. Scherer, *Chem. Ber.* , **1993**, *126*, 331

[115] F. Benetello, G. Bombieri, C. Bisi Castellani, W. Jahn and R. D. Fischer, *Inorg. Chim. Acta.*, **1985**, *110*, L7

[116] G. B. Deacon, B. M. Gatehouse, S. N. Platts and D. L. Wilkinson, *Aust. J. Chem.*, **1987**, *40*, 907

[117] H. Schumann, E.C.E. Rosenthal, J. Demtschuk and G. A. Molander, *Orgnometallics*, **1998**, *17*, 5324

[118] H. Schumann, F. Erbstein, D. F. Karasiak, I. L. Fedushkin, J. Demtschuk, and F. Girgdies, *Z. Anorg. Allg. Chem.*, **1999**, *625*, 781
[119] K. P. Krut'ko, *Russ. Chem. Bull., Int. Ed.*, **2009**, *58*, 1745
[120] G. Trouvé, D. A. Laske, A. Meetsma and J. H. Teuben, *J. Organomet. Chem.*, **1996**, *511*, 255
[121] A. A. H. van der Zeijden, C. Mattheis and R. Fröhlich, *Organometallics*, **1997**, *16*, 2651
[122] A. A. H. van der Zeijden, C. Mattheis and R. Fröhlich, *Acta. Cryst.*, **1998**, *C54*, 458
[123] D. P. Krut'ko, M. V. Borzov, R. S. Kirsanov, A. V. Churakov and L. G. Kuz'mina, *J. Organomet. Chem.*
[124] L. F. Braun, T. Dreier, M. Christy and J. L. Petersen, *Inorg. Chem.*, **2004**, *43*, 3976
[125] D. P. Krut'Ko, M. V. Borzov, E. N. Veksler, A. V. Churakov and A. K. Howard, *Polyhedron*, **1998**, *17*, 3889
[126] D. P. Krut'Ko, M. V. Borzov, E. N. Veksler, A. V. Churakov and L. G. Kuz'mina, *J. Organomet. Chem.*, **2005**, *690*, 4036
[127] F. Amor, K. E. Plooy, T. P. Spaniol and J. Okuda, *J. Organomet. Chem.*, **1998**, *558*, 139
[128] T.-F. Wang, T.-Y. Lee, J.-W. Chou and C.-W. Ong, *J. Organomet. Chem.*, **1992**, *423*, 31
[129] Z. Pang, R. F. Johnston and D. G. VanDerveer, *J. Organomet., Chem.* **1996**, *526*, 25
[130] P. Jutzi, M. O. Kristen, J. Dahlhaus, B. Neumann and H.-G. Stammler, *Organometallics*, **1993**, *12*, 2980
[131] P. Jutzi, M. O. Kristen, B. Neumann and H.-G. Stammler, *Organometallics*, **1994**, *13*, 3854
[132] P. Jutzi, T. Redeker, B. Neumann, H-G Stammler, *J. Organomet. Chem.*, **1995**, *498*, 127
[133] P. Jutzi and J. Dahlhaus, *Phosphorus, Sulphur and Silicon*, **1994**, *87*, 73
[134] A. Kunicki, R. Sadowski and J. Zachara, *J. Organomet. Chem.*, **1996**, *508*, 249
[135] D. F. Grant, R. C. G. Killean and L. J. Lawrence, *Acta. Crystallogr., Sect. B.*, **1969**, *25*, 377
[136] T. E. Bitterwolf, K. A. Lott and A. J. Rest, *J. Organomet. Chem.*, **1991**, *408*, 137
[137] P. Jutzi, H. Schmedt, B. Neumann and H.-G. Stammler, *J. Organomet. Chem.*, **1995**, *499*, 7
[138] N. Feeder, A. D. Hopkins, R. A. Layfield and D. S. Wright, *J. Chem. Soc., Dalton Trans.*, **2000**, 2247
[139] P. Jutzi, A. Becker, C. Leue, H.-G.Stammler, B. Neumann, M. B. Hursthouse and A. Karaulov, *Organometallics*, **1995**, *499*, 7
[140] G. Schultz, J. Tremmel, I. Hargittai, I. Berecz, S. Bohatka, N. D. Kagramanov, A. K. Maltsev and O. M. Nefedov, *J. Mol. Struct. Chem.*, **1979**, *11*, 61
[141] L. Fernholt, A. Haaland, P. Jutzi, F. X. Kohl and R. Seip, *Acta Chem. Scand., Ser. A.*, **1984**, *38*, 211
[142] J. Clayden, N. Greeves, s. Warren and P. Wothers, *Organic Chemistry*, Oxford University Press, Oxford, New York, 2001
[143] R. D. Ernst, *Chem. Rev.*, **1988**, *88*, 1255
[144] R. D. Ernst, *Comm. Inorg. Chem.*, **1999**, *21*, 285

[145] R. B. Bates, S. Brenner, C. M. Cole, E. W. Davidson, G. D. Forsythe, D. A. McCombs and A. S. Roth, *J. Am. Chem. Soc.*, **1973**, *95*, 926

[146] W. T. Ford and Martin Newcomb, *J. Am. Chem. Soc.*, **1974**, *96*, 309

[147] P. Atkins and J. De Paula, *Elements of Physical Chemistry*, Oxford University Press, Oxford, New York, 2005

[148] H. Yasuda, T. Nishi, S. Miyanaga, and A. Nakamura, *Organometallics*, **1985**, *4*, 359

[149] M. Schlosser and G. Rauchschwalbe, *J. Am. Chem. Soc*, **1978**, *100*, 3258

[150] H. Yasuda and A. Nakamura, *J. Organomet. Chem.*, **1985**, *285*, 15

[151] H. Yasuda, T. Nishi, K. Lee and A. Nakamura, *Organometallics*, **1983**, *2*, 21

[152] L. M. Pratt and A. Streitwieser, *J. Org. Chem.*, **2000**, *65*, 290

[153] E. Cerpa, F. J. Tenorio, M. Contraras, M. Villanueva, H. I. Beltán, T. Heine, K. J. Donald and G. Merino., *Organometallics*, **2008**, *27*, 827

[154] L. Gong, N. Hu, Z. Jin and W. Chen, *J. Organomet. Chem.*, **1988**, *352*, 62

[155] R. E. Dinnebier, U. Behrens and F. Olbrich, *Organometallics*, **1997**, *16*, 3855

[156] H. Yasuda, M. Yamauchi, A. Nakamura, T. Sei, Y. Kai, N. Yasuoka and N. Kasai, *Bull. Chem. Soc. Jpn.*, **1980**, *53*, 1089

[157] H. Yasuda, Y. Ohnuma, A. Nakamura, Y. Kai, N. Yasuoka and N. Kasai, *Bull. Chem. Soc. Jpn.*, **1980**, *53*, 1101

[158] J. S. Overby and T. P. Hanusa, *Angew. Chem. Int. Ed. Engl.*, **1994**, *33*, 2191

[159] L. M. Engelhardt, P. C. Junk, C. L. Raston and A. H. White, *J. Chem. Soc., Chem. Commun.*, **1988**, 1500

[160] R. D. Ernst and T. H. Cymbaluk, *Organometallics*, **1982**, *1*, 708

[161] J. H. Burns, W. H. Baldwin and F. H. Fink, *Inorg. Chem.*, **1974**, *13*, 1916

[162] M. R. Kunze, D. Steinborn, K. Merzweiler, C. Wagner, J. Sieler and R. Taube, *Z. Anorg. Allg. Chem*, **2007**, *633*, 1451

[163] N. Hu, L. Gong, Z. Jin and W. Chen, *J. Inorg. Chem. (China)*, **1989**, *5*, 107

[164] X. Qui and J.-Z. Liu, *Chin. J. Chem.*, **1991**, 10

[165] S.-B. Zhang, D.-M. Chui, J.-H. Cheng, J.-Z. Jin, N.-H. Hu, W.-Q. Chen and J.-Z. Liu, *Chin. J. Appl. Chem.*, **2001**, *18*, 330

[166] J. Jin, S. Jin, Z. Jin and W. Chen, *J. Chem. Soc., Chem. Commun.*, **1991**, 1328

[167] S. Zhang, J. Jin, G. Wei, W. Chen and J. Jin, *J. Organomet. Chem.*, **1994**, *483*, 57

[168] H. Schumann and A. Dietrich, *J. Organomet. Chem.*, **1991**, *401*, C33

[169] D. Baudry, E. Bulot, P. Charpin, M. Ephritikhine, M. Lance, M. Nierlich and J. Vigner, *J. Organomet. Chem.*, **1989**, *371*, 163

[170] T. J. Kealy and P. L. Pauson, *Nature*, **1951**, *168*, 1039

[171] A. L McKnight and R. M. Waymouth, *Chem. Rev.*, **1998**, *98*, 2587

[172] S. Harder, *Coord. Chem. Rev*, **1998**, *176*, 17

[173] J.-Z. Liu and R. D. Ernst, *J. Am. Chem. Soc.*, **1982**, *104*, 3737

[174] R. W. Gedridge, A. M. Arif and R. D. Ernst, *J. Organomet. Chem.*, **1995**, *501*, 95

[175] D. R. Wilson, J.-Z. Liu and R. D. Ernst, *J. Am. Chem. Soc.*, **1982**, *104*, 1120

[176] C. F. Campana, R. D. Ernst, D. R. Wilson and J.-Z. Liu, *Inorg. Chem.*, **1984**, *23*, 2732

[177] F. H. Köhler, R. Mölle, W. Strauss, B. Weber, R. W. Gedridge, R. Basta, W. Trakarnpruk, R. Tomaszewski, A. M. Arif and R. D. Ernst, *Organometallics*, **2003**, *22*, 1923

[178] A. M. Arif, R. D. Ernst E. Meléndez, A. L. Rheingold and T. E. Waldman, *Organometallics,* **1995**, *14*, 1761

[179] D. R. Wilson, A. A. DiLullo and R. D. Ernst, *J. Am. Chem. Soc.,* **1980**, *102*, 5930

[180] D. R. Wilson, R. D. Ernst and T. H. Cymbaluk, *Organometallics*, **1983**, *2*, 1220

[181] L. Stahl, H. Ma, R. D. Ernst, I. Hyla-Kryspin, R. Gleiter and M. L. Ziegler, *J. Organomet. Chem.,* **1987**, *326*, 257

[182] J.-C. Han, J. P. Hutchinson and R. D. Ernst, *J. Organomet. Chem.*, **1987**, *321*, 389

[183] W. Trakarnpruk, A. M. Arif and R. D. Ernst, *J. Organomet. Chem.,* **1995**, *485*, 25

[184] L. Stahl and R. D. Ernst, *Organometallics*, **1983**, *2*, 1229

[185] R. U. Kirss, A. Quazi, C. H. Lake and M. R. Churchill, *Organometallics*, **1993**, *12*, 4145

[186] I. A. Guzei, M. E. Sánchez-Castro, A. Ramirez-Monroy, M. Cervantes-Vásquez, I. R. A. Figueroa and M. A. Paz-Sandoval, *Inorg. Chim. Acta.*, **2006**, *359*, 701

[187] R.D. Ernst, H. Ma, G. Sergeson, T. Zahn and M. L. Ziegler, *Organometallics*, **1987**, *6*, 848

[188] J. Müller, C. Schiller, P. E. Gaede, M. Kempf, *Z. Anorg. Allg. Chem.*, **2005**, *631*, 38

[189] R. Rienäcker and H. Yoshiura, *Angew. Chem. Int. Ed. Engl.*, **1969**, *8*, 677

[190] C. Krüger, *Angew. Chem. Int. Ed. Engl.*, **1969**, *8*, 678

[191] R. K. Bohm and A. Haaland, *J. Organomet. Chem.,* **1966**, *5*, 470

[192] W. Oppolzer, S. C. Burford and F.Marazza, *Helvetica Chim. Acta.,* **1980**, *63*, 555

[193] M. Schlosser, O. Desponds, R. Lehmann, E. Moret and G. Rauchschwalbe, *Tetrahedron*, **1993**, *49*, 10175

[194] M. Schlosser, A. Zellner and F. Leroux, *Synthesis*, **2001**, *12*, 1830

[195] M. Roux, M. Santelli, J. L. Parrain, *Org. Lett.*, **2000**, *2*, 1701

[196] D. H. O'Brien, A. J. Hart and C. R. Russell¸ *J. Am. Chem. Soc.,* **1975**, *97*, 4410

[197] G. M. Sheldrick, SHELXTL Version 6.10, Bruker AXS Inc, Madison, Wisconsin, 1997.